

ANNALS OF THE NEW YORK ACADEMY OF SCIENCES

Issue: *Building the Knowledge Base for Climate Resiliency*

NPCC 2015 Contributors and Reviewers

New York City Panel on Climate Change

Cynthia Rosenzweig (Co-chair), NASA Goddard Institute for Space Studies and Columbia University, Earth Institute, Center for Climate Systems Research

William Solecki (Co-chair), Hunter College, City University of New York, CUNY Institute for Sustainable Cities

Reginald A. Blake, New York City College of Technology

Malcolm J. Bowman, Stony Brook University

Vivien Gornitz, Columbia University, Earth Institute, Center for Climate Systems Research

Klaus H. Jacob, Columbia University, Lamont-Doherty Earth Observatory

Patrick L. Kinney, Columbia University, Mailman School of Public Health

Howard Kunreuther, University of Pennsylvania

Yochanan Kushnir, Columbia University, Lamont-Doherty Earth Observatory

Robin M. Leichenko, Rutgers University

Ning Lin, Princeton University

Guy J.P. Nordenson, Princeton University

Michael Oppenheimer, Princeton University

Gary W. Yohe, Wesleyan University

New York City Government

Katherine Greig, New York City Mayor's Office of Recovery and Resiliency

Leah Cohen, formerly New York City Mayor's Office of Long Term Planning and Sustainability

Project Manager

Daniel Bader, Columbia University, Earth Institute, Center for Climate Systems Research

NOAA Consortium for Climate Risk in the Urban Northeast (CCRUN) Technical Team

Radley Horton (Lead), Columbia University, Earth Institute, Center for Climate Systems Research

CUNY Institute for Sustainable Cities (CISC) Technical Team

Lesley Patrick (Co-lead)

William Solecki (Co-lead)

Stevens Institute of Technology Technical Team

Alan Blumberg (Co-lead)

Philip Orton (Co-lead)

doi: 10.1111/nyas.12626

Ann. N.Y. Acad. Sci. 1336 (2015) 1–2 © 2015 New York Academy of Sciences.

NPCC2 Work Groups

Climate Science: Daniel Bader, Reginald Blake, Vivien Gornitz, Radley Horton (Lead), Yochanan Kushnir, Christopher Little, Michael Oppenheimer, Cynthia Rosenzweig

Sea Level Rise/Coastal Storms and Flooding: Daniel Bader, Alan Blumberg, Vivien Gornitz, Radley Horton (Lead), Klaus Jacob, Ning Lin, Christopher Little, Michael Oppenheimer, Philip Orton

Mapping: Klaus Jacob, Guy Nordenson, Philip Orton, Lesley Patrick, William Solecki (Lead)

Health: Mark Arend, Patrick Kinney (Lead), Kim Knowlton, Jaime Madrigano, Thomas Matte, Elisaveta Petkova, Julie Pullen, Ashlinn Quinn, Kate Weinberger

Indicators and Monitoring: Mark Arend, Reginald Blake (Lead), Alex de Sherbinin, Wendy Dessy, Stuart Gaffin, Klaus Jacob, Kathryn Lane, Thomas Matte, Fred Moshary, Bernice Rosenzweig, Cynthia Rosenzweig, William Solecki, Geraldine Sweeney

Expert Reviewers

John M. Balbus, National Institutes of Health

Kenneth Broad, University of Miami

Virginia Burkett, United States Geological Survey

Brian A. Colle, Stony Brook University

Hannah M. Cooper, Florida Atlantic University

Kristie L. Ebi, ClimAdapt, LLC

Anthony C. Janetos, Boston University

Robert E. Kopp, Rutgers University

David C. Major, Columbia University

Nate Mantua, University of Washington

Gina Maranto, University of Miami

Kenneth G. Miller, Rutgers University

Adam Parris, National Oceanic and Atmospheric Administration

Kathleen J. Tierney, University of Colorado

Rae Zimmerman, New York University

ANNALS OF THE NEW YORK ACADEMY OF SCIENCES

Issue: *Building the Knowledge Base for Climate Resiliency*

New York City Panel on Climate Change 2015 Report Introduction

The climate of the New York City metropolitan region is changing—annual temperatures are hotter, heavy downpours are increasingly frequent, and the sea is rising. These trends, which are also occurring in many parts of the world, are projected to continue and even worsen in the coming decades because of higher concentrations of greenhouse gases in the atmosphere caused by burning of fossil fuels and clearing of forests for agriculture. These changing climate hazards increase the risks for the people, economy, and infrastructure of New York City. As was demonstrated by Hurricane Sandy, coastal and low-lying areas, the elderly and very young, and lower-income neighborhoods are highly vulnerable. In response to these climate challenges, New York City is developing a broad range of climate resiliency policies and programs, as well as the knowledge base to support them. The knowledge base includes up-to-date climate, sea level rise, and coastal flooding projections; a Climate Resiliency Indicators and Monitoring System; and resiliency studies. A special attribute of the New York City response to these challenges is the recognition that both the knowledge base and the programs and policies it supports need to evolve through time as climate risks unfold in the coming decades.

In early September 2012, just weeks before Hurricane Sandy hit, the New York City Council passed Local Law 42 that established the New York City Panel on Climate Change (NPCC) as an ongoing body serving the City of New York. The NPCC is required to meet at least twice each calendar year to review recent scientific data on climate change and its potential impacts, and to make recommendations on climate projections for the coming decades to the end of the century. These projections are due within one year of the publication of the Intergovernmental Panel on Climate Change Assessment Reports (<http://www.ipcc.ch>), or at least every three years. The NPCC also advises the Mayor's Office of Sustainability and the Mayor's Office of Recovery and Resiliency (ORR) on the development of a community- or borough-level communications strategy intended to ensure that the public is informed about the findings of the panel, including the creation of a summary of the climate change projections for dissemination to city residents.

Initially formed as a scientific panel in 2008, the first NPCC was comprised of academic and private-sector experts in climate science, infrastructure, social science, and risk management. It established a risk management framework for the city's critical infrastructure throughout the extended metropolitan region under climate change. The first NPCC developed downscaled climate projections and derived new climate risk information, created adaptation assessment guidelines and protocols, and determined how climate protection levels would need to change to respond to evolving climate conditions (NPCC, 2010).

Following Hurricane Sandy, the City convened the Second New York City Panel on Climate Change (NPCC2) in January 2013 to provide up-to-date scientific information and analyses on increasing climate risks for the creation of *A Stronger, More Resilient New York* (City of New York, 2013). In response, the NPCC2 published the Climate Risk Information 2013 Report (CRI; NPCC, 2013) in June 2013 (<http://ccrun.org/NPCC-2013>). The Climate Risk Information 2013 Report presented quantitative and qualitative information about future climate hazards for the 2020s and 2050s, focusing on temperature, precipitation, and sea level, as well as providing future coastal flood risk maps.

This NPCC2 Report (NPCC, 2015) presents the full work of the NPCC2 from January 2013 to January 2015. The aim is to increase current and future resiliency of the communities, citywide systems, and infrastructure of New York City to a range of climate risks. NPCC2 follows the risk management and resilience approach developed by the first NPCC (Yohe & Leichenko, 2010). In this approach, climate hazards are extreme climatic or weather events that cause harm and damage, and climate risk is the product of the likelihood of a climate hazard occurring and the magnitude of consequences should that event occur. The NPCC 2010 Report found that climate risks are spatially varied across the city because different levels of vulnerability are present within and across communities and infrastructure systems, resulting in different outcomes. Recognizing that risk management strategies need to evolve through time in response to continuous climate risk assessment, the NPCC developed a flexible adaptation pathways approach to guide the city in developing greater resiliency (NPCC, 2010). The New York City flexible adaptation framework encompasses both adaptation and mitigation and enables the consideration of long-range goals as well as their translation into short-term objectives.

The NPCC uses the definition of the term *resilience* presented by the Intergovernmental Panel on Climate Change (IPCC) in *Managing the Risks of Extreme Events and Disasters to Advance Climate Change Adaptation* (Lavell *et al.*, 2012), but with emphasis on *improvement* of city systems in contrast to their simple restoration.

“Resilience is the ability of a system and its component parts to anticipate, absorb, accommodate, or recover from the effects of a potentially hazardous event in a timely and efficient manner, including through ensuring the preservation, restoration, or *improvement of its essential basic structures.*”

The information in the NPCC2 Report has been co-generated by scientists, stakeholders, and decision-makers in New York City. The NPCC2 established Work Groups on Climate Science, Sea Level Rise/Coastal Storms and Flooding, Mapping, Health, and Indicators and Monitoring. Scientists and managers of critical city systems met in a series of stakeholder meetings and workshops to discuss climate risks and how they could best be understood and presented to aid in sound decision-making. Some of these diverse contributors are authors of the report’s chapters.

This volume is a continuation of the NPCC assessment process that began in 2008 with some significant advances that reflect the growing sophistication of climate science research and the evolving policy agenda to which it must respond. The report provides the City of New York with projections of its climate to the end of the century, both static and dynamic coastal storm surge modeling, and next steps in the development of an indicators and monitoring system for climate change impacts and adaptation. The assessment process is innovative because it looks beyond critical infrastructure and its vulnerability to climate change (a highlight of the first NPCC), and more directly focuses on what a more dynamic climate will mean for the everyday experience of the city’s residents—for example, regarding health impacts.

The report documents recent observed climate trends and extends the CRI 2013 projections to the 2080s and 2100 for temperature and precipitation (Chapter 1) and sea level rise (Chapter 2). It explains the spatial applicability of the projections to the wider New York metropolitan region and compares the NPCC2 methods to the recently published Fifth Assessment Report of the IPCC (IPCC, 2013). It presents new maps for the flood risks to the 2080s and 2100 for the current 100- and 500-year coastal flood event^a (Chapter 3). The report characterizes future coastal flooding through enhanced dynamic flood inundation (storm surge) modeling that includes the effects of sea level rise (Chapter 4) and provides a review of key issues related to climate change and health relevant to the citizens of New York City (Chapter 5). It then develops a process for establishing an indicators and monitoring system to track data related to climate hazards, risks, impacts, and adaptations, and presents metrics for evaluating the NYC Cool Roofs Program and its effect on the urban heat island (Chapter 6). The report ends with conclusions and recommendations

^aThe 100-year coastal flood event refers to the flood with a 1% annual chance of occurrence. The 500-year coastal flood event refers to the flood with a 0.2% annual chance of occurrence.

with regard to both increasing climate change resiliency for the city and advancing the research required to build it. The report includes two appendices that provide climate risk and projections infographics for stakeholders and technical details for each of the chapters.

Ongoing assessments such as those of the NPCC must be flexible in response to changing science and policy demands, yet also must provide a foundation for inter-assessment comparison and benchmarking through time. The NPCC2 assessment arose from the urgent post-Hurricane Sandy need for forward thinking on extreme events and resiliency. Implicit in its assessment approach is that as the new “normal” of climate non-stationarity^b emerges, so the way forward must be clear for developing a new and better knowledge base for policy (Solecki & Rosenzweig 2014; Rosenzweig & Solecki 2014).

Finally, the NPCC works to improve ways to communicate data and information on climate risks both to citizens and to potential users at multiple levels of government, including city, state, and national. While specific to New York City and its metropolitan region, the approaches developed by the NPCC can contribute to efforts to enhance resiliency as they are undertaken across governmental scales as well as in other locations.

CYNTHIA ROSENZWEIG AND WILLIAM SOLECKI

References

- City of New York. 2013. *A Stronger, More Resilient New York*. 438 pp.
- IPCC. 2013. *Climate Change 2013: The Physical Science Basis. Contribution of Working Group I to the Fifth Assessment Report of the Intergovernmental Panel on Climate Change*. Cambridge University Press.
- Lavell, A. *et al.* 2012. Climate change: new dimensions in disaster risk, exposure, vulnerability, and resilience. pp. 25–64.
- Milly, P.C.D., J. Betancourt, M. Falkenmark, *et al.* 2008. Stationarity is dead: whither water management? *Science* **319**: 573–574.
- New York City Panel on Climate Change (NPCC). 2013. *Climate Risk Information 2013: Observations, Climate Change Projections, and Maps*. Prepared for use by the City of New York Special Initiative on Rebuilding and Resiliency.
- NPCC. 2010. Climate Change Adaptation in New York City: Building a Risk Management Response. C. Rosenzweig and W. Solecki, Eds. *Ann. N.Y. Acad. Sci.* **1196**: 1–354.
- NPCC. 2015. Building the Knowledge Base for Climate Resiliency: New York City Panel on Climate Change 2015 Report. C. Rosenzweig and W. Solecki, Eds. *Ann. N.Y. Acad. Sci.* **1336**: 1–149.
- Rosenzweig, C., and W. Solecki. 2014. Hurricane Sandy and adaptation pathways in New York: Lessons from a first-responder city. *Glob. Environ. Change* **28**: 395–408, doi:10.1016/j.gloenvcha.2014.05.003.
- Solecki, W. & C. Rosenzweig. 2014. Climate Change, Extreme Events, and Hurricane Sandy: From Non-Stationary Climate to Non-Stationary Policy. *J. Extreme Events* **1**: 1–20.
- Yohe, G. & R. Leichenko. 2010. “Chapter 2: Adopting a risk-based approach.” In *Climate Change Adaptation in New York City: Building a Risk Management Response*. C. Rosenzweig & W. Solecki, Eds. *Ann. N.Y. Acad. Sci.* **1196**: 29–40.

^b*Stationarity* is defined as having common statistical properties over time (e.g., mean, variance, and other statistics are all constant). Now that the climate system is changing, non-stationarity has become the new normal (Milly *et al.*, 2010).

ANNALS OF THE NEW YORK ACADEMY OF SCIENCES

Issue: *Building the Knowledge Base for Climate Resiliency*

Foreword to *Building the Knowledge Base for Climate Resiliency: New York City Panel on Climate Change 2015 Report*

Dear Friends,

Climate change is an existential threat to New Yorkers and the world. Together, we are rising to the challenge by dramatically reducing our contributions to its causes, while protecting ourselves against its risks. New York City has committed to reducing our emissions 80%, from 2005, by 2050, making us the largest city in the world to commit to this ambitious and necessary goal, while simultaneously implementing an aggressive, comprehensive climate resiliency plan.

With this report, the New York City Panel on Climate Change (NPCC) provides critical climate and impact projections needed to inform decision-makers so as to make New Yorkers safer and to enhance the city's long-term resiliency. The buildings and infrastructure we construct and improve today will be with New Yorkers for generations. As we prepare our city for extreme weather and rising sea levels, we must use the best possible information and projections regarding the risks we face.

The NPCC is a consortium of local world-class scientists that began advising the city in 2008. Thanks to their tireless work, our understanding of the risks we face continues to improve. This year, for the first time, we have local sea level rise projections through 2100. We know that New York City's sea level is increasing at almost twice the global average. We also understand with greater certainty that local climate change will very likely result in warmer regional temperatures, and that heat waves are very likely to increase.

In 2014, we created the Mayor's Office of Recovery and Resiliency, the first-ever city office focused on climate resiliency. This office is leading the city's short- and long-term efforts to strengthen coastal defenses, upgrade buildings, protect infrastructure and critical services, and make homes, businesses, and neighborhoods safer and more vibrant. With the projections and analysis of climate change provided by the NPCC, we can continue to track our progress, monitor our risks, and ensure that we make New York City a safe and accessible place for all New Yorkers for years to come.



BILL DE BLASIO
Mayor of New York City

ANNALS OF THE NEW YORK ACADEMY OF SCIENCES

Issue: *Building the Knowledge Base for Climate Resiliency*

Preface to *Building the Knowledge Base for Climate Resiliency: New York City Panel on Climate Change 2015 Report*

This volume is the New York City Panel on Climate Change (NPCC) 2015 Report. It contains the Executive Summary, chapters of the report including the Conclusions and Recommendations, one appendix developed with and for stakeholders on climate risk and projections, and a second appendix that provides technical details. The NPCC 2015 Report may be found online at www.wileyonlinelibrary.com/journal/annals and www.nyc.gov/planycreports.

It has been an honor to work with the Mayor's Office of Recovery and Resiliency and the Mayor's Office of Sustainability. We especially thank Katherine Grieg, Daniel Zarrilli, Leah Cohen, and Sergej Mahnovski; they are exemplary professionals committed to developing effective ways to confront climate change resiliency challenges.

This report is the product of the work of the members of the NPCC and its work groups. We express our sincere thanks to each of them for their contributions, and to their institutions for supporting their participation. We thank Daniel Bader for his dedicated work as the NPCC project manager, without whom the NPCC could not have completed its tasks in such a concerted way. At the Columbia University Center for Climate Systems Research, we thank Danielle Peters for research assistance and Shari Lifson for graphics. We also thank the expert reviewers of the NPCC2 Report without whom the independent provision of sound science for climate change resiliency could not proceed.

We are proud that the NPCC 2015 Report is being published in *Annals of the New York Academy of Sciences*, one of the oldest continuously published scientific journals in the United States, by the third-oldest scientific society. We would like to thank especially Douglas Braaten, editor-in chief, and the *Annals'* staff, for their partnership in the publication of this volume.

Support for the printing of the report was provided by a grant administered by the New York State Division of Homeland Security and Emergency Services and the U.S. Department of Homeland Security. Points of view in this document are those of the authors and do not necessarily represent the official position or policies of the New York State Division of Homeland Security and Emergency Services or the U.S. Department of Homeland Security.

CYNTHIA ROSENZWEIG AND WILLIAM SOLECKI
Co-chairs of the New York City Panel on Climate Change

ANNALS OF THE NEW YORK ACADEMY OF SCIENCES

Issue: *Building the Knowledge Base for Climate Resiliency*

New York City Panel on Climate Change 2015 Report Executive Summary

The climate of the New York metropolitan region is changing—annual temperatures are hotter, heavy downpours are increasingly frequent, and the sea is rising. These trends, which are also occurring in many parts of the world, are projected to continue and even worsen in the coming decades due to higher concentrations of greenhouse gases (GHGs) in the atmosphere caused by burning of fossil fuels and clearing of forests for agriculture. These changing climate hazards increase the risks for the people, economy, and infrastructure of New York City. As was demonstrated by Hurricane Sandy, populations living in coastal and low-lying areas, the elderly and very young, and lower-income neighborhoods are highly vulnerable. In response to these climate challenges, New York City is developing a broad range of climate resiliency policies and programs as well as the knowledge base to support them.

Initially formed as a scientific panel in 2008, the first New York City Panel on Climate Change (NPCC) was comprised of academic and private sector experts in climate science, infrastructure, social science, and risk management. It established a risk-management framework for the city's critical infrastructure throughout the extended metropolitan region under climate change (NPCC, 2010). Following Hurricane Sandy, the City convened the Second New York City Panel on Climate Change (NPCC2) in January 2013 to provide up-to-date scientific information and analyses on climate risks for the creation of *A Stronger, More Resilient New York* (City of New York, 2013). This report (NPCC, 2015) presents the work of the New York City Panel on Climate Change from January 2013 to January 2015.

The report documents recently observed climate trends and climate projections for the New York metropolitan region up to 2100. It compares the NPCC2 methods and projections for the local scale to those done at the global scale by the Fifth Assessment Report of the Intergovernmental Panel on

Climate Change (IPCC, 2013). The report presents new maps that show increasing flood risks due to climate change defined for the 100- and 500-year coastal flood event^a in the 2020s, 2050s, 2080s and 2100. It compares future coastal flooding simulated by static and dynamic modeling that include the effects of sea level rise. The report reviews key issues related to climate change and health relevant to the citizens of New York City and sets forth a process for developing a system of indicators and monitoring to track data related to climate change hazards, risks, impacts, and adaptation strategies. Research needs and recommendations for climate resiliency are provided.

Climate observations and projections

Observations show that temperatures and precipitation in New York City are increasing. In the New York metropolitan region, projections from global climate models (GCMs) indicate significant future changes in temperature and precipitation, and thus the potential for large impacts. Reducing greenhouse gas emissions now will reduce the likelihood of more extreme climate risks in the future.

Observations

- **Mean annual temperature** has increased at a rate of 0.3°F per decade (total of 3.4°F) over the 1900 to 2013 period in Central Park, although the trend has varied substantially over shorter periods.
- **Mean annual precipitation** has increased at a rate of approximately 0.8 inches per decade (total of 8 inches) over 1900 to 2013 in Central Park. Year-to-year (and multi-year) variability of precipitation has also become more pronounced, especially since the 1970s.

^aThe 100-year coastal flood event refers to the flood with a 1% annual chance of occurrence. The 500-year coastal flood event refers to the flood with a 0.2% annual chance of occurrence.

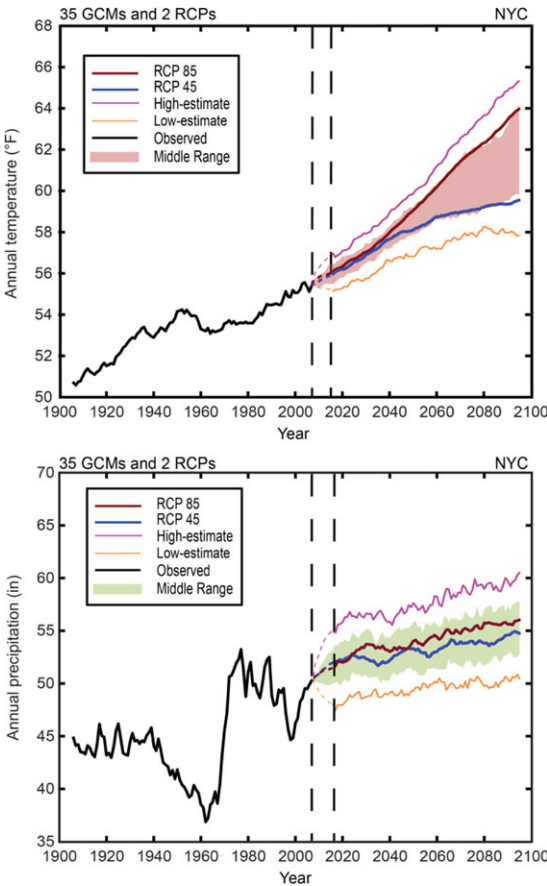


Figure ES.1. Observed and projected temperature and precipitation. Projected global climate model changes through time are applied to the observed historical data.^c

Future projections

Climate change is extremely likely^b to bring warmer temperatures to the New York metropolitan region.

^bProbability of occurrence and likelihood defined as (IPCC, 2007): virtually certain, >99% probability of occurrence; extremely likely, >95% probability of occurrence; very likely, >90% probability of occurrence; likely, >66% probability of occurrence; more likely than not, >50% probability of occurrence; about as likely as not, 33% to 66% probability of occurrence.

Likelihoods are assigned for the direction and characterization of change of projected climate hazards based on observations, model projections, physical understanding, literature review, and expert judgment.

^cThe two thick lines show the average for each representative concentration pathway (RCP) across the 35 global climate models (GCMs). Shading shows the middle range

- **Mean annual temperatures** are projected by GCMs to increase by 4.1 to 5.7°F^d by the 2050s and by 5.3 to 8.8°F by the 2080s.^e

Total annual precipitation will likely increase.

- **Mean annual precipitation** increases projected by the GCMs are 4 to 11 percent by the 2050s and 5 to 13 percent by the 2080s.

Heat waves and extreme precipitation days^f are also very likely to increase.

- The frequency of **heat waves** is projected to triple by the 2080s, and extreme cold events are projected to decrease.
- The frequency of **extreme precipitation days** is projected to increase, with approximately one and a half times more events per year possible by the 2080s compared to the current climate.

Figure ES.1 shows observed annual trends and future projections for temperature and precipitation in New York City. The range of NPCC2 projections increases to the end of the century.

Sea level rise and coastal storms

Sea level rise in New York City is a significant hazard, increasing the risks posed to coastal communities, infrastructure, and ecosystems.

(25th to 75th percentile). The bottom and top lines respectively show each year’s low-estimate and high-estimate projections across the suite of simulations. A 10-year smoothing filter has been applied to the observed data and model output. The dotted area between 2007 and 2015 represents the time period that is not covered because of the smoothing procedure.

^dMiddle range (25th to 75th percentile) of model-based projections.

^eSpecific quantitative projections are not assigned a likelihood due to uncertainties in future greenhouse gas concentrations, sensitivity of the climate system to changes in greenhouse gases, climate variability, and changes in regional and local processes.

^fThe NPCC defines heat waves as three or more consecutive days with maximum temperatures at or above 90°F. Extreme precipitation days are defined as days with total precipitation of 1 inch or more.

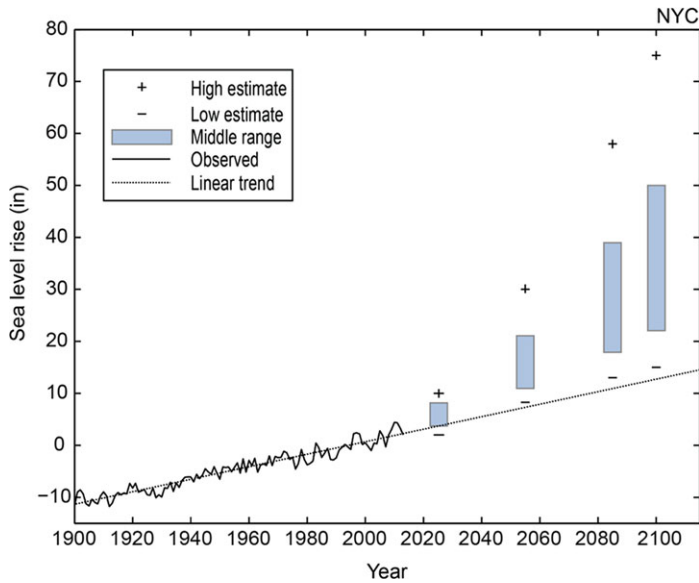


Figure ES.2. New York City sea level rise observations and projections. Projections shown are the low estimate (10th percentile), middle range (25th to 75th percentiles), and the high estimate (90th percentile). The historical trend is also included. Projections are relative to the 2000 to 2004 base period.

Observations

- **Sea level rise** in New York City has averaged 1.2 inches per decade (total of 1.1 feet) since 1900, nearly twice the observed global rate of 0.5 to 0.7 inches per decade over a similar time period.

Projections

Sea level rise in New York City is projected to continue to exceed the global average. Sea level rise is very likely to accelerate as the century progresses.

- Projections for **sea level rise** in New York City are 11 to 21 inches by the 2050s, 18 to 39 inches by the 2080s, and could reach as high as 6 feet by 2100.

It is virtually certain that sea level rise alone will lead to an increased frequency and intensity of coastal flooding as the century progresses.

- Projected sea level changes alone would increase the frequency and intensity of **coastal flooding**, leading to (absent any change in storms themselves) between a doubling and an approximately 10- to 15-fold increase in the frequency of the current 100-year coastal flood by the 2080s.

Figure ES.2 shows the observed trend and future projections for sea level rise in New York City. The NPCC2 projections take global and local components into account.

Projected changes in the frequency and intensity of coastal storms are uncertain at local scales. The two types of storms with the largest influence on the coastal areas of the New York metropolitan region are tropical cyclones (hurricanes and tropical storms) and nor’easters.

- It is more likely than not that the number of the **most intense hurricanes** will increase in the North Atlantic Basin, along with extreme winds associated with these storms.
- As the ocean and atmosphere continue to warm, **intense precipitation from hurricanes** in the North Atlantic Basin is more likely than not to increase.
- It is currently not known how **nor’easters** in the New York metropolitan region may change in the future.

Static coastal flood mapping

Mapping climate hazards is an essential part of an overall risk management strategy for densely populated urban areas such as the New York metropolitan region. The strength of a flood-mapping tool

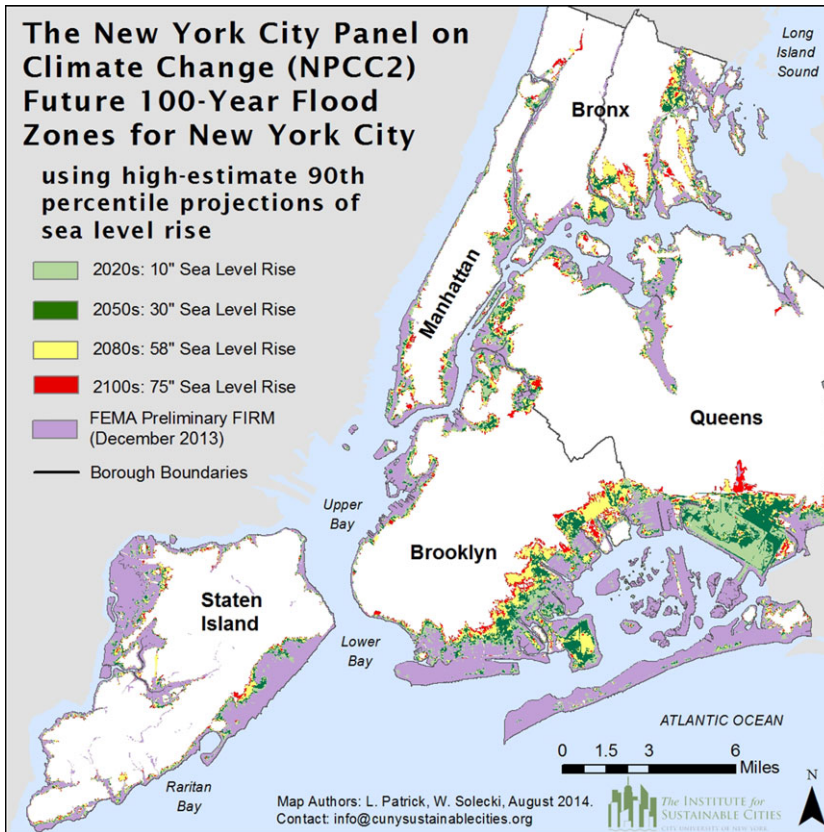


Figure ES.3. Potential areas that could be impacted by the 100-year flood in the 2020s, 2050s, 2080s, and 2100 based on projections of the high-estimate 90th percentile NPCC2 sea level rise scenario. Map developed using the static approach. **NOTE:** This map is subject to limitations in accuracy as a result of the quantitative models, data sets, and methodology used in its development. The map and data should not be used to assess actual coastal hazards, insurance requirements, or property values or be used in lieu of FIRMS issued by FEMA. The flood areas delineated in no way represent precise flood boundaries but rather illustrate three distinct areas of interest: (1) areas currently subject to the 100-year flood that will continue to be subject to flooding in the future; (2) areas that do not currently flood but are expected to potentially experience the 100-year flood in the future; and (3) areas that do not currently flood and are unlikely to do so in the timeline of the climate scenarios used in this research (end of the current century).

depends on the quality of the underlying data and the techniques used for presentation. The updated future 100-year and 500-year flood maps by the NPCC2 show large-scale coastal vulnerability.

- Higher sea level elevations result in greater floodplain areas, with the extent of landward flooding dependent on elevation and slope of land, presence of man-made structures, permeability of soils, vegetation, and other impediments to movement of water.
- For the 100-year flood, sea level rise by 2100 roughly doubles the affected area compared to the December 2013 FEMA Preliminary Flood

Insurance Rate Maps (FIRMS); for the 500-year flood, sea level rise by 2100 increases the affected area by 50% compared to the December 2013 FEMA FIRMS 500-year flood area.

- Queens is the borough with the most land area at risk of future coastal flooding due to sea level rise, followed by Brooklyn, Staten Island, the Bronx, and Manhattan.

Figure ES.3 presents the updated future 100-year flood map for New York City for the 90th percentile projections of sea level rise for the 2020s, 2050s, 2080s, and 2100 compared to FEMA’s December 2013 FIRMS.

Dynamic modeling of future coastal flood hazards

Sea level rise interacts with coastal storms to cause increased flood heights and expanded floodplains. The static approach to projecting coastal flooding adds sea level rise onto current storm tide levels, and dynamic models capture the roles of friction and wind as well as sea level rise and tides.

- NPCC2 results generally support the finding that both static and dynamic modeling approaches are valid and reliable approximations of coastal flooding for most locations in the New York metropolitan region.
- For results with hurricanes only, the static approach projects lower coastal flood heights and reduced flood zone areas for several locations in the New York metropolitan region, compared to results of the dynamic modeling approach.
- Many sources, including sea level rise, type of storm, errors in elevation data, and statistical methods, contribute to uncertainties in coastal flooding projections.

Figure ES.4 illustrates the differences between the dynamic and static approaches for the 100-year

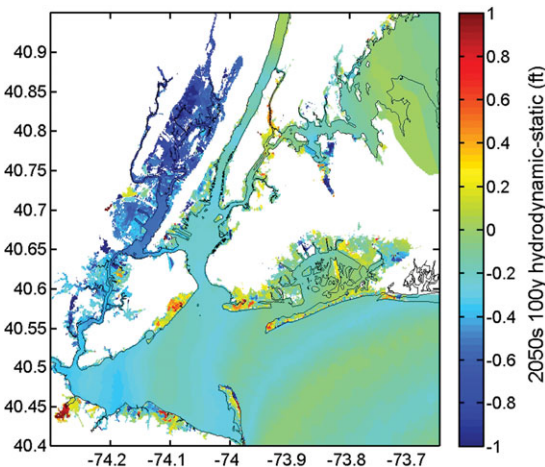


Figure ES.4. Difference between dynamic and static mapping results for 100-year flood elevations (2050s 90th percentile NPCC sea level rise scenario). Results show the combined assessment of extratropical cyclones and tropical cyclones (extratropical cyclones are coastal storms existing or occurring outside of the tropical latitudes).

flood elevations for the 2050s, using the NPCC2 90th percentile sea level rise projections.

Public health impacts and resiliency

New York City faces potential health risks related to two principal climate hazards: increasing temperatures and heat waves and coastal storms with flooding, as well as a range of secondary hazards related to air pollution, pollen, vector-borne diseases, and water/food-borne illnesses. Recent experience from Hurricane Sandy and other extreme events has clearly demonstrated that the health of New Yorkers can be compromised by these hazards.

- Health impacts from exposure to extreme weather events include direct loss of life, increases in respiratory and cardiovascular diseases, and compromised mental health. The risk of these impacts is projected to increase in the future.
- Rising temperatures over the coming century are projected to increase the number of heat-related deaths that occur in Manhattan. However, uncertain future trends in the use of home air conditioning, improved population health, and better air quality during heat waves make it difficult to predict the magnitude of these increases.
- The health impacts of Hurricane Sandy varied across the city considerably due to local effects of storm and tidal surges, differing housing types, the degree to which energy, water, and/or transportation infrastructure was disrupted, and the underlying health and resilience factors of the affected population.
- Vulnerable groups include the old and the very young; women; those with preexisting physical, mental, or substance-abuse disorders; residents of low-income households; members of disadvantaged racial/ethnic groups; workers engaged in recovery efforts; and those with weak social networks.

Figure ES.5 shows projected increases in heat mortality in New York City for two GHG emissions scenarios (A2 and B1).

Indicators and monitoring

Climate change indicators are defined as empirically based quantities that can be tracked over time

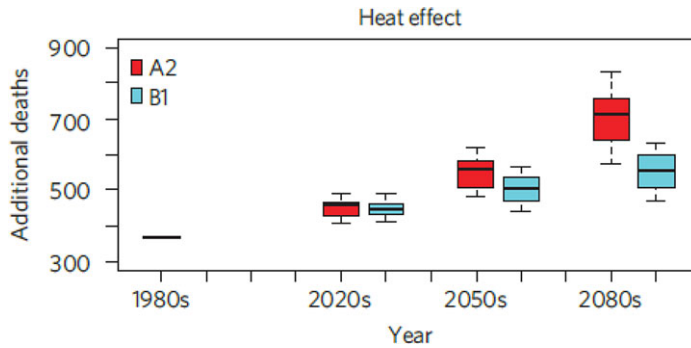


Figure ES.5. Heat-related deaths in the 1980s (observed), 2020s, 2050s, and 2080s for 16 global climate models and the A2 and B1 GHG scenarios. Source: Li *et al.*, 2013.

to provide relevant information for stakeholder decisions on climate resiliency and on the efficacy of resiliency measures to reduce vulnerability and risk. The three main categories of climate change indicators are (1) physical climate change variables; (2) exposure, vulnerability, and impact metrics; and (3) adaptation measures and their effectiveness.

and monitoring systems for tracking the effectiveness of adaptation measures.

An example of data tracked as part of the NYC Cool Roofs Program is shown in Figure ES.6, which illustrates that white roofs are more effective than black roofs in reducing peak temperatures.

Research needs

- New York City maintains an extensive set of indicators and monitoring programs that can be harmonized and expanded to provide targeted information about current and emerging climate risks, impacts, and adaptation. This will provide key information for climate resiliency decision-making in regard to critical infrastructure, ecosystems, and health.
- Building on current tracking efforts, New York City is well placed to develop an expanded Climate Resiliency Indicators and Monitoring System for the New York metropolitan region.
- Developing an effective indicators and a monitoring system involves seven steps, which include interacting with stakeholders to ascertain information needs and key decisions; determining what data are available; developing a preliminary set of indicators; presenting indicators to stakeholders for feedback; revising preliminary indicators based on stakeholder input; setting up and maintaining the monitoring system; and conducting indicator evaluations through time to track general trends and to evaluate specific adaptation interventions.
- The NYC Cool Roofs Program provides a valuable testbed for the establishment of indicators

There is a need for ongoing research across a broad spectrum of areas in order to provide the people of New York City and the surrounding metropolitan region with the knowledge required to enhance climate resiliency through the coming decades. Economic studies of potential damages and costs of adaptation are critical to provide the knowledge base needed for wise climate change policy. It is important that budgetary resources are focused on building the scientific basis for resiliency planning.

Climate

Although there is a growing understanding of how the New York metropolitan region as a whole may be impacted by climate change, more research is needed on neighborhood-specific hazards and impacts. High-resolution regional climate modeling is needed to illuminate how projected changes vary throughout the city due to factors including coastal breezes, topography, and different urban land surfaces.

Sea level rise and coastal storms

More research is needed on how the Greenland and West Antarctic ice sheets will respond to climate change because these ice sheets are the largest long-term source of “high-end” sea level rise uncertainty. Future research efforts should also explore the

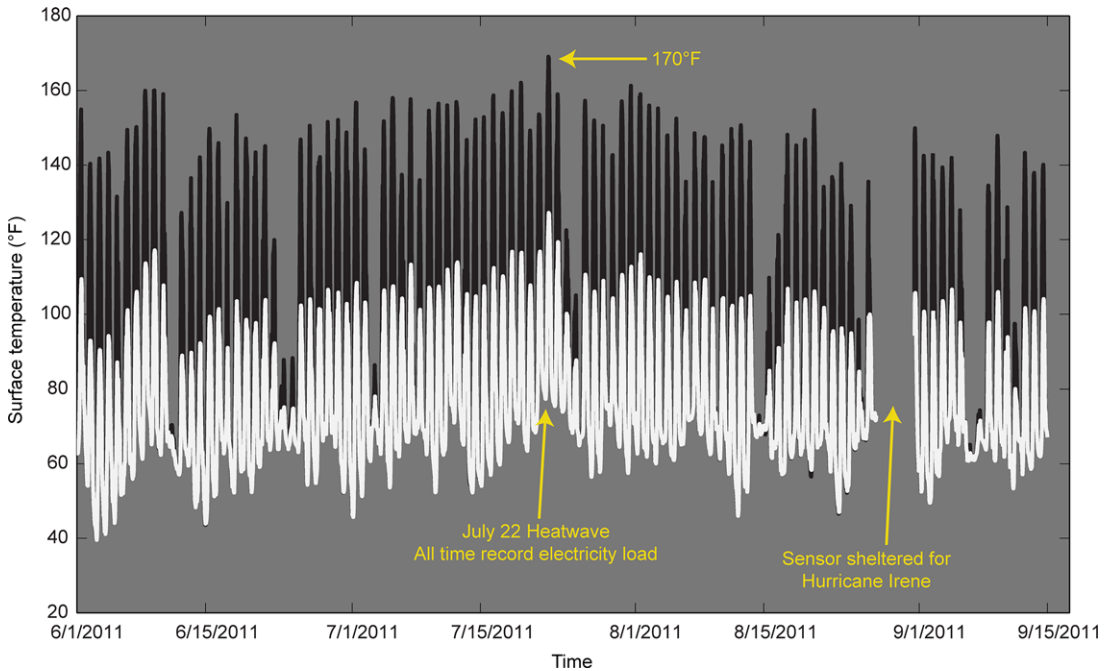


Figure ES.6. Surface temperatures for a freshly painted white roof compared to those of a control black roof at the Museum of Modern Art, Queens, NY. Source: Gaffin *et al.*, 2012.

relationships among the different sea level rise components as well as the relationships between those sea level rise components and coastal storm risk in the Northeast. An additional key area of study is how coastal storms may change in the future.

Static coastal flood mapping

Future work should focus on quantifying the sources of uncertainty in the datasets used to develop flood maps, on the mapping process, and on displaying these uncertainties on the maps themselves. An overall flood vulnerability index that combines both social and biophysical vulnerability should be utilized because it can characterize site-specific levels of risk to flood hazards. This will also help to identify communities in the New York metropolitan region that may require special attention, planning efforts, and mobilization to respond to and recover from disasters and hazards.

Dynamic coastal flood modeling

More research should be done on historical events and on probabilistic hazard assessment methods to identify and reduce the uncertainty in defining flood hazards for the New York metropolitan region. Investigations are needed of the local geographical and

storm conditions that lead to different flood heights in static and dynamic models. Studies should explore the comparability between the use of the static and dynamic approaches to projecting coastal zone flooding.

Public health impacts and resiliency

Additional knowledge will be essential for New York City to anticipate and avoid future health impacts from extreme weather events in a changing climate. Key areas include understanding the factors that lead to unhealthy levels of exposure to heat inside New York City apartment buildings, where most deaths occur during heat events. Research is needed to analyze the health impacts resulting from climate adaptation and mitigation measures, including effects on indoor air quality. Actions that result in climate adaptation and mitigation co-benefits including positive health outcomes are particularly important to identify.

Indicators and monitoring

Studies are needed to identify opportunities where existing monitoring systems in the New York metropolitan region can easily be enhanced for climate change and situations where more extensive

adjustments are needed. Focused analyses should be conducted on the identification of urban system tipping points in response to stresses in order to enhance capacity for early action.

Recommendations for climate resiliency

Although there remain significant uncertainties regarding long-term climate change, the NPCC 2015 report supports the large body of evidence indicating that decision-makers are better served by consideration of the future climate risks rather than reliance on the climate of the past in development of resiliency and rebuilding programs. Specific recommendations for climate resiliency include:

- Continue to follow the risk-based Flexible Adaptation Pathways approach to climate resiliency, set forth by the NPCC in 2010. This approach enhances the ability of the region to periodically assess, adjust, and tailor future development plans under changing climate conditions, updated by the NPCC as mandated by New York City's Local Law 42.
- Make progress on achieving the initiatives in *A Stronger, More Resilient New York* (City of New York, 2013). Because of the short- and long-term challenges posed by increasing risks of temperature extremes, heavy downpours, and coastal flooding, these need to be strengthened and expanded to the entire New York metropolitan region.
- An integrated approach that includes engineering, ecosystems, and social strategies is vital to ensuring climate resiliency in the coming decades. Land use planning for sustainable infrastructure systems, particularly in coastal zones and low-lying areas, is especially important.
- At the same time, develop and support programs and policies (such as *One City: Built to Last*; City of New York, 2014) that work to reduce GHG emissions in order to limit the rate of future climate change and the magnitude of the associated risks. Consider co-benefits of adaptation and mitigation.
- Establish the New York City Climate Resiliency Indicators and Monitoring System. Associated Working Groups should be convened to develop and analyze key information for decision-making on critical infras-

structure, ecosystems, and health. Build wider networks to monitor indicators and actively support their operation and long-term maintenance throughout the New York metropolitan region.

- Coordinate with state and federal partners on climate change projections and resiliency programs such as Rebuild by Design and the U.S. Army Corps of Engineers North Atlantic Comprehensive Study. FEMA should incorporate local sea level rise projections into its coastal flood methodology and mapping. This enables residents as well as planners to utilize the best available information as they develop and implement climate resiliency strategies.
- While the 100-year coastal flood is widely used to inform decision-making, other risk thresholds should be examined to improve risk-reduction decisions in the future. The goal is dynamic performance-based risk management across a range of probabilistic hazards established for current and future climates.

Throughout all of the above activities:

- It is essential to facilitate an ongoing and continuous process of stakeholder–scientist interactions, with cross-linkages between the NPCC, other experts, the City, the other municipalities of the New York metropolitan region, New York State, relevant agencies of the federal government, and the U.S. National Climate Assessment.

Collaboration across multiple scales of government will help to ensure that the climate science developed for the New York metropolitan region informs and draws from the best available information, thereby positioning residents and planners to confront expected future changes in the most effective way possible.

References

- City of New York. 2013. New York City Special Initiative on Rebuilding and Resiliency. 'A Strong More Resilient New York', 438 pp.
- City of New York. 2014. *One City: Built to Last*. New York, NY: Mayor's Office of Long Term Planning and Sustainability, 114 pp.

- Gaffin, S.R., M. Imhoff, C. Rosenzweig, *et al.* 2012. Bright is the new black –multi-year performance of high-albedo roofs in an urban climate. *Environ. Res. Letter.*, **7**: 014029.
- IPCC. 2007. *Climate Change 2007: The Physical Science Basis. Contribution of Working Group I to the Fourth Assessment Report of the Intergovernmental Panel on Climate Change.* Cambridge University Press.
- IPCC. 2013. *Climate Change 2013: The Physical Science Basis. Contribution of Working Group I to the Fifth Assessment Report of the Intergovernmental Panel on Climate Change.* Cambridge University Press.
- Li, T., R.M. Horton, & P.L. Kinney. 2013. Projections of seasonal patterns in temperature- related deaths for Manhattan, New York. *Nature Clim. Change*, **3**: 717–721.
- NPCC. 2010. Climate Change Adaptation in New York City: Building a Risk Management Response. C. Rosenzweig and W. Solecki, Eds. *Ann. N.Y. Acad. Sci.* **1196**: 1–354.
- NPCC. 2015. Building the Knowledge Base for Climate Resiliency: New York City Panel on Climate Change 2015 Report. C. Rosenzweig and W. Solecki, Eds. *Ann. N.Y. Acad. Sci.* **1336**: 1–149.

ANNALS OF THE NEW YORK ACADEMY OF SCIENCES

Issue: *Building the Knowledge Base for Climate Resiliency*

New York City Panel on Climate Change 2015 Report

Chapter 1: Climate Observations and Projections

Radley Horton,^{1,a} Daniel Bader,^{1,a} Yochanan Kushnir,² Christopher Little,³ Reginald Blake,⁴ and Cynthia Rosenzweig⁵

¹Columbia University Center for Climate Systems Research, New York, NY. ²Ocean and Climate Physics Department, Lamont-Doherty Earth Observatory, Columbia University, Palisades, NY. ³Atmospheric and Environmental Research, Lexington, MA. ⁴Physics Department, New York City College of Technology, CUNY, Brooklyn, NY. ⁵Climate Impacts Group, NASA Goddard Institute for Space Studies; Center for Climate Systems Research, Columbia University Earth Institute, New York, NY

Address for correspondence: Radley Horton, Associate Research Scientist, Columbia University Center for Climate Systems Research, 2880 Broadway, New York, NY 10025. rh142@columbia.edu

Contents

- 1.1 The global climate system
- 1.2 Observed climate
- 1.3 Climate projections
- 1.4 Conclusions and recommendations

Introduction

During 2013 and 2014, numerous international (IPCC, 2013) and national (Melillo *et al.*, 2014; Gordon, 2014) reports have concluded that human activities are changing the climate, leading to increased vulnerability and risk. Since the industrial revolution, fossil fuel burning, industrial activity, and land use changes have led to a 40% increase in heat-trapping carbon dioxide (CO₂), and an approximately 150% increase in methane (CH₄), another powerful greenhouse gas (GHG), has been observed. Global temperatures have increased by close to 1°C since 1880 as the upper oceans have warmed and polar ice has retreated. These and other climate changes are projected to accelerate as greenhouse gas concentrations continue to rise.

In the coming decades, climate change is extremely likely to bring warmer temperatures in the New York metropolitan region (see Box 1.1 and Fig. 1.1 for key definitions and terms). Heat waves are very likely to increase; total annual precipitation will likely increase and brief, intense rainstorms are very likely to increase.

Because of incomplete knowledge about exactly how much climate change will occur, choosing among policies for reducing future damages requires prudent risk management (Yohe and Leichenko, 2010; Kunreuther *et al.*, 2013). Given differing risk tolerances among stakeholders, a risk management approach allows for a range of possible climate change outcomes to be examined with associated uncertainties surrounding their likelihoods.

The New York City Panel on Climate Change 2 (NPCC2) projections can be used to inform planning across multiple governmental scales (e.g., city, county, state) in the New York metropolitan region. Such coordinated efforts can serve as test cases for successful local, state, and federal coordination for integrated climate adaptation initiatives.

This chapter describes the global climate system, and presents observed temperature and precipitation trends and projections for the region. Chapter 2 (NPCC, 2015) focuses on sea level rise and possible changes in coastal storms. Chapter 3 and Chapter 4 (NPCC, 2015) describe efforts to better understand the region's vulnerability to coastal flooding during coastal storms.

The treatment of likelihood related to the NPCC projections is similar to that developed by the Intergovernmental Panel on Climate Change Fourth and Fifth Assessment Reports (IPCC, 2007; 2013), with six likelihood categories (Box 1.1 and Fig. 1.1). The assignment of climate hazards to these categories is

^aLead authors.

Box 1.1. Definitions and terms

Climate change

Climate change refers to a significant change in the state of the climate that can be identified from changes in the average state or the variability of weather and that persists for an extended time period, typically decades to centuries or longer. Climate change can refer to the effects of (1) persistent anthropogenic or human-caused changes in the composition of the atmosphere and/or land use, or (2) natural processes such as volcanic eruptions and Earth's orbital variations (IPCC, 2013).

Global climate models (GCMs)

A GCM is a mathematical representation of the behavior of the Earth's climate system over time that can be used to estimate the sensitivity of the climate system to changes in atmospheric concentrations of greenhouse gases (GHGs) and aerosols. Each model simulates physical exchanges among the ocean, atmosphere, land, and ice. The NPCC2 uses 35 GCMs for temperature and precipitation projections.

Representative concentration pathways (RCPs)

RCPs are sets of trajectories of concentrations of GHGs, aerosols, and land use changes developed for climate models as a basis for long-term and near-term climate-modeling experiments (Figure 1.2; Moss *et al.*, 2010). RCPs describe different climate futures based on different amounts of climate forcings^b. These data are used as inputs to global climate models to project the effects of these drivers on future climate. The NPCC2 uses a set of global climate model simulations driven by two RCPs, known as 4.5 and 8.5, which had the maximum number of GCM simulations available from World Climate Research Programme/Program for Climate Model Diagnosis and Intercomparison (WCRP/PCMDI). RCP 4.5 and RCP 8.5 were selected to bound the range of anticipated GHG forcings at the global scale.

Climate change risk information

On the basis of the selection of the 2 RCPs and 35 GCM simulations, local climate change information is developed for key climate variables—temperature, precipitation, and associated extreme events. These results and projections reflect a range of potential outcomes for the New York metropolitan region (for a full description of projection methods, see Section 1.3).

Climate hazard

A climate hazard is a weather or climate state such as a heat wave, flood, high wind, heavy rain, ice, snow, and drought that can cause harm and damage to people, property, infrastructure, land, and ecosystems. Climate hazards can be expressed in quantified measures, such as flood height in feet, wind speed in miles per hour, and inches of rain, ice, or snowfall that are reached or exceeded in a given period of time.

Uncertainty

Uncertainty denotes a state of incomplete knowledge that results from lack of information, natural variability in the measured phenomenon, instrumental and modeling errors, and/or from disagreement about what is known or knowable (IPCC, 2013). See Box 1.3 for information on sources of uncertainty in climate projections.

based on observed data, global climate model simulations, published literature, and expert judgment.

^bA climate forcing is a mechanism that alters the global energy balance, causing the climate to change. Examples of climate forcings include variations in GHG concentrations and volcanic aerosols.

1.1 The global climate system

The global climate system is comprised of the atmosphere, biosphere, hydrosphere, cryosphere, and lithosphere. The components of the climate system interact over a wide range of spatial and temporal scales. The Earth's climate is largely driven by the energy it receives from the sun. This incoming solar

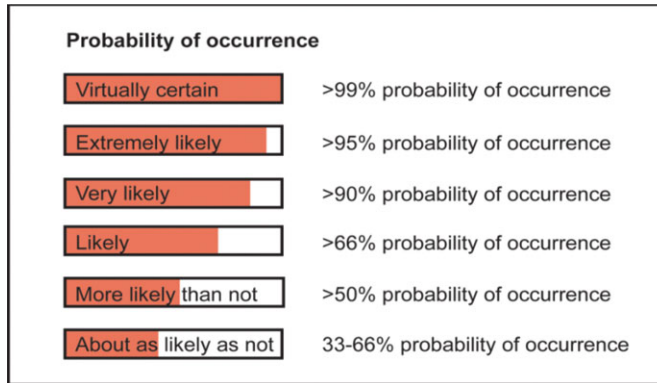


Figure 1.1. Probability categories used by NPCC2. Source: IPCC, 2007; 2013.

radiation (shortwave radiation) is partly absorbed, partly scattered, and partly reflected by gases in the atmosphere, by aerosols, by the Earth’s surface, and by clouds. The Earth reemits the energy it receives

from the sun in the form of longwave, or infrared, radiation.

Under equilibrium conditions, there is an energy balance between the outgoing terrestrial longwave

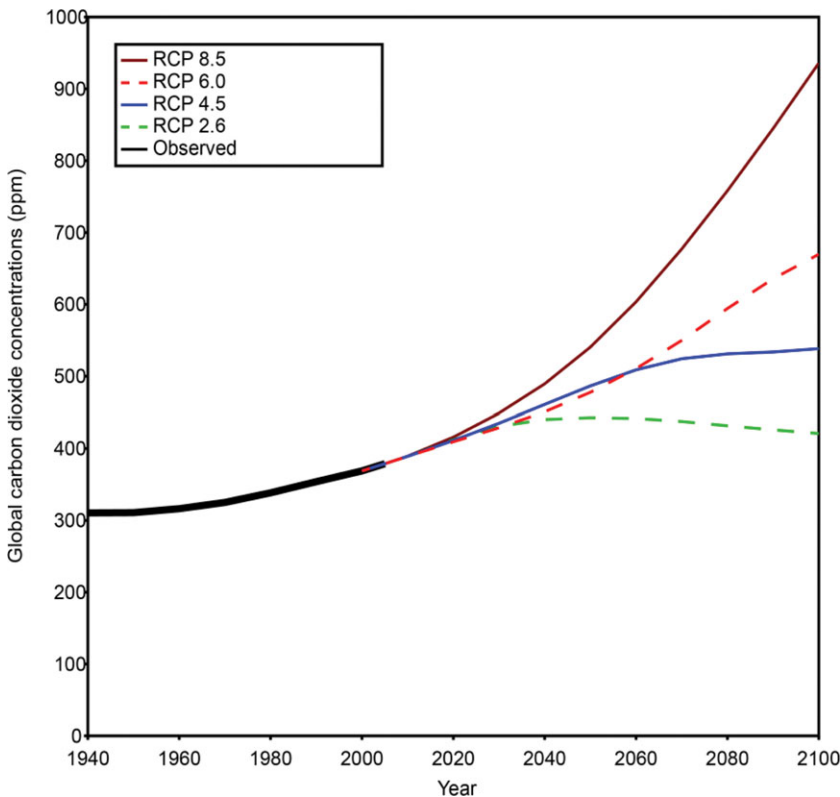


Figure 1.2. Observed CO₂ concentrations through 2005 and future CO₂ concentrations consistent with four representative concentration pathways (RCPs). NPCC2 climate projections are based on RCP 4.5 and RCP 8.5. Carbon dioxide and other GHG concentrations are driven by a range of factors, including carbon intensity of energy used, population and economic growth, and diffusion and adoption of new technologies including green energy and energy efficiency.

radiation and the incoming solar radiation. Without the presence of naturally occurring GHGs in the atmosphere, this balance would be achieved at temperatures of approximately -33°F (-18°C). An atmosphere containing GHGs is relatively opaque to terrestrial radiation. Such a planet achieves radiative balance at a higher surface temperature than it would without GHGs. On Earth, the increase in GHG concentrations due to human activities such as fossil fuel combustion, cement making, deforestation, and land use changes has led to a surface warming of almost 1.8°F (1°C) and a range of climate changes including upper ocean warming, and loss of land and sea ice. Key components of Earth's radiative balance are illustrated in Figure 1.3.

In the 2013 Fifth Assessment Report (IPCC AR5), the IPCC documented a range of observed climate trends. Global surface temperature has increased about 1.5°F (0.85°C) since 1880. Both hemispheres have experienced decreases in net snow and ice cover, and global sea level has risen by approximately 0.5 to 0.7 inches (1.3 to 1.7 cm) per decade over the past century (Hay *et al.*, 2015). More recently,

since the 1990s, the global sea level rise rate has accelerated to approximately 1.3 inches (3.2 cm) per decade (see Chapter 2, NPCC, 2015, for New York metropolitan region sea level rise observations and projections). Droughts (in regions such as but not limited to the Mediterranean and West Africa) have grown more frequent and longer in duration. In the United States, Canada, and Mexico (as well as other regions), intense precipitation events have become more common. Hot days and heat waves have become more frequent and intense, and cold events have decreased in frequency. The upper oceans have warmed and become more acidic (IPCC, 2013). As temperatures have warmed in the atmosphere and ocean, biological systems have responded as well; for example, spring has been arriving earlier, and fall has been extending later into the year, in many mid- and high-latitude regions (IPCC, 2014).

The IPCC AR5 states that there is a greater than 95% chance that warming temperatures since the mid-20th century are primarily due to human activities. Atmospheric concentrations of the major GHG carbon dioxide (CO_2) are now approximately

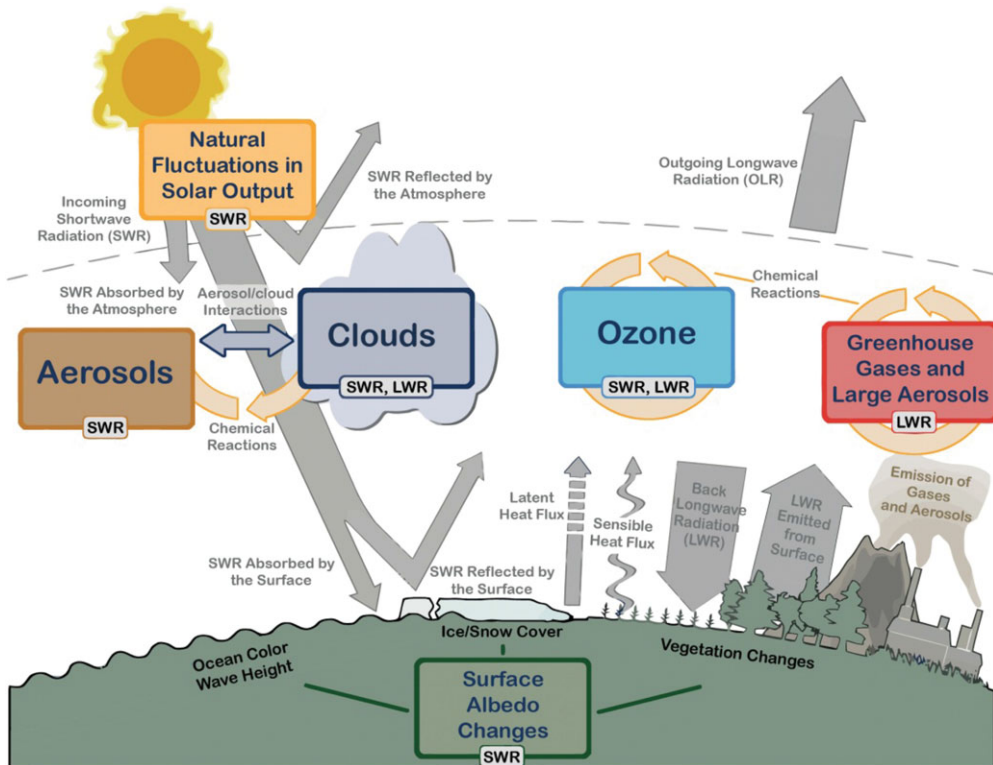


Figure 1.3. The main drivers of climate change. Source: IPCC, 2013.

40% higher than in preindustrial times. Concentrations of other important GHGs, including methane (CH₄) and nitrous oxide (N₂O), have increased by close to 150% and close to 20%, respectively, since preindustrial times. The warming that occurred globally over the 20th century cannot be reproduced by GCMs unless human contributions to historical GHG concentrations are taken into account (Fig. 1.4).

Further increases in GHG concentrations are extremely likely to lead to accelerated temperature increases. Depending on these future emissions and concentrations, by the 2081 to 2100 time period, global average temperatures are projected to increase by 2.0°F to 4.7°F (1.1°C to 2.6°C) or as high as 4.7°F to 8.6°F (2.6°C to 4.8°C)^c (IPCC, 2013). The large range is due to uncertainties both in future GHG concentrations and the sensitivity^d of the climate system to GHG concentrations. Warming is projected to be greatest in the high latitudes of the northern hemisphere. Throughout the globe, land areas are generally expected to warm more than ocean regions.

High-latitude precipitation is projected to increase in both hemispheres, while many dry regions at subtropical latitudes, such as the Mediterranean region, are projected to become drier.

Globally, it is virtually certain that the hottest temperatures will increase in frequency and magnitude, and the coldest temperatures will decrease in frequency and magnitude, although there could be regional exceptions (IPCC, 2012). Both land ice and sea ice volumes are projected to decrease. Ocean acidification is projected to increase as CO₂ concentrations rise.

1.2 Observed local climate

This section describes the critical climate hazards related to temperature and precipitation in the New York metropolitan region. For sea level and coastal storms, see Chapters 2 and 4 (NPCC, 2015). Both

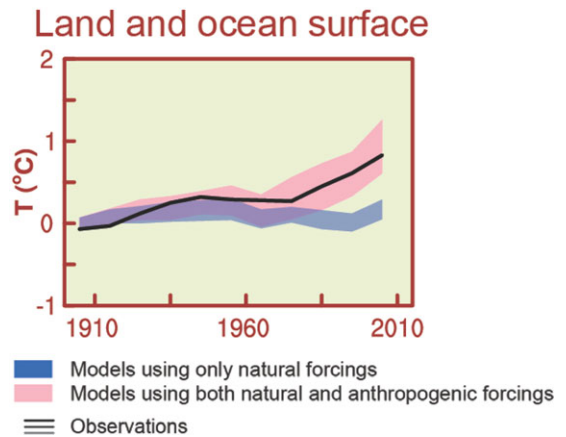


Figure 1.4. Twentieth-century observations and global climate model results. Source: IPCC, 2013.

mean (e.g., annual averages) and extreme (e.g., heavy downpours) quantities are presented. Observations for New York City are placed in a broader context because trends over large spatial scales (regional, national and global) are an important source of predictability with respect to New York City's future climate.

Temperature

Summers in New York City are warm, with cool winters. Annual mean air temperature in New York City (using data from the Central Park weather station) was approximately 54°F from 1971 to 2000. Mean annual temperature has increased at a rate of 0.3°F per decade over the 1900 to 2013 period in Central Park, although the trend has varied substantially over shorter periods (Fig. 1.5). For example, the first and last 30-year periods were characterized by warming (0.38°F per decade and 0.79°F per decade, respectively), whereas the middle segment experienced negligible cooling (−0.04°F per decade). This absence of warming in the middle of the 20th century is evident nationally and globally as well and has been linked to a combination of high sulphate aerosol emissions (a cooling factor) and natural variability.

The temperature trend since 1900 for the New York metropolitan region is broadly similar to the trend for the northeast United States (Fig. 1.6).^e Specifically, most of the Northeast has experienced

^cEstimates based on RCP 4.5 and RCP 8.5.

^dClimate sensitivity is defined by the IPCC (IPCC, 2007) as the equilibrium or final increase in global temperature associated with a doubling of CO₂ from preindustrial levels. More generally, sensitivity refers to how much climate change is associated with a given climate-forcing agent, such as CO₂.

^eThe Northeast as defined in the U.S. National Climate Assessment consists of Connecticut, Delaware, Maine,

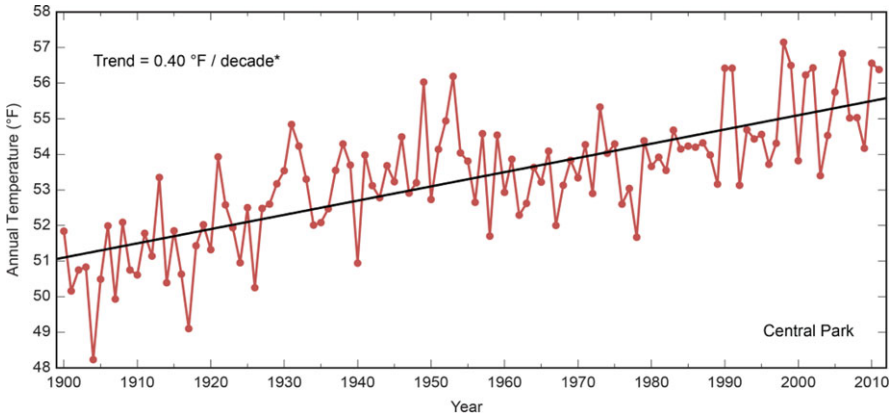


Figure 1.5. Observed annual temperature trend in New York City (Central Park) for 1900 to 2013. Data are from NOAA United States Historical Climatology Network (USHCN) Version 2.5 (Menne *et al.*, 2013). *Trend is significant at the 99% level.

a trend toward higher temperatures, especially in recent decades. This trend is present in both rural and urban weather stations, so it cannot be explained by the urban heat island effect.^f

Precipitation

New York City experiences significant precipitation throughout the year, with relatively little variation from month to month in the typical year. Annual average precipitation ranges between approximately 43 and 50 inches, depending on the location within the city. Precipitation has increased at a rate of approximately 0.8 inches per decade from 1900 to 2013 in Central Park (Fig. 1.7).

Year-to-year (and multiyear) variability of precipitation has also become more pronounced,

especially since the 1970s. The standard deviation, a measure of variability, increased from 6.1 inches from 1900 to 1956 to 10.3 inches from 1957 to 2013.

Precipitation in many parts of the larger Northeast region has also increased since the 1900s

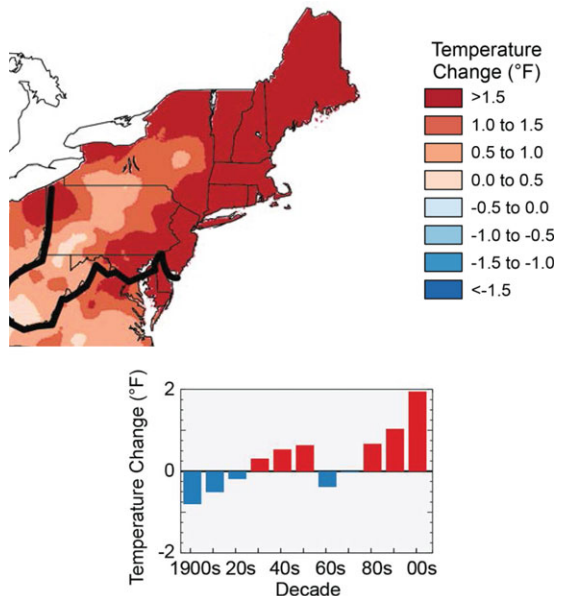


Figure 1.6. Observed temperature changes in the Northeast. The map shows temperature changes over the past 22 years (1991–2012) compared to the 1901–1960 average. The bars on the graph show the average temperature change by decade for 1901–2012 (relative to the 1901–1960 average). The far right bar (2000s decade) includes 2011 and 2012. Source: Melillo *et al.*, 2014; Horton *et al.*, 2014.

Maryland, Massachusetts, New Hampshire, New Jersey, New York, Pennsylvania, Rhode Island, Vermont, and West Virginia (NCA; Melillo *et al.*, 2014; Horton *et al.*, 2014).

^fUrbanization is often associated with elevated surface air temperature, a condition referred to as the urban heat island (UHI). Urban centers and cities are often several degrees warmer than their surrounding areas. Because of the low albedo (reflectivity) of urban surfaces (such as dark rooftops and asphalt roadways) and reduced evapotranspiration, cities “trap” heat (Blake *et al.*, 2011, and references therein). The future projections described in this chapter primarily reflect the influences of global processes. New York City’s long-term baseline surface temperature is higher than those of surrounding areas in part due to the urban heat island effect, but the UHI cannot explain New York City’s long-term warming trend.

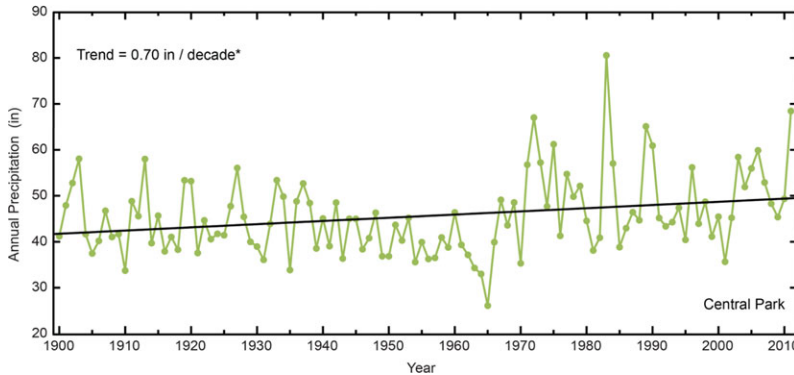


Figure 1.7. Observed annual precipitation trend in New York City (Central Park) for 1900 to 2013. Data are from NOAA United States Historical Climatology Network (USHCN) Version 2.5 (Menne *et al.*, 2013). *Trend is significant at the 99% level.

(Fig. 1.8). However, this long-term trend in the Northeast generally cannot be distinguished from natural variability.

Extreme events

Both temperature and precipitation extremes have significant impacts on New York City. When a single climate variable or combinations of variables approach the tails of their distribution, this

is referred to as an extreme event (see Fig. 1.9 for an example of how an extreme is defined). Extreme precipitation timescales are highly asymmetrical: heavy precipitation events generally range from less than an hour to a few days, whereas meteorological droughts can range from months to years. With its location in the midlatitudes, New York City frequently experiences heat waves in summer and periods of cold weather in winter.

Trends in extreme events at local scales such as the New York metropolitan region are often not statistically significant due to high natural variability and limited record length (Horton *et al.*, 2011). However, some changes in extreme events (such as daily maximum and minimum temperatures and

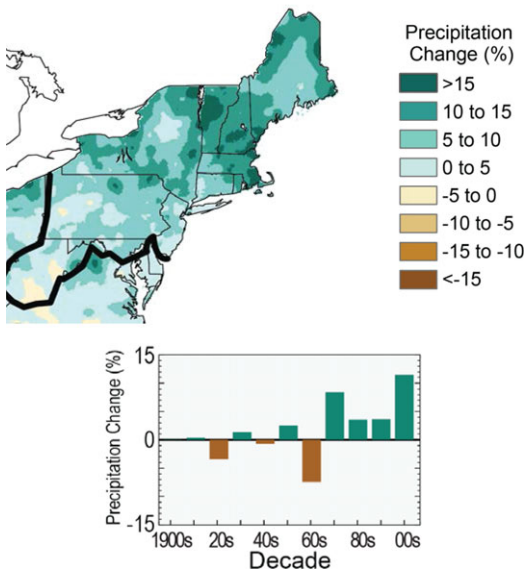


Figure 1.8. Observed precipitation changes in the Northeast. The map shows annual total precipitation changes (%) for 1991–2012 compared to the 1901–1960 average. The bars on the graphs show average precipitation changes (%) by decade for 1901–2012 (relative to the 1901–1960 average). The far right bar is for 2001–2012. Source: Melillo *et al.*, 2014; Horton *et al.*, 2014.

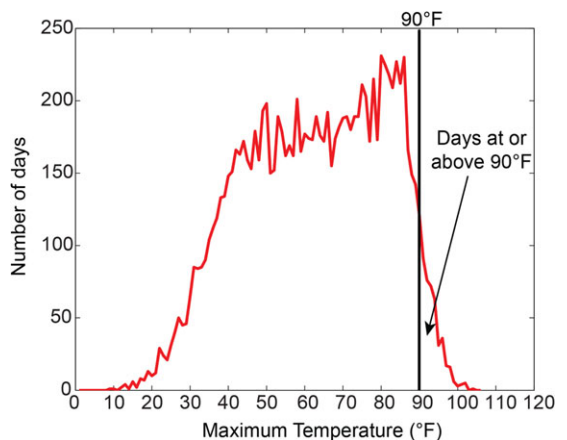


Figure 1.9. Distribution of observed cumulative daily maximum temperatures in Central Park from 1971 to 2000 with an extreme event threshold of days with maximum temperature at or above 90°F. Source: NCDC

extreme precipitation) at large spatial scales can be attributed to human influences on global climate (IPCC, 2012). The IPCC Special Report on Managing the Risks of Extreme Events and Disasters to Advance Climate Change Adaptation (SREX) report concluded that it is very likely that there have been an overall decrease in the number of cold days and cold nights and an overall increase in the number of warm days and warm nights globally for most land areas with sufficient data, including North America, Europe, and Asia. The SREX also found that there have been statistically significant trends in the number of heavy precipitation events in some regions around the world (e.g., Canada and Mexico).

Hurricane Sandy has focused attention on the significant effects that extreme climate events have on New York City (see Chapter 2, Box 2.1). Other recent events in the United States, such as the widespread drought of 2012 or the “polar vortex” winter of 2013/2014 (see Box 1.2), also raised awareness of the impacts of weather and climate extremes. Although it is not possible to attribute any one extreme event such as Hurricane Sandy to climate change, sea level rise already occurring in the New York metropolitan region, in part due to climate change, increased the extent and magnitude of coastal flooding during the storm (see also Chapter 2, NPCC, 2015). This is an example of how long-term trends in climate variables can modify the risk of extremes.

Extreme temperature. Extreme temperature events can be defined in several ways using daily data from New York City (Central Park weather station) since 1900.^g Here, we use the following metrics:

- Individual days with maximum temperatures at or above 90°F
- Individual days with maximum temperatures at or above 100°F
- Heat waves, defined as three consecutive days with maximum temperatures at or above 90°F
- Individual days with minimum temperatures at or below 32°F

^gTemperatures from the meteorological station in Central Park tend to be lower than those in some other parts of New York City. This is due to the close proximity of the weather station to extensive vegetation.

From 1971 to 2000, New York City averaged 18 days per year with maximum temperatures at or above 90°F, 0.4 days^h per year at or above 100°F, and two heat waves per year.

The number of extreme events in a given year is highly variable. For example, New York City recently recorded three consecutive years (2010–2012) with at least one day with maximum temperatures at or above 100°F. Prior to 2010, the last day at or above 100°F was in 2001, and there has only been one other time on record (1952–1955) where New York City experienced more than two years in a row with maximum temperatures at or above 100°F.

From 1971 to 2000, Central Park averaged 71 days per year with minimum temperatures at or below 32°F. As is the case for hot days, the number of cold days in a given year also varies from one year to the next. In the cool season of 2013/2014, there were 92 days at or below 32°F, whereas in 2011/2012, there were only 37 days. The former is the greatest number of cool season days at or below 32°F since 1976/1977.

Extreme precipitation. Extreme precipitation events are defined here as the number of occurrences per year of precipitation at or above 1, 2, and 4 inches per day for New York City (at the weather station in Central Park) since 1900. Between 1971 and 2000, New York City averaged 13 days per year with 1 inch or more of rain, 3 days per year with 2 inches or more of rain, and 0.3 days per year with 4 inches or more of rain. As with extreme temperatures, year-to-year variations in extreme precipitation events are large.

There has been a small but not statistically significant trend toward more extreme precipitation events in New York City since 1900. For example, the four years with the greatest number of events with 2 inches or more of rain have all occurred since 1980 (1983, 1989, 2007, and 2011). Because extreme precipitation events tend to occur relatively infrequently, long time-series of measurements over large areas are needed to identify trends; there is a relatively large burden of proof required to distinguish a significant trend from random variability. Over the larger Northeast region, intense precipitation events (defined as the heaviest 1% of all daily

^hFor extreme events, decimal places are shown for values less than 1, although this does not indicate higher precision/certainty.

events) have increased by approximately 70% over the period from 1958 to 2011 (Horton *et al.*, 2014).

1.3 Climate projections

This section presents New York City–specific climate projections for the 21st century along with the methods used to develop the projections. Quantitative global climate model–based projections are provided for means and extremes of temperature and precipitation. This section also describes the potential for changes in other variables (e.g., heat indices and heavy downpours) qualitatively because quantitative projections are either unavailable or considered less reliable. See Appendices I and IIA (NPCC, 2015) for infographics of the projections and further details.

Uncertainty and risk management

Scientific understanding of climate change and its impacts has increased dramatically in recent years. Nevertheless, there remain substantial uncertainties that are amplified at smaller geographical scales (Box 1.3) (IPCC, 2007; 2012).

The NPCC2 seeks to present climate uncertainties clearly in order to facilitate risk-based decision-making for the use of policy tools such as incentives, regulations, and insurance. The goal is to make New York City and the surrounding metropolitan region more resilient to mean changes in climate and to future extreme events (e.g., Lempert *et al.*, 1996; Kunreuther *et al.*, 2013).

Methods

The NPCC2 generates a range of climate model-based outcomes for temperature and precipitation from GCM simulations based on two representative concentration pathways (Moss *et al.*, 2010). The RCPs represent a range of possible future global concentrations of GHGs, other radiatively important agents such as aerosols, and land use changes over the 21st century. Simulation results from 35 GCMs are used to produce temperature and precipitation projections for the New York metropolitan region.

For some variables, climate models do not provide results, the model results are too uncertain, or there is not a long-enough history of observations to justify quantitative model-based projections. For these variables, a qualitative projection of the likely direction of change is provided on the basis of expert judgment. Both the quantitative and qualitative

approaches parallel methods used in the IPCC AR5 report (IPCC, 2013).

Global climate models. GCMs are mathematical representations of the behavior of the Earth’s climate system over time that can be used to estimate the sensitivity of the climate system to changes in atmospheric concentrations of GHGs and aerosols. Each model simulates physical exchanges among the ocean, atmosphere, land, and ice. Over the past several decades, climate models have increased in both complexity and computational power as physical understanding of the climate system has grown.

The GCM simulations used by the NPCC2 are from the Coupled Model Intercomparison Project Phase 5 (CMIP5; Taylor *et al.*, 2011) and were developed for the IPCC AR5. Compared to the previous climate model simulations from CMIP3 used in the first NPCC (NPCC, 2010), the CMIP5 models generally have higher spatial resolution and include more diverse model types (Knutti and Sedlacek, 2013).

The CMIP5 global climate models include some Earth system models that allow interactions among chemistry, aerosols, vegetation, ice sheets, and biogeochemical cycles (Taylor *et al.*, 2011). For example, warming temperatures in an Earth system model lead to changes in vegetation type and the carbon cycle, which can then “feed back” on temperature, either amplifying (a positive feedback) or damping (a negative feedback) the initial warming. There have also been a number of improvements in model-represented physics and numerical algorithms. Some CMIP5 models include better treatments of rainfall and cloud formation that can occur at small “subgrid” spatial scales. These and other improvements have led to better simulation of many climate features, such as Arctic sea ice extent (Stroeve *et al.*, 2012).

Local projections. Local projections are based on GCM output from the single land-based model grid boxⁱ covering the New York metropolitan region.

ⁱ GCMs divide the Earth into a series of grid boxes, which represent the finest spatial resolution of the climate model. In each grid box, physical equations (e.g., of motion and moisture conservation) are solved to determine the evolution of the climate in space and time.

Box 1.2. The polar vortex and climate change

The winter of 2013/2014 serves as a timely reminder that unusually cold conditions can still be expected to occur from time to time as the climate warms, especially at regional and local scales. Cold conditions extended throughout the Eastern United States, where the Great Lakes reached their second highest ice cover amount in the 41-year satellite record. However, averaged over the continental United States, cold conditions in the East were largely canceled out by warm conditions in the Western United States, where a few states experienced their warmest winter on record. Globally, 2013 tied for the fourth warmest year on record (NOAA, 2013). The planet has not experienced a month with below-normal temperatures since February 1985.

The fact that global temperatures continue to climb as GHG concentrations continue to rise does not rule out the possibility that individual regions could cool or that weather could become more extreme in either direction. An emerging body of observational and modeling studies (e.g., Liu *et al.*, 2012) is investigating whether rapid reduction in Arctic sea ice could be producing a wavier jet stream characterized by more, and more persistent, weather extremes. This is an active research topic [counterarguments have been made by Screen and Simmonds (2013) and Wallace *et al.* (2014), for example]. However, the potential consequences are large, given the expected continued retreat of Arctic sea ice (Liu *et al.*, 2013) and the high societal vulnerability to climate extremes.

The precise coordinates of the grid box vary from GCM to GCM because GCMs differ in spatial resolution (i.e., the unit area over which calculations are made). These spatial resolutions range from as fine as ~50 miles by ~40 miles (80 by 65 km) to as coarse as ~195 miles by ~195 miles (315 by 315 km), with an average resolution of approximately 125 miles by 115 miles (200 by 185 km). The changes reported by the NPCC2 in temperature and precipitation through time (e.g., 3 degrees of warming by a given future time period) are specific to the New York metropolitan region.

The spatial area of applicability of the NPCC2 projections is larger for mean changes in temperature and precipitation than for the number of days exceeding extreme event thresholds. The mean changes in temperature and precipitation generally apply across at least a 100-mile land radius. For example, the precise quantitative mean temperature and precipitation change projections for Philadelphia (approximately 78 miles from Manhattan) and New Haven (approximately 70 miles from Manhattan) differ only slightly from those for New York City (i.e., $\pm 4\%$).^j These small differences are well within the bounds

of the climate uncertainty in any long-term projections.

Similarly, the qualitative projections for changes in extreme events (such as heat indices and extreme winds) are expected to be generally applicable across an approximately 100-mile radius. However, the quantitative projections of changes in the frequency of extreme event thresholds (e.g., days over 90°F) can be highly variable spatially, even within the confines of a city itself. For example, there is large spatial variation in the number of days over 90°F across the region as a result of factors such as the urban heat island and the distance from the Atlantic Ocean. The percentage change in the number of days over 90°F is variable as well (Meir *et al.*, 2013).

Although the NPCC2 projections for total sea level change are applicable for the New York metropolitan region (see Chapter 2, NPCC, 2015), projected changes in flood extent will vary substantially within the 100-mile radius, and within the city itself, as shown in the NPCC2 coastal flood maps (Chapter 3, NPCC, 2015). This is primarily because coastal topography differs throughout the region;

^j Spatial variation in mean temperature and precipitation projections across these three cities is based on the com-

parison of the 35-GCM ensemble for RCP 8.5. The climate projections described here illustrate changes for the 2050s relative to the 1980s base period.

for example, the relatively flat south shores of Brooklyn and Queens are in contrast to the steep shorelines where northern Manhattan and the Bronx meet the Hudson River.

Time slices. Although it is not possible to predict future temperature or precipitation for a particular day, month, or year, GCMs are valuable tools for projecting the likely range of changes over multi-decadal time periods. The NPCC2 projections use time slices of 30-year intervals, expressed relative to the baseline period 1971 to 2000, for temperature and precipitation. The NPCC uses three time slices (the 2020s, 2050s, and 2080s) centered around a given decade. For example, the 2050s time slice refers to the period from 2040 to 2069.^k

The NPCC2 has also provided climate projections for 2100. Projections for 2100 require a different methodological approach from the 30-year time slices discussed above. The primary difference is that because the majority of climate model simulations end in 2100, it is not possible to make a projection for the 30-year time slice centered on the year 2100. Projections for 2100 are an average of two methods that involve adding a linear trend to the final time slice (2080s) and extrapolating that trend to 2100 (see Appendix IIA).

Uncertainties grow over the timeframe of the NPCC projections toward the end of the century (Box 1.3). For example, the RCPs do not sample all the possible carbon and other biogeochemical cycle feedbacks associated with climate change. The few Earth system models in CMIP5 used by the NPCC2 could possibly underestimate the potential for increased methane and carbon release from the thawing Arctic permafrost under extreme warming scenarios. More generally, the potential for surprises, such as technological innovations that could remove carbon from the atmosphere, increases the further into the future one considers.

Model-based probability. The combination of 35 GCMs and two RCPs produces a 70 (35 × 2)-member matrix of outputs for temperature and precipitation. For each time period, the results con-

stitute a climate model-based range of outcomes, which can be used in risk-based decision-making. Equal weights were assigned to each GCM and to each of the two selected RCPs.

The results for future time periods are compared to the climate model results for the baseline period (1971 to 2000). Mean temperature change projections are calculated via the delta method, a type of bias-correction^l whereby the difference between each model's future and baseline simulation is used, rather than "raw" model outputs. The delta method is a long-established technique for developing local climate-change projections (Gleick, 1986; Arnell, 1996; Wilby *et al.*, 2004; Horton *et al.*, 2011). Mean precipitation change is similarly based on the ratio of a given model's future precipitation to that of its baseline precipitation (expressed as a percentage change^m).

Methods for projecting changes in extreme events. The greatest impacts of extreme temperature and precipitation (with the exception of drought) occur on daily rather than monthly timescales. Because monthly output from climate models is considered more reliable than daily output (Grotch and MacCracken, 1991), the NPCC2 uses a hybrid projection technique for extreme events.

Modeled changes in monthly temperature and precipitation are based on the same methods described for the annual data. Monthly changes through time in each of the GCM-RCP combinations are then applied (added in the case of degrees of temperature change and multiplied in the case of percentage change in precipitation) to the observed daily 1971 to 2000 temperature and precipitation data from Central Park to generate 70 time-series of daily data. This simplified approach to projections of extreme events does not account for possible changes in

^kThirty-year time slices are required to minimize the effects of natural variability, which is largely unpredictable. For sea level rise (see Chapter 2), 10-year time slices are sufficient due to smaller natural variability.

^lBias correction is a standard practice when climate model outputs are used because long-term changes through time are considered more reliable than actual values, especially when an area like the New York metropolitan region, that is smaller than the size of a climate model grid box, is assessed.

^mThe ratio approach is used for precipitation because it minimizes the impact of climate model biases in average baseline precipitation, which can be large for some models at monthly scales.

Box 1.3. Sources of uncertainty in climate projections

Sources of uncertainty in climate projections include:

Future concentrations of GHGs, aerosols, black carbon, and land use change. Future GHG concentrations will depend on population and economic growth, technology, and biogeochemical feedbacks (e.g., methane release from permafrost in a warming Arctic). Multiple emissions scenarios and/or RCPs are used to explore possible futures.

Sensitivity of the climate system to changes in GHGs and other “forcing” agents. Climate models are used to explore how much warming and other changes may occur for a given change in radiatively important agents. The direct temperature effects of increasing CO₂ are well understood, but models differ in their feedbacks (such as changes in clouds, water vapor, and ice with warming) that determine just how much warming ultimately will occur. A set of climate models is used to sample the range of such outcomes.

Regional and local changes that may differ from global and continental averages. Climate model results can be statistically or dynamically downscaled (e.g., using regional models embedded within global models), but some processes may not be captured by existing downscaling techniques. Examples include changes in land–sea breezes and the urban heat island effect on a warming planet.

Natural variability that is largely unpredictable, especially in midlatitude areas such as the New York metropolitan region. As a result, even as increasing GHG concentrations gradually shift weather and climate, random elements will remain important, especially for extreme events and over short time periods (e.g., a cold month). Chaos theory has demonstrated that natural variability can be driven by small initial variations that amplify thereafter. Other sources of natural variability include the El Niño Southern Oscillation and solar cycles. Averaging short-term weather over long periods of time (e.g., 30 years) can average out much of the natural variability, but it does not eliminate it entirely.

Observations include uncertainties as well. Sources of observational uncertainty include poor siting of weather stations, instrument errors, and errors involved in the processing of data using models.

submonthly variability over time, which are not well understood.

Projections for the New York metropolitan region

This section presents climate projections for the 2020s, 2050s, 2080s, and 2100 for temperature, precipitation, and extreme events.

Mean annual changes. Higher temperatures are extremely likely for the New York metropolitan region in the coming decades. All simulations project continued increases through the end of this century. Most GCM simulations indicate small increases in precipitation, but some do not. Natural precipitation variability is large; thus, precipitation projections are less certain than temperature projections.

Future temperature. The projected future temperature changes shown in Table 1.1 and Figure 1.10 indicate that by the 2080s, New York City’s mean

temperatures throughout a “typical” year may bear similarities to those of a city like Norfolk, Virginia, today. The middle range of projections show temperatures increasing by 2.0°F to 2.8°F by the 2020s, 4.0°F to 5.7°F by the 2050s, and 5.3°F to 8.8°F by the 2080s. By 2100, temperatures may increase by 5.8°F to 10.3°F. Temperature increases are projected to be comparable for all months of the year.

The two RCPs project similar temperature changes up to the 2020s; after the 2020s, temperature changes produced by RCP 8.5 are higher than those produced by RCP 4.5. It takes several decades for the different RCPs to produce large differences in climate due to the long lifetime of GHGs in the atmosphere and the inertia or delayed response of the climate system and the oceans especially.

Future precipitation. Table 1.1 indicates that regional precipitation is projected in the middle range to increase by approximately 1–8% by the

Table 1.1. Mean annual changes

a. Temperature			
Baseline (1971–2000) 54°F	Low estimate (10th percentile)	Middle range (25th to 75th percentile)	High estimate (90th percentile)
2020s	+1.5°F	+2.0–2.9°F	+3.2°F
2050s	+3.1°F	+4.1–5.7°F	+6.6°F
2080s	+3.8°F	+5.3–8.8°F	+10.3°F
2100	+4.2°F	+5.8–10.4°F	+12.1°F
b. Precipitation			
Baseline (1971–2000) 50.1 in	Low estimate (10th percentile)	Middle range (25th to 75th percentile)	High estimate (90th percentile)
2020s	–1 percent	+1–8%	+10%
2050s	+1 percent	+4–11%	+13%
2080s	+2 percent	+5–13%	+19%
2100	–6 percent	–1% to +19%	+25%

NOTE: Based on 35 GCMs and two RCPs. Baseline data cover the 1971–2000 base period and are from the NOAA National Climatic Data Center (NCDC). Shown are the low estimate (10th percentile), middle range (25th percentile to 75th percentile), and high estimate (90th percentile). These estimates are based on a ranking (from most to least) of the 70 (35 GCMs times 2 RCPs) projections. The 90th percentile is defined as the value that 90 percent of the outcomes (or 63 of the 70 values) are the same or lower than. Like all projections, the NPCC climate projections have uncertainty embedded within them. Sources of uncertainty include data and modeling constraints, the random nature of some parts of the climate system, and limited understanding of some physical processes. The NPCC characterizes levels of uncertainty using state-of-the-art climate models, multiple scenarios of future greenhouse gas concentrations, and recent peer-reviewed literature. Even so, the projections are not true probabilities and the potential for error should be acknowledged.

2020s, 4–11% by the 2050s, and 5–13% by the 2080s. By 2100, projected changes in precipitation range from –1 to +19%. In general, the projected changes in precipitation associated with increasing GHGs in the global climate models are small relative to year-to-year variability. Figure 1.11 shows that precipitation is characterized by large historical variability, even with 10-year smoothing. One example is the New York metropolitan region’s multi-year drought of record in the 1960s.

Precipitation increases are expected to be largest during the winter months. Projections of precipitation changes in summer are inconclusive, with approximately half the models projecting precipitation increases and half projecting decreases (see Appendix IIA for seasonal projections).

Future extreme events. Despite their brief duration, extreme events can have large impacts on New York City’s infrastructure, natural systems, and population. This section describes how the frequencies of heat waves, cold events, and intense precipitation in the New York metropolitan

region are projected to change in the coming decades. The extreme event projections shown in Table 1.2 are based on observed data for Central Park.

Future heat waves and cold events. The total number of hot days, defined as days with a maximum temperature at or above 90°F or 100°F, is expected to increase as the 21st century progresses (Table 1.2). By the 2020s, the frequency of days at or above 90°F may increase by more than 50% relative to the 1971 to 2000 base period; by the 2050s, the frequency may more than double; by the 2080s, the frequency may more than triple. Although 100°F days are expected to remain relatively rare, the percentage increase in their frequency of occurrence is projected to exceed the percentage change in days at or above 90°F.

The frequency and duration of heat waves, defined as three or more consecutive days with maximum temperatures at or above 90°F, are very likely to increase. In contrast, the frequency of extreme cold events, defined as the number of days per year with minimum temperatures at or below 32°F, is projected to decrease approximately 25% by the

Table 1.2. Extreme events

a. 2020s	Baseline (1971–2000)	Low estimate (10th percentile)	Middle range (25th to 75th percentile)	High estimate (90th percentile)
Numbers of heat waves per year	2	3	3–4	4
Average heat wave duration (days)	4	5	5	5
Number of days per year with				
Maximum temperature at or above 90°F	18	24	26–31	33
Maximum temperature at or above 100°F	0.4	0.7	1–2	2
Minimum temperature at or below 32°F	71	50	52–58	60
Rainfall at or above 1 inch	13	13	14–15	16
Rainfall at or above 2 inches	3	3	3–4	5
Rainfall at or above 4 inches	0.3	0.2	0.3–0.4	0.5
b. 2050s	Baseline	Low estimate (10th percentile)	Middle range (25th to 75th percentile)	High estimate (90th percentile)
Numbers of heat waves per year	2	4	5–7	7
Average heat wave duration (days)	4	5	5–6	6
Number of days per year with				
Maximum temperature at or above 90°F	18	32	39–52	57
Maximum temperature at or above 100°F	0.4	2	3–5	7
Minimum temperature at or below 32°F	71	37	42–48	52
Rainfall at or above 1 inch	13	13	14–16	17
Rainfall at or above 2 inches	3	3	4–4	5
Rainfall at or above 4 inches	0.3	0.3	0.3–0.4	0.5
c. 2080s	Baseline	Low estimate (10th percentile)	Middle range (25th to 75th percentile)	High estimate (90th percentile)
Numbers of heat waves per year	2	5	6–9	9
Average heat wave duration (days)	4	5	5–7	8
Number of days per year with				
Maximum temperature at or above 90°F	18	38	44–76	87
Maximum temperature at or above 100°F	0.4	2	4–14	20
Minimum temperature at or below 32°F	71	25	30–42	49
Rainfall at or above 1 inch	13	14	15–17	18
Rainfall at or above 2 inches	3	3	4–5	5
Rainfall at or above 4 inches	0.3	0.2	0.3–0.5	0.7

NOTE: Projections for temperature and precipitation are based on 35 GCMs and 2 RCPs. Baseline data are for the 1971 to 2000 base period and are from the NOAA National Climatic Data Center (NCDC). Shown are the low estimate (10th percentile), middle range (25th to 75th percentile), and high estimate (90th percentile) 30-year mean values from model-based outcomes. Decimal places are shown for values less than one, although this does not indicate higher precision/certainty. Heat waves are defined as three or more consecutive days with maximum temperatures at or above 90°F. Like all projections, the NPCC climate projections have uncertainty embedded within them. Sources of uncertainty include data and modeling constraints, the random nature of some parts of the climate system, and limited understanding of some physical processes. The NPCC characterizes levels of uncertainty using state-of-the-art climate models, multiple scenarios of future greenhouse gas concentrations, and recent peer-reviewed literature. Even so, the projections are not true probabilities and the potential for error should be acknowledged.

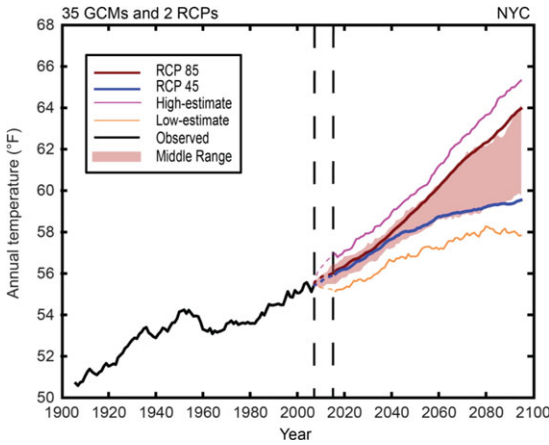


Figure 1.10. Combined observed (black line) and projected temperature (colored lines). Projected model changes through time are applied to the observed historical data. The two thick lines (blue and red) show the average for each representative concentration pathway across the 35 GCMs. Shading shows the middle range. The bottom and top lines respectively show each year’s low-estimate and high-estimate projections across the suite of simulations. A smoothing procedure/10-year filter has been applied to the observed data and model output to remove unpredictable short-term natural variability and highlight longer-term signals associated with climate and climate change. The dotted area between 2007 and 2015 represents the time period that is not covered due to the smoothing procedure.

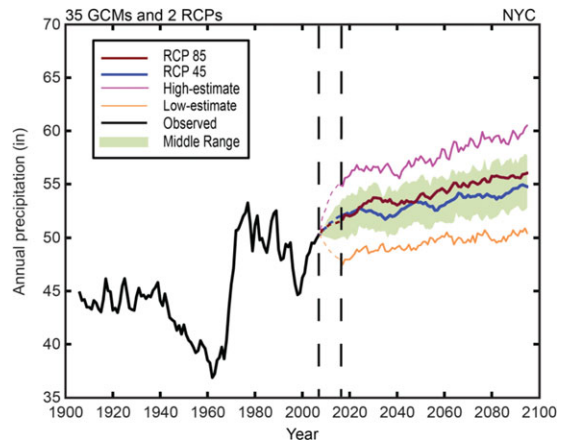


Figure 1.11. Combined observed (black line) and projected precipitation (colored lines). Projected model changes through time are applied to the observed historical data. The two thick lines (blue and red) show the average for each representative concentration pathway across the 35 GCMs. Shading shows the middle range. The bottom and top lines respectively show each year’s low-estimate and high-estimate projections across the suite of simulations. A smoothing procedure/10-year filter has been applied to the observed data and model output to remove unpredictable short-term natural variability and highlight longer-term signals associated with climate and climate change. The dotted area between 2007 and 2015 represents the time period that is not covered due to the smoothing procedure.

2020s, more than 33% by the 2050s, and approximately 50% by the 2080s.

Future extreme precipitation. Although the percentage increase in annual precipitation is expected to be relatively small, larger percentage increases are expected in the frequency, intensity, and duration of extreme precipitation (defined in this report as at least 1, 2, or 4 inches) at daily timescales (Table 1.2). Because some parts of New York City, including parts of coastal Brooklyn and Queens, currently experience significantly fewer extreme precipitation days than does Central Park, they may experience fewer extreme precipitation days than those shown in the table for Central Park in the future as well.

Qualitative extreme events. For some of the extreme climate events, future changes are too uncertain at local scales to allow quantitative projections. For example, the relationships between short duration extreme precipitation events and different types of storms, and between droughts and temperature/precipitation, are complex. For these, the NPCC makes qualitative projections based on scientific literature and expert judgment (Table 1.3).

By the end of the century, heat indices⁷ are very likely to increase, both directly due to higher temperatures and because warmer air can hold more moisture. The combination of high temperatures and high humidity can produce severe additive effects by restricting the human body’s ability to cool itself and thereby induce heat stress (see Chapter 5, NPCC, 2015).

Downpours, defined as intense precipitation at subdaily, and often subhourly, timescales, are very likely to increase in frequency and intensity. Changes in lightning are currently too uncertain to support even qualitative statements.

By the end of the century, it is more likely than not that late-summer short-duration droughts will increase in the New York metropolitan region (Rosenzweig *et al.*, 2011). It is unknown how multiyear drought risk in the New York metropolitan region may change in the future.

⁷The heat index (HI) or “apparent temperature” is an approximation of how hot it “feels” for a given combination of air temperature and relative humidity (American Meteorological Society, 2013).

Table 1.3. Qualitative changes in extreme events

	Spatial scale of projection	Direction of change by the 2080s	Likelihood	Sources
Heat index	New York metropolitan region	Increase	Very likely	NPCC, 2010; IPCC, 2012; Fischer and Knutti, 2012
Short-duration drought	New York metropolitan region	Increase	More likely than not	Rosenzweig <i>et al.</i> , 2011
Multi-year drought	New York metropolitan region	Unknown	—	Dai, 2013
Seasonal snowfall	New York metropolitan region	Decrease	Likely	IPCC, 2007; 2012; Liu <i>et al.</i> , 2012
Ice storms/freezing rain	New York metropolitan region	Unknown	—	NPCC, 2010; Rosenzweig <i>et al.</i> , 2011
Downpours	New York metropolitan region	Increase	Very likely	IPCC, 2012; Melillo <i>et al.</i> , 2014
Lightning	New York metropolitan region	Unknown	—	Melillo <i>et al.</i> , 2014; Price and Rind, 1994

As the century progresses, snowfall is likely to become less frequent, with the snow season decreasing in length (IPCC, 2007). Possible changes in the intensity of snowfall per storm are highly uncertain. It is unknown how the frequency and intensity of ice storms and freezing rain may change.

1.4 Conclusions and recommendations

Projections for the New York metropolitan region from the current generation of global climate models indicate large climate changes and thus the potential for large impacts. In the coming decades, the NPCC projects that climate change is extremely likely to bring warmer temperatures to New York City and the surrounding region. Heat waves are very likely to increase. Total annual precipitation is likely to increase, and brief, intense rainstorms are very likely to increase. It is more likely than not that short-duration, end-of-summer droughts will become more severe. Although there remain significant uncertainties regarding long-term climate change, these projections would move the city's climate outside what has been experienced historically.

This chapter offers critical information that can be used to support resiliency, but a central message is that the high-end scenarios of extreme warming may challenge even a great city like New York's adaptive capacity. The best steps to avoid extreme warming are to ramp up the reductions in GHG emissions already undertaken in New York City (City of New York, 2014). Although GHG emissions are a global issue, New York City's leadership on emissions reduction in the United States and internationally is crucially important.

Although the NPCC has a growing understanding of how the city as a whole may be affected by climate change, more research is needed on neighborhood-by-neighborhood impacts. Neighborhood- and building-level indicators and monitoring (see Chapter 6, NPCC, 2015) of temperature, precipitation, air quality, and other variables will be critical in the era of "big data." High-resolution regional climate modeling will also illuminate how projected changes vary throughout the city due to factors including coastal breezes, topography, and different urban land surfaces.

The NPCC risk-based approach emphasizes a range of possible outcomes and lends itself to updated projections as new information and climate model results become available. Such updates are essential as the science of climate change advances.

References

- American Meteorological Society, 2013.
- Arnell, N.W. 1996. *Global Warming, River Flows, and Water Resources*. New York: Wiley.
- Blake, R., A. Grimm, T. Ichinose, R. Horton, S. Gaffin, S. Jiong, D. Bader and D.W. Cecil. 2011. Urban climate: Processes, trends, and projections. *Climate Change and Cities: First Assessment Report of the Urban Climate Change Research Network*, C. Rosenzweig, W.D. Solecki, S.A. Hammer, and S. Mehrotra, Eds., Cambridge University Press, 43–81.
- City of New York. 2014. *One City: Built to Last*. New York, NY: Mayor's Office of Long Term Planning and Sustainability. 114 pp.
- Colle, B.A., Z. Zhang, K.A. Lombardo, *et al.* 2013. Historical evaluation and future prediction of eastern North American and western Atlantic extratropical cyclones in the CMIP5 models during the cool season. *J. Climate* **26**: 6882–6903.
- Dai, A. 2013. Increasing drought under global warming in observations and models. *Nature Clim. Change* **3**: 52–58.
- Fischer, E.M. and R. Knutti. 2013. Robust projections of combined humidity and temperature extremes. *Nature Clim. Change* **3**: 126–130.
- Gleick, P.H. 1986. Methods for evaluating the regional hydrologic effects of global climate changes. *J. Hydrology* **88**: 97–116.
- Gordon, K. 2014. *Risky Business: The Economic Risks of Climate Change in the United States*.
- Grotch, S.L. and M.C. MacCracken. 1991. The use of general circulation models to predict regional climatic change. *J. Climate* **4**: 286–303.
- Hay, Carling C., E. Morrow, R.E. Kopp, and J.X. Mitrovica. 2015. Probabilistic reanalysis of twentieth-century sea-level rise. *Nature* **517**: 481–484.
- Horton, R., *et al.* 2014. Chapter 16: Northeast. In *Climate Change Impacts in the United States: The Third National Climate Assessment*. J. M. Melillo, T. C. Richmond & G. W. Yohe, Eds., U.S. Global Change Research Program. 371–395.
- Horton, R.M., V. Gornitz, D.A. Bader, *et al.* 2011. Climate hazard assessment for stakeholder adaptation planning in New York City. *J. Appl. Meteorol. Climatol.* **50**: 2247–2266.
- IPCC. 2007. *Climate Change 2007: The Physical Science Basis. Contribution of Working Group I to the Fourth Assessment Report of the Intergovernmental Panel on Climate Change*. Cambridge: Cambridge University Press.
- IPCC. 2012. *Managing the Risks of Extreme Events and Disasters to Advance Climate Change Adaptation*. Cambridge: Cambridge University Press.
- IPCC. 2013. *Climate Change 2013: The Physical Science Basis. Contribution of Working Group I to the Fifth Assessment Report of the Intergovernmental Panel on Climate Change*. Cambridge: Cambridge University Press.
- IPCC. 2014. *Climate Change 2014: Impacts, Adaptation, and Vulnerability. Part A: Global and Sectoral Aspects. Contribution of Working Group II to the Fifth Assessment Report of the Intergovernmental Panel on Climate Change*. Cambridge: Cambridge University Press.
- Knutti, R. and J. Sedlacek. 2013. Robustness and uncertainties in the new CMIP5 climate model projections. *Nature Clim. Change* **3**: 369–373.
- Kunreuther, H., G. Heal, M. Allen, *et al.* 2013. Risk management and climate change. *Nature Clim. Change* **3**: 447–450.
- Lempert, R.J., M.E. Schlesinger and S. C. Bankes. 1996. When we don't know the costs or the benefits: adaptive strategies for abating climate change. *Climatic Change* **33**: 235–274.
- Liu, J., M. Song, R. M. Horton and Y. Hu. 2013. Reducing spread in climate model projections of a September ice-free Arctic. *Proc. Natl. Acad. Sci. USA* **110**: 12571–12576.
- Liu, J., J.A. Curry, H. Wang, *et al.* 2012. Impact of declining Arctic sea ice on winter snowfall. *Proc. Natl. Acad. Sci. USA* **109**: 4074–4079.
- Meir, T., P.M. Orton, J. Pullen, *et al.* 2013. Forecasting the New York City urban heat island and sea breeze during extreme heat events. *Weather Forecast* **28**: 1460–1477.
- Melillo, J., T. Richmond, G. Yohe, and Eds. 2014. *Climate Change Impacts in the United States: The Third National Climate Assessment*, 841 pp.
- Menne, M.J., C.N. Williams Jr., and R.S. Vose. 2013. United States Historical Climatology Network (USHCN) Version 2.5 Serial Monthly Dataset.
- Milly, P.C.D., J. Betancourt, M. Falkenmark, *et al.* 2008. Stationarity is dead: whither water management? *Science* **319**: 573–574.
- Moss, R. H., *et al.* 2010. The next generation of scenarios for climate change research and assessment. *Nature* **463**: 747–756.
- NOAA. 2013. NOAA National Climatic Data Center, State of the Climate: Global Analysis for Annual 2013, published online December 2013.
- NPCC. 2010. *Climate Change Adaptation in New York City: Building a Risk Management Response*. C. Rosenzweig and W. Solecki, Eds. *Ann. N.Y. Acad. Sci.* **1196**: 1–354.
- NPCC. 2015. *Building the Knowledge Base for Climate Resiliency: New York City Panel on Climate Change 2015 Report*. C. Rosenzweig and W. Solecki, Eds. *Ann. N.Y. Acad. Sci.* **1336**: 1–149.
- Price, C. and D. Rind. 1994. Modeling Global Lightning Distributions in a General Circulation Model. *Monthly Weather Review* **122**: 1930–1939.
- Rosenzweig, C., W.D. Solecki, A. DeGaetano, M. O'Grady, S. Hassol, and P. Grabhorn, Eds. 2011. Responding to climate change in New York State: The ClimAID integrated assessment for effective climate change adaptation in New York State. *Ann. N.Y. Acad. Sci.* 1244: 1–460.
- Screen, J.A. and I. Simmonds. 2013. Exploring links between Arctic amplification and mid-latitude weather. *Geophys. Res. Lett.* **40**: 959–964.
- Stroeve, J.C., M.C. Serreze, M.M. Holland, *et al.* 2012. The Arctic's rapidly shrinking sea ice cover: a research synthesis. *Climatic Change* **110**: 1005–1027.

- Taylor, K.E., R.J. Stouffer and G.A. Meehl. 2011. An overview of CMIP5 and the experiment design. *Bull. Am. Meteorol. Soc.* **93**: 485–498.
- Wallace, J. M., I. M. Held, D. W. J. Thompson, *et al.* 2014. Global warming and winter weather. *Science* **343**: 729–730.
- Wilby, R., S. Charles, E. Zorita, B. Timbal, P. Whetton, and L. Mearns. 2004. Guidelines for use of climate scenarios developed from statistical downscaling methods. *Supporting material for the Intergovernmental Panel on Climate Change*.
- Yohe, G. and R. Leichenko. 2010. Adopting a risk-based approach. *Ann. N.Y. Acad. Sci.* **1196**: 29–40.

ANNALS OF THE NEW YORK ACADEMY OF SCIENCES

Issue: *Building the Knowledge Base for Climate Resiliency*

New York City Panel on Climate Change 2015 Report

Chapter 2: Sea Level Rise and Coastal Storms

Radley Horton,¹ Christopher Little,² Vivien Gornitz,¹ Daniel Bader,¹ and Michael Oppenheimer³¹Columbia University Center for Climate Systems Research, New York, NY. ²Atmospheric and Environmental Research, Lexington, MA. ³Woodrow Wilson School and Department of Geosciences, Princeton University, Princeton, NJ

Address for correspondence: Radley Horton, Associate Research Scientist, Columbia University Center for Climate Systems Research, 2880 Broadway, New York, NY 10025. rh142@columbia.edu

Contents

- 2.1 Observed changes
- 2.2 Sea level rise and coastal storm projections
- 2.3 Conclusions and recommendations

Introduction

New York City's low-lying areas are home to a large population, critical infrastructure, and iconic natural, economic and cultural resources. These areas are currently exposed to coastal flooding by warm-season tropical storms such as Hurricane Sandy^a (Box 2.1) and cold-season nor'easters. Sea level rise increases the frequency and intensity of coastal flooding. For example, the ~12 inches of sea level rise in New York City since 1900 may have expanded Hurricane Sandy's flood area by approximately 25 square miles, flooding the homes of more than 80,000 *additional* people^b in New York and New Jersey alone (Climate Central 2013, as reported in Miller *et al.*, 2013; see also Chapter 3, NPCC, 2015).

This chapter presents an overview of observed sea level rise and coastal storms for the New York metropolitan region, sea level rise projection methods and results, coastal storm projections, and recommendations for future research.

^aWe hereafter refer to Sandy as a hurricane or tropical cyclone, although it also can be referred to as a hybrid storm. The storm completed its transition to an extratropical storm just prior to making landfall in New Jersey (Blake *et al.*, 2013).

^bRelative to the number of people who would have experienced flooding in the absence of the ~12 inches of sea level rise since 1900.

2.1 Observed changes

This section describes observed sea level rise and coastal storms.

Sea level rise

Since 1900, the global rate of sea level rise has averaged 0.5 to 0.7 inches per decade (Church *et al.*, 2013; Hay *et al.*, 2015; Church and White, 2011). As with temperature, the long-term upward trend in sea level has varied over the decades. For example, there were lower rates of increase during the early part of the 20th century and much of the 1960s and 1970s; sea level rise increased more rapidly during the 1930s through the 1950s. Since 1993, satellite observations and tide gauges show a global sea level rise of $\sim 1.3 \pm 0.1$ inches per decade (Church *et al.*, 2013; Nerem *et al.*, 2010). There may be a small, yet statistically significant global sea level acceleration of 0.004 ± 0.002 inches per decade between 1900 and 2009 (Church and White, 2011).

There are multiple processes that contribute to sea level rise, including changes in ocean mass distribution and density; changes in the mass of glaciers, ice caps, and ice sheets; water storage on land; vertical land movements; and gravitational, elastic, and rotational effects resulting from ice mass loss. Historically, the majority of the observed rise in global mean sea level has been attributed to thermal expansion. More recently, the contribution of land-based ice loss to global mean sea level rise has begun to rival that of thermal expansion (Church *et al.*, 2011; 2013).

Each of these processes has a unique local signature. Sea level rise in New York City has averaged 1.2 inches per decade since 1900 (Fig. 2.1).

Box 2.1. Hurricane Sandy

Hurricane Sandy was directly responsible for approximately 150 deaths (Blake *et al.*, 2013) and \$70 billion in losses (NOAA, 2013). About half of the deaths occurred in the Caribbean and half in the United States, including 44 in New York City (Blake *et al.*, 2013). Sandy's 14.1-foot elevation (above mean low low water; MLLW) set the record at the Battery tide gauge (Blake *et al.*, 2013). Several factors caused the extreme surge. Sandy's minimum pressure was the lowest ever recorded^c at landfall north of Cape Hatteras, NC. With a tropical storm-force wind field of close to 1000 miles in diameter, Sandy was among the largest storms as well. Hurricane Sandy's unusual westward-turning track also concentrated storm surge, wind, and waves in the New York metropolitan region. Part of the extensive coastal flooding was due to the fact that Sandy's peak surge coincided with high tide.

This is nearly twice the observed global rate. In New York City, approximately 40% of the observed sea level rise is due to land subsidence,^d with the remaining sea level rise driven by climate-related factors (Peltier, 2004; Engelhart and Horton, 2012).

A faster rate of *local* New York City sea level rise has also been observed in recent decades relative to earlier in the 20th century. Tide gauges along the Atlantic coast show a distinct regional sea level acceleration “hotspot” from Cape Cod to Cape Hatteras since the early 1990s (Sallenger *et al.*, 2012; Boon, 2012; Ezer and Corlett, 2012), although the acceleration is still too short to attribute to climate change because of high interannual-multidecadal ocean variability (Kopp, 2013).

Coastal storms

The two types of storms with the largest influence on the coastal areas of the New York metropolitan region are tropical cyclones (hurricanes and tropical storms) and nor'easters. Tropical cyclones strike New York City very infrequently, generally between July and October, and can produce large storm surges and wind damage (Lin *et al.*, 2010). Nor'easters, which tend to occur during the cold season (November to April), are generally associated with smaller surges and weaker winds than hurricanes. Nevertheless, nor'easters affect New York

City more frequently (several times a year) than do hurricanes (Karvetski *et al.*, 2009), and their impacts can be large, in part because their lengthy duration leads to longer periods of high winds and high water than are experienced during tropical cyclones.

The greatest coastal inundation occurs when the surge caused by a storm's wind and wave effects coincides with high astronomical (or “non-storm”) tides. At the Battery, the mean range of tide^e is 4.5 feet but can be as large as 7.7 feet^f during the most extreme spring tides^g (NOAA Tides and Currents, 2013; Orton *et al.*, 2012).

Because of the complexity of the New York City coastline, there is often a large spatial variation in the extent and timing of flooding associated with any particular storm. High tides and waves associated with nor'easters can lead to significant flooding and beach erosion (Hondula and Dolan, 2010). In the case of Hurricane Sandy (see Box 2.1), one of the reasons coastal flooding was so devastating for southern parts of New York City was that the peak storm surge occurred near high tide. Had the storm struck a few hours earlier or later than it did, coastal flood damage would have been much higher elsewhere, including other parts of the city such as Hunts Point in the Bronx.

^cThe 1938 hurricane probably had lower pressure at landfall, but it went unrecorded.

^dLand can subside or “sink” for many reasons. At the Battery, the primary cause is a process known as glacial isostatic adjustment, whereby the land is still responding to the retreat of the ice sheets during the last ice age.

^eThe mean range of tide is defined as the difference in height between mean high water and mean low water (NOAA Tides and Currents, 2013).

^fThe maximum range of tide is defined as the difference in height between NOAA's highest astronomical tide (HAT) and lowest astronomical tide (LAT).

^gA tide near the time of a new or full moon, when there is the greatest difference between high and low water.

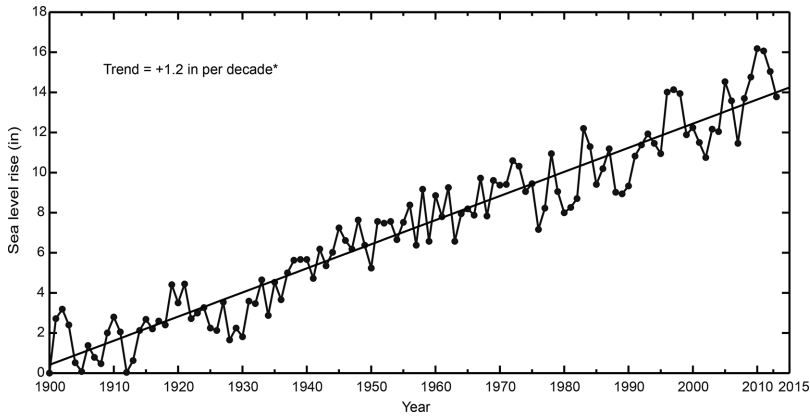


Figure 2.1. Observed sea level rise in New York City (the Battery) from 1900 to 2013. Data are from Permanent Service for Mean Sea Level (PSMSL). *Trend is significant at the 99% level.

Observed changes in the frequency and intensity of coastal storms can also be provided for large geographic regions. There has been an increase in the overall strength of hurricanes and in the number of strong (category 4 and 5) hurricanes in the North Atlantic Basin since the early 1980s (Melillo *et al.*, 2014). However, it is unclear how much of the observed trend is due to natural variability (Seniveratne *et al.*, 2012), increases in greenhouse gas (GHG) concentrations (Hegerl *et al.*, 2007), and/or other changes such as a reduction in aerosol pollution^h in recent decades (Booth *et al.*, 2012). There is also some evidence of an overall increase in storm ac-

^hAerosols can influence hurricanes both by blocking sunlight from heating the upper ocean and through local changes in cloud formation.

tivity near the northeastern U.S. coastline during the second half of the 20th century from 1950 to 2010 (Melillo *et al.*, 2014). Studies have also noted increases in coastal flooding during the past century along the United States East Coast (Grinsted *et al.*, 2012) and in the New York metropolitan region (Talke *et al.*, 2014). Coastal flooding has been influenced by historical changes in sea level in addition to changes in storm frequency and intensity.

2.2 Sea level rise and coastal storm projections

This section describes the methods used to project future sea level rise for New York City and presents the projections (see Appendix I for infographics of projections and Appendix IIB for details of the methods (NPCC, 2015)).

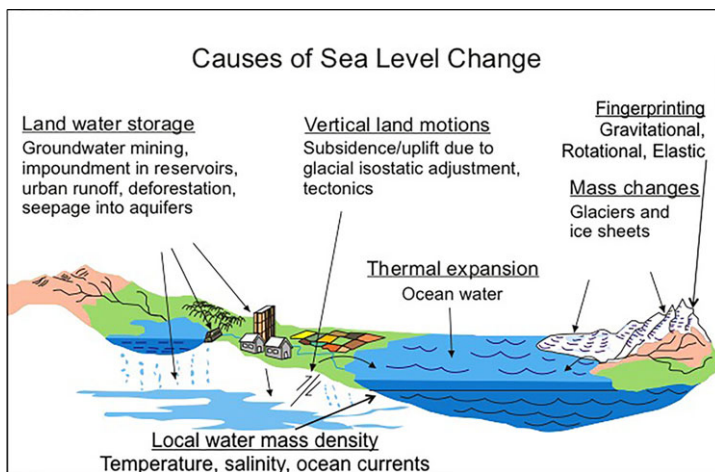


Figure 2.2. Causes of sea level change.

Table 2.1. Sea level rise projection components

Sea level rise component	Scale	Description	Method	Sources
Global thermal expansion	Global	Ocean water expands as it warms	Single globally-averaged value from CMIP5 models	http://cmip-pcmdi.llnl.gov/cmip5
Local changes in ocean height	Local	Changes in ocean water density and circulation	Local values from CMIP5 models	http://cmip-pcmdi.llnl.gov/cmip5
Loss of ice from Greenland and Antarctic ice sheets	Global	Addition of freshwater to the ocean	Bamber and Aspinall expert elicitation surveys of 26 ice sheet experts, with additional probabilistic analysis	Bamber and Aspinall, 2013
Loss of ice from glaciers and ice caps	Global	Addition of freshwater to the ocean	Range from two recent analyses	Radić <i>et al.</i> , 2014; Marzeion <i>et al.</i> , 2012
Gravitational, rotational, and elastic “fingerprints” [*] of ice loss	Local	Regional sea level changes due to ice mass change are modified by gravitational, rotational, and “fast” (elastic) isostatic responses	Ice loss from each ice sheet and the glaciers/ice caps is multiplied by a local NYC coefficient reflecting the aggregate effect	Mitrovica <i>et al.</i> , 2009; Perrette <i>et al.</i> , 2013; Gomez <i>et al.</i> , 2010
Vertical land movements/glacioisostatic adjustments (GIA)	Local	Local land subsidence is an ongoing slow response to the last deglaciation	Peltier’s Glacial Isostatic Adjustment (GIA model)	Peltier, 2004
Land-water storage	Global	Addition or subtraction of freshwater stored in reservoirs and groundwater	Global estimates derived from recent literature	Church <i>et al.</i> , 2011; Milly <i>et al.</i> , 2010

^{*} See Appendix IIB for a full description of the “fingerprints.”

Sea level rise methods and components

The NPCC2 sea level rise projections for New York City have been developed using a component-by-component analysis (Fig. 2.2; Table 2.1).

Other published studies (e.g., Kopp *et al.*, 2014; Perrette *et al.*, 2013; Slangen *et al.*, 2012) have taken a similar regionalized approach to sea level rise projections using different sources of informa-

tion (e.g., set of climate models) and assumptions (e.g., for vertical land motion and ice sheet mass loss).

For each of the components of sea level change, the NPCC2 estimated the 10th, 25th, 75th, and 90th percentiles of the distribution. The sum of all components at each percentile is assumed to give the aggregate sea level rise projection.

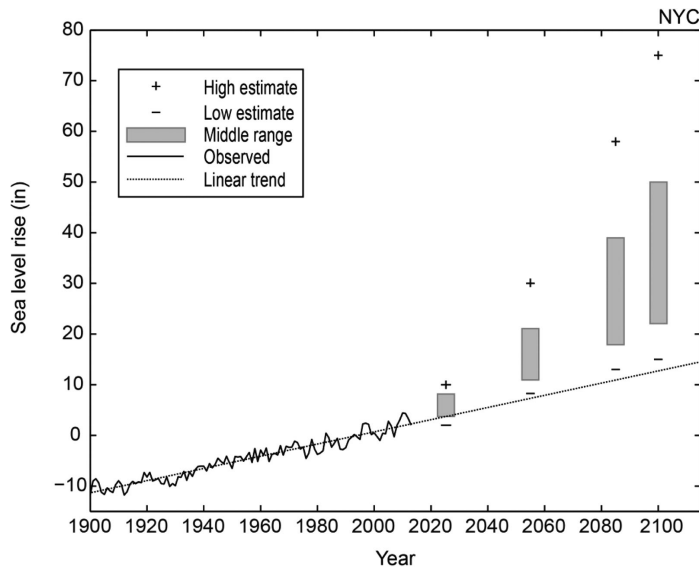


Figure 2.3. New York City sea level rise trends and projections. Projections shown are the low estimate (10th percentile), middle range (25th to 75th percentiles), and the high estimate (90th percentile). The historical trend is also included. Projections are relative to the 2000 to 2004 base period.

Projections for sea level rise are relative to the 2000 to 2004 base period. The three time slices for sea level rise (2020s, 2050s, 2080s) are centered on a given decade. For example, the 2050s time slice refers to the decadal period from 2050 to 2059. Decadal time slices were used for sea level rise (in contrast to the 30-year periods used for the climate variables; see Chapter 1) because natural variability of sea level is lower than that of temperature and precipitation. The sea level rise projections were also extended to 2100 (the methodology is described in Appendices IIA and IIB).

The NPCC2 90th percentile projections are generally comparable to the rapid ice melt scenario of NPCC 2010. Whereas NPCC 2010 included two sea level rise projection techniques, NPCC2 consolidates the projections for all percentiles into a single methodology.

Future sea level rise

As shown in Table 2.2 and Figure 2.3, the middle-range (25th to 75th percentile) sea level rise projection in New York City is an increase of 4 to 8 inches in the 2020s, 11 to 21 inches in the 2050s, 18 to 39 inches in the 2080s, and 22 to 50 inches by 2100. Sea level rise is projected to accelerate as the century progresses and could reach as high as 75 inches by 2100 under the high estimate (90th percentile).

New York City’s sea level rise projections exceed the global average, primarily due to local land subsidence and global climate model projections that ocean height along the Northeast coastline may increase faster than global average ocean height due in part to projected weakening of the Gulf Stream current (Yin *et al.*, 2009, 2010). The range of projected sea level rise grows as the century progresses, primarily because of uncertainties about how much the ice sheets will melt as temperatures rise.

At the 90th percentile, the NPCC2 late-century sea level rise projections are higher than those of Kopp *et al.* (2014). This is primarily due to (1) differing representation of the tail of the sea level rise distribution in Kopp *et al.*, which is based on a combination of Bamber and Aspinnall’s (2013) estimate and that of IPCC AR5 (Church *et al.*, 2013), and (2) the assumption by Kopp *et al.* that sea level rise components are independent.

Flood heights and recurrence intervals

Sea level rise is projected to yield large changes in the frequency and intensity of coastal flooding, even if storms themselves do not change at all (Table 2.3). By the 2050s, the middle range sea level rise projections are associated with approximately a doubling of the probability of the historical 100-year coastal flood (the 100-year coastal flood event refers to the

Table 2.2. New York City sea level rise projections

Baseline (2000–2004) 0 in	Low estimate (10th percentile)	Middle range (25th to 75th percentile)	High estimate (90th percentile)
2020s	2 in	4–8 in	10 in
2050s	8 in	11–21 in	30 in
2080s	13 in	18–39 in	58 in
2100	15 in	22–50 in	75 in

NOTE: Projections are based on a six-component approach that incorporates both local and global factors. The model-based components are from 24 global climate models and two representative concentration pathways. Projections are relative to the 2000–2004 base period.

Table 2.3. Future coastal flood heights and recurrence intervals at the Battery, New York

	Low estimate (10th percentile)	Middle range (25th to 75th percentile)	High estimate (90th percentile)
2020s			
Annual chance of today's 100-year flood (1%)	1.1%	1.1–1.4%	1.5%
Flood heights associated with 100-year flood (11.3 ft)	11.5 ft	11.6–12.0 ft	12.1 ft
2050s			
Annual chance of today's 100-year flood (1%)	1.4%	1.6–2.4%	3.6%
Flood heights associated with 100-year flood (11.3 ft)	12.0 ft	12.2–13.1 ft	13.8 ft
2080s			
Annual chance of today's 100-year flood (%)	1.7%	2.0–5.4%	12.7%
Flood heights heights associated with 100-year flood	12.4 ft	12.8–14.6 ft	16.1 ft

NOTE: Flood heights are derived by adding the sea level–rise projections for the corresponding percentiles to the baseline values. Baseline flood heights associated with the 100-year flood are based on the FEMA stillwater elevations (i.e., without wave height). Flood height elevations are referenced to the NAVD88 datum.

flood with a 1% annual chance of occurrence). By the 2080s under the middle range, the historical 100-year event is projected to occur approximately 2 to 4 times more often. Even under the low sea level rise estimate, coastal flood frequency would approximately double by the 2080s. Under the high sea level rise estimate, coastal flood frequency would increase more than ten-fold, turning the 100-year flood into an approximately once per eight year event. The next section addresses potential changes in coastal storms themselves.

Coastal storms

The balance of evidence suggests that the strongest hurricanes in the North Atlantic Basin may become

more frequent in the future, although the total number of tropical storms may decrease slightly (Christensen *et al.*, 2013; see Table 2.4).ⁱ The implications for the New York metropolitan region, however, are unclear because individual storm tracks are highly variable, and potential changes in tropical cyclone tracks are poorly understood (Kozar *et al.*, 2013; Christensen *et al.*, 2013). As the ocean and atmosphere continue to warm, intense precipitation from

ⁱ A few recent studies based on downscaled CMIP5 global climate models have projected an increase in the number of 21st-century tropical storms (Emanuel, 2013), at least through midcentury (Villarini and Vecchi, 2012; 2013).

Table 2.4. Projected changes in coastal storms

	Spatial scale of projection	Direction of change by the 2080s	Likelihood
Tropical cyclones			
Total number	North Atlantic Basin	Unknown	—
Number of intense hurricanes	North Atlantic Basin	Increase	More likely than not ^a
Extreme hurricane winds	North Atlantic Basin	Increase	More likely than not
Intense hurricane precipitation	North Atlantic Basin	Increase	More likely than not
Nor'easters (number and intensity)	New York City metropolitan region	Unknown	—

^a >50% probability of occurrence

Sources: Melillo, 2014; IPCC, 2012; Colle *et al.*, 2013.

hurricanes will more likely than not increase on a global scale (Knutson *et al.*, 2010; IPCC, 2012), although the implications for the more limited New York metropolitan region are unclear because so few tropical cyclones impact the region. It is unknown how nor'easters in the region may change in the future.^j

2.3 Conclusions and recommendations

Sea level rise in the New York metropolitan region is projected to accelerate as the century progresses and could reach as high as 75 inches by 2100 under the NPCC2 high estimate. New York City's sea level rise is projected to exceed the global average due to land subsidence and changes in ocean circulation, increasing the hazard posed to the New York metropolitan region's coastal population, infrastructure, and other built and natural assets. Although projected changes in coastal storms are uncertain, it is virtually certain (>99% probability of occurrence) that sea level rise alone will lead to an increased frequency and intensity of coastal flooding as the century progresses.

Although these sea level rise projections are New York region specific, projections based on similar methods would not differ greatly throughout the coastal corridor from Boston to Washington, DC (see e.g., Tebaldi *et al.*, 2012; Kopp *et al.*, 2014). Exceptions would include locations experiencing more

rapid changes in local land height, such as land subsidence due to excess groundwater extraction.

In the face of uncertainty about the future frequency and intensity of coastal storms, two critical messages are that (1) New York City is highly vulnerable to coastal storms today, and (2) even low-end sea level projections can be expected to increase the frequency and intensity of coastal flooding, absent any changes in storms themselves.

Although the NPCC projections have focused on the 21st century, sea level rise is projected to accelerate into the 22nd century even if heat-trapping GHG concentrations stabilize later this century. Reducing GHG emissions in the near term is critical to minimizing that long-term acceleration.

More research is needed on how the Greenland and West Antarctic ice sheets will respond to climate change because these ice sheets are the largest long-term source of "high-end" uncertainty. Future research efforts should also explore the relationship between the different sea level rise components as well as the relationship between those sea level rise components and coastal storm risk. For example, research is needed on the potential correlation between dynamic sea level along the northeastern U.S. coast and coastal storm risk (Horton and Liu, 2014).

As understanding grows of how coastal storms may change with climate change, it will become possible to combine changing storm and sea level hazards into integrated projections of coastal flood exposure. Another important area of research is how sea level rise may impact coastal flooding and wave damage associated with a given coastal storm.

^j One recent study (Colle *et al.*, 2013) using CMIP5 models projects that nor'easter tracks could shift to the west.

References

- Bamber, J.L., & W.P. Aspinall. 2013. An expert judgement assessment of future sea level rise from the ice sheets. *Nature Clim. Change*, **3**: 424–427.
- Blake, E. S., Kimberlain, T. B., Berg, R. J., Cangialosi, J. P., and J. L. Beven II. 2013. Tropical Cyclone Report: Hurricane Sandy (AL182012) 2229 October 2012. 157. *National Hurricane Center*.
- Boon, J.D. 2012. Evidence of sea level acceleration at U.S. and Canadian tide stations, Atlantic coast, North America. *Journal of Coastal Research* 1437–1445.
- Booth, B., N.J. Dunstone, P.R. Halloran, *et al.* 2012. Aerosols implicated as a prime driver of twentieth-century North Atlantic climate variability. *Nature* **484**: 228–232.
- Christensen, J.H., *et al.* 2013. Climate phenomena and their relevance for future regional climate change. In *Climate Change 2013: The Physical Science Basis. Contribution of Working Group I to the Fifth Assessment Report of the Intergovernmental Panel on Climate Change*, T.F. Stocker *et al.*, Eds. Cambridge: Cambridge University Press. 1218–1308.
- Church, J.A., & N.J. White. 2011. Sea-level rise from the late 19th to the early 21st century. *Surv. Geophys.* **32**: 585–602.
- Church, J.A., *et al.* 2011. Revisiting the Earth's sea-level and energy budgets from 1961 to 2008. *Geophys. Res. Lett.* **38**: L18601.
- Church, J.A., *et al.* 2013. Sea level change. In *Climate Change 2013: The Physical Science Basis. Contribution of Working Group I to the Fifth Assessment Report of the Intergovernmental Panel on Climate Change*, T.F. Stocker *et al.*, Eds. Cambridge: Cambridge University Press. 1137–1216.
- Colle, B.A., Z. Zhang, K.A. Lombardo, *et al.* 2013. Historical evaluation and future prediction of eastern North American and western Atlantic extratropical cyclones in the CMIP5 models during the cool season. *J. Climate* **26**: 6882–6903.
- Emanuel, K.A. 2013. Downscaling CMIP5 climate models shows increased tropical cyclone activity over the 21st century. *Proc. Nat. Acad. Sci. USA* **110**: 12219–12224.
- Engelhart, S.E., & B.P. Horton. 2012. Holocene sea level database for the Atlantic coast of the United States. *Quat. Sci. Rev.* **54**: 12–25.
- Ezer, T., & W.C. Corlett. 2012. Is sea level rise acceleration in the Chesapeake Bay? A demonstration of a novel new approach for analyzing sea level data. *Geophys. Res. Lett.* **39**: L19606.
- Gomez, N., J.X. Mitrovica, P. Huybers, & P.U. Clark. 2010. Sea level as a stabilizing factor for marine-ice-sheet grounding lines. *Nature Geosci.* **3**: 850–853.
- Grinsted, A., J.C. Moore, & S. Jevrejeva. 2012. Homogeneous record of Atlantic hurricane surge threat since 1923. *Proc. Natl. Acad. Sci. USA* **109**: 19601–19605.
- Hay, Carling C., E. Morrow, R.E. Kopp, and J.X. Mitrovica. 2015. Probabilistic reanalysis of twentieth-century sea-level rise. *Nature* **517**: 481–484.
- Hegerl, G.C., *et al.* 2007. Understanding and attributing climate change. In *Climate Change 2007: The Physical Science Basis. Contribution of Working Group I to the Fourth Assessment Report of the Intergovernmental Panel on Climate Change*, S. Solomon *et al.*, Eds. Cambridge: Cambridge University Press, 663–745.
- Hondula, D.M., & R. Dolan. 2010. Predicting severe winter coastal storm damage. *Environ. Res. Lett.* **5**.
- Horton, R.M., & J. Liu. 2014. Beyond Hurricane Sandy: what might the future hold for tropical cyclones in the North Atlantic? *J. Extreme Events* 1450007.
- IPCC. 2012. *Managing the Risks of Extreme Events and Disasters to Advance Climate Change Adaptation*. Cambridge: Cambridge University Press.
- Karvetski, C., R.B. Lund, & F. Parisi. 2009. A statistical study of extreme nor'easter snowstorms. *Involve* **2**: 341–350.
- Knutson, T.R., *et al.* 2010. Tropical cyclones and climate change. *Nature Geosci.* **3**: 157–163.
- Kopp, R.E. 2013. Does the mid-Atlantic United States sea level acceleration hot spot reflect ocean dynamic variability? *Geophys. Res. Lett.* **40**: 3981–3985.
- Kopp, R.E., *et al.* 2014. Probabilistic 21st and 22nd century sea-level projections at a global network of tide gauge sites. *Earth's Future* **2**: 383–406.
- Kozar, M.E., M.E. Mann, K.A. Emanuel, & J.L. Evans. 2013. Long-term variations of North Atlantic tropical cyclone activity downscaled from a coupled model simulation of the last millennium. *J. Geophys. Res.: Atmospheres* **118**: 13383–13392.
- Lin, N., K.A. Emanuel, J.A. Smith, & E. Vanmarcke. 2010. Risk assessment of hurricane storm surge for New York City. *J. Geophys. Res.: Atmospheres* **115**: D18121.
- Marzeion, B., A.H. Jarosch, & M. Hofer. 2012. Past and future sea-level change from the surface mass balance of glaciers. *Cryosphere* **6**: 1295–1322.
- Melillo, J., T. Richmond, G. Yohe, & Eds. 2014. *Climate Change Impacts in the United States: The Third National Climate Assessment*. 841 pp.
- Miller, K.G., R.E. Kopp, B.P. Horton, *et al.* 2013. A geological perspective on sea-level rise and its impacts along the U.S. mid-Atlantic coast. *Earth's Future* **1**: 3–18.
- Milly, P.C.D., *et al.* 2010. Terrestrial water-storage contributions to sea-level rise and variability. In *Understanding Sea-Level Rise and Variability* New York: Wiley-Blackwell, 226–255.
- Mitrovica, J.X., N. Gomez, & P.U. Clark. 2009. The sea-level fingerprint of West Antarctic collapse. *Science*, **323**: 753.
- Nerem, R.S., D.P. Chambers, C. Choe, & G.T. Mitchum. 2010. Estimating mean sea level change from the TOPEX and Jason altimeter missions. *Marine Geodesy* **33**: 435–446.
- NOAA: Tides and Currents. Available online at <http://tidesandcurrents.noaa.gov>.
- NPCC. 2015. *Building the Knowledge Base for Climate Resiliency: New York City Panel on Climate Change 2015 Report*. C. Rosenzweig and W. Solecki, Eds. *Ann. N.Y. Acad. Sci.* **1336**: 1–149.
- Orton, P., N. Georgas, A. Blumberg, & J. Pullen. 2012. Detailed modeling of recent severe storm tides in estuaries of the New York City region. *J. Geophys. Res.: Oceans (1978–2012)* **117**.
- Peltier, W.R. 2004. Global glacial isostasy and the surface of the ice-age Earth: The ICE-5G (VM2) model and GRACE. *Annu. Rev. Earth Planetary Sci.* **32**: 111–149.
- Perrette, M., F. Landerer, R. Riva, *et al.* 2013. A scaling approach to project regional sea level rise and its uncertainties. *Earth Syst. Dynam.* **4**: 11–29.
- Radić, V., A. Bliss, A.C. Beedlow, R. Hock, E. Miles, & J.G. Cogley. 2014. Regional and global projections of twenty-first century glacier mass changes in response to climate scenarios from global climate models. *Clim. Dyn.* **42**: 37–58.

- Sallenger, A.H., K.S. Doran, & P.A. Howd. 2012. Hotspot of accelerated sea-level rise on the Atlantic coast of North America. *Nature Clim. Change* **2**: 884–888.
- Senevirante, S.I., *et al.* 2012. *Managing the Risks of Extreme Events and Disasters to Advance Climate Change Adaptation. A Special Report of Working Groups I and II of the Intergovernmental Panel on Climate Change.* 109–230.
- Slangen, A.B.A., C.A. Katsman, R.S.W. *et al.* 2012. Towards regional projections of twenty-first century sea-level change based on IPCC SRES scenarios. *Clim. Dynam.* **38**: 1191–1209.
- Talke, S.A., P. Orton, & D.A. Jay. 2014. Increasing storm tides in New York Harbor, 1844–2013. *Geophysical Research Letters*.
- Tebaldi, C., B.H. Strauss, & C.E. Zervas. 2012. Modelling sea level rise impacts on storm surges along US coasts. *Environ. Res. Lett.* **7**: 014032.
- Villarini, G., & G.A. Vecchi. 2012. Twenty-first-century projections of North Atlantic tropical storms from CMIP5 models. *Nature Clim. Change* **2**: 604–607.
- Villarini, G., & G.A. Vecchi. 2013. Projected increases in North Atlantic tropical cyclone intensity from CMIP5 models. *J. Climate* **26**: 3231–3240.
- Yin, J., M.E. Schlesinger, & R.J. Stouffer. 2009. Model projections of rapid sea-level rise on the northeast coast of the United States. *Nature Geosci.* **2**: 262–266.
- Yin, J., S.M. Griffies, & R.J. Stouffer. 2010. Spatial variability of sea level rise in twenty-first century projections. *J. Climate* **23**, 4585–4607.

ANNALS OF THE NEW YORK ACADEMY OF SCIENCES

Issue: *Building the Knowledge Base for Climate Resiliency*

New York City Panel on Climate Change 2015 Report

Chapter 3: Static Coastal Flood Mapping

Lesley Patrick,^{1,a} William Solecki,^{1,a} Klaus H. Jacob,² Howard Kunreuther,³
and Guy Nordenson⁴

¹City University of New York, CUNY Institute for Sustainable Cities, New York, NY. ²Lamont-Doherty Earth Observatory, Columbia University, Palisades, NY. ³Risk Management and Decision Process Center, Wharton School, University of Pennsylvania, Philadelphia, PA. ⁴School of Architecture, Princeton University, Princeton, NJ.

Address for correspondence: Lesley Patrick, Department of Earth and Environmental Sciences, The Graduate Center, City University of New York (CUNY) 365 Fifth Avenue, New York, NY 10016

Contents

- 3.1 Mapping risks, hazards, and uncertainty
- 3.2 GIS flood-mapping approach
- 3.3 Future flood map products
- 3.4 Mapping limitations
- 3.5 Conclusions and recommendations

Introduction

The objective of this chapter is to describe the coastal flood-mapping methods used by the second New York City Panel on Climate Change (NPCC2) and the coastal flood-mapping products. The chapter illustrates the technical approach used to create the NPCC2 maps of projected future flood extents. Uncertainties in the coastal flood-mapping process are explained and associated caveats are presented. See Box 3.1 for key definitions and terms.

3.1 Mapping risk, hazards, and uncertainty

Risk and hazard mapping has a long and rich tradition, and presenting spatial risks and hazards has been applied in a wide range of contexts. The strength of the map as an information tool depends on the quality of data and the techniques used to translate the data onto a flat surface. Flood-hazard mapping has its roots in 1930s conservation-era watershed and flood-hazard management (Mileti, 1999). The most significant advance since that time, besides the dynamic growth of computational mapping and geographic information systems (GIS) (Clarke, 1997), has been the application of model-based projections of flood extents and periodicity

(recurrence intervals) to the empirically based data on flood extents and elevation (see Chapters 2 and 4, NPCC, 2015).

New York City hazards and climate risks

Mapping natural hazards and climate risks is an essential part of an overall emergency management strategy for densely populated urban areas such as New York City and can be an effective part of an overall risk reduction plan. In 2009, the New York City Office of Emergency Management (OEM) developed the first FEMA-approved hazard mitigation plan (HMP) for the City, a document designed to serve as a guideline for protecting New York City from the effects of natural hazards. The HMP assesses hazard vulnerabilities including those related to climate, identifies risk reduction opportunities, and helps to secure funding for hazard mitigation; it is updated every five years.

The most current plan (NYCHMP, 2014) contains maps and tables that depict a broad range of both physical hazards and social vulnerabilities. The maps of potential flood inundation are used to illustrate the City's Hurricane Evacuation Zones and to inform the general public about their risk from individual flood hazard events. These are worst-case scenario maps based on the Sea, Lake, and Overland Surges from Hurricanes (SLOSH) model^b and are

^bThe SLOSH model is a computerized numerical model developed by the National Weather Service (NWS) to estimate storm surge heights resulting from historical, hypothetical, or predicted hurricanes by taking into account atmospheric pressure, size, forward speed, and storm track data. These parameters are used to create a model of the wind field that drives storm surge.

^aLead authors.

Box 3.1. Definitions and terms

Base flood elevation (BFE)

FEMA term for the 100-year flood elevation that specifically includes the elevation of wave crests above the stillwater elevation as well as estimated effects of wave runup and overtopping of sea walls.

Dynamic coastal flood modeling

Physics-based computer simulation techniques that include the effects of factors such as wind, atmospheric pressure, and friction in calculation of coastal flood elevations (also known as *hydrodynamic modeling*).

Extratropical cyclone

Coastal storms existing or occurring outside of the tropical latitudes, displaying poleward displacement and conversion of the primary energy source from the release of latent heat of condensation to baroclinic (temperature contrast between warm and cold air masses) processes. Cyclones can become extratropical and still retain winds of hurricane or tropical storm force.

Flood exceedance curves

Relationship between flood intensity and different levels of frequency; each curve represents the flood intensity that will be equaled or exceeded once in a certain number of years, indicated as the frequency of that curve.

Flood hazard assessment

Statistical evaluation of the annual likelihood of a given flood event for a range of different flood elevations.

Flood zone and floodplain

A flood zone is statistically-defined region whereby each point within is subject to a flooding at a given annual probability. A floodplain is a geologic term that refers to a broad, relatively flat land area subject to flooding from a river, lake, ocean, or other water body.

Return period/recurrence

The average interval, in years, between occurrences of two floods of equal or greater magnitude. It is based on the probability that the given flood event will be equaled or exceeded in any given year.

Static coastal flood modeling

A common technique for mapping flood extents whereby a flood elevation is extrapolated landward until it reaches the equivalent contour height on land (see Chapter 4 for further discussion of the static approach). Topographic elevations at or lower than this height are considered flooded. This approach—also referred to as a “bathtub” model—is commonly used for sea level inundation scenarios applied to surfaces of constant elevation such as a tidal datum, but it has also been applied to SLOSH model output.

Stillwater elevation

FEMA terminology for combined storm surge and tide, that is, total water elevation during a storm. It is the water elevation in the absence of waves. NPCC2 utilizes stillwater elevation to create its 500-year map products.

Storm surge/storm tide

Storm surge is a wind-driven and atmospheric pressure-driven increase in water level and combines with tides to form the total water elevation during a storm, also known as the storm tide.

Tropical cyclone

A warm-core, non-frontal synoptic-scale cyclone, originating over tropical or subtropical waters with organized deep convection and a closed surface wind circulation about a well-defined center.

Wave setup

The rise in stillwater elevation that is driven by the unidirectional effect of waves breaking, thus pushing water onshore.

utilized by city agencies and stakeholders to develop plans to protect their at-risk infrastructure. FEMA Flood Insurance Rate Maps (FIRMs) are represented in the HMP. New York City's comprehensive climate resiliency plan, *A Stronger, More Resilient New York* (City of New York, 2013), also uses flood mapping to assess risks and plan for the future.

FEMA Flood Insurance Rate Maps and Hurricane Sandy

A Flood Insurance Study (FIS) is a document developed by FEMA that contains information about flooding in a community and is produced in conjunction with a flood rate insurance map (FIRM). Both coastal flooding and riverine flooding are included (the NPCC2 only considered coastal flooding). A FIS describes the flooding history of a community, explains the engineering methods and data sources used to develop the FIRMs, and provides flood heights and profiles for various recurrence probabilities.

FIRMs display flood hazard boundaries and base flood elevation (BFE) information essential to setting insurance rates and building design standards, and for the implementation of floodplain management and regulation practices. They are used by federal agencies, state and local governments, lending institutions, insurance agencies, surveyors, and the National Flood Insurance Program (Crowell *et al.*, 2007).

The initial Flood Insurance Study for the City of New York became effective in 1983 and then, in 1991, 1992, 1994, 2001, and 2007, underwent a series of revisions such as redelineations, and the incorporation of approved amendments requested by property owners. Despite these updates, the original coastal flood-hazard analysis for New York City was not fully revised until 2013.

FEMA was in the process of updating the FIS and FIRMs for New York City when Hurricane Sandy struck on October 29, 2012. The Hurricane Sandy field-verified inundation area (Fig. 3.1), a surface interpolated using field-verified high-water marks and storm-sensor data from the U.S. Geological Survey, clearly equaled and exceeded the 1983 100- and 500-year floodplains, most strikingly along the southern coasts of Brooklyn and Queens and along the eastern and southern shores of Staten Island. Northern Queens and the Bronx experienced less flooding relative to the other boroughs in part because the Long

Island Sound was at low tide when Sandy made landfall (Georgas *et al.*, 2014).

It is critical that coastal flood maps are updated regularly. As a result of not having updated maps, many people were caught unaware and without flood insurance during Hurricane Sandy. The flood maps from the 2010 NPCC Report, *Climate Change Adaptation in New York City*, were based on the 1983 FEMA FIS, thus making them less useful than they were intended to be.

In December 2013, FEMA released Preliminary Flood Insurance Rate Maps for New York City based on their 2013 Flood Insurance Study. These maps were a significant update from the first FEMA Flood Insurance Study conducted in 1983. They incorporated changes that included:

- Revised flood hazard analysis and mapping for the 520 miles of coastal shoreline of New York City
- Base map updated to 2008 aerial photography
- Incorporation of 2010 digital topographic data provided by New York City
- Incorporation of validated Letters of Map Change (LOMCs), which are FEMA-issued documents that reflect official revisions/amendments to FIRMs
- Conversion of the geodetic datum from the National Geodetic Vertical Datum of 1929 (NAVD29) to the North American Vertical Datum of 1988 (NAVD88).

In comparison to the 1983 FIRMs, the revised preliminary FIRMs delineate a larger 100-year flood zone, extending the zone of flooding further inland in nearly all areas of the city and encompassing 50 square miles of land relative to the 100-year flood zone of 1983 that covered 33 square miles (Fig. 3.2).

3.2 GIS flood-mapping approach

In the first NPCC Report and in the post-Hurricane Sandy NPCC Climate Risk Information 2013 that followed (NPCC, 2010; 2013), the NPCC provided future flood maps for New York City depicting projected flood areas under the NPCC sea level rise scenarios. The sea level rise scenarios were an essential component of the future flood-mapping exercise because, as sea levels rise through the 21st century, a coastal flood of a given volume will reach higher elevations and greater aerial extents than previously experienced.

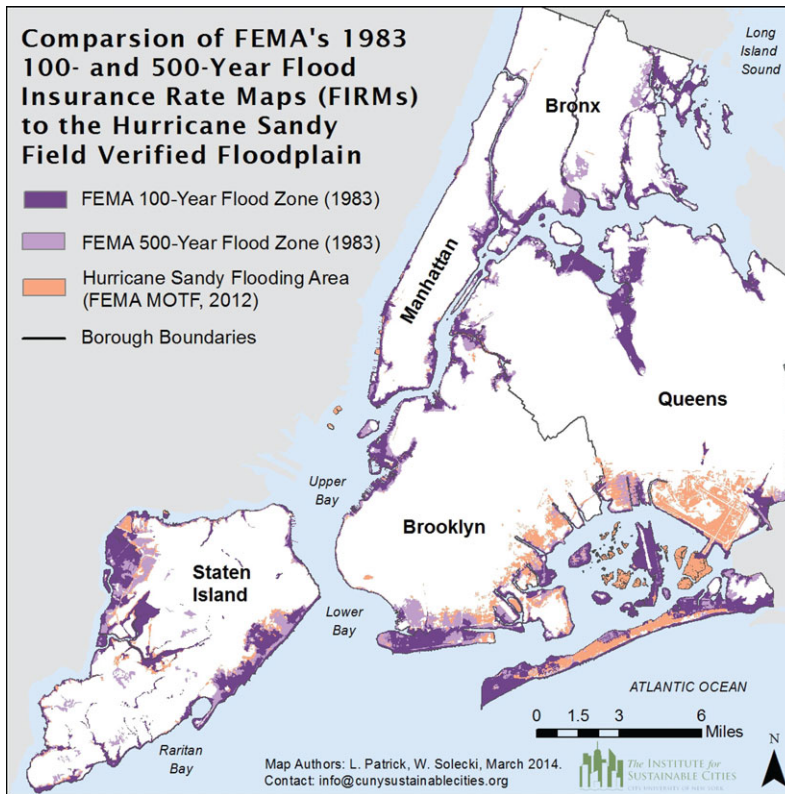


Figure 3.1. FEMA's 1983 projections of the 100-year and 500-year flood zones^c in New York City compared to the field-verified post-Hurricane Sandy flooding area. Source: FEMA.

The projected flood areas created by the NPCC2 for the 100- and 500-year flood events in the 2020s, 2050s, 2080s, and 2100 were developed using a static coastal flood-modeling technique that uses outputs from FEMA's hydrologic and hydraulic models and modifies these outputs in a GIS by adding the NPCC sea level rise projections (see Appendix IIC NPCC, 2015 for further details). This static "bathtub" approach to mapping sea level effects on coastal flood zones is simple in logic. It assumes that floodwaters will continue to move landward until they reach an equivalent topographic elevation (see Chapter 4, NPCC, 2015, for further discussion of the static approach) (Titus and Richman, 2001; Wu *et al.*, 2002; Kleinosky *et al.*, 2006; Poulter and Halpin, 2008; Gesch, 2009; Li *et al.*, 2009).

^cThe 100-year coastal flood event refers to the flood with a 1% annual chance of occurrence. The 500-year coastal flood event refers to the flood with a 0.2% annual chance of occurrence.

The FEMA FIRMs were chosen as the base dataset (and not the hurricane storm-surge inundation areas derived from SLOSH) because the FIRMs are used for New York City Building Code regulations and floodplain management. Selection of the FIRMs produces maps that are compatible and comparable for stakeholder and planner use. However, the FEMA Regional 2 Coastal Storm Surge Study (FEMA, 2014) suggests the 2013 FIRM flood elevations and extents may be on the high end of previous estimates (see Chapter 4 of NPCC, 2015 for further discussion).

Following on from this approach, the NPCC2 has also conducted analyses and created maps that combine sea level rise directly with dynamic coastal flood models that include wave effects (see Chapter 4). Despite its limitations (discussed below), the static approach is a useful tool for planners and stakeholders and can be used to inform decisions on infrastructure investments and land use policy. The static approach is relatively simple, requires less

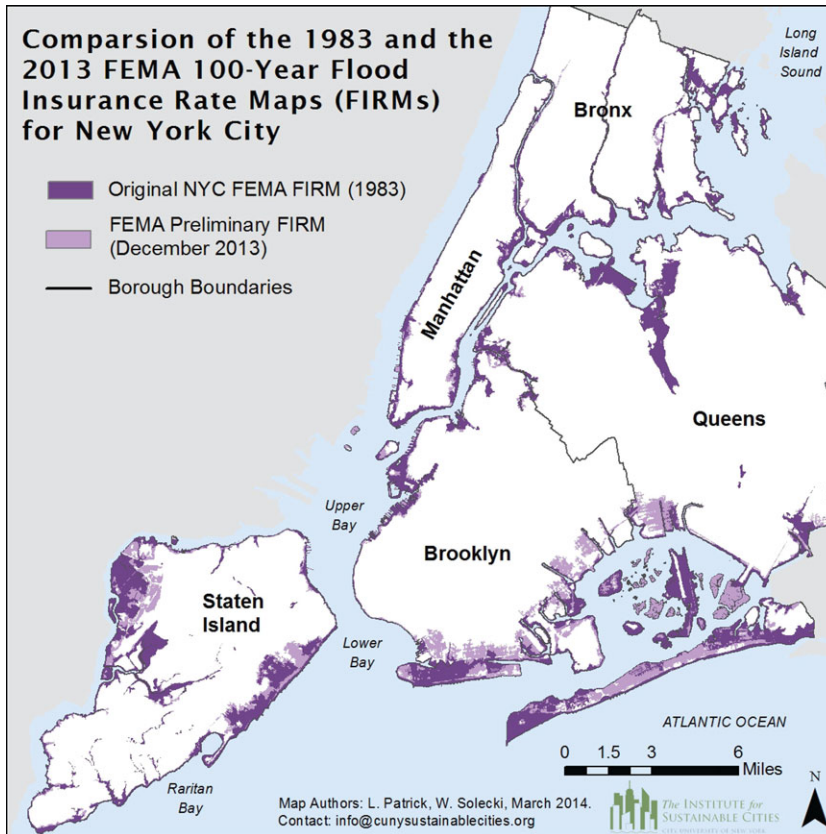


Figure 3.2. Comparison of FEMA’s 100-year floodplains for New York City as first developed in 1983 and revised in 2013.

time, and is less computer-intensive than dynamic approaches.

The methodology for developing the static GIS maps described in the NPCC 2010 Report has been revised slightly for the NPCC2 mapping products that have followed. The following section details the GIS mapping approach, methodology and limitations regarding data use and map interpretation, and describes the vertical accuracy of the topographic data. It notes where current data-sets and methods differ from previous mapping efforts.

Data sets used for mapping

The following data sets were used to develop the NPCC2 flood maps:

1. The 90th-percentile value projections of sea level rise elevations for the 2020s, 2050s, 2080s, and 2100 developed by NPCC2.
 - 2020s, 10 inches; 2050s, 30 inches; 2080s, 58 inches; 2100, 75 inches
 - Prepared February–December 2013
2. Preliminary 2013 FIRMs derived from the FEMA 2013 Preliminary Flood Insurance Study for the City of New York, NY.
 - Flood extent and base flood elevation (BFE) information (relative to the North American Vertical Datum of 1988 [NAVD88]) for the 100-year floodplain
 - Release date: December 5, 2013
3. The 0.2% (500-year) Annual Chance Flood Hazard Area Stillwater Elevation Raster, derived from the FEMA Preliminary Flood Insurance Study and FIRMs for the City of New York, NY.
 - Flood extent and stillwater elevation (SWEL) information (relative to NAVD88) for the 500-year floodplain
 - Release date: December 5, 2013
4. Digital Elevation Model (DEM), 2010 for New York City.
 - Surface developed from LiDAR data collected in spring 2010 over New York City

- Nominal pulse spacing (NPS) of LiDAR: < 1 meter (>1 pulse/m²)
 - LiDAR points interpolated to create a 1-foot resolution surface with cell values corresponding to ground-elevation values in feet above NAVD88
 - Horizontal positional accuracy: root mean square error (RMSE) of LiDAR data 33.08 cm
 - Horizontal datum: North American 1983
 - Vertical positional accuracy: root mean square error (RMSE) of LiDAR data 9.5 cm
 - Vertical datum: NAVD88^d
5. New York City borough boundaries (New York City Department of City Planning).
 - Release date: September 2008

Static coastal flood mapping methodology

Vector shapefiles and maps of areas that could be impacted by future 100- and 500-year floods were created using spatial processing techniques in ESRI ArcGIS software.^e In 2010 and again in 2013, the NPCC developed a GIS-based methodology to map projected flood scenarios based on given increments of sea level rise. That work was based on the following assumptions:

1. Sea level rise will result in greater 100- and 500-year flood extents and higher flood elevations than are currently modeled in the FEMA FIRMs.
2. Floodwaters will continue to move onshore until they reach an equivalent topographic elevation.
3. Low-elevation land areas must have direct connectivity to the open water in order to flood (i.e., they are not surrounded by areas of higher elevation).^f

^dThe NAVD88 is an orthometric datum that is approximately 2.5 inches above mean sea level at the Battery, NY tide gauge station.

^eESRI's ArcGIS software is a platform that is used for creating maps and geographic information products.

^fIt is possible that areas not hydrologically connected to open water can flood via subterranean tunnels or pipes or via a storm surge-induced increase in hydrostatic pressure that raises water tables relatively distant from shoreline. However, this flooding is not indicated on the NPCC maps.

4. Wave contributions to flood elevations will remain unchanged from those found in the FEMA FIRMs.

Flood-elevation values change as floodwaters move inland, most often but not always decreasing in elevation as they move from the coast to areas onshore. NPCC2 projections of the 90th percentile of sea level rise elevations of 10 inches for the 2020s, 30 inches for the 2050s, 58 inches for the 2080s, and 75 inches for 2100 were added to the BFE and SWEL elevation values at the most landward locations of flooding to show how a rise in sea level could increase those values and extend the 100- and 500-year floodplains further inland.

FEMA's BFE and SWEL elevations vary both parallel and perpendicular to the shoreline and thus are not at a constant elevation. The transitions in flood elevation values along the coasts should be reflected in the landward movement of floodwaters, such that the inland shape and extent of the flood zone reflect the changing base flood elevation values nearer to shore. The NPCC2 static approach incorporates these lateral variations in flood elevation values by assuming that landward values of floodwater elevation are likely to be more similar to neighboring flood-elevation values and less similar to more distant values (see Appendix IIC, NPCC, 2015).

3.3 Future flood map products

The NPCC2 maps illustrate the estimated potential inundation extent associated with projected sea level rise elevations for four time slices (see Figs. 3.3 and 3.4). Using the static approach, the NPCC2 created two specific map products:

1. GIS shape files of the future 100-year flood extent for the 2020s, 2050s, 2080s, and 2100 based on FEMA's Preliminary FIRMs (December 2013) for New York City and the NPCC2 high-estimate (90th percentile) sea level rise projections of 10 inches for the 2020s, 30 inches for the 2050s, 58 inches for the 2080s, and 75 inches for 2100.
2. GIS shape files of the future 500-year flood extent for the 2020s, 2050s, 2080s, and 2100 based on stillwater elevation (SWEL) raster data for New York City (December 2013) and

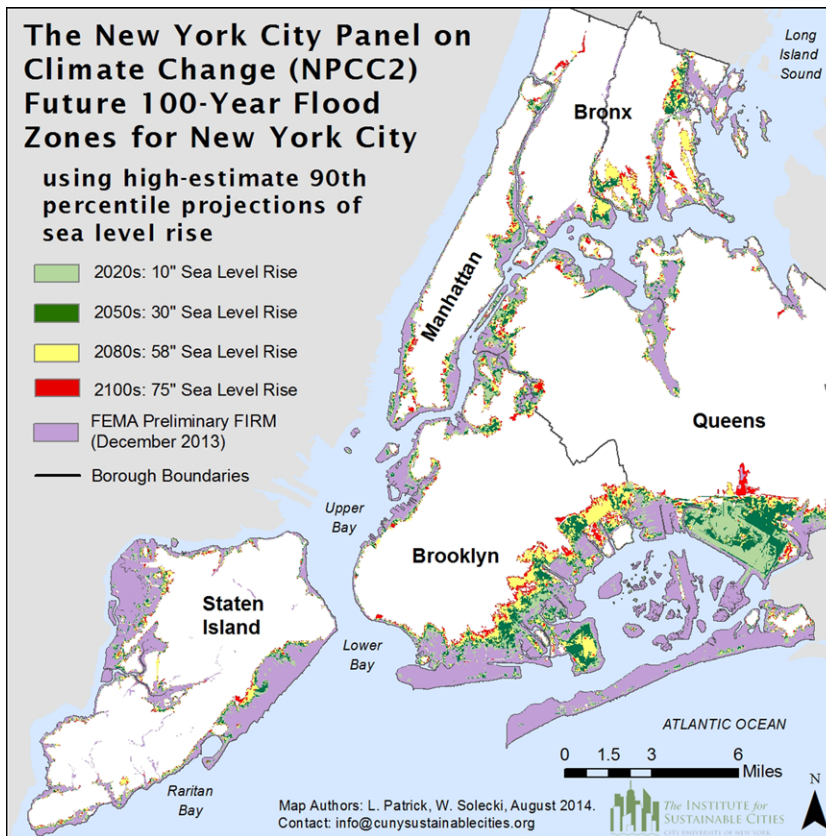


Figure 3.3. Potential areas that could be impacted by the 100-year flood in the 2020s, 2050s, 2080s, and 2100 based on NPCC2 projections of the high-estimate 90th-percentile sea level rise scenario.

NOTE: This map is subject to limitations in accuracy as a result of the quantitative models, datasets, and methodology used in its development. The map and data should not be used to assess actual coastal hazards, insurance requirements, or property values or be used in lieu of FIRMS issued by FEMA. The flood areas delineated above in no way represent precise flood boundaries but rather illustrate three distinct areas of interest: (1) areas currently subject to the 100-year flood that will continue to be subject to flooding in the future; (2) areas that do not currently flood but are expected to potentially experience the 100-year flood in the future; and (3) areas that do not currently flood and are unlikely to do so in the timeline of the climate scenarios used in this research (end of the current century).

the NPCC2 high-estimate (90th percentile) sea level rise projections of 10 inches for the 2020s, 30 inches for the 2050s, 58 inches for the 2080s, and 75 inches for 2100.

The GIS shape files were used to create the projected future 100- and 500-year flood zone maps for New York City shown in Figures 3.3 and 3.4. These maps illustrate that higher sea level elevations result in greater floodplain areas, with the extent of landward movement dictated by the elevation and slope of the land. In each scenario, Queens is the borough with the most affected land area, followed by Brooklyn, Staten Island, the Bronx, and Manhattan.

The relationship between sea level elevation and flood extent is illustrated by the calculations of flood area inundation in Table 3.1.

3.4 Mapping limitations

The maps contain numerous sources of uncertainty as a result of the datasets and methodologies used in their development and as such are limited in their accuracy. FEMA's methodology for creating coastal BFEs and SWEL data involves simulating the dynamic processes of flooding using detailed hydrologic and hydraulic models (FEMA, 2013). These models have a range of uncertainty associated with their output, even before sea level rise

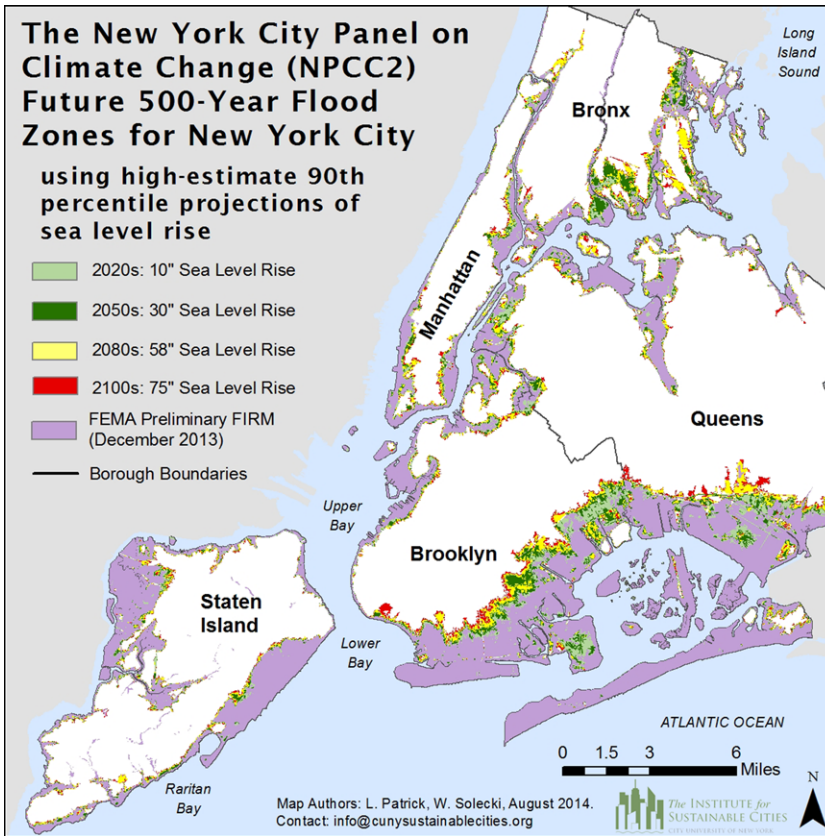


Figure 3.4. Potential areas that could be impacted by the 500-year flood in the 2020s, 2050s, 2080s, and 2100 based on NPCC2 projections of the high-estimate 90th-percentile sea level rise scenario.

NOTE: This map is subject to limitations in accuracy as a result of the quantitative models, datasets, and methodology used in its development. The map and data should not be used to assess actual coastal hazards, insurance requirements or property values or be used in lieu of FIRMS issued by FEMA. The flood areas delineated above in no way represent precise flood boundaries but rather illustrate three distinct areas of interest: (1) areas currently subject to the 1-in-500-year flood that will continue to be subject to flooding in the future; (2) areas that do not currently flood but are expected to potentially experience the 1-in-500-year flood in the future; and (3) areas that do not currently flood and are unlikely to do so in the timeline of the climate scenarios used in this research (end of the current century).

projections are added (see Box 3.2). As mentioned above, FEMA’s 2013 Preliminary FIRMs and 500-year Flood Hazard Still Water Elevation Raster present flood elevations and extents that are on the high end of previous estimates (see Chapter 4 of NPCC, 2015 for further discussion). Projecting future sea level rise impacts on the 100- and 500-year flood areas also involves uncertainties regardless of the methodology. Uncertainty in the elevation data, the sea level rise projections, and FEMA model outputs (BFE and SWEL data) contribute to uncertainty that is difficult to quantify.

In addition, the static coastal flood-modeling methodology involves different uncertainties than

those encountered in the dynamic modeling methodology. The static GIS-based methodology does not take into consideration the effects of soils, vegetation, surface permeability, infrastructure (e.g., drainage systems), structures, friction, and other factors that can act to limit or increase the extent of flooding at local scales (in most cases these factors will likely limit the extent of flooding). For example, the landward extents of FEMA’s dynamically modeled 100- and 500-year flood areas do not simply follow topographic contours but are influenced by shoreline protection features (e.g., rip-rap, bulkheads), land use/land cover, and infrastructure obstructions. Because these are not taken

Box 3.2. NPCC2 mapping data limitations

Critical issues related to future coastal flood mapping are the vertical accuracy of the elevation data, the consistency of flood elevation data, and the inherent uncertainties in the information presented. (See Appendix IIC for further details.)

Vertical accuracy of elevation data

The absolute vertical accuracy of the topographic elevation dataset must be known in order to determine if the sea level rise increments used are supported by the underlying elevation data. Using sea level rise increments that are smaller than the bounds of the statistical uncertainty of the elevation data, defined as the linear error at 95% confidence, will yield questionable results. The 90th-percentile NPCC2 sea level rise projections of 10 inches (25.4 cm) for the 2020s, 30 inches (76.2 cm) for the 2050s, 58 inches (145.3 cm) for the 2080s, and 75 inches (190.5 cm) for 2100 all exceed the 95% error bounds of the elevation data.

Dataset consistency

Because base flood elevations incorporating wave heights and wave runup were not calculated for the 2013 Preliminary FIRM 500-year flood extent, 500-year SWEL data were used as a proxy.

Table 3.1. Inundation areas for current and projected 100- and 500-year flood scenarios. Sources: 100-year flood scenario from *A Stronger, More Resilient New York*; 500-year flood scenario calculated by NPCC2.

100-year flood scenario	Area (mi ²)
FEMA 2013 Preliminary FIRM	50
Projected 2020s, 10"	59
Projected 2050s, 30"	72
Projected 2080s, 58"	85
Projected 2100s, 75"	91
500-year flood scenario	Area (mi ²)
FEMA preliminary FIRM	66
Projected 2020s, 10"	76
Projected 2050s, 30"	84
Projected 2080s, 58"	94
Projected 2100s, 75"	99

into account in the static modeling approach, the NPCC2 future flood maps may overestimate flood extent in areas where shoreline features such as seawalls and bulkheads have a large effect on floodwater movement. See Chapter 4 for a comparison of the results using the static and the dynamic modeling approaches for future flood mapping.

The NPCC2 maps do, however, account for hydrologic connectivity in the flood area, such that only land areas with direct connection to the ocean or flooded waterways are considered flooded.

Hydrologic connectivity is a useful refinement to a static coastal flood-modeling approach that effectively eliminates from inclusion low-elevation areas surrounded by areas of higher elevation. That said, it is possible to experience inland flooding in areas not connected to the ocean or other water bodies due to flooding in underground passageways (e.g., transportation tunnels, sewers, utility conduits) or to an increase in hydrostatic pressure that elevates groundwater levels at inland locations. Neither static nor dynamic modeling takes this into account. Without a method to account for such underground water movement, future flood maps may underestimate the extent of flooded inland areas.

Further, the NPCC2 future flood maps do not contain flood-elevation information and should not be used to evaluate site-specific flood hazards or be used in lieu of FEMA FIRMs to determine building elevation or insurance requirements. The presence of man-made structures, permeable soils, vegetation, and other impediments to water movement will affect the extent of flooding, and these effects are not captured in the maps.

3.5 Conclusions and recommendations

The NPCC2 100- and 500-year future flood maps are presented as two-dimensional delineations of potential flood extent. Their intent and value lie in illustrating three distinct citywide areas of interest

that should be monitored as sea level rise projections are updated through the 21st century: (1) areas currently within the 100- and 500-year flood areas; (2) areas that are not currently within the 100- and 500-year flood areas but will potentially be in the future; and (3) areas that are not currently in the 100- and 500-year flood areas and are unlikely to be in flood areas during the time slices used in this report. In Chapter 4 (NPCC, 2015) the NPCC2 sea level rise projections are incorporated into a dynamic storm surge model to more fully explore future flooding potential and to compare methodologies.

Future work should focus on quantifying the sources of uncertainty in both the data sets used to develop these maps and in the mapping process, and in displaying this uncertainty on the maps themselves. Known vertical uncertainties include those associated with the estimates of sea level rise and with the topographic LiDAR data (see Appendix IIC, NPCC, 2015).

Additional mapping work should consider alternative methods of assessing the extent of coastal flooding associated with different return periods and considering directly the effects of projected climate conditions using dynamic models with synthetic hurricanes (Emmanuel *et al.*, 2006; Lin *et al.*, 2012). Hurricane models such as these typically use large-scale atmospheric and oceanic data as input, which can be generated from global climate models (GCMs). Dynamic models with synthetic hurricanes could be used to prepare maps for both current and future climate conditions using the same methodology. This proposed future work will allow for the consideration of both 100- and 500-year average return periods as well as events with lower probabilities of occurrence that may produce large flooding extents similar to that which occurred during Hurricane Sandy.

Other future work of particular interest to stakeholders and planners are site-specific flood depth calculations. Estimates of uncertainty associated with the elevation, sea level rise, and FEMA flood heights should be used to determine to what degree of confidence flood depth calculations could be determined. Although the 90th-percentile sea level rise projections exceed the 95% error bounds of the elevation data, other sources of error such as those associated with FEMA's base flood elevations may not. The error associated with flood-depth calculations may exceed the value of those depths themselves.

Finally, future work should also consider the biophysical and social vulnerabilities to current and future flood events through the development of indices (Cutter *et al.*, 2000, 2003; Cutter and Finch, 2008; Flanagan *et al.*, 2011; Kleinosky *et al.*, 2006; Maantay *et al.*, 2009; Rygel *et al.*, 2006; Wu *et al.*, 2002). Storms are not "equal-impact events" because social and physical geographies interact to expose vulnerable populations to elevated risk (Cutter, 1996). Not all populations are exposed to the same degree of flooding: some will experience more wave action and greater flood heights than others, and not all populations have the same capacity to prepare for, respond to, and recover from a flood event. An overall flood vulnerability index that combines both social and biophysical vulnerability can characterize site-specific levels of risk to flood hazards and identify communities that may require special attention, planning efforts, and mobilization to respond to and recover from such disasters and hazards.

References

- City of New York. 2013. New York City Special Initiative on Rebuilding and Resiliency, *A Stronger, More Resilient New York*. New York: 438pp.
- Clarke, K.C. 1997. *Getting Started with Geographic Information Systems*. Upper Saddle River, NJ: Prentice Hall.
- Crowell, M., E. Hirsch, and T.L. Hayes. 2007. Improving FEMA's coastal risk assessment through the National Flood Insurance Program: an historical overview. *Mar. Technol. Soc. J.* **41**: 18–27.
- Cutter, S.L., 1996. Vulnerability to environmental hazards. *Prog. Human Geography* **20**(4): 529–539.
- Cutter, S., B. Boruff, and W.L. Shirley. 2003. Social vulnerability to environmental hazards. *Soc. Sci. Q.* **84**: 242–261.
- Cutter, S.L. and C. Finch. 2008. Temporal and spatial changes in social vulnerability to natural hazards. *Proc. Natl. Acad. Sci. USA*, **105**: 2301–2306.
- Cutter, S.L., J.T. Mitchell, J.T., and M.S. Scott. 2000. Revealing the vulnerability of people and places: a case study of Georgetown County, South Carolina. *Ann. Assoc. Am. Geogr.* **90**: 713–737.
- Emmanuel, K., S. Ravela, E. Vivant, and C. Risi. 2006. A statistical deterministic approach to hurricane risk assessment. *Bull. Am. Meteor. Soc.* **87**: 299–314.
- Federal Emergency Management Agency (FEMA). 2013. *Flood Insurance Study: City of New York, New York, Bronx County, Richmond County, New York County, Queens County, Kings County*, 131. Washington, DC: FEMA.
- Flanagan, B.E., E. Gregory, E. Hallisey, *et al.* 2011. A social vulnerability index for disaster management. *J. Homel. Secur. Emerg. Manag.* **8**(1): Article 3.
- Georgas, N., P. Orton, A. Blumberg, *et al.* 2014. The impact of tidal phase on Hurricane Sandy's flooding around New York City and Long Island Sound. *J. of Extr. Even.* **01**: 1450006.

- Gesch, D.B. 2009. Analysis of Lidar elevation data for improved identification and delineation of lands vulnerable to sea-level rise. *J. Coastal Res. Special Issue* **53**: 49–58.
- Kleinosky, L., B. Yarnal, and A. Fisher. 2006. Vulnerability of Hampton Roads, Virginia to storm-surge flooding and sea-level rise. *Natural Hazards* **40**: 43–70, doi:10.1007/s11069-006-0004-z.
- Li, X., R.J. Rowley, J.C. Kostelnick, *et al.* 2009. GIS analysis of global impacts from sea level rise. *Photogrammetric Eng. Remote Sens.* **75**: 807–818.
- Lin, N., K. Emanuel, M. Oppenheimer, and E. Vanmarcke. 2012. Physically based assessment of hurricane surge threat under climate change. *Nat. Clim. Change* **2**: 462–467.
- Maantay, J., A. Maroko, and G. Culp. 2009. Using geographic information science to estimate vulnerable urban populations for flood hazard and risk assessment in New York City. In *Geospatial Techniques in Urban Hazard and Disaster Analysis*. pp. 71–91. P.S. Showalter and Y. Lu, Eds. Dordrecht: Springer Netherlands.
- Mileti, D. 1999. *Disasters by Design: A Reassessment of Natural Hazards in the United States*. New York: Joseph Henry Press.
- NPCC. 2010. Climate Change Adaptation in New York City: Building a Risk Management Response, New York City Panel on Climate Change 2010 Report. C. Rosenzweig and W. Solecki, Eds. *Ann. N.Y. Acad. Sci.* **1196**: 1–354.
- NPCC. 2013. *Climate Risk Information 2013: Observations, Climate Change Projections, and Maps*. New York: New York.
- NPCC. 2015. Building the Knowledge Base for Climate Resiliency: New York City Panel on Climate Change 2015 Report. C. Rosenzweig and W. Solecki, Eds. *Ann. N.Y. Acad. Sci.* **1336**: 1–149.
- NYCHMP. 2014. The City of New York Hazard Mitigation Plan. Accessed at http://www.nyc.gov/html/oem/html/planning_response/planning_hazard_mitigation_2014.shtml.
- Poulter, B., and P.N. Halpin. 2008. Raster modelling of coastal flooding from sea-level rise. *Int. J. Geograph. Info. Sci.* **22**: 167–182.
- Rygel, L., D. O’Sullivan, and B. Yarnal. 2006. A method for constructing a social vulnerability index: an application to hurricane storm surges in a developed country. *Mitig. Adapt. Strateg. Glob. Change* **11**: 741–764.
- Titus, J.G. and C. Richman. 2001. Maps of lands vulnerable to sea level rise: modeled elevations along the U.S. Atlantic and Gulf coasts. *Climate Res.* **18**: 205–228.
- Wu, S.-Y., B. Yarnal, and A. Fisher. 2002. Vulnerability of coastal communities to sea-level rise: a case study of Cape May County, New Jersey. *Climate Res.* **22**: 255–270.

ANNALS OF THE NEW YORK ACADEMY OF SCIENCES

Issue: *Building the Knowledge Base for Climate Resiliency*

New York City Panel on Climate Change 2015 Report

Chapter 4: Dynamic Coastal Flood Modeling

Philip Orton,^{1,a} Sergey Vinogradov,^{2,a} Nickitas Georgas,^{1,a} Alan Blumberg,^{1,a} Ning Lin,³
 Vivien Gornitz,⁴ Christopher Little,⁵ Klaus Jacob,⁶ and Radley Horton⁴

¹Stevens Institute of Technology, Hoboken, NJ. ²Earth Resources Technology/National Atmospheric and Oceanic Administration, Silver Spring, MD. ³Department of Civil and Environmental Engineering, Princeton University, Princeton, NJ. ⁴Columbia University Center for Climate Systems Research, New York, NY. ⁵Atmospheric and Environmental Research, Lexington, MA. ⁶Lamont-Doherty Earth Observatory, Palisades, NY.

Address for correspondence: philip.orton@stevens.edu

Contents

- 4.1 Background
- 4.2 Methods
- 4.3 Results and discussion
- 4.4 Conclusions and recommendations

Introduction

Storm surge is an increase in water level caused by winds and low atmospheric pressure and combines with tides to form the total water elevation during a storm, also known as the storm tide or stillwater elevation. Storm tides are among the world's most costly and deadly hazards, bringing floodwaters and waves capable of damaging and disabling infrastructure, homes, and property, as well as threatening human life and health. Sea level rise in the New York metropolitan region has already been increasing the number of coastal flood events (see e.g., Colle *et al.*, 2010; Sweet *et al.*, 2013; Talke *et al.*, 2014). Coastal flood heights are projected to increase and coastal flood zones to expand as sea levels continue to rise due to climate change, as documented in Chapters 2 and 3.

Until now, the New York City Panel on Climate Change (NPCC) has utilized a static mapping approach to assess future coastal flood hazards (see NPCC, 2010; 2013; 2015). One assumption of static mapping is that the flood elevation is spatially uniform over inland flood areas, although peak water elevation for a major hurricane can have strong

spatial variations (Fig. 4.1), potentially violating this assumption. In this chapter, the second NPCC (NPCC2) advances these methods by testing the use of a dynamic model that explicitly accounts for more of the forces acting on the water and the resulting water movement. The NPCC2 has undertaken dynamic modeling of future coastal flooding based on the Federal Emergency Management Agency's (FEMA) flood-mapping framework, which includes the effects of tides, storm surge, and wave setup (see Chapter 3, Box 3.1, NPCC, 2015) on water elevations and maps overland flood areas. This chapter presents the methods for the dynamic modeling of coastal flooding and compares results from the static approach (discussed in more detail in Chapter 3, NPCC, 2015) and dynamic modeling approaches.

The NPCC2's exploration of dynamic modeling was, in part, motivated by a desire to test whether there were considerable differences between dynamic modeling and static mapping outcomes. In addition, FEMA uses dynamic models for its flood-mapping studies (e.g., FEMA, 2014a), and the National Oceanic and Atmospheric Administration (NOAA) similarly uses dynamic models for forecasting neighborhood flooding during hurricanes. Further, prior studies of New York Harbor have shown that dynamic models can reproduce past storm-tide events with a typical accuracy of 0.5 ft (e.g., Colle *et al.*, 2008; Orton *et al.*, 2012; Georgas *et al.*, 2014).

In addition, under the Biggert-Waters Flood Insurance Reform Act of 2012, FEMA is required to convene a Technical Mapping Advisory Council to develop recommendations on "how to ensure that the Federal Emergency Management Agency

^aLead authors.

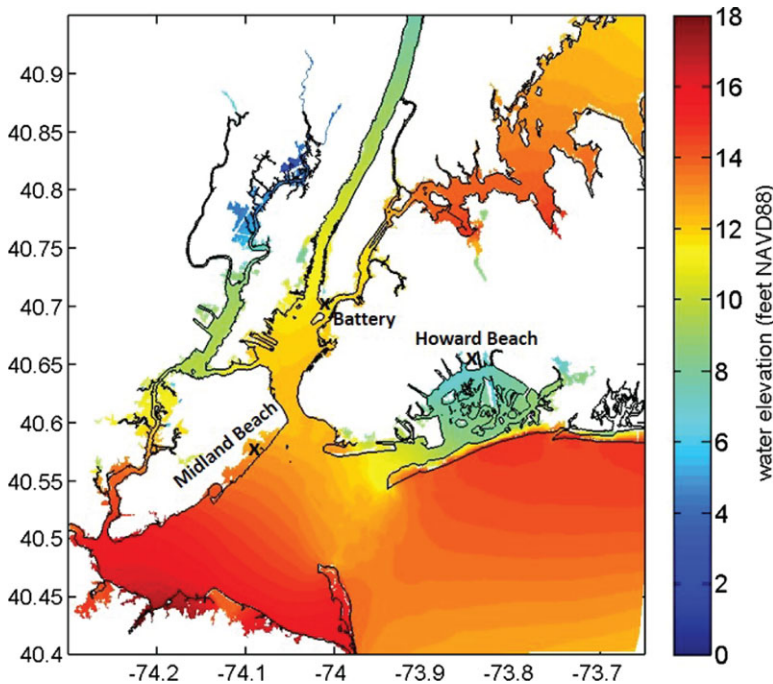


Figure 4.1. Study region for NPCC2 dynamic coastal flood modeling, with peak water elevation data for the synthetic tropical cyclone NJa_0007_006 shown in Figure 4.2.

uses the *best available methodology* to consider the impact of the rise in sea level.”^b New York City relies on FEMA’s Flood Insurance Rate Maps (FIRMs) as the basis to understand current flood risk and to inform floodplain management regulations. Therefore New York City and the NPCC2 have an interest in developing methods for assessing future flood hazards that are consistent with FEMA’s approach for mapping present-day flood zones.

Here, we set out to inform this discussion by utilizing both static and dynamic methods of calculating the effects of sea level rise on FEMA stillwater elevation estimates and then comparing results. The broader goal of this work is to contribute to the methods by which New York City and other coastal cities can evaluate and address the future impacts of sea level rise on coastal flooding.

4.1 Background

As discussed in Chapter 2 (NPCC, 2015), both tropical cyclones (e.g., hurricanes) and extratropical

cyclones (e.g., nor’easters) strike the New York metropolitan region and are important to defining flood zones and elevations for the “100-year” and “500-year” floods, known respectively as the 1% and 0.2% annual chance floods (FEMA, 2014a, Chapter 2). Currently almost 400,000 New Yorkers live within the new 100-year FEMA flood zone, as defined by FEMA’s Preliminary FIRMs (City of New York, 2013a; FEMA, 2014a), and Hurricane Sandy flooded many of these neighborhoods (see Chapter 2, FEMA, 2014a).

Hurricanes strike New York City infrequently but have produced the highest two flood events on record at the Battery at the southern tip of Manhattan—Hurricane Donna in 1960 (7.2 feet, NAVD88) and Hurricane Sandy in 2012 (11.3 feet, NAVD88). Extratropical cyclones such as nor’easters typically have small-to-moderate surges but occur more frequently. Their effects can be large because they can last for several days, leading to more extended periods with high storm surge. This makes it more likely for the storm surge to coincide with high tide, as occurred with the December 11–12, 1992 nor’easter (Colle *et al.*, 2010).

^b42 USC 4101a(d) (emphasis added), available at <http://www.law.cornell.edu/uscode/text/42/4101a>.

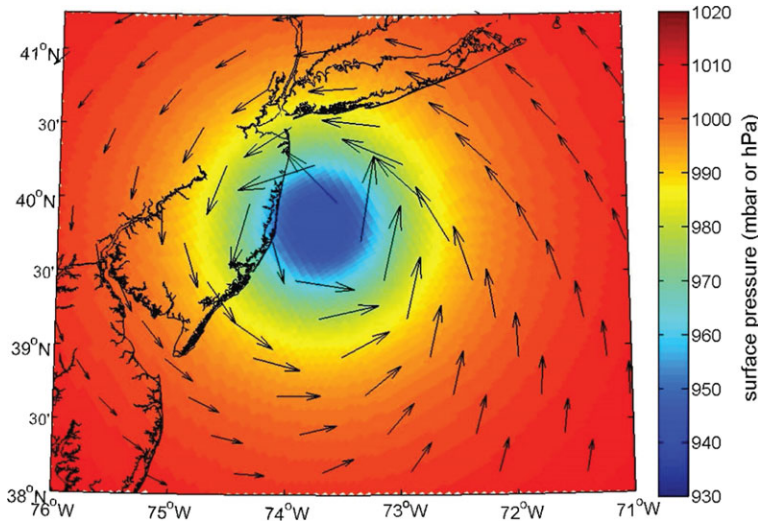


Figure 4.2. Atmospheric pressure and wind vectors for synthetic tropical cyclone NJa_0007_006, one of the worst in the FEMA storm set for New York metropolitan region flooding used in NPCC2 dynamic coastal flood modeling. The longest vector represents a maximum sustained wind speed of 124 mph, a Category-3 hurricane.

Flood-mapping methods for future sea levels

In Chapter 3 (NPCC, 2015), NPCC, 2010, and NPCC, 2013, static approaches were used to estimate the future impacts of sea level rise, adding sea level rise projections to FEMA's 100- and 500-year flood elevations, and to map flood zones with projected sea level rise (Horton *et al.*, 2010; NPCC, 2010; 2013). The static approach was applied to FEMA flood elevations for 100- and 500-year floods, with the additional criterion that low-elevation land areas must have direct connectivity to the open water in order to flood. Whereas the first NPCC maps relied on older FEMA flood elevations from the 2007 FIRMs, the NPCC2 updates use newer, higher flood elevations from the recently released FEMA Preliminary FIRMs and coastal flood study (FEMA, 2014a).

Dynamic flood modeling is a physics-based computer simulation technique that includes the effects of factors such as wind, atmospheric pressure, and friction in the calculation of flood elevations (this technique is also known as *hydrodynamic modeling*). A limited number of studies have compared static mapping and dynamic modeling to quantify the impact of sea level rise on coastal flooding. One study of low-lying populated regions around Miami found that dynamic modeling gave higher flood heights than static flood-mapping methods (Zhang *et al.*, 2013). A study of the New York metropolitan region that did not include overland flooding found

that simple superposition of sea level rise on top of storm tide (used in the static mapping technique) was an excellent approximation to dynamic modeling results (Lin *et al.*, 2012). This NPCC2 study uses a hazard assessment framework, dynamically simulates water elevation (including the effects of tides, storm surge, and wave setup) and identifies overland flood areas.

4.2 Methods

The overall strategy of the NPCC2 dynamic modeling is to incorporate sea level rise projections into the dynamic coastal flood-modeling procedure used in the recent FEMA Region II Coastal Storm Surge Study (FEMA, 2014a). The aim is to produce compatible future flood exceedance curves and flood zones (see Appendix IID for details). The NPCC2 baseline simulations used the same dynamic model, grid parameters (e.g., bottom friction, bathymetry/land elevation), storm sets, and forcing data input files (wind, atmospheric pressure, and tide). Statistical methods were also similar between the NPCC2 dynamic modeling and the FEMA study, although there are small discrepancies in results that suggest minor differences in computation.

The study region for the NPCC2's dynamic coastal flood modeling is shown in Figure 4.1, with three areas that were highlighted for special focus: The Battery, Manhattan; the Midland Beach, Staten

Island neighborhood; and the Howard Beach, Queens neighborhood. The flood maps and hazard assessment presented in this chapter include the surrounding parts of New Jersey around the New York Harbor. These interconnected areas are a crucial part of the New York metropolitan region's transportation, energy, and food distribution systems.

The first step was to conduct a baseline reproduction of the FEMA (2014a) model simulations that do not include the effects of sea level rise. The ADCIRC (ADvanced CIRCulation)/SWAN (Simulating WAVes Nearshore) (Booij *et al.*, 1996; Luettich *et al.*, 1992) computer model was used to conduct the storm-surge simulations. The NPCC2 baseline results were then compared to FEMA (2014a) results to test for consistency.

The storm set developed by FEMA for use in the Region 2 Coastal Storm Surge Study includes the 30 strongest extratropical cyclones from the period 1950–2009, based on ranking storm surge heights from tide gauges in the region. Tropical cyclones are harder to characterize because they are rare, so FEMA defined a set of 159 synthetic tropical cyclones that span a wider range of possible storms (see e.g., Fig. 4.2).

In the second step, the same modeling procedure was followed, incorporating NPCC2 sea level rise projections. Chapter 2 (NPCC, 2015) presents the NPCC2 sea level rise projections for the 10th, 25th, 75th and 90th percentiles for the 2020s, 2050s, 2080s and 2100. The NPCC2 dynamic coastal flood modeling used the 90th percentile sea level projections in order to focus on high-end risks. Time periods simulated were the 2020s, 2050s and 2080s (11, 31, and 58 inches of sea level rise, respectively^c). Only a subset of the storms were simulated with sea level rise, focused on 100-year to 500-year events, but the final results take into account the full range of storms (see Appendix IID).

Dynamic coastal flood mapping

Temporal maximum water elevation data (e.g., Fig. 4.2) at each location over the entire domain for

each storm were utilized for statistical analysis. For each of the 188,390 grid points in the study area that covers the spatial extent shown in Figure 4.2, probability distributions of water elevation were built separately for tropical cyclones (TCs) and extratropical cyclones (ETCs). A detailed description of the statistical methods utilized for converting these distributions to flood exceedance curves (return period versus water elevation; Fig. 4.3) is given in Appendix IID. As a consistency check, statistical codes and ADCIRC modeling outputs closely reproduced FEMA flood exceedance curves, generally within 2 inches (e.g., Fig. 4.3).

For dynamic flood maps of the baseline and future decades, the 100-year and 500-year stillwater elevation values were taken from the flood exceedance curves for each grid location. The resulting water elevation data were imported into ArcMAP and interpolated (inverse-distance weighting, IDW) to form a raster surface over the entire region (New York City and the New Jersey Harbor regions). The ADCIRC land surface elevation (essentially a coarse, 70-m-resolution digital elevation model) was also interpolated using IDW to the same cell size as the water elevation rasters. The land surface raster was subtracted from each water elevation raster to compute a map (raster) of flood depth, and the zero contour is the boundary of that event's floodplain. Static mapping methods were generally equivalent to those summarized in Chapter 3, but were performed using a 70-m-resolution digital elevation model (DEM) to enable equivalent comparison to the dynamic mapping results (see Appendix IID, NPCC, 2015 for details).

4.3 Results and discussion

This section presents the dynamic coastal flood modeling results and examines differences between the dynamic and static flood-mapping results. The sensitivity of the flood elevations to potential climate change–driven increases in the frequency of tropical cyclones is then analyzed. Finally, the section outlines and discusses some limitations of this study as well as how further research can address them.

Dynamic modeling of future coastal floods

Contours for the 100-year (1% annual chance) flood zone, baseline versus the 2080s, are shown in Figure 4.4. The regions where sea level rise will cause

^cThe values used here differ slightly from the 10, 30, and 58 inches presented in Chapter 2 (NPCC, 2015); the Chapter 2 values include additional information incorporated after the release of the IPCC Fifth Assessment Report. The small differences are within the bounds of climate uncertainty in the long-term projections.

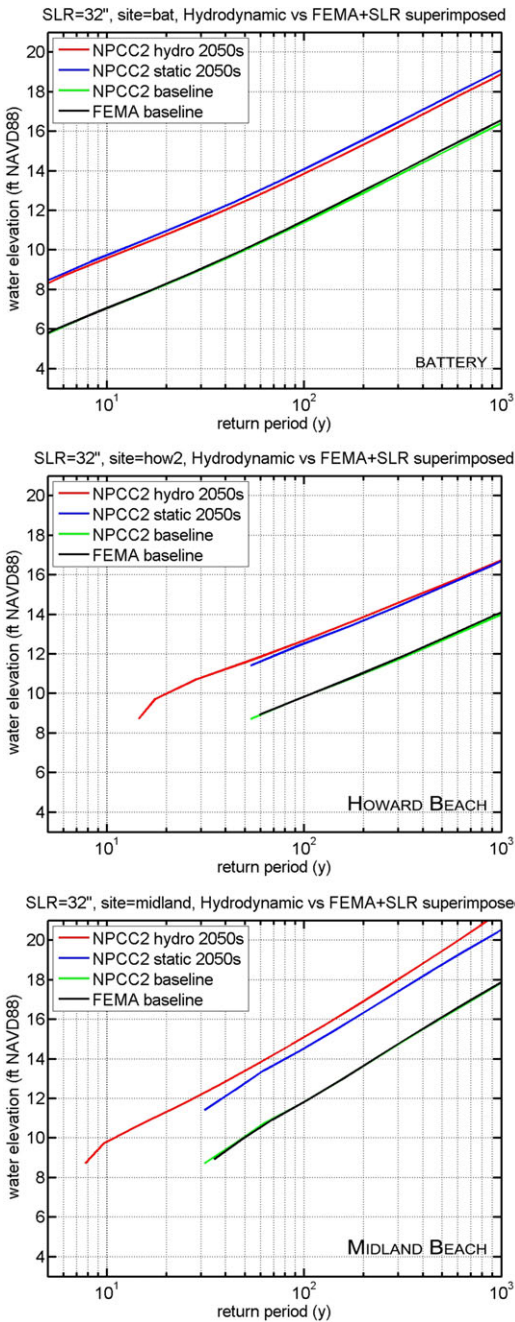


Figure 4.3. Comparison of NPCC2 (green) with FEMA (black) baseline flood exceedance curves as well as NPCC2 static (blue) and dynamic (red) flood exceedance curves for the NPCC2 2050s 90th-percentile sea level rise. Each curve shows the average return period for a flood that exceeds a given flood elevation. Source: Stevens Institute of Technology.

the greatest change in the 100-year flood zone are in the broad flat land area (a floodplain in geographic terms) of southern Queens and eastern Brooklyn around Jamaica Bay. There are other increases in the flooding area across the entire region, including the southern Bronx (the Bronx and Hutchinson River floodplains), and northern Brooklyn (Newtown and Gowanus Creek floodplains).

Contrasting dynamic and static flood assessment approaches

A comparison of the dynamic and static assessments of flood zone boundary contours in the 2050s is shown in Figures 4.5 and 4.6. The results are similar, especially when considering the entire region.

Many New York City floodplain regions in Figure 4.6 show dynamic mapping results that are similar to static mapping results—in many cases the two are only inches higher or lower. Variations in these results arise due to factors such as wind direction (which can blow up higher sea levels in downwind areas) and friction (which initially reduces flood height for a shallow flow, then eventually has little effect as the flow becomes deeper). (For full details, see Appendix IID, NPCC, 2015.)

Results of stillwater elevations for the three specific study locations are compared in Figure 4.3 and Table 4.1. At the Battery, the site of the New York City financial district and a historical tide gauge station off lower Manhattan, the results show dynamic stillwater elevations that are just below those calculated with the static method. At Howard Beach, a neighborhood in southern Queens with a slightly sloping floodplain on the north shore of Jamaica Bay, the dynamic results are equal to or a few inches higher than the static results. At Midland Beach, a neighborhood on the eastern shore of Staten Island that is only a few feet above normal high tides, the dynamic results for the 2050s are substantially higher (>0.5 ft) than the static results, but for the 2080s they are substantially lower (>1.0 ft; Table 4.1). Reasons for these results are discussed below.

A spatial view of the difference between dynamic and static 100-year flood calculations is presented in Figure 4.6. Like the Battery, most other deep-water, estuarine, or open coastal locations show dynamic flood elevations equal to or a few inches lower than the static results.

One exception is the Meadowlands in New Jersey, where dynamic modeling results are close to 1 foot

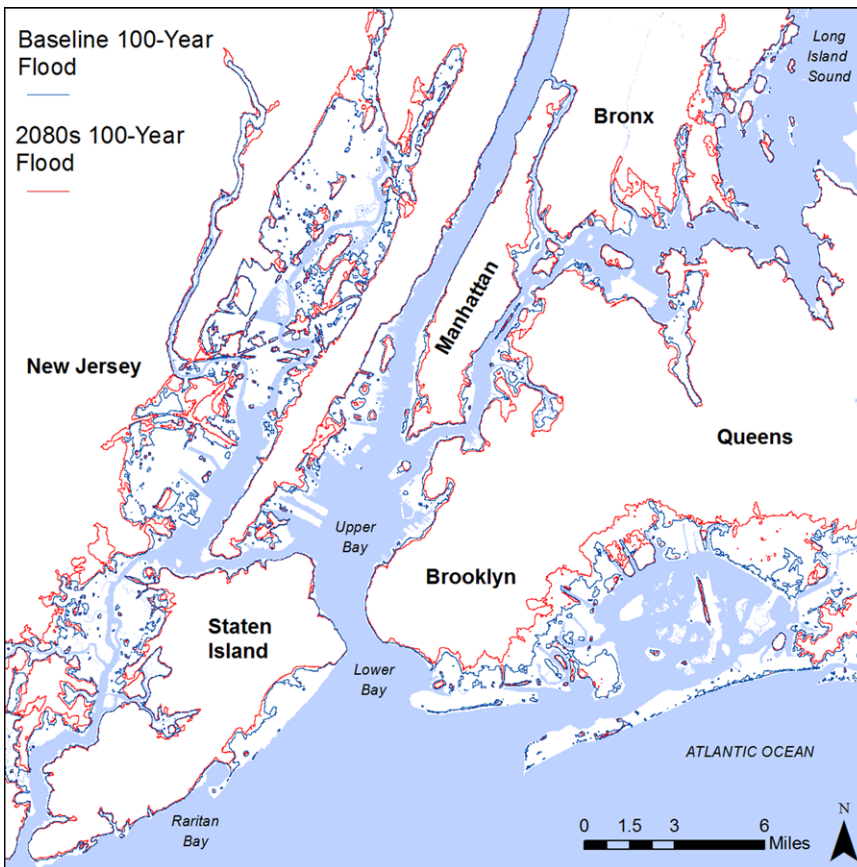


Figure 4.4. The 100-year flood zone for baseline sea level (mean sea level, 1983–2001, as used by FEMA) and for the NPCC2 2080s 90th-percentile sea level rise scenario using the dynamic model.

lower than those of the static mapping approach. These differences are likely related to several factors. First, as flood levels rise with sea level rise, the flood-plain cross-section across which the flood travels is expanding. Thus, some volume of water is spreading outward and inland instead of just rising upward as noted in a prior study of the area (Moore *et al.*, 1981). Second, the result could be related to interactions between the tide and the storm surge or to changes to the resonance of the tides (e.g., Zhong *et al.*, 2008). Third, the differences could also be related to the frictional effects of wetlands (e.g., Resio and Westerink, 2008). These and other mechanisms need to be evaluated further.

There are also a small number of locations where the static methods underestimate future flood heights by more than 0.5 feet. For example, Midland Beach dynamic results for the 2050s are greater than the static results by more than 0.5 feet,

yet for the 2020s and 2080s they are equal or in one case lower than the static results (the 2080s 500-year water elevation) (Table 4.1). These dynamic modeling results for Midland Beach are also found in FEMA’s results for 100-year flood elevations, where the lowest-lying area of Midland Beach has ~0.5 feet lower stillwater elevations than the surrounding more elevated regions.

The results at Midland Beach stem from two combined factors: (1) the dominance of only one extratropical cyclone in the FEMA assessment; and (2) the placement of the low-lying neighborhood behind an elevated waterfront land berm, which makes the statistical analysis of flood zones complex. In the FEMA study, areas that are not flooded for a given storm are referred to as “upland points” (FEMA, 2014b), and the dynamic model-based statistics are supplemented for nonflooding storms with water elevations from nearby flooded areas (effectively

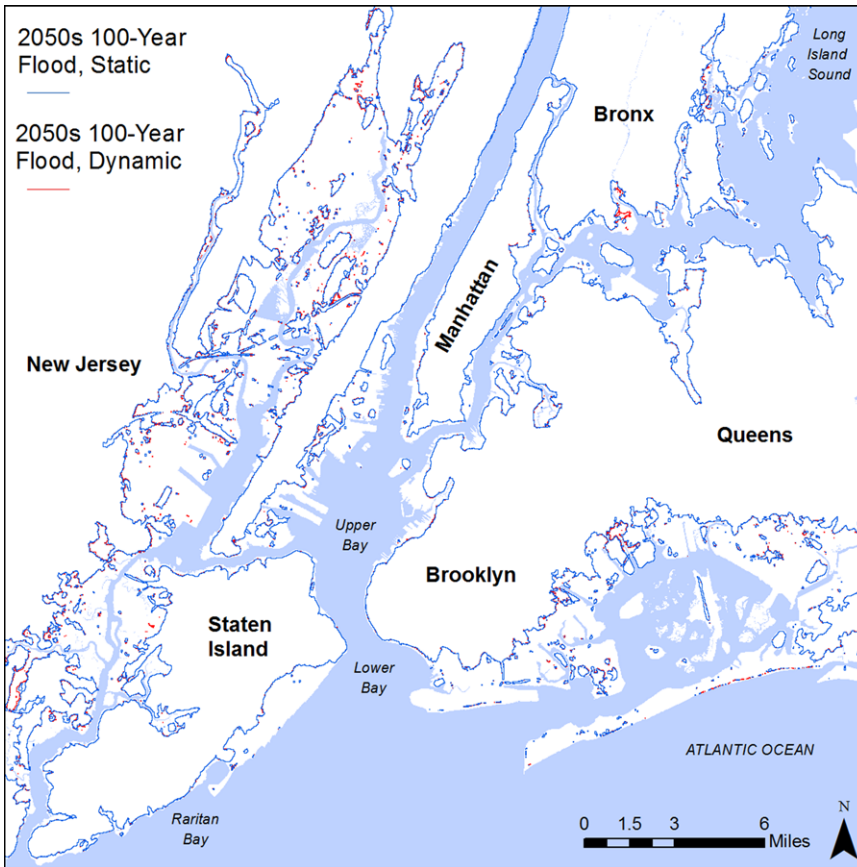


Figure 4.5. Comparison of dynamic model and static flood area contours for the 100-year flood area of the NPCC2 2050s 90th-percentile sea level rise scenario.

a static flood-mapping method). The combination of these two factors leads to erratic results in the assessment of the impact of sea level rise for Midland Beach; however, berm-protected sites are relatively rare in the broader New York metropolitan region.

Cases where the dynamic and static results differ by more than 0.5 feet are more widespread in the case of flooding from tropical cyclones only (Fig. 4.6, bottom). The difference between these results for the combined flood assessment (Fig. 4.6, top; note different color scales) occurs because the extratropical cyclone 100-year flood height is higher than the tropical cyclone 100-year flood height in the FEMA study, and thus, the extratropical cyclones more strongly influence the combined assessment. The larger differences (dynamic versus static) for tropical cyclones are likely driven by the very strong winds during tropical cyclones that can drive up

large sea level gradients, particularly in shallow areas of flooding. Friction and water velocity, which combine to reduce inland penetration of a fast-moving storm surge (e.g., a hurricane surge) and have less effect on a slow-moving storm surge (e.g., a nor'easter), also play a role.

These results indicate that the static flood-mapping approach is not always the “conservative” method (i.e., erring on the side of a high risk bias and therefore leading to a more risk-averse response) of estimating the effect of sea level rise on flood heights. Future studies should use both dynamic and static methods in the absence of funding constraints. Continuing use of static mapping methods allows for comparisons to previous assessments.

An ancillary benefit of dynamic modeling of flood hazards is the availability of the model for adaptation experiments. During the development of the City’s comprehensive climate resiliency plan,

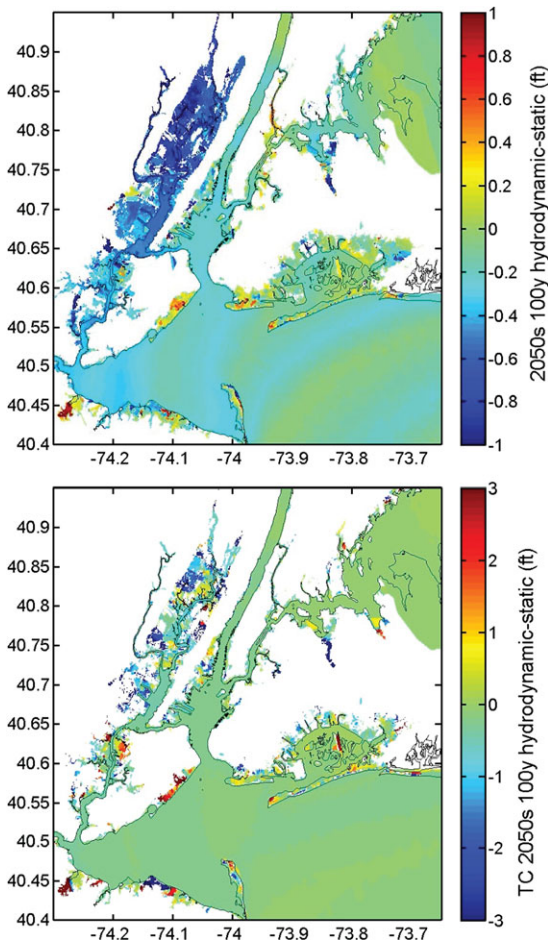


Figure 4.6. Difference between dynamic and static mapping results for 100-year flood elevations (NPCC2 2050s 90th-percentile sea level rise). Top panel shows results for the combined assessment of extratropical cyclones and tropical cyclones; bottom panel shows results for tropical cyclones only. Note difference in color scales.

A Stronger, More Resilient New York, dynamic modeling was used to test the effects of coastal adaptation options such as storm-surge barriers, breakwaters, and wetlands (City of New York, 2013b). The dynamic modeling provided quantitative information on the efficacy of these flood adaptations and on how they could be iteratively adjusted to address problems such as “backdoor flooding” (flood waters that do not go over high ground at the front of a barrier island but instead go around the low-lying area behind the island, as occurs with Coney Island).

Sensitivity analysis of storm climatology change

Storm climatology changes are changes to the frequencies or intensities of storms for a given area. Like sea level changes, storm climatology changes can alter return periods for a given flood level (Lin *et al.*, 2012). Recent evidence suggests this may already be occurring due to both regional reductions in aerosol emissions (Villarini and Vecchi, 2012) and atmospheric warming (Grinsted *et al.*, 2013; see Chapter 2). Grinsted *et al.* (2012) found a doubling of “Katrina-level” tropical cyclones in years with warm global air temperatures, based on analysis of historical tide gauge data in the U.S. East and Gulf Coasts.

A sensitivity test was conducted based on this finding, where the annual rates of tropical cyclones were doubled in the statistical analysis. For the same test no change was imposed for extratropical cyclones, as there is no consensus on how climate change will affect their storm surges in the New York metropolitan region (Chapter 2, NPCC, 2013). The results were that the 100-year and 500-year flood for the Battery increased by 0.7 and 0.6 feet, respectively, under doubled annual rates of tropical cyclones. These are relatively small increases compared to the increases driven by sea level rise because extratropical cyclones dominate the impact of storm surge in the FEMA and NPCC2 assessments. For a discussion of this dominance, see the last three paragraphs of the next section.

Study limitations

The use of NPCC2 90th-percentile, high-end projections of sea level rise is useful for conservative, risk-averse planning, but the lack of a similar assessment using median estimates of sea level rise is a limitation of this study. The sea level rise projections are near-worst-case scenarios for the specific future decades that the projections are targeting.

Besides uncertainty in the amount of projected sea level rise, there is also uncertainty about the time it will take to arrive at a given amount. Sea level rise is expected to occur and to be unavoidable due to greenhouse gases already added to the atmosphere, but the exact amount and timing are difficult to project (see Chapter 2 of Levermann *et al.*, 2013). However, the conclusions of this chapter on the differences between dynamic and static coastal flooding calculation methods are independent of

Table 4.1. 100-year and 500-year still water elevations (NAVD88) for baseline 1983–2001 sea level^a and future decades with NPCC2 sea level rise projections, comparing dynamic (D) and static (S) modeling results

Sea level	The Battery, Manhattan				Howard Beach, Queens				Midland Beach, Staten Island			
	100-year return (ft)		500-year return (ft)		100-year return (ft)		500-year return (ft)		100-year return (ft)		500-year return (ft)	
	D	S	D	S	D	S	D	S	D	S	D	S
Baseline (1983– 2001)	11.3	–	14.8	–	9.7	–	12.5	–	11.7	–	16.0	–
2020s	12.3	12.3	15.7	15.8	10.8	10.7	13.5	13.6	12.7	12.7	16.8	17.0
2050s	13.8	14.0	17.3	17.5	12.6	12.4	15.4	15.2	15.0	14.4	19.3	18.7
2080s	15.9	16.2	19.4	19.7	15.0	14.7	17.6	17.5	16.6	16.6	19.6	20.9

^aThe 1983–2001 values are from the current NPCC2 statistical analysis and are nearly identical (within 0.1 ft) to FEMA’s results. However, the earlier NPCC Climate Risk Information 2013 report cites baseline (1983–2001) values for the Battery that are 0.4–0.5 ft lower (10.8, 14.4 ft). This difference arose because the earlier NPCC report utilized a location from the FEMA FIRMs in Battery Park, whereas the work for this chapter utilizes the location of the in-water tide gauge in the FIRMs for the purposes of historical comparison and cross-comparisons with other studies.

the uncertainty in the rate at which the sea level rise occurs.

This NPCC2 study relied on the FEMA hazard assessment approach, which is an extremely detailed study of the region’s storms and flooding; yet the FEMA approach has limitations. One limitation is that Hurricane Sandy is not included in the storm set because the storm climatology assessment was completed before Sandy hit the New York metropolitan region. This raises the question of how Sandy’s storm track and record-setting storm surge would have affected results. Future studies will need to utilize data for Hurricane Sandy as well as more recent storms to build a more complete storm climatology in what are currently data-poor conditions.

A further limitation is that tropical cyclones in the New York metropolitan region often take on extratropical characteristics (Colle *et al.*, 2008), as was the case with Sandy (Blake *et al.*, 2013). The FEMA study utilized representations of idealized tropical cyclones (e.g., Fig. 4.1) that lack the more complex characteristics of extratropical cyclones. Further study of hybrid storms, transitions between tropical and extratropical storms, and methods for representing synthetic tropical cyclone wind and pressure fields will be useful for improving the accuracy of future hazard assessment studies.

The FEMA study found that the hazard assessment results for New York Harbor at the Battery for the flood elevations of 100- and 500-year storm tides are influenced predominantly by the extratropical cyclones. However, a recent study has recovered storm tide data from the 1800s and has shown that the three highest storm tides from 1821 to the present were either tropical cyclones (the major storm of 1821 and Hurricane Donna in 1960) or tropical-extratropical hybrid storms (Sandy) (Talke *et al.*, 2014). Yet, the largest *storm surge* within the time period used by FEMA (1927–2009) was an extratropical cyclone on November 25, 1950, at 7.6 feet. That storm surge peaked at the time of low tide, and the *storm tide* was only the sixth highest from 1821 to present (Talke *et al.*, 2014). Thus, the relative importance of extratropical cyclones, tropical cyclones, and hybrid storms for defining the region’s flood hazards is an important topic for further research.

Uncertainties in flood hazard assessment for the New York metropolitan region (e.g., defining the 100-year flood elevation) are large, and more research should be done on historical events and on hazard assessment methods to reduce these uncertainties. The recent FEMA hazard assessment found substantially higher estimates of 100-year and 500-year storm tides for New York City (except

for the upper East River and Long Island Sound) than those of other studies or data analyses.

For example, the FEMA (2014a) estimate of the 100-year flood elevation at the Battery tide gauge is 11.3 feet (NAVD88), whereas a statistical analysis by NOAA of observed storm tides from 1893 to 2013 results in a 100-year flood elevation of 7.86 feet (NAVD88) (<http://tidesandcurrents.noaa.gov/est>), a difference of 3.4 feet. Putting this into perspective, Hurricane Sandy produced an 11.3-foot storm tide at the Battery. Prior to the new FEMA study, FEMA's old estimate for the 100-year flood elevation was estimated to be 8.6 feet (NAVD88) based on USACE Waterways Experiment Station Implicit Flood Model results in the 1980s (Horton *et al.*, 2010). A recent study of tropical cyclone storm tides concluded that the 100-year tropical cyclone storm tide is 6.45 feet (NAVD88) (Lin *et al.*, 2012), compared with the FEMA 100-year tropical cyclone storm tide of 8.83 feet (FEMA, 2014a). Discrepancies for 500-year storm tides are similarly large. Again, further research is needed to understand and reduce these large discrepancies and uncertainties.

4.4 Conclusions and recommendations

The static and dynamic flood-mapping methods for projecting the effects of sea level rise on coastal flood elevations in the New York metropolitan region give similar results for most locations, usually within ± 0.5 feet. Therefore, the flood zone boundaries produced from these two methods are very similar.

In a small number of areas, the methods differ by more than 0.5 feet. These exceptions are geographically more widespread in regard to flooding from tropical cyclones (hurricanes) than from extratropical cyclones (nor'easters).

Uncertainties in flood hazard assessment for the New York metropolitan region (e.g., defining the 100-year flood elevation) and in the rate of future sea level rise are much larger than differences between the dynamic and static flood-mapping methods. Recent studies assessing the present-day 100-year flood elevation for the Battery have differed substantially (a range of 3.4 feet), while the 80% uncertainty range (90th percentile minus the 10th percentile) in NPCC2 sea level rise predictions for the 2080s is 3.75 feet.

Research recommendations

More research should be done on historical storm events and on hazard assessment methods to reduce the uncertainty in defining New York City flood hazards. The 100-year and 500-year flood heights from FEMA's (2014a) present-day hazard assessment are influenced predominantly by the extratropical cyclones, but new storm tide data from the 1800s demonstrate that the three highest storm tides from 1821 to the present came from tropical cyclones.

Future dynamic modeling efforts should study a broader set of sea level scenarios. However, computational dynamic modeling of storm surges for hazard assessment is time intensive, and this limits the potential for simulating many different scenarios. Therefore, either faster models, different statistical techniques, or a much larger allocation of computational resources will be required.

Research is needed to understand the geography and storm conditions that cause some locations to have higher (or lower) dynamic modeling flood heights than static flood-mapping heights.

Resiliency recommendations

Dynamic modeling identified some locations in the New York metropolitan region where results differed from static flood-mapping methods. Therefore, it is recommended that dynamic modeling continue to be used alongside static flooding assessments as resources allow. An ancillary benefit of dynamic modeling of flood hazards is the ability to conduct adaptation experiments such as testing locations for storm surge barriers.

For more complete probabilistic risk analyses and cost-benefit studies in the context of sea level rise and adaptation strategies for important infrastructure and coastal land-use planning, it would be highly advisable to consider the storm tide elevations for much longer recurrence periods (e.g., 1000 to 5000 years), together with a thorough quantification of their uncertainties.

Acknowledgments

This research was supported by FEMA Region II and the City of New York Office of Emergency Management and Office of Long-Term Planning and Sustainability, through FEMA's Cooperating Technical Partnership grant program as well as by a National Oceanic and Atmospheric Administration (NOAA) Regional Integrated Sciences and

Assessments (RISA) program project (Consortium for Climate Risk in the Urban Northeast), and by a NOAA Coastal Ocean Climate Applications project (Award NA12OAR4310107). This research was also supported in part by a grant of computer time from the City University of New York High-Performance Computing Center under NSF Grants CNS-0855217, CNS-0958379, and ACI-1126113. Special thanks to Hugh Roberts, Zach Cobell, Casey Dietrich, Alan Niederoda, Taylor Asher, Chris Reed, Gabriel Toro, Paul Muzio, Andrew Martin, Alan Springett, Cynthia Rosenzweig, Daniel Bader, Leah Cohen, Carrie Grassi, and others at their respective organizations.

References

- Blake, E.S., T.B. Kimberlain, R.J. Berg, *et al.* 2013. *Tropical Cyclone Report: Hurricane Sandy (AL182012)*. Miami, FL: National Hurricane Center.
- Booij, N., L. Holthuijsen, and R. Ris. 1996. The “SWAN” wave model for shallow water. *Coastal Engineering Proceedings*. **1**: 668–676.
- City of New York. 2013a. Chapter 2: Climate Analysis. In *A Stronger, More Resilient New York*. New York: New York City Economic Development Corporation.
- City of New York. 2013b. Chapter 3: Coastal Adaptation. In *A Stronger, More Resilient New York*. New York: New York City Economic Development Corporation.
- Colle, B.A., F. Buonaiuto, M.J. Bowman, *et al.* 2008. New York City’s vulnerability to coastal flooding. *Bull. Am. Meteorol. Soc.* **89**: 829–841.
- Colle, B.A., K. Rojowsky, and F. Buonaiuto. 2010. New York City storm surges: climatology and an analysis of the wind and cyclone evolution. *J. Appl. Meteorol. Climatol.* **49**: 85–100.
- FEMA. 2014a. *Region II Coastal Storm Surge Study: Overview*. Washington, DC: Federal Emergency Management Agency.
- FEMA. 2014b. *Final Draft Report: Joint Probability Analysis of Hurricane Flood Hazards for New York–New Jersey*. Washington, DC: Federal Emergency Management Agency.
- Georgas, N., P. Orton, A. Blumberg, *et al.* 2014. The impact of tidal phase on Hurricane Sandy’s flooding around New York City and Long Island Sound. *J. Extreme Events* **01**: 1450006–16.
- Grinsted, A., J.C. Moore, and S. Jevrejeva. 2012. Homogeneous record of Atlantic hurricane surge threat since 1923. *Proc. Natl. Acad. Sci. USA* **109**: 19601–19605.
- Grinsted, A., J.C. Moore, and S. Jevrejeva. 2013. Projected Atlantic hurricane surge threat from rising temperatures. *Proc. Natl. Acad. Sci. USA* **110**: 5369–5373.
- Horton, R., V. Gornitz, M. Bowman, and R. Blake. 2010. Climate observations and projections. In *Climate Change Adaptation in New York City: Building a Risk Management Response*. C. Rosenzweig and W. Solecki, Eds. *Ann. N.Y. Acad. Sci.* **1196**: 41–62.
- Levermann, A., P.U. Clark, B. Marzeion, *et al.* 2013. The multimillennial sea-level commitment of global warming. *Proc. Natl. Acad. Sci. USA* **110**: 13745–13750.
- Lin, N., K. Emanuel, M. Oppenheimer, and E. Vanmarcke. 2012. Physically based assessment of hurricane surge threat under climate change. *Nature Climate Change* **2**: 462–467.
- Luetlich, R., J. Westerink, and N.W. Scheffner 1992. *ADCIRC: An Advanced Three-Dimensional Circulation Model for Shelves, Coasts, and Estuaries. Report 1. Theory and Methodology of ADCIRC-2DDI and ADCIRC-3DL*. Vicksburg, MS.
- Moore, C., S. Dendrou, and R. Taylor 1981. *New York City Flood Insurance Study Report no. 7*. Prepared for the New York Department of Environmental Conservation.
- NPCC. 2010. *Climate Change Adaptation in New York City: Building a Risk Management Response*. C. Rosenzweig and W. Solecki, Eds. *Ann. N.Y. Acad. Sci.* **1196**: 1–354.
- NPCC. 2013. *Climate Risk Information 2013: Climate Change Scenarios and Maps*. New York: New York City Panel on Climate Change.
- NPCC. 2015. *Building the Knowledge Base for Climate Resiliency: New York City Panel on Climate Change 2015 Report*. C. Rosenzweig and W. Solecki, Eds. *Ann. N.Y. Acad. Sci.* **1336**: 1–149.
- Orton, P., N. Georgas, A. Blumberg, and J. Pullen. 2012. Detailed modeling of recent severe storm tides in estuaries of the New York City region. *J. Geophys. Res.* **117**: C09030.
- Resio, D.T., and J.J. Westerink. 2008. Modeling the physics of storm surges. *Physics Today* **61**: 33–38.
- Sweet, W., C. Zervas, S. Gill, and J. Park. 2013. Section 6: Hurricane Sandy inundation probabilities today and tomorrow. *Bull. Am. Meteorol. Soc.* **94**: S17–S20.
- Talke, S., P. Orton, and D. Jay. 2014. Increasing storm tides at New York City, 1844–2013. *Geophys. Res. Lett.* **41**: 3149–3155.
- Villarini, G., and G.A. Vecchi. 2012. Twenty-first-century projections of North Atlantic tropical storms from CMIP5 models. *Nature Climate Change* **2**: 604–607.
- Zhang, K., Y. Li, H. Liu, *et al.* 2013. Comparison of three methods for estimating the sea level rise effect on storm surge flooding. *Climatic Change* **118**: 487–500.
- Zhong, L., M. Li, and M. Foreman. 2008. Resonance and sea level variability in Chesapeake Bay. *Cont. Shelf Res.* **28**: 2565–2573.

ANNALS OF THE NEW YORK ACADEMY OF SCIENCES

Issue: *Building the Knowledge Base for Climate Resiliency*

New York City Panel on Climate Change 2015 Report

Chapter 5: Public Health Impacts and Resiliency

Patrick L. Kinney,¹ Thomas Matte,² Kim Knowlton,^{1,3} Jaime Madrigano,⁴ Elisaveta Petkova,¹ Kate Weinberger,¹ Ashlinn Quinn,¹ Mark Arend,⁵ and Julie Pullen⁶

¹Mailman School of Public Health, Columbia University, New York, NY. ²New York City Department of Health and Mental Hygiene, New York, NY. ³Natural Resources Defense Council, New York, NY. ⁴School of Public Health, Rutgers University, New Brunswick, NJ. ⁵NOAA CREST, City College of New York, CUNY, New York, NY. ⁶DHS National Center of Excellence for Maritime Security, Stevens Institute of Technology, Hoboken, NJ

Address for correspondence: Patrick L. Kinney, Mailman School of Public Health, Columbia University, 722 West 168th Street New York, NY 10032

Contents

- 5.1 Coastal storms and flooding
- 5.2 Extreme heat
- 5.3 Air pollution, aeroallergens, and vector-borne, water-borne, and food-borne diseases
- 5.4 Resiliency recommendations
- 5.5 Research recommendations
- 5.6 Looking ahead

Introduction

Recent experience from Hurricane Sandy and high-temperature episodes has clearly demonstrated that the health of New Yorkers can be compromised by extreme coastal storms and heat events. Health impacts that can result from exposure to extreme weather events include direct loss of life, increases in respiratory and cardiovascular diseases, and compromised mental health. Other related health stressors—such as air pollution, pollen, and vector-borne, water-borne, and food-borne diseases—can also be influenced by weather and climate. Figure 5.1 illustrates the complex pathways linking extreme weather events to adverse health outcomes in New York City. New York City and the surrounding metropolitan region face potential health risks related to two principal climate hazards: (1) increasing temperatures and heat waves, and (2) coastal storms and flooding. The health impacts of these hazards depend in turn on myriad pathways, the most important of which are illustrated in the figure.

Although New York City is one of the best-prepared and most climate-resilient cities in the world, there remain significant potential vulnerabilities related to climate variability and change. As part of the NPCC2 process, a team of local climate and health specialists was mobilized to assess current vulnerabilities and to identify strategies that could enhance the resilience of New York City to adverse health impacts from climate events. The goal was to highlight some of the important climate-related health challenges that New York City is currently facing or may face in the future due to climate variability and change, based on emerging scientific understanding.

As indicated in Figure 5.1, health vulnerabilities can be magnified when critical infrastructure is compromised. Critical infrastructure is a highly complex, heterogeneous, and interdependent mix of facilities, systems, and functions that are vulnerable to a wide variety of threats, including extreme weather events. For example, delivery of electricity to households depends on a multi-faceted electrical grid system that is susceptible to blackouts that can occur during heat waves. These, in turn, can expose people to greater risk of contact with exposed wires or to greater heat stress due to failure of air conditioning. Understanding and predicting the impacts that extreme weather events may have on health in New York City require careful analysis of these interactions.

Two recent plans to enhance climate resiliency in New York City have been released. *A Stronger, More Resilient New York* (City of New York, 2013)

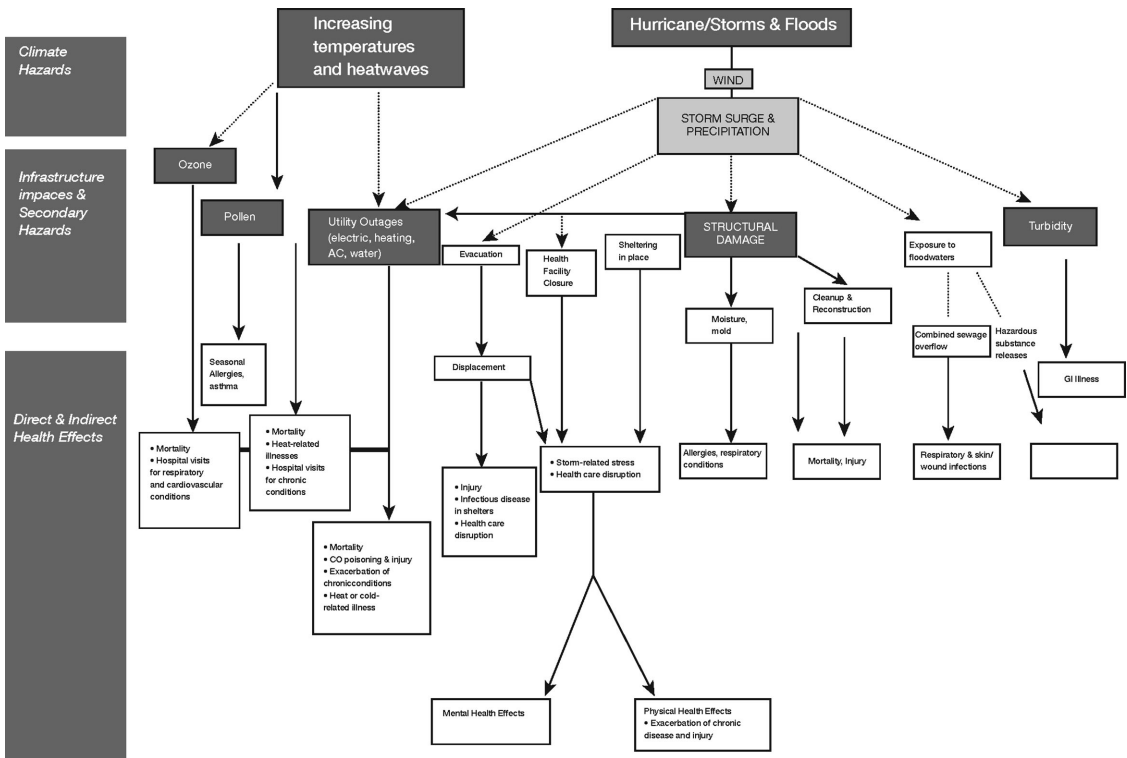


Figure 5.1. Pathways linking climate hazards to health impacts in New York City.

was developed in the aftermath of Hurricane Sandy by a task force of representatives from City agencies and consultants. This plan was informed by a detailed analysis of the impacts of Hurricane Sandy on infrastructure and the built environment and by the NPCC’s updated 2013 climate projections for the New York metropolitan region. It includes more than 250 initiatives and actionable recommendations addressing 14 domains of the built environment and infrastructure including the healthcare system and several other domains relevant to protecting public health.

In addition, the 2014 *New York City Hazard Mitigation Plan (HMP)* (City of New York, 2014), developed by the NYC Office of Emergency Management in collaboration with the Department of City Planning, updated the 2009 HMP and assesses risks from multiple hazards that threaten New York City. These include but are not limited to several climate-related hazards such as coastal storms and heat waves, and it lays out comprehensive strategies and plans to address these hazards. Many of the

measures recommended by *A Stronger, More Resilient New York* and the HMP have already been implemented, are in progress, or are planned (City of New York, 2013; 2014). This chapter does not include a detailed review of these plans, which would be beyond the expertise and charge of the contributors. Nonetheless, the recommendations in this chapter do broadly support the plans laid out in *A Stronger, More Resilient New York* and the 2014 HMP, and these are referenced at several points where they are especially relevant. Here we focus on summarizing and synthesizing the emerging scientific knowledge on climate-related health hazards, knowledge that can inform ongoing preparedness planning.

Key terms related to climate variability and change as they are applied in the health sector are defined in Box 5.1. This is followed by sections describing health risks, vulnerabilities, and resilience strategies for coastal storms and extreme heat events. We then briefly discuss the interactions of climate change with air pollution, pollen, vector-borne diseases, and water- and food-borne

Box 5.1. Definitions of key cross-cutting terms in the health context

Adaptation

Initiatives and measures to reduce the vulnerability of natural and human systems against actual or expected climate change effects. Various types of adaptation exist, such as anticipatory and reactive, private and public, and autonomous and planned. For health, physiological adaptation is also relevant.

Infrastructure

The man-made built environment and supporting systems and facilities, including buildings, land use (e.g., parks and green space), transportation systems, and utilities (e.g., electricity, running water).

Critical infrastructure

Systems and assets, whether physical or virtual, so vital to the United States that the incapacity or destruction of such systems and assets would have a debilitating impact on security, national economic security, national public health or safety, or any combination of those matters. In the health sector, examples include the electrical grid, water supply, and access to functioning health care facilities. Source: §1016(e) of the U.S. Patriot Act of 2001 (42 U.S.C. §5195c(e)).

Environmental public health indicators

Summary measures that provide information about a population's health status in relation to environmental factors. Ongoing collection, integration, analysis, and dissemination of indicators can be used to:

- Quantify the magnitude of a public health problem
- Detect trends in health, exposures, and hazards
- Identify populations at risk of environmentally related diseases or of exposure to hazards
- Generate hypotheses about the relationship between health and the environment
- Direct and evaluate control and prevention measures and individual actions
- Facilitate policy development

Source: U.S. CDC (2014).

Vulnerability

The propensity for the health of individuals or groups to be adversely affected as a result of exposure to a climate hazard. Vulnerability is an internal characteristic of the affected system and includes the characteristics of persons or groups and their situation that influence their capacity to anticipate, cope with, resist, and recover from an adverse climate event. Different levels of vulnerability will lead to different levels of health damage and loss under similar conditions of exposure to physical events of a given magnitude. Source: IPCC (2012).

Resilience

Resilience is the ability of a system and its component parts to anticipate, absorb, accommodate, or recover from the effects of a potentially hazardous event in a timely and efficient manner, including through ensuring the preservation, restoration, or improvement of its essential basic structures. Source: Lavell *et al.* (2012).

diseases. We conclude with recommendations for research and resiliency planning.

5.1. Coastal storms and flooding

Storm surge-related health risks will be compounded in the future as sea level continues to rise and with the potential for more intense storms in a changing climate (Lane *et al.*, 2013a; Chapter 2).

Large and growing numbers of people live near coasts and within areas likely to be impacted by coastal storms (Walsh *et al.*, 2014).

The health risks related to coastal storms can vary widely and in ways that are hard to predict due to differences in the severity, timing, and location of landfall, the topographic and infrastructure characteristics of affected areas, and the capacity for preparedness and response.

Storm health impact pathways

There are at least seven pathways through which storm events can adversely affect health, including:

1. Direct exposure to storm hazards
2. Evacuation
3. Exposure to secondary hazards related to utility outages and sheltering in place in inadequate housing after the storm
4. Exposure to secondary hazards including contaminated drinking water, contact with contaminated floodwaters, and mold and moisture in housing
5. Population displacement and disruption of services
6. Mental health effects from traumatic or stressful experiences during and after the storm
7. Health and safety risks from cleanup and recovery activities

These pathways and their interactions are elaborated in Figure 5.1. Storms can impact health not only through direct exposure to climate hazards such as wind and flood waters but also via a range of secondary hazards, many of which operate through disruptions in critical infrastructure. These hazards, for which few data often exist, can result in a range of short-term and long-term health outcomes.

Direct exposure to storm hazards. Adverse health effects due to direct exposure to storm hazards include deaths and injuries from drowning, electrocution, or physical trauma. All of these health effects were observed in the immediate aftermath of Hurricane Sandy (see Box 5.2). Flash flooding, due to excessive rainfall, although often a key risk factor for drowning during extreme storm events in many locations (French *et al.*, 1983; Rosenzweig *et al.*, 2011), is generally not a major threat to life safety in New York City and was not observed for Sandy.

Evacuation. Evacuation before, during, or after a storm event can result in health impacts, including those due to traffic accidents. An inability to evacuate in advance of a storm due to age, disability, or lack of economic resources, or an unwillingness to evacuate in order to protect one's home and/or property, increases vulnerability to direct storm hazards (Jonkman and Kelman, 2005; Zoraster, 2010). Evacuation from health care and nursing home facilities presents complex challenges because of the unique

needs of patients and elderly individuals (Klein and Nagel, 2007).

Secondary hazards from utility outages and sheltering in place. Widespread power outages can occur from storm events due to flooding and wind damage to infrastructure. Lack of electricity can make it difficult or impossible to control interior climate, refrigerate food, pump water to upper floors of high-rise buildings, move within buildings, and operate medical support equipment (Beatty *et al.*, 2006). These infrastructure disruptions can lead to a wide range of adverse health effects depending on the age, health, and economic resources of residents in the affected households. For example, exposure to ambient heat or cold in the absence of climate control may lead to heat- or cold-related illness or exacerbate underlying chronic conditions. Carbon monoxide poisoning from backup generators or cooking equipment used improperly is another potential risk. Increases in overall mortality rates have been observed after widespread power outages (Anderson and Bell, 2012).

Secondary hazards from contaminated drinking water, floodwaters, and mold and moisture. Intense rainfall and wind can compromise water quality via mobilization of pathogens and/or toxins. Untreated sewage in urban areas sometimes contaminates surface waters when heavy rainfall leads to combined sewer overflows. Toxic waste reservoirs can also disperse pollutants (Rotkin-Ellman *et al.*, 2010; Ruckart *et al.*, 2008). Flooding of structures is a strong risk factor for mold growth and may result in subsequent respiratory symptoms such as cough or wheeze and be a risk factor for childhood asthma exacerbation (Barbeau *et al.*, 2010; Jaakkola *et al.*, 2005).

Research conducted by the New York City Environmental Justice Alliance's (NYC-EJA)^a Waterfront

^aThe NYC-EJA is a nonprofit New York City-wide membership network linking grassroots organizations from low-income communities of color in their struggle for environmental justice. NYC-EJA coalesces its member organizations around common issues to advocate for improved environmental conditions and against inequitable burdens by coordinating campaigns designed to affect City and State policies. The Waterfront Justice Project is an advocacy campaign created by NYC-EJA to (1) research

Box 5.2. Hurricane Sandy and health in New York City

Hurricane Sandy showed in stark terms the extent to which the health of New Yorkers can be rapidly put at risk by powerful coastal storms. In its initial landfall on October 29, 2012, Sandy caused 44 deaths in New York City, nearly four-fifths of which occurred by drowning due to the storm-driven tidal surge. The remaining deaths were caused by falling trees, falls, electrocution, and other trauma. Nearly half of fatalities occurred among adults aged 65 or older. Although these deaths represent the most obvious and tragic impact of Sandy, they do not account for the storm's full impact on excess mortality from accidental and natural causes, as well as other nonfatal health impacts, in impacted communities.

Hurricane Sandy had substantial impacts due to its unusually large size and low pressure, a massive storm surge, and the fact that its landfall coincided with high tide (see Box 2.1). Further, impacts differed considerably across locations within the flood zone due to local variations in the storm and tidal surges, differing housing types, the extent to which energy, water, and/or transportation infrastructure was disrupted, and underlying population health and resilience.

Five acute-care hospitals in New York City shut down due to Sandy, three of which required evacuation of patients after the storm hit due to flooding and damage to energy infrastructure in lower floors (NYU Langone Medical Center, Bellevue Hospital, and Coney Island Hospital). Other health facilities affected by Sandy included a psychiatric hospital, nursing homes, long-term-care facilities, outpatient and ambulatory care facilities, community-based providers, and pharmacies.

After Hurricane Sandy made landfall, 2 million of New York City residents lost power at some point during the storm. However, even after the electric grid had been largely restored, many residential buildings in storm-inundated areas still lacked electric power, heat, or running water, often because of saltwater flood damage to electrical and heating systems. Many people who did not evacuate in advance of the storm sheltered in place in housing conditions that lacked one or more of these essential services.

Developing a fuller understanding of the health impacts of Sandy requires careful analysis of health data, only some of which have so far been available. For example, in the days following Sandy, health department surveillance data showed the impact of people living without power or heat and, in some cases, trying to provide power or heat in unsafe ways. From the storm impact until November 9 (10 days), carbon monoxide (CO)-related emergency department visits and Poison Control Center (PCC) calls related to CO exposure were elevated for the time of year; PCC data frequently identified storm-related sources of exposure including charcoal grills and household cooking appliances used for heating, as well as portable generators. Calls to the PCC about gasoline exposures, often due to siphoning, were also elevated, although no serious outcomes were reported (<http://www.ncbi.nlm.nih.gov/pubmed/24237625>). On the other hand, there was no observed increase in reportable infectious diseases (<http://www.ncbi.nlm.nih.gov/pubmed/24274131>).

A more complete accounting for immediate, delayed, and longer-term Sandy health impacts, including those related to health-care facilities, power outages, stress and mental health disorders, and flood damage to homes requires longer-term study and access to data that were not immediately available, such as all-cause mortality data, hospital discharge data, and follow-up surveys. Several ongoing studies aim to characterize these impacts with funding by the Centers for Disease Control and Prevention (http://www.cdc.gov/phpr/science/hurricane_sandy_recovery_research.html).

potential threats affecting industrial waterfront communities based on local vulnerabilities; (2) identify proactive policies and programs to promote climate resiliency that reflect local priorities; and (3) convene local communities, government agencies, and private-sector representatives to share priorities and resources. Current members

include UPROSE (Southwest Brooklyn), El Puente (North Brooklyn); Morningside Heights-West Harlem Sanitation Coalition (Upper Manhattan); Nos Quedamos (South Bronx); The Point CDC (South Bronx); Youth Ministries for Peace & Justice (South Bronx); and Sustainable South Bronx (South Bronx). For more information see: <http://www.nyc-eja.org>.

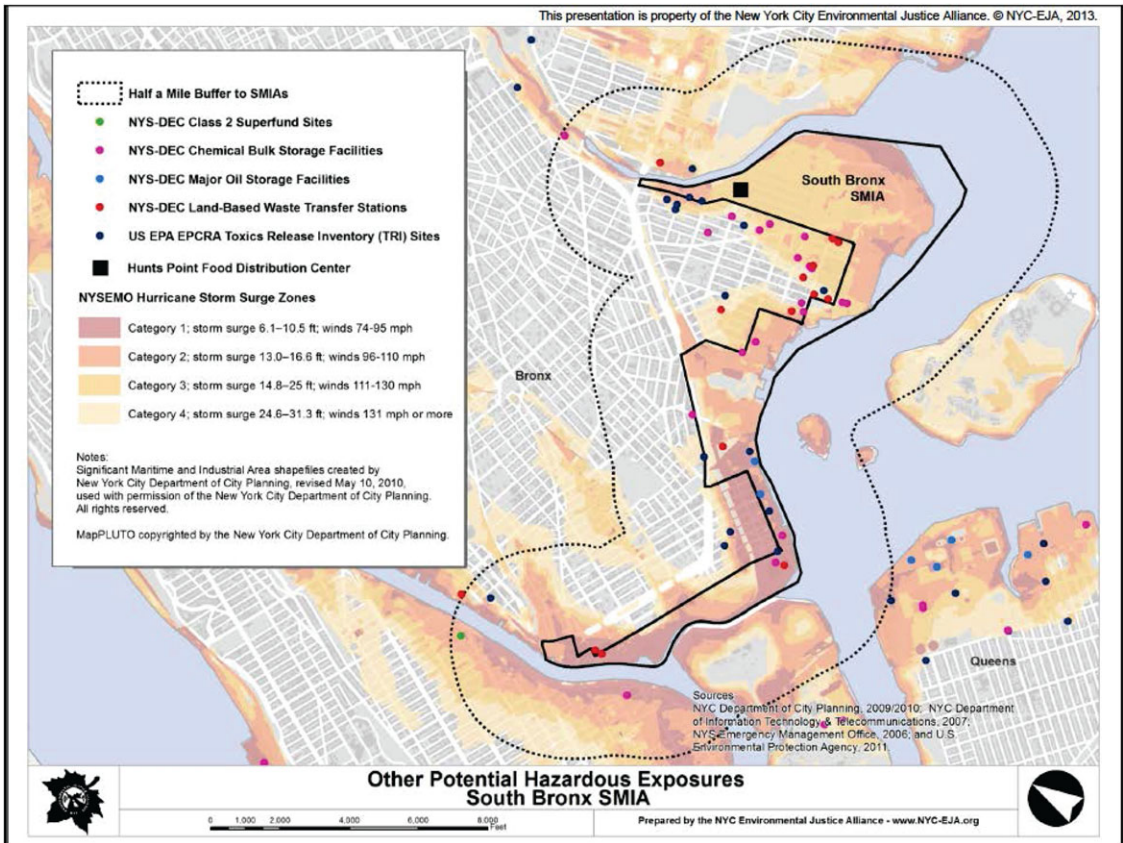


Figure 5.2. Storm surge zones and sources of potentially hazardous materials in the South Bronx. Source: Bautista *et al.*, 2014

Justice Project has raised awareness about how hazardous substances handled, stored, or transferred in waterfront industrial neighborhoods may be accidentally released in the event of storm surge. For example, Figure 5.2 shows the close proximity of industrial facilities, residential neighborhoods, and food distribution facilities to storm surge zones in the Hunts Point neighborhood of the South Bronx (NYC-EJA, 2014).

Damage to healthcare facilities, population displacement and disruption of services. As demonstrated by Hurricane Sandy, critical healthcare infrastructure can be damaged and made inoperable for extended periods by coastal flooding events (see *A Stronger, More Resilient New York: City of New York*, 2013). Institutions that provide care that can be impacted by coastal storms include hospitals, nursing homes, adult-care facilities, correctional facilities, primary and mental health-care facilities, and pharmacies.

In addition, for people who evacuate flood-prone neighborhoods, living for extended periods in shelters is associated with increased risk of communicable diseases and with interruption in medical care that could otherwise prevent complications from chronic health conditions (Arrieta *et al.*, 2009). Loss of medical record information, medications (including information regarding names and dosages), and access to routine medical care can exacerbate health problems.

Mental health. Exposure to direct and secondary storm hazards and their aftermath, including displacement, can have adverse consequences for mental health, exacerbating existing disease or contributing to new cases (Pietrzak *et al.*, 2012; Galea *et al.*, 2007). Post-traumatic stress disorder (PTSD) is a common observation following natural disasters. Some important predictors of mental-health impacts include storm-related physical illness or injury, physical adversity, and property loss. Mental

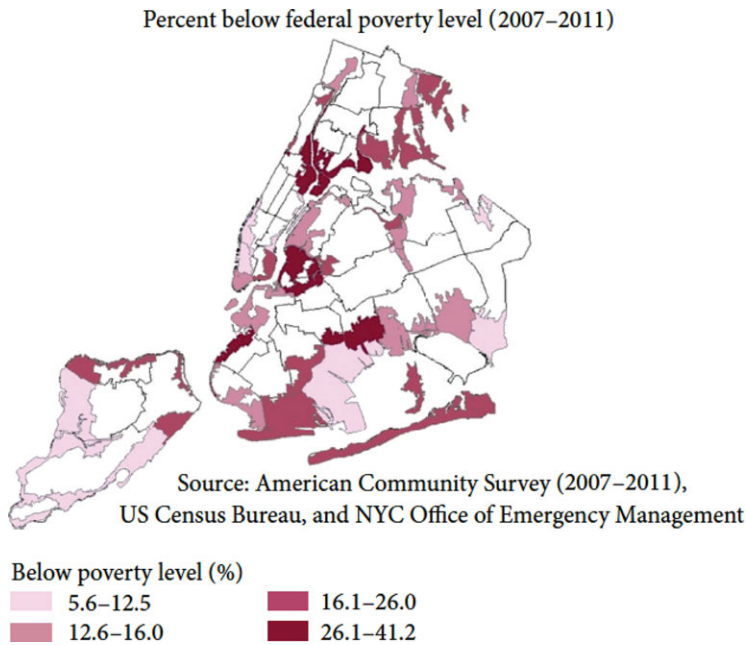


Figure 5.3. Poverty rate within 2012 NYC hurricane evacuation zones. Note that the prevalence estimates represent the entire United Hospital Fund neighborhood but are displayed only within the evacuation zone. Source: Lane *et al.* (2013a).

health impacts can linger or intensify long after storm events as emergency support services wind down; however, this is an area for which more study is needed.

Clean-up and recovery work. Recovery efforts can include risks related to demolition and renovation work, including traumatic injuries and exposure to dust and to fumes from temporary generators. Mold remediation can potentially expose workers as well as residents to unhealthy levels of mold if precautions are not taken.

Health vulnerability factors for storms

Although the pathways linking coastal storm events to adverse health outcomes are numerous and complex, increased vulnerability tends to be associated with a number of factors:

- Both the old and very young tend to be more vulnerable due to lack of mobility
- Women tend to be more vulnerable with respect to economic resources available for recovery
- Preexisting physical, mental, or substance-abuse disorders can impede safety-seeking behaviors

- Residents of low-income households have fewer resources for relocation and/or sheltering in place. Figure 5.3 maps the percentage of people living below poverty within New York City flood evacuation zones
- Workers engaged in recovery efforts, owing to their exposure to toxic contaminants and injury risks
- Those with weak social networks, hindering safety-seeking behaviors
- Those especially dependent on critical infrastructure such as electric power, putting them at risk of disruption of those services

Vulnerability tends to be greater where multiple individual factors are present.

Improving health resilience to coastal storms^b

On the basis of our experience with Hurricane Sandy as well as lessons learned from other coastal storm

^bRecommendations regarding improving health resiliency to coastal storms were distilled from discussions that occurred during the December 13, 2013 NPCC2 Health Workshop held at Columbia University's Mailman School of Public Health.

events, we can highlight several ways in which health resiliency can be enhanced in the face of coastal storm events.

Enhancing community engagement is critical.

Health resilience can be enhanced if communities in flood zones and evacuation zones are actively engaged to develop neighborhood-level climate-health vulnerability maps, deliver messages about ways to prepare for storms and other climate emergencies, create systems to locate vulnerable people, and disseminate information on locations of shelters and other types of care centers. Health impacts can be reduced by enhancing capacity for immediate post-storm door-to-door outreach, assessment of medical and other urgent needs, and assistance to populations stranded or sheltering in place, with a focus on the most vulnerable. To ensure effective responses, it is important to enhance communication among community-based volunteer organizations and government agencies involved in outreach and response.

Planning and preparation are needed for both short-term and long-term sheltering of evacuees. For those who take shelter, special effort is required to minimize the disruption of physical and mental health care and medication access. New York City's Hazard Mitigation Plan (City of New York, 2014) includes the City's Shelter Plan within the overall Coastal Storm Plan and describes efforts to develop more and improved post-disaster interim housing options.

Speedy restoration of electrical power and natural gas distribution and local delivery systems is key to public health protection in the aftermath of extreme weather events. People living in housing that lacks essential utilities (power, heat, and running water) face numerous health risks. Thus, measures to harden critical infrastructure against projected flooding and high wind risks will protect health as well as critical infrastructure. Transportation and communications infrastructure systems are also critical for public health.

Continuity of healthcare services is essential to protecting public health. Measures that can reduce disruptions of service delivery and/or speed recovery of services for the health system include building patient-care areas above flood elevation, elevating or flood-proofing back-up generators and

fuel and other essential building systems from storm damage, preparedness for hospital evacuation decision-making and safety, systems to track displaced clients/residents, backup communications systems, and plans to ensure continuity of care and safe sheltering in place at storm-hardened facilities. Many health-system resiliency measures are addressed in the City's Hazard Mitigation Plan (City of New York, 2014) and *A Stronger, More Resilient New York* (City of New York, 2013); some, including new design standards for facilities, are already being addressed in pending and enacted laws^c and initiatives.^d

5.2. Extreme heat

More frequent and more severe coastal flooding events are not the only climate-related health hazards faced by New York City due to climate change in the coming decades. Warming temperatures will result in longer and more intense summer heat waves.

Heat was the largest of weather-related^e causes of death in the United States in 2012, as it has been on average since NOAA began reporting data for heat in 1988 (NOAA, 2014). Furthermore, heat-related morbidity (disease events such as emergency room visits or hospital admissions) and mortality (deaths) are the most well understood, measurable, and yet preventable impacts of climate change on human health (Confalonieri *et al.*, 2007).

In recognition of the significance of these impacts, New York City is making substantial progress in building long-term resiliency to heat via enhanced messaging to the public and healthcare providers, advance warning of heat events, improved access to cooling centers, and other measures.

As are other large cities in the Northeast and upper Midwest of the United States and cities just over the border in Canada, New York City is particularly susceptible to the impacts of heat and will face challenges in the years to come. Factors that contribute to vulnerability in such cities include the urban heat island effect that can amplify the impacts of rising temperatures (Rosenzweig *et al.*, 2009) and a relatively high proportion of older housing stock

^c<http://www.nyc.gov/html/dob/downloads/pdf/1195of2013.pdf>.

^d<http://stormrecovery.ny.gov/e-FINDS>.

^eIncludes lightning, tornados, floods, hurricanes, and cold snaps.

Box 5.3. Heat: Key concepts

Heat exposure metrics

Various exposure metrics such as minimum, mean, or maximum temperature or composite indices of temperature, humidity, and/or other meteorological variables have been utilized to quantify the effects of heat on morbidity and mortality. In a recent analysis, various exposure metrics performed similarly as predictors of heat-related mortality in New York City (Metzger *et al.*, 2010).

Health and heat waves

Heat waves are broadly defined as periods of unusually hot weather over an extended period of time, relative to local conditions. In New York, a heat wave is defined as a period of at least three consecutive days with temperatures $\geq 90^{\circ}\text{F}$ (32°C) (See Chapter 1). However, it is worth noting that health impacts can occur when only one or two days of elevated temperatures are experienced.

NYC heat health warning system

In New York City, a citywide heat emergency response is triggered when an extreme heat event is forecast, defined as any one day reaching a heat index (HI)^f of 100°F or any two or more consecutive days reaching 95°F HI. These thresholds are based on studies of the relationship between temperature and excess mortality in NYC (Metzger *et al.*, 2010).

Urban heat island effect

“Urban heat island effect” refers to the occurrence of substantially higher temperatures (especially at night) within an urban area than in surrounding less-built-up areas. A recent study in New York City found that the city’s heat island effect can reach 8°F (Rosenzweig *et al.*, 2009). The urban heat island may enhance the health risks of climate-related warming.

that may be poorly adapted to hot weather and lack air conditioning compared to many southern U.S. cities. In addition to hotter summers expected in the years to come, New York City’s population is aging, and the prevalence of obesity in adults has been increasing. Being elderly, obese, and/or diabetic are risk factors for heat-related morbidity and mortality (Basu and Samet, 2002).

Evidence for heat and health responses

A large number of studies have characterized health responses during and following severe heat waves such as the European heat wave of 2003 (Le Tertre *et al.*, 2006) and the 1995 heat wave in Chicago (Whitman *et al.*, 1997; Klinenberg, 2002) (Box 5.3). Early studies in New York City focused on specific heat-wave episodes (Marmor, 1975; Ellis and Nelson, 1978). More recent studies have assessed health responses in relation to less severe but more

frequent temperature extremes. These more recent studies usually fit an exposure–response function that can be used to quantify the excess mortality that occurs when temperatures rise above certain levels (Fig. 5.4).

An example of a temperature exposure–health response function for Manhattan from Li *et al.* (2013) is reproduced in Figure 5.4. This shows that both cold and warm temperatures can increase risk of premature death. The gap in the curve at the bottom indicates the range of temperatures in Manhattan in which there is no observable mortality risk.

Most studies investigating the impacts of heat have focused on premature deaths (i.e., mortality) (Barnett, 2007; Basu *et al.*, 2008; Curriero *et al.*, 2002; Medina-Ramón and Schwartz, 2007). Heat has a direct impact on total daily deaths, with most deaths occurring on the same day or shortly after exposure to heat. Deaths due to specific causes also have been associated with high temperatures. For example, in New York City, daily deaths from cardiovascular disease were associated with higher warm-season temperatures in a recent study (Ito *et al.*, 2010). Most deaths occur at home, but studies

^fThe heat index (HI) or “apparent temperature” is an approximation of how hot it “feels” for a given combination of air temperature and relative humidity (American Meteorological Society, 2013).

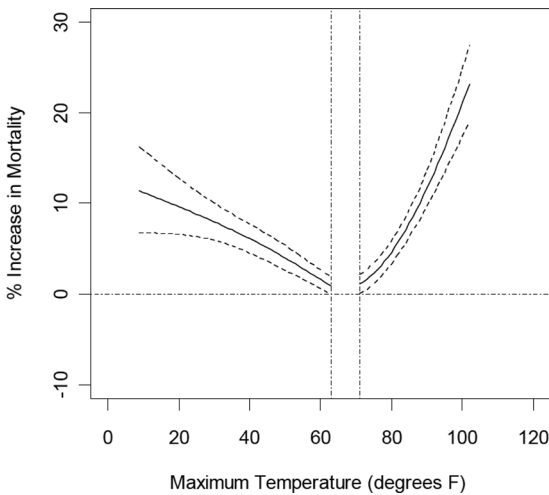


Figure 5.4. Exposure–response function for temperature-related mortality in Manhattan, NY, based on daily data from 1982 to 1999 (Li *et al.*, 2013). Both cold and warm temperatures are associated with increased risk of premature death. The dashed lines indicate the 95% confidence bounds.

have also reported an increase in emergency room visits and hospital admissions for heat-sensitive diseases during heat episodes (Knowlton *et al.*, 2006; Lin *et al.*, 2009). According to a recent report based on data between 2000 and 2011, approximately 447 heat-related emergency department visits, 152 hospital admissions, and 13 deaths occurred annually in New York City (U.S. CDC, 2013c). Exposure to elevated temperatures may also have an impact on birth outcomes. For example, a recent study reported an association between high ambient temperature and pre-term births (Basu *et al.*, 2010).

Heat-related deaths determined on death certificates often underestimate the full burden because of difficulties in establishing a conclusive diagnosis, especially for the large number of deaths that occur at home during extreme heat events (Nixdorf-Miller *et al.*, 2006) (see Box 5.4). After a severe 10-day heat wave in New York City in 2006, for example, there were only approximately 40 deaths coded as heat stroke on death certificates, whereas there were 100 excess deaths that occurred in association with the heat wave as determined by NYC DOHMH (2006).

Morbidity and mortality effects of heat may be especially severe if a blackout occurs during an extreme heat event. Blackouts are more likely during heat waves due to the increased demand for electric power for air conditioning, an effect that places stress on the systems that supply and deliver electric-

ity. On the other hand, air conditioning provides important protection from exposure to heat, limiting health impacts. When blackouts occur, exposure to heat increases, with a corresponding increase in health risks. Blackouts can also increase risk of carbon monoxide poisoning from improper use of generators and cooking equipment.

During August 2003, the largest blackout in U.S. history occurred in the Northeast. Although this particular blackout did not coincide with a heat wave, it occurred during warm weather and resulted in approximately 90 excess deaths and an increase in respiratory hospitalizations (Lin *et al.*, 2012; Anderson and Bell, 2012). As a result of higher summertime temperatures (with a corresponding increase in electricity usage) and an already-stressed electricity grid, climate change may bring frequent blackouts. Other indirect health impacts of heat may be associated with increased violence and crime (Hsiang *et al.*, 2013).

Projecting future heat-related health risks in a changing climate. Projecting potential future health impacts from warming temperatures involves linking together projections about future climate, the underlying health status of the population, the size and age distribution of the population, and the exposure–response function.

A recent study by Li and colleagues used down-scaled temperature projections from an ensemble of 16 global climate models and two greenhouse gas emission scenarios (high and low) to project heat-related mortality in Manhattan over the current century in the face of climate change (Li *et al.*, 2013). Results are summarized in Figure 5.5, which plots statistically estimated heat-related deaths in an 18-year baseline period centered on the 1980s, and projected heat-related deaths in three future decades.

Comparisons of recent heat impacts with mortality reported during severe heat waves in the 1970s suggest that in New York City vulnerability to heat waves may be decreasing over time, as has been reported in other locations (Carson *et al.*, 2006). A recent study by Columbia University documents a decreasing trend in heat impacts over the 20th century (Petkova *et al.*, 2014). Increasing use of home air conditioning and better air quality during heat waves may have played a role in reducing vulnerability. Vulnerability aside, continuing climate

Box 5.4. Definitions of heat-related deaths

Two different approaches are commonly employed to quantify the impacts of high ambient temperatures on deaths:

- The first identifies individual deaths that have been listed as heat-related on death certificates.
- The second estimates “statistical heat-related deaths” based on a statistical analysis of deaths from total daily death counts in relation to daily temperatures.

The advantage of the first method—based on death certificates—is that this information is available quickly, and these deaths can be individually counted and investigated to better understand risk factors, including housing conditions, the presence of air conditioning, levels of social isolation, and other factors that are key to informing prevention. However, this method substantially underestimates the total burden of heat-related deaths.

The advantage of the second method—based on statistical analysis—is that it potentially provides a fuller accounting for the total burden of heat-related deaths. However, the statistical analyses require multiple years of data as inputs, averaged over time and the population. In addition, there is no standardized method for the statistical estimation of heat deaths, leading to inconsistencies across assessments.

warming and urbanization mean more people will migrate to cities, and more people will be exposed to extreme heat. Whether future trends in these parameters or the growing populations of elderly and obese individuals in New York City will produce a net increase or decrease in heat-related health outcomes is uncertain.

Vulnerability mapping

Several studies have found that certain subpopulations—the elderly, African-Americans, and those with less education—are more susceptible to the health impacts of temperature (Anderson and Bell, 2009; Medina-Ramón *et al.*, 2006). A recent investigation in New York City (J. Madrigano, personal communication, 2014) found that during heat waves (compared to other warm-season days), deaths were more likely to occur in African-American individuals than other groups, more likely to occur at home than in institutions and hospital settings, and more likely among those living in census tracts where more households received public assistance. Finally, deaths during heat waves were more likely among residents in areas of the city with higher relative daytime summer surface temperature and less likely among residents living in areas with more green space. Air conditioning prevalence also varies among New York City neighborhoods (NYC DOHMH, 2007).

Understanding within-city vulnerability can help guide efforts to prevent heat-related deaths, including urban planning measures that apply susceptibility and exposure information to prioritize urban heat island reduction efforts, public messaging during heat waves, and provision of air conditioners and electric power subsidies (Lane *et al.*, 2013b).

At-home deaths could be a marker of social isolation, lack of mobility, or both. In previous major heat waves in Chicago (1995) and Paris (2003), social isolation and lack of mobility were determined to be major risk factors for death (Semenza *et al.*, 1996; Vandentorren *et al.*, 2006). Public-awareness campaigns on the dangers posed by extreme heat events could help encourage New Yorkers to check in on neighbors and relatives who may be particularly vulnerable.

The burden of heat-related mortality experienced by socioeconomically disadvantaged populations is likely the result of a complex interplay of factors, but one explanatory factor is the lack of access to air conditioning. A recent telephone survey indicated that approximately 11% of New Yorkers do not have a functioning air conditioner, and an additional 14% do not use their air conditioner regularly (Lane *et al.*, 2013b). The most frequently cited reason for lack of air conditioning ownership was cost, followed by the perception that it was not needed and a dislike of air conditioning. In addition to making air conditioning and cooling centers accessible,

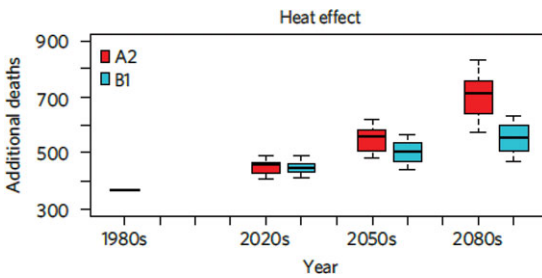


Figure 5.5. Distribution of heat-related deaths in the 1980s (observed), 2020s, 2050s, and 2080s for 16 global climate models and two greenhouse gas emission scenarios. The A2 scenario assumes relatively high, and the B1 assumes relatively low, greenhouse gas emissions over the 21st century. Source: Li *et al.* (2013).

emphasis also needs to be placed on educating New York City residents on heat health risks and how they can be alleviated.

Climate health indicators are measurable characteristics that potentially offer tools to track or give early warning of more complex health-relevant climate conditions. Some of the top-priority proposed health indicators for New York City and the New York metropolitan region that emerged from NPCC2 discussions are shown in Table 5.1 with a complete listing in Appendix IIE (NPCC, 2015).

Improving health resilience to heat extremes

A range of measures is available to reduce heat-health risks before and during extreme heat events.^g

Programs are needed to enhance availability of air conditioning for people who are most vulnerable to heat. They should also aim to improve energy efficiency, curtail wasteful use of air conditioning in overcooled spaces, implement urban heat island mitigation measures, and reduce overall citywide power demand during heat waves. A lack of air conditioning at home increases the risk of heat-related death (O’Neill *et al.*, 2005). However, air conditioning also contributes to higher electrical demand during heat waves, which increases the risk of power disruptions or blackouts and increases emissions of greenhouse gases.

The city operates large numbers of cooling shelters during heat emergencies, although a relatively

small proportion of vulnerable New Yorkers use them (Lane *et al.*, 2013b). It is therefore especially important to identify and enhance outreach to assist vulnerable individuals—those who are old, sick, and poor—with getting to a cool place or staying cool at home. This can operate through caregivers, community organizations, neighbors, and so on. Improved health education around heat extremes will assist in this regard.

Urban-scale cooling strategies are needed. Because green spaces reduce local temperatures (Harlan *et al.*, 2006), tree planting can be an important strategy for urban cooling, especially when targeted to vulnerable neighborhoods. Green and light-colored roofs are additional strategies with potential for local cooling. Several ongoing New York City programs are contributing to reducing impacts of the urban heat island^h (see Chapter 6, NPCC, 2015).

The development and application of a heat-health vulnerability index, mapped to the block level, can help to target urban heat interventions. In the longer term, building design standards can be revised to reduce heat load related to facades and other building treatments and improve passive ventilation and thermal performance, especially during power outages.

Health resiliency during extreme heat events depends on a well-functioning electrical grid. Robust electrical infrastructure, especially in vulnerable neighborhoods and public housing, is thus essential.

5.3. Air pollution, aeroallergens, and vector-borne, water-borne, and food-borne diseases

New York City residents face a variety of climate-related health impacts in addition to the direct effects of storms and extreme heat. Four important additional risks are air pollution, aeroallergens, vector-borne diseases, and water and food-borne diarrheal illnesses.

^gHere we summarize suggestions discussed at the December 13, 2013, NPCC2 Health Workshop held at Columbia University’s Mailman School of Public Health.

^hNYC Cool Roofs (<http://www.nyc.gov/html/coolroofs/html/home/home.shtml>); MillionTreesNYC (<http://www.milliontreesnyc.org/html/home/home.shtml>); Green Infrastructure Plan (http://www.nyc.gov/html/dep/html/stormwater/nyc_green_infrastructure_plan.shtml).

Table 5.1. Proposed priority Climate–Health Indicators for New York City (see Appendix IIE (NPCC, 2015) for detailed, complete set of suggested indicators).

Climate hazard	Type of indicator	Indicator
Heat	Health outcome	<ul style="list-style-type: none"> • Emergency department visits and hospital admissions for heat illness • Heat stroke deaths • Excess natural-cause mortality
Heat	Vulnerability	<ul style="list-style-type: none"> • Surface temperature • % vegetative cover
Power outages	Health outcome	<ul style="list-style-type: none"> • Carbon monoxide (CO) exposure incidents • CO hospital admissions and emergency department visits • CO deaths
Extreme weather	Health outcome	<ul style="list-style-type: none"> • Injuries and death due to extreme weather events
Coastal storms/floods	Vulnerability	<ul style="list-style-type: none"> • Storm surge zones that take into account regularly updated climate projections • Health facilities and critical infrastructure located within storm surge zones
Heat, power outages	Vulnerability	<ul style="list-style-type: none"> • % with no air conditioning
All	Vulnerability	<ul style="list-style-type: none"> • % aged ≥ 5 years with a disability • % below federal poverty line

Air pollution

Climate change has the potential to increase morbidity and mortality from respiratory and cardiovascular causes through its effects on air pollution. Respiratory diseases such as childhood asthma are a major public health challenge in New York City, and cardiovascular disease is the most common cause of death in New York State (NYC DOHMH, 2003; U.S. CDC, 2008). In 2008, asthma prevalence among children in New York State was 10.8% compared to 9.4% in the United States as a whole (U.S. CDC, 2010; 2011). Within New York City, asthma prevalence varies dramatically among neighborhoods, with the prevalence of asthma among children under the age of 5 in New York City neighborhoods varying from 3% to 19% (NYC DOHMH, 2003).

An important air pollutant in the context of climate change is ground-level ozone, which is produced on hot, sunny days from a combination of nitrogen oxides, carbon monoxide, and volatile organic compounds. Ozone production is dependent on temperature and the presence of sunlight, with higher temperatures and still, cloudless days leading to increased production. Thus, ground-level ozone concentrations have the potential to increase in some regions in response to climate change (Ebi

and McGregor, 2008; Tsai *et al.*, 2008; Cheng *et al.*, 2011; Polvani *et al.*, 2011; Hogrefe *et al.*, 2004).

Exposure to ozone is associated with decreased lung function, increased premature mortality, increased cardiopulmonary mortality, increased hospital admissions, and increased emergency room visits (Dennekamp and Carey, 2010; Kampa and Castanas, 2008; Kinney, 2008; Smith *et al.*, 2009). In New York City, ozone-related emergency room visits for asthma among children under the age of 18 have been projected to rise by 7.3% by the 2020s versus the 1980s as the result of climate change-induced increases in ozone concentrations (Sheffield *et al.*, 2011a). The New York Climate and Health Project, a multidisciplinary study of climate change and human health in the New York metropolitan area, reported potential increases in ozone-related deaths in New York City ranging from 4% to 6% across the five boroughs by 2050 (Fig. 5.6) (Knowlton *et al.*, 2008).

Particulate matter (PM) is another important air pollutant in New York City from a human health perspective. The most health-relevant PM is emitted by the combustion of fuels—by cars, diesel vehicles, power plants, and heating systems. Combustion particles are small enough to penetrate deep into lungs and contain toxic components. Some

Other aeroallergens such as mold also contribute to the burden of respiratory and allergic disease and have been linked to indoor air quality (IAQ) and climate change (IOM, 2011). Increased temperatures, coastal flooding, and heavy precipitation events can present ideal conditions for the growth of mold and other fungi in the indoor environment (Fisk *et al.*, 2007; Mudarri and Fisk, 2007; Wolf *et al.*, 2010; Spengler, 2012) (see Section 5.1, above).

Vector-borne diseases

Vector-borne diseases are spread by organisms such as ticks and mosquitoes. Cases of several types of vector-borne diseases have been reported in New York State, including Lyme disease, West Nile virus, and dengue fever (Knowlton *et al.*, 2009; Centers for Disease Control and Prevention, 2013a). Vector-borne disease incidence is influenced by climate factors such as temperature and precipitation, on multiple timescales. For example, there is evidence that the Lyme disease vector, the tick species *Ixodes scapularis*, has expanded its range northward into Canada over the last several decades in part due to warming temperatures (Ogden *et al.*, 2009, 2010). Thus, climate change may lead to changes in the seasonal cycle and spatial distribution of some vector-borne diseases or even expand their ranges, although it is important to note that climate is only one of many drivers of vector-borne disease distribution (Lafferty, 2009; McGregor, 2012; Wilson, 2009).

Water- and food-borne illnesses

Humans can be exposed to water- and food-borne pathogens through a variety of routes, including through the consumption of polluted drinking water and ingestion of contaminated food (Rose *et al.*, 2001). A number of pathogens that cause water and food-borne illnesses in humans are sensitive to projected climate parameters, including increased temperature, changing precipitation patterns, more frequent extreme precipitation events, and associated changes in seasonal patterns in the hydrological cycle. Although specific relationships vary by pathogen, increased temperatures appear to increase the incidence of common North American diarrheal diseases such as campylobacteriosis and salmonellosis (Curriero *et al.*, 2001; European Centre for Disease Prevention and Control, 2012; Semenza *et al.*, 2012). Water-borne illnesses from exposures to pathogens in recreational waters increase in the hours after extreme rainfall events and

are projected to increase in the Great Lakes region as climate change continues (Patz *et al.*, 2008).

Improving resilience to public health threats

Air pollution. Because ozone production is especially sensitive to warming temperatures, strategies to control anthropogenic emissions of ozone precursors, including nitrogen oxides from vehicles and other fuel-combustion sources, and volatile organic compounds from fuel storage and refueling operations, will be more important than ever in a changing climate. New York City and surrounding regions are frequently exposed to unhealthy levels of ozone concentrations and other air pollutants.ⁱ Because of the regional nature of ozone, success in reducing episodic ozone concentrations necessitates a regional approach via cooperation with upwind states and cities. New York City should also consider enhancing early-warning systems for forecasted air pollution episodes, keeping in mind the potential compounding influences of heat waves and ozone precursors.

Aeroallergens. In the short term, health impacts from earlier or more severe pollen seasons can be potentially reduced by early-warning systems that inform patients and health-care providers at the start of the pollen season so they have adequate supplies of allergy and asthma medications. Populations who lack access to primary care need to be reached through other means. New York City should include allergenicity as a criterion for species selection in future tree-planting programs.

Vector-borne diseases. Surveillance of infected disease vectors is an integral part of health systems to enhance resilience to risks, including networks to routinely trap and analyze vector organisms such as mosquitos and ticks. Long-term surveillance of vectors should take place not only in areas where they are known to exist but also in areas where they may expand to in a warming climate in order to assess range expansion as well as the introduction of invasive species. Health professionals and the general public need to be educated about the signs and symptoms of now-rare diseases that may occur more often with projected climate change, such as dengue fever. Mosquito vector control can be enhanced via

ⁱ www.epa.gov/airtrends/ozone.html#ozloc.

the reduction of standing water and community education about the importance of reducing it.

Water- and food-borne illnesses. Continued and enhanced protection of New York City's watershed in the face of changing development, temperature, and precipitation patterns will be essential to ensuring an adequate supply of fresh water over the coming decades. Stormwater drainage is another critical infrastructure system in New York City. Extreme rain events can overwhelm the capacity of the combined sewer system, leading to direct contamination of surrounding waters by untreated sewage. Efforts to retain and slow the drainage of storm water via green infrastructure can address this problem to some extent (Rosenzweig *et al.*, 2011). Assessments of the water quality and heat island benefits of these initiatives are needed.

5.4. Research recommendations

Further knowledge generation will be essential for New York City to anticipate and avoid future health impacts from extreme weather events in a changing climate. To promote research that has the greatest potential value for resiliency planning, it is recommended that a climate-health partnership involving local university researchers and city practitioners be established and supported. Recognizing that information needs will evolve over time, the NPCC2 Health Work Group identified a set of immediate areas in which research knowledge is needed.

Specific near-term research recommendations include

- **Evaluate and quantify the efficacy of cool roofs** and other urban heat island mitigation measures for public health protection.
- **Understand the factors (structural, behavioral, etc.)** that lead to unhealthy levels of exposure to heat inside New York City apartment buildings, where most deaths occur during heat events.
- **Develop vulnerability indicators of health risks** from both coastal storms and extreme heat events that can be applied at fine spatial (e.g., block or neighborhood) scales to target resiliency initiatives.
- **Examine risks of coupled extreme events.** Worst-case health impacts could occur when

multiple climate-related extreme events happen simultaneously or in rapid succession, for example, a heat event followed by a coastal storm and/or an air pollution episode. Research is needed to examine these scenarios, quantify their probabilities and health impacts, and devise response strategies.

- **Conduct studies that couple infrastructure system failures with human health impacts.** Analysis and quantification of linkages between critical infrastructure systems and human health would provide essential information for risk planning in New York City.
- **Evaluate expansion of the current syndromic heat-illness surveillance program,** a NYC DOH initiative that tracks emergent cases of heat-related illnesses at hospitals, to more locations in the New York metropolitan region to aid in early warning for communities with disproportionate heat-health burdens.
- **Analyze and quantify potential health co-benefits and possible negative consequences of climate adaptation and mitigation** measures at the local level in New York City, including effects on indoor air quality. Take actions to mitigate greenhouse gas emissions and adapt to warming temperatures that result in reductions in air pollution or changes in other health-relevant factors such as increased green space or physical activity.

5.5. Resiliency recommendations

In reviewing the current knowledge base on climate impacts and vulnerability in New York City, we identify several opportunities for further resiliency planning. These generally fall within the broad categories of *engagement* with preparedness planning; *enhancement* of social networks and linkages; and *evaluation* of existing resilience efforts with a health lens.

Coastal storms

New York City has a number of programs and initiatives under way to build resilience to more intense coastal flooding in response to projected climate change effects on sea level rise and storm surge. Strategies addressing community preparedness and infrastructure measures are described in the City's Hurricane Sandy After Action Report, the NYC

Hazard Mitigation Plan, and *A Stronger, More Resilient New York*.^j

The NPCC2 Health Workgroup highlighted short-term and long-term recommendations to build health-related coastal storm resilience in New York City.

Short-term resilience strategies include:

- **Enhance communications to vulnerable sites, neighborhoods, and populations.** This should draw on baseline surveys of locational risks including industrial waste sites, concentrations of at-risk or isolated populations, neighborhoods with infrastructure problems and locations (e.g., schools and daycare centers that often become shelters). Working with leaders in the most vulnerable communities and at-risk populations, the City should conduct flood emergency drills and practices, prioritizing public housing.
- **Leverage local community-based organizations, social networks, and business leaders in designing effective targeted responses.** Businesses and community-based organizations that assess baseline vulnerability should evaluate potential hazardous exposures and disproportionate health impacts immediately postflooding. Rapid-response teams that assess pre- and post-storm impacts and infrastructure breakdowns in highly vulnerable neighborhoods should include community groups, social networks, and health and safety professionals.

Infrastructure improvements for longer-term flood resiliency include:

- **Assess public health aspects of New York City's resiliency plan.** The city's resiliency investments in critical infrastructure are crucial—not only to prevent future damage and promote faster recovery but also for protecting against adverse health impacts from these events. It is important to understand the complex linkages between infrastructure and

health in New York City and to use this knowledge to anticipate and account for the health improvements that can be achieved via infrastructure investments.

Heat events

Although some programs are already in place to adapt to more frequent, intense, and longer-lasting heat waves in New York City, several preparedness gaps have been identified.

Recommendations for short-term resilience strategies to enhance heat-wave preparedness in New York City include:

- **Enhance communication before heat waves, targeting those most at risk.** Heat-risk awareness should be targeted to vulnerable populations and their caregivers (e.g., doctors, teachers, meals-on-wheels programs) and include pharmacists who should provide information about heat-health risks when they disperse medications that increase susceptibility to heat illness.
- **During heat waves, ensure access to cool indoor spaces while avoiding power outages.** Approaches to increasing use of cooling centers in high-risk areas should be considered. Consideration should also be given to the needs of people who are unable to travel to cooling centers. Neighbor look-in programs to check on people at risk from heat stress should be activated.
- **Develop robust public messaging that promotes use of air conditioning by those who are vulnerable while discouraging excessive cooling of residential and commercial spaces.** Ample evidence exists of the benefits of air conditioning for people most vulnerable to heat-related health risks.
- **Expand use of multimedia to reduce vulnerabilities.** Wider use of mobile devices, social media, and mainstream media to disseminate heat warnings can help reduce health risks, especially for prolonged heat waves and complex disasters.

Recommendations for longer-term resilience strategies that could enhance New York City's heat-wave preparedness include:

^j *Hurricane Sandy After Action Report* (City of New York, 2013), *Hazard Mitigation Plan* (City of New York, 2014), and *A Stronger, More Resilient New York* (City of New York, 2013).

- **Conduct urban heat island vulnerability assessments.** Develop a combined heat vulnerability index that includes local exposures and susceptibilities to target and prioritize urban heat island interventions in the hottest city neighborhoods and perform before/after health outcome evaluations.
- **Develop programs for built environment upgrades** to increase green spaces, making sure all buildings have windows that can open and provide air conditioners to those who need relief from heat but cannot afford the cost of purchase or operation.
- **Improve energy resilience** of the power grid by increasing energy efficiency and using alternative energy sources for cooling, especially in vulnerable neighborhoods and public housing. To reduce electrical load, the City should combine heat island mitigation (white roofs, greening, etc.), efficiency improvements, expanded marketing of voluntary conservation measures (such as setting thermostats to avoid excessive cooling), and promoting—in collaboration with electric utilities—expanded participation in load-shaving programs.

5.6. Looking ahead

New York City is in the fortunate position of having a wealth of research capacity for projecting how climate change will affect flooding and extreme heat conditions locally. These NPCC2 projections afford the city a certain independence from relying on federal agency sources for these data. However, it is increasingly important for federal agencies to provide a national source of locally relevant information on the effects of climate change (Parris, 2014). The inclusion of sea level rise in FEMA's flood risk maps is one example.^k One pathway for provision of regionally focused climate information is NOAA's Regional Integrated Science and Assessment (RISA) network. In particular, the NOAA-funded Consortium for Climate Risks in the Urban Northeast (CCRUN) is a source of climate information for urban decision-makers in the northeastern states.^l

^kSee <http://www.globalchange.gov/browse/sea-level-rise-tool-sandy-recovery>.

^l<http://www.ccrun.org>.

To advance the recommendations in this chapter, New York City should improve its ability to monitor and evaluate the ongoing local effects of climate change on the public's health (see Chapter 6 of NPCC, 2015). This means establishing networks to monitor climate-health indicators, such as emergency room visits and hospital admissions for heat illness, or injuries and deaths due to extreme weather events, and actively supporting their operation and long-term maintenance in New York City and the surrounding metropolitan region. Other important data needs relate to expanded monitoring of pollen levels and disease vectors over time and space in New York City. Gathering information on these health indicators should become part of the City's standard operating procedure. This will establish baselines and build a suite of city- and neighborhood-specific climate-health indicators for analysis of trends over time.

References

- Anderson, B.G., and M.L. Bell. 2009. Weather-related mortality: how heat, cold, and heat waves affect mortality in the United States. *Epidemiology* **20**: 205–213.
- Anderson, G.B., and M.L. Bell. 2012. Lights out: impact of the August 2003 power outage on mortality in New York, NY. *Epidemiology* **23**: 189–193.
- Arrieta, M.I., R.D. Foreman, E.D. Crook, and M.L. Icenogle. 2009. Providing continuity of care for chronic diseases in the aftermath of Katrina: from field experience to policy recommendations. *Disaster Med. Publ. Health Prep.* **3**: 174–182.
- Barbeau, D.N., L.F. Grimsley, L.E. White, *et al.* 2010. Mold exposure and health effects following Hurricanes Katrina and Rita. *Annu. Rev. Publ. Health* **31**: 165–178.
- Barnett, A.G. 2007. Temperature and cardiovascular deaths in the US elderly: changes over time. *Epidemiology* **18**: 369–372.
- Basu, R., and J.M. Samet. 2002. Relation between elevated ambient temperature and mortality: a review of the epidemiologic evidence. *Epidemiol. Rev.* **24**: 190–202.
- Basu, R., W.Y. Feng, and B.D. Ostro. 2008. Characterizing temperature and mortality in nine California counties. *Epidemiology* **19**: 138–145.
- Basu, R., B. Malig, and B. Ostro. 2010. High ambient temperature and the risk of preterm delivery. *Am. J. Epidemiol.* **172**: 1108–1117.
- Bautista, E., E. Hanhardt, J.C. Osorio, and N. Dwyer. 2014. New York City Environmental Justice Alliance Waterfront Justice Project. *Local Environment*, 1–19.
- Beatty, M.E., S. Phelps, C. Rohner, and I. Weisfuse. 2006. Blackout of 2003: public health effects and emergency response. *Public Health Reports* **121**: 36–44.
- Bjorksten, F., I. Suoniemi, and V. Koski. 1980. Neonatal birch-pollen contact and subsequent allergy to birch pollen. *Clin. Exp. Allergy* **10**: 585–591.

- Cakmak, S., R.E. Dales, R.T. Burnett, *et al.* 2002. Effect of airborne allergens on emergency visits by children for conjunctivitis and rhinitis. *Lancet* **359**: 947–948.
- Carson, C., S. Hajat, B. Armstrong, and P. Wilkinson. 2006. Declining vulnerability to temperature-related mortality in London over the 20th century. *Am. J. Epidemiol.* **164**: 77–84.
- Centers for Disease Control and Prevention (U.S. CDC). 2010. Current asthma prevalence percents by age, United States: National Health Interview Survey, 2008. Available online at <http://www.cdc.gov/asthma/nhis/08/table4-1.htm>.
- Centers for Disease Control and Prevention (U.S. CDC). 2011. Asthma in New York state. Available online at http://www.cdc.gov/asthma/stateprofiles/Asthma_in_NYS.pdf.
- Centers for Disease Control and Prevention (U.S. CDC). 2013a. *New York: Burden of Chronic Diseases*. Available online at http://www.cdc.gov/chronicdisease/states/pdf/new_york.pdf.
- Centers for Disease Control and Prevention (U.S. CDC). 2013b. Current asthma prevalence percents by age, United States: National Health Interview Survey 2008. Available online at <http://www.cdc.gov/asthma/nhis/08/table4-1.htm>.
- Centers for Disease Control and Prevention (U.S. CDC). 2013c. Heat Illness and Deaths—New York City, 2000–2011. Available online at <http://www.cdc.gov/mmwr/pdf/wk/mm6231.pdf>.
- Centers for Disease Control and Prevention (U.S. CDC). 2014a. *Asthma in New York State*. Available online at http://www.cdc.gov/asthma/stateprofiles/Asthma_in_NYS.pdf.
- Centers for Disease Control and Prevention (U.S. CDC). 2014b. *Environmental Public Health Tracking*. Available online at <http://ephtracking.cdc.gov/showIndicatorsData.action>.
- Cheng, C.H., S.F. Huang, and H.J. Teoh. 2011. Predicting daily ozone concentration maxima using fuzzy time series based on a two-stage linguistic partition method. *Comput. Math. Appl.* **62**: 2016–2028.
- City of New York. 2013. Healthcare. In *A Stronger, More Resilient New York*.
- City of New York. 2013. *Hurricane Sandy After Action Report: Report and recommendations to Mayor Michael R. Bloomberg*.
- City of New York. 2014. *City of New York, Hazard Mitigation Plan*.
- Confalonieri, U., *et al.* 2007. Human health. In *Climate Change 2007: Impacts, Adaptation, and Vulnerability. Contribution of Working Group II to the Fourth Assessment Report of the Intergovernmental Panel on Climate Change*, M.L. Parry, O.F. Canziani, J.P. Palutikof, *et al.*, Eds. Cambridge: Cambridge University Press, 391–431.
- Curriero, F.C., J.A. Patz, J.B. Rose, and S. Lele. 2001. The association between extreme precipitation and waterborne disease outbreaks in the United States, 1948–1994. *Am. J. Epidemiol.* **91**: 1194–1199.
- Curriero, F.C., K.S. Heiner, J.M. Samat, *et al.* 2002. Temperature and mortality in 11 cities of the eastern United States. *Am. J. Epidemiol.* **155**: 80–87.
- D’Amato, G., and L. Cecchi. 2008. Effects of climate change on environmental factors in respiratory allergic diseases. *Clin. Exp. Allergy* **38**: 1264–1274.
- D’Amato, G., L. Cecchi, M. D’Amato, and G. Liccardi. 2010. Urban air pollution and climate change as environmental risk factors of respiratory allergy: an update. *J. Invest. Allergol. Clin. Immunol.* **20**: 95–102.
- Darrow, L.A., J. Hess, C.A. Rogers, *et al.* 2012. Ambient pollen concentrations and emergency department visits for asthma and wheeze. *J. Allergy Clin. Immunol.* **130**: 630–638.
- Delfino, R.J., R.S. Zeiger, J.M. Seltzer, *et al.* 2002. Association of asthma symptoms with peak particulate air pollution and effect modification by anti-inflammatory medication use. *Environ. Health Perspect.* **110**: A607–A617.
- Delfino R.J., N. Staimer, T. Tjoa, *et al.* 2010. Associations of primary and secondary organic aerosols with airway and systemic inflammation in an elderly panel cohort. *Epidemiology* **21**: 892–902.
- Dennekamp, M., and M. Carey. 2010. Air quality and chronic disease: why action on climate change is also good for health. *N.S.W. Public Health Bull.* **21**: 115–121.
- Diaz-Sanchez, D., A. Tsein, J. Fleming, and A. Saxon. 1997. Combined diesel exhaust particulate and ragweed allergen challenge markedly enhances human in vivo nasal ragweed-specific IgE and skews cytokine production to a T helper cell 2-type pattern. *J. Immunol.* **158**: 2406–2413.
- Diaz-Sanchez, D., M.P. Garcia, M. Wang, *et al.* 1999. Nasal challenge with diesel exhaust particles can induce sensitization to a neoallergen in the human mucosa. *J. Allergy Clin. Immunol.* **104**: 1183–1188.
- Ebi, K.L., and G. McGregor. 2008. Climate change, tropospheric ozone and particulate matter, and health impacts. *Environ. Health Perspect.* **116**: 1449–1455.
- Ellis, F.P., and F. Nelson. 1978. Mortality in the elderly in a heat wave in New York City, August 1975. *Environ. Res.* **15**: 504–512.
- Emberlin, J., M. Detandt, R. Gehrig, *et al.* 2002. Responses in the start of *Betula* (birch) pollen seasons to recent changes in spring temperatures across Europe. *Int. J. Biometeorol.* **46**: 159–170.
- European Center for Disease Control and Prevention. 2012. Assessing the potential impacts of climate change on food- and waterborne diseases in Europe.
- Finlay, S.E., A. Moffat, R. Gazzard, *et al.* 2012. Health impacts of wildfires. *PLoS Currents* **4**.
- Fisk, W.J., Q. Lei-Gomez, and M.J. Mendell. 2007. Meta-analyses of the associations of respiratory health effects with dampness and mold in homes. *Indoor Air* **17**: 284–296.
- French, J., R. Ing, S.V. Allmen, and R. Wood. 1983. Mortality from flash floods: a review of national weather service reports, 1969–81. *Public Health Rep.* **98**: 584–588.
- Galea, S., *et al.* 2007. Exposure to hurricane-related stressors and mental illness after Hurricane Katrina. *Arch. Gen. Psychiatry* **64**: 1427–1434.
- Gutiérrez, E., J.E. González, R. Bornstein, *et al.* 2013. A new modeling approach to forecast building energy demands during extreme heat events in complex cities. *J. Sol. Energy Eng.* **135**: 040906.
- Handmer, J., *et al.* 2012. Changes in impacts of climate extremes: human systems and ecosystems. In *Managing the Risks of Extreme Events and Disasters to Advance Climate Change Adaptation. A Special Report of Working Groups I and II of the Intergovernmental Panel on Climate Change*, C.B. Field *et al.*, Eds. Cambridge: Cambridge University Press. 231–290.

- Harlan, S.L., A.J. Brazel, L. Prashad, *et al.* 2006. Neighborhood microclimates and vulnerability to heat stress. *Soc. Sci. Med.* **63**: 2847–2863.
- Hogrefe, C., B. Lynn, K. Civerolo, J. Y. Ku, *et al.* 2004. Simulating changes in regional air pollution over the eastern United States due to changes in global and regional climate and emissions. *Journal of Geophysical Research: Atmospheres* **109**: D22301.
- Hsiang, S.M., M. Burke, and E. Miguel. 2013. Quantifying the influence of climate on human conflict. *Science* **341**: 1235367.
- Institute of Medicine (IOM). 2011. *Climate Change, the Indoor Environment, and Health*. Washington, DC: National Academies Press.
- IPCC. 2012. Managing the Risks of Extreme Events and Disasters to Advance Climate Change Adaptation. A Special Report of Working Groups I and II of the Intergovernmental Panel on Climate Change [Field, C.B., V. Barros, T.F. Stocker, D. Qin, D.J. Dokken, K.L. Ebi, M.D. Mastrandrea, K.J. Mach, G.-K. Plattner, S.K. Allen, M. Tignor, and P.M. Midgley (eds.)]. Cambridge University Press, Cambridge, UK, and New York, NY, USA, 582 pp.
- Ito, K., R. Mathes, Z. Ross, *et al.* 2010. Fine Particulate Matter Constituents Associated with Cardiovascular Hospitalizations and Mortality in New York City. *Environmental health perspectives* **119**: 467–473.
- Jaakkola, J.J.K., B.F. Hwang, and N. Jaakkola. 2005. Home dampness and molds, parental atopy, and asthma in childhood: a six-year population-based cohort study. *Environ. Health Perspect.* **113**: 357–361.
- Jonkman, S.N., and I. Kelman. 2005. An analysis of the causes and circumstances of flood disaster deaths. *Disasters* **29**: 75–97.
- Kampa, M., and E. Castanas. 2008. Human health effects of air pollution. *Environ. Pollution* **151**: 362–367.
- Kihlström, A., G. Lilja, G. Pershagen, and G. Hedlin. 2003. Exposure to high doses of birch pollen during pregnancy, and risk of sensitization and atopic disease in the child. *Allergy* **58**: 871–877.
- Kinney, P.L. 2008. Climate change, air quality, and human health. *Am. J. Prev. Med.* **35**: 459–467.
- Kistemann, T., A. Rechenburg, C. Höser, *et al.* 2012. Assessing the potential impacts of climate change on food- and waterborne diseases in Europe.
- Klein, K.R., and N.E. Nagel. 2007. Mass medical evacuation: Hurricane Katrina and nursing experiences at the New Orleans airport. *Disaster Manage. Resp.* **5**: 56–61.
- Klinenberg, E. 2002. *Heat wave: a social autopsy of disaster in Chicago*. Chicago: University of Chicago Press.
- Knowlton, K., G. Solomon & M. Rotkin-Ellman. 2009. Fever pitch: Mosquito-borne dengue fever threat spreading in the Americas. Natural Resources Defense Council (July 2009 Issue Paper), 22 pp.
- Knowlton, K., C. Hogrefe, B. Lynn, *et al.* 2008. Impacts of heat and ozone on mortality risk in the New York City metropolitan region under a changing climate. In *Seasonal Forecasts, Climatic Change and Human Health*, M.C. Thomson, R. Garcia-Herrera, and M. Benniston, Eds. Dordrecht: Springer Netherlands, 143–160.
- Knowlton, K., M. Rotkin-Ellman, G. King, *et al.* 2009. The 2006 California heat wave: impacts on hospitalizations and emergency department visits. *Environ. Health Perspect.* **117**: 61–67.
- Knowlton, K., *et al.* 2004. Assessing ozone-related health impacts under a changing climate. *Environ. Health Perspect.* **112**: 1557–1563.
- Lafferty, K.D. 2009. The ecology of climate change and infectious diseases. *Ecology* **90**: 888–900.
- Lane, K., K. Charles-Guzman, K. Wheeler, *et al.* 2013a. Health effects of coastal storms and flooding in urban areas: a review and vulnerability assessment. *J. Environ. Public Health* **15**: 1–13.
- Lane, K., *et al.* 2013b. Extreme heat awareness and protective behaviors in New York City. *J. Urban Health*, **91**: 403–414.
- Lavell, A., M. Oppenheimer, C. Diop, *et al.*, 2012: Climate change: new dimensions in disaster risk, exposure, vulnerability, and resilience. In: Managing the Risks of Extreme Events and Disasters to Advance Climate Change Adaptation [Field, C.B., V. Barros, T.F. Stocker, D. Qin, D.J. Dokken, K.L. Ebi, M.D. Mastrandrea, K.J. Mach, G.-K. Plattner, S.K. Allen, M. Tignor, and P.M. Midgley (eds.)]. A Special Report of Working Groups I and II of the Intergovernmental Panel on Climate Change (IPCC). Cambridge University Press, Cambridge, UK, and New York, NY, USA, pp. 25–64.
- Le Tertre, A., *et al.* 2006. Impact of the 2003 heatwave on all-cause mortality in 9 French cities. *Epidemiology* **17**: 75–79.
- Li, T., R.M. Horton, and P.L. Kinney. 2013. Projections of seasonal patterns in temperature-related deaths for Manhattan, New York. *Nature Clim. Change* **3**: 717–721.
- Lin, S., M. Luo, R.J. Walker, *et al.* 2009. Extreme high temperatures and hospital admissions for respiratory and cardiovascular diseases. *Epidemiology* **20**: 738–746.
- Lin, S., W.H. Hsu, A.R.V. Zutphen, *et al.* 2012. Excessive Heat and Respiratory Hospitalizations in New York State: Estimating Current and Future Public Health Burden Related to Climate Change. *Environmental Health Perspectives* **120**: 1571–1577.
- Madrigano, J. 2014. personal communication.
- Marmor, M. 1975. Heat wave mortality in New York City, 1949 to 1970. *Arch. Environ. Health* **30**: 130–136.
- McGregor, G.R. 2012. Human biometeorology. *Prog. Phys. Geography* **36**: 93–109.
- Medina-Ramón, M., and J. Schwartz. 2007. Temperature, temperature extremes, and mortality: a study of acclimatisation and effect modification in 50 US cities. *Occup. Environ. Med.* **64**: 827–833.
- Medina-Ramón, M., M. Zanobetti, D.P. Cavanagh, and J. Schwartz. 2006. Extreme temperatures and mortality: assessing effect modification by personal characteristics and specific cause of death in a multi-city case-only analysis. *Environ. Health Perspect.* 1331–1336.
- Metzger, K.B., K. Ito, and T.D. Matte. 2010. Summer heat and mortality in New York City: how hot is too hot? *Environ. Health Perspect.* 80–86.
- Mudarra, D., and W.J. Fisk. 2007. Public health and economic impact of dampness and mold. *Indoor Air*, **17**: 226–235.
- National Oceanic and Atmospheric Administration (NOAA). 2014. *U.S. weather related fatalities*. Available online at http://www.nws.noaa.gov/om/hazstats/resources/weather_fatalities.pdf.

- National Weather Service (NWS). 2013. *U.S. Natural Hazard Statistics*. Available online at <http://www.nws.noaa.gov/om/hazstats.shtml>.
- New York City Department of Health and Mental Hygiene (NYC DOHMH), cited 2014: NYC Vital Signs Investigation Report. Available online at <http://www.nyc.gov/html/doh/downloads/pdf/survey/survey-2006heatdeaths.pdf>.
- New York City Department of Health and Mental Hygiene (NYC DOHMH). 2007. *Epiquery: NYC Interactive Health Data System—Community Health Survey 2007*. Available online at <http://www.nyc.gov/epiquery>.
- New York City Department of Health and Mental Hygiene (NYC DOHMH). 2014. *NYC Vital Signs Investigation Report*. Available online at <http://www.nyc.gov/html/doh/downloads/pdf/survey/survey-2006heatdeaths.pdf>.
- NPCC. 2015. Building the Knowledge Base for Climate Resiliency: New York City Panel on Climate Change 2015 Report. C. Rosenzweig and W. Solecki, Eds. *Ann. N.Y. Acad. Sci.* **1336**: 1–149.
- NYC Environmental Justice Alliance, personal communication. 2014.
- Nixdorf-Miller, A., D.M. Hunsaker, and J.C. Hunsaker III. 2006. Hypothermia and hyperthermia medicolegal investigation of morbidity and mortality from exposure to environmental temperature extremes. *Arch. Pathol. Lab. Med.* **130**: 1297–1304.
- Ogden, N.H., R.L. Lindsay, M. Morshed, *et al.* 2009. The emergence of Lyme disease in Canada. *CMAJ* **180**: 1221–1224.
- Ogden, N.H., *et al.* 2010. Active and passive surveillance and phylogenetic analysis of *Borrelia burgdorferi* elucidate the process of Lyme disease risk emergence in Canada. *Environ. Health Perspect.* **118**: 909–914.
- O’Neill, M.S., A. Zanobetti, and J. Schwartz. 2005. Disparities by race in heat-related mortality in four US cities: the role of air conditioning prevalence. *J. Urban Health* **82**: 191–197.
- Parris, A. 2014. How Hurricane Sandy tamed the bureaucracy. *Issues Sci. Technol.* **30**.
- Patz, J.A., S.J. Vavrus, C.K. Uejio, and S.L. McLellan. 2008. Climate change and waterborne disease risk in the Great Lakes region of the U.S. *Am. J. Prev. Med.* **35**: 451–458.
- Petkova, E.P., A. Gasparrini, and P.L. Kinney. 2014. Heat and mortality in New York City since the beginning of the 20th century. *Epidemiology* **25**: 554–560.
- Pietrzak, R.H., *et al.* 2012. Resilience in the face of disaster: prevalence and longitudinal course of mental disorders following Hurricane Ike. *PLoS ONE* **7**: e38964.
- Polvani, L.M., D.W. Waugh, G.J.P. Correa, and S.W. Son. 2011. Stratospheric ozone depletion: the main driver of twentieth-century atmospheric circulation changes in the southern hemisphere. *J. Climate* **24**: 795–812.
- Porsbjerg, C., M.L. Linstow, S.C. Nepper-Christensen, *et al.* 2002. Allergen sensitization and allergen exposure in Greenlandic Inuit residing in Denmark and Greenland. *Respir. Med.* **96**: 736–744.
- Reiss, N.M., and S.R. Kostic. 1976. Pollen season severity and meteorologic parameters in central New Jersey. *J. Allergy Clin. Immunol.* **57**: 609–614.
- Rose, J.B., P.R. Epstein, E.K. Lipp, *et al.* 2001. Climate variability and change in the United States: potential impacts on water- and foodborne diseases caused by microbiologic agents. *Environ. Health Perspect.* **109**(Suppl. 2): 211–221.
- Rosenzweig, C., C.W. Solecki, A. DeGaetano, *et al.*, Eds. 2011. Responding to climate change in New York State: The ClimAID integrated assessment for effective climate change adaptation in New York State. *Ann. N.Y. Acad. Sci.* **1244**: 1–460.
- Rosenzweig, C., *et al.* 2009. Mitigating New York City’s heat island: integrating stakeholder perspectives and scientific evaluation. *Bull. Am. Meteorol. Soc.* **90**: 1297–1312.
- Rotkin-Ellman, M., G. Solomon, C.R. Gonzales, *et al.* 2010. Arsenic contamination in New Orleans soil: temporal changes associated with flooding. *Environ. Res.* **110**: 19–25.
- Ruckart, P.Z., M.F. Orr, K. Lanier, and A. Koehler. 2008. Hazardous substances releases associated with Hurricanes Katrina and Rita in industrial settings, Louisiana and Texas. *J. Hazard. Mater.* **159**: 53–57.
- Semenza, J.C., J.E. Suk, V. Estevez, *et al.* 2012. Mapping climate change vulnerabilities to infectious diseases in Europe. *Environ. Health Perspect.* **120**: 385–392.
- Semenza, J.C., C.H. Rubin, K.H. Falter, *et al.* 1996. Heat-related deaths during the July 1995 heat wave in Chicago. *N. Engl. J. Med.*, **335**: 84–90.
- Sheffield, P.E., K. Knowlton, J.L. Carr, and P.L. Kinney. 2011a. Modeling of regional climate change effects on ground-level ozone and childhood asthma. *Am. J. Prev. Med.*, **41**: 251–257.
- Sheffield, P.E., K.R. Weinberger, K. Ito, *et al.* 2011b. The association of tree pollen concentration peaks and allergy medication sales in New York City: 2003–2008. *ISRN Allergy*, **2011**: 7.
- Sheffield, P.E., K.R. Weinberger, and P.L. Kinney. 2011c. Climate change, aeroallergens, and pediatric allergic disease. *Mt. Sinai J. Med.* **78**: 78–84.
- Singer, B.D., L.H. Ziska, D.A. Frenz, *et al.* 2005. Increasing Amb a 1 content in common ragweed (*Ambrosia artemisiifolia*) pollen as a function of rising atmospheric CO₂ concentration. *Functional Plant Biol.* **32**: 667–670.
- Smith, K.R., *et al.* 2009. Public health benefits of strategies to reduce greenhouse-gas emissions: health implications of short-lived greenhouse pollutants. *Lancet* **374**: 2091–2103.
- Spengler, J.D. 2012. Climate change, indoor environments, and health. *Indoor Air* **22**: 89–95.
- Tsai, D.H., J.L. Wang, C.H. Wang, and C.C. Chan. 2008. A study of ground-level ozone pollution, ozone precursors and subtropical meteorological conditions in central Taiwan. *J. Environ. Monit.* **10**: 109–118.
- U.S. EPA. 2008. *A review of the impact of climate variability and change on aeroallergens and their associated effects. Final report*. Washington, DC: EPA.
- Vandentorren, S., *et al.* 2006. August 2003 heat wave in France: risk factors for death of elderly people living at home. *Eur. J. Public Health* **16**: 583–591.
- Villeneuve, P.J., M.S. Doiron, D. Stieb, *et al.* 2006. Is outdoor air pollution associated with physician visits for allergic rhinitis among the elderly in Toronto, Canada? *Allergy* **61**: 750–758.
- Walsh, J., D. Wuebbles, K. Hayhoe, *et al.* 2014. Our changing climate. In *Climate Change Impacts in the United States: The Third National Climate Assessment*. J.M. Melillo, T.T.C. Richmond & G.W. Yohe, Eds.: 19–67. U.S. Global Change Research Program.

- Whitman, S., G. Good, E.R. Donoghue, *et al.* 1997. Mortality in Chicago attributed to the July 1995 heat wave. *Am. J. Public Health* **87**: 1515–1518.
- Wilson, K. 2009. Climate change and the spread of infectious ideas. *Ecology* **90**: 901–902.
- Wolf, J., N.R. O'Neill, C.A. Rogers, *et al.* 2010. Elevated atmospheric carbon dioxide concentrations amplify *Alternaria alternata* sporulation and total antigen production. *Environ. Health Perspect.* **118**: 1223–1228.
- Ziska, L.H., and F.A. Caulfield. 2000. Rising CO₂ and pollen production of common ragweed (*Ambrosia artemisiifolia* L.), a known allergy-inducing species: implications for public health. *Aust. J. Plant Physiol.* **27**: 893–898.
- Ziska, L.H., D.E. Gebhard, D.A. Frenz, *et al.* 2003. Cities as harbingers of climate change: common ragweed, urbanization, and public health. *J. Allergy Clin. Immunol.* **111**: 290–295.
- Ziska, L., *et al.* 2011. Recent warming by latitude associated with increased length of ragweed pollen season in central North America. *Proc. Natl. Acad. Sci. USA* **108**: 4248–4251.
- Zoraster, R.M. 2010. Vulnerable populations: Hurricane Katrina as a case study. *Prehosp. Disaster Med.* **25**: 74–78.

ANNALS OF THE NEW YORK ACADEMY OF SCIENCES

Issue: *Building the Knowledge Base for Climate Resiliency*

New York City Panel on Climate Change 2015 Report

Chapter 6: Indicators and Monitoring

William Solecki,^{1,a} Cynthia Rosenzweig,^{2,a} Reginald Blake,^{3,a} Alex de Sherbinin,⁴ Tom Matte,⁵ Fred Moshary,⁶ Bernice Rosenzweig,⁷ Mark Arend,⁶ Stuart Gaffin,⁸ Elie Bou-Zeid,⁹ Keith Rule,¹⁰ Geraldine Sweeny,¹¹ and Wendy Dessy¹¹

¹City University of New York, CUNY Institute for Sustainable Cities, New York, NY. ²Climate Impacts Group, NASA Goddard Institute for Space Studies, Center for Climate Systems Research, Columbia University Earth Institute, New York, NY. ³Physics Department, New York City College of Technology, CUNY, Brooklyn, NY; Climate Impacts Group, NASA Goddard Institute for Space Studies. ⁴Center for International Earth Science Information Network (CIESIN), Columbia University, Palisades, NY. ⁵New York City Department of Health and Mental Hygiene, New York, NY. ⁶NOAA CREST, City College of New York, CUNY, New York, NY. ⁷CUNY Environmental Crossroads, City College of New York, CUNY, New York, NY. ⁸Center for Climate Systems Research, Columbia University Earth Institute, New York, NY. ⁹Department of Civil & Environmental Engineering, Princeton University, Princeton, NJ. ¹⁰Princeton Plasma Physics Laboratory, Princeton, NJ. ¹¹New York City Mayor's Office of Operation, New York, NY

Address for correspondence: William Solecki, Department of Geography, Hunter College (CUNY), New York, NY 10021

Contents

- 6.1 Background and framework
- 6.2 New York City environmental indicators
- 6.3 Climate resilience indicators and monitoring test bed—reducing the urban heat island
- 6.4 Conclusions and recommendations

Introduction

Among the crucial challenges for climate change facing New York City are measurement, monitoring, and evaluation of critical indicators of climate change. This involves developing indicators not only of the climate itself and its impacts, but also of resiliency measures. These need to be tracked over time in order to provide relevant information on the effectiveness of current and future response strategies. Required are a manageable set of climate change indicators and a monitoring system that enables evaluation of the dynamic processes associated with climate change, its associated impacts, and flexible adaptation and resiliency practices (see Box 6.1 for definition of climate change indicators).

The first report by the New York City Panel on Climate Change (NPCC, 2010) set out an approach to indicators and monitoring for tracking climate

risks and presented potential sources of data from existing monitoring systems in the city (NPCC, 2010; Jacob *et al.*, 2010). Building on this approach, the objective of this chapter is to identify how New York City can establish a Climate Resiliency Indicators and Monitoring System that is more responsive to current and future climate change.

A logic similar to the climate protection level (CPL) discussion of the first NPCC is employed (Solecki *et al.*, 2010). The CPL analysis focused on a basic question: Given that there were already an extensive number of codes and standards designed to protect critical infrastructure and human well-being from climate risks, how can the existing legal, managerial, and operational climate protection strategies be adjusted and enhanced to be responsive to future climate change? Because the City (along with its state and federal partners) already maintains an extensive set of environmental indicator and monitoring programs to track a variety of environmental quality and human and ecological health indicators, this chapter explores how, and under what conditions, the City of New York can expand these programs to be fully capable of assessing climate risks and resiliency opportunities as they evolve. Specifically, this chapter addresses three questions:

^aLead authors.

Box 6.1. Definition of climate change indicators

Climate change indicators are defined as empirically-based quantities that can be tracked over time to provide relevant information for stakeholder decisions on climate resiliency and on the efficacy of resiliency measures to reduce vulnerability and risk.

1. What indicator and monitoring systems are currently in place within the City of New York?
2. What are the opportunities and challenges to establishing the New York City Climate Resiliency Indicators and Monitoring System?
3. What can be learned from a case study on the existing urban heat island indicator and monitoring system within the City?

The chapter identifies opportunities and gaps in the existing systems with respect to monitoring and adapting to climate change and illustrates some conditions under which these gaps could be filled. The use of innovative monitoring methods including remote sensing, flexible systems (e.g., mobile), and microsensors is highlighted. The chapter uses the urban heat island as a test bed to evaluate the specific requirements for an indicator and monitoring system associated with a particular resiliency strategy. The existing NYC Cool Roofs Program reveals several real-world issues and demands on indicators and monitoring systems that include evaluation challenges and the need to maintain efficiency and effectiveness over time.

6.1 Background and framework

Augmenting the approach developed in NPCC 2010, this section presents an overview of the NPCC2 indicators and monitoring framework and indicator system design and process.

NPCC 2010 approach

The first report by the NPCC established three selection criteria for indicators: policy relevance, analytical soundness, and measurability (NPCC, 2010; Jacob *et al.*, 2010). The climate change indicators were seen as creating a mechanism for alerting stakeholders to emerging climate change and related risk information; warning decision-makers of potential system-level thresholds (which may lead to tipping points that could alter elements in the risk-assessment process); and providing decision triggers

for altering adaptation pathways. Three categories of indicator variables were highlighted: (1) physical climate change variables; (2) risk exposure, vulnerability, and impact metrics; and (3) adaptation measures and their effectiveness. For each category, a variety of potential indicators were presented and discussed.

NPCC2 framework 2015

Monitoring frameworks have been developed for urban climate resiliency (Tyler *et al.*, 2014; Moench *et al.*, 2011), urban vulnerability (Swart *et al.*, 2012; Romero Lankao and Qin, 2011), urban sustainability (Shen *et al.*, 2011), and urban environmental performance (EIU, 2012). Building on earlier work, the NPCC2 has developed an indicator and monitoring framework that relates to climate hazards, impacts, and resiliency and that strengthens the potential for identification of system-level tipping points or thresholds. The NPCC2 monitoring framework is tailored to the purpose of the indicator set, and encapsulates the conceptual linkages between climate change and different urban systems.

Indicator development process

Cities need a robust yet flexible process for climate change indicator development that includes multiple stakeholders. Cities already track a large number of indicators, and the challenge is to evolve current systems of indicators and monitoring to include climate change. The NPCC2 process for development of climate resiliency indicators consists of seven steps (Fig. 6.1):

1. Meet with stakeholders to decide relevant climate adaptation and resilience decision areas, information needs, and key questions
2. Determine what data are available and how they can be accessed
3. Conduct indicator research to develop a small set of preliminary indicators
4. Present set of preliminary indicators to stakeholders for feedback and to scope implementation

5. Revise indicators based on stakeholder feedback
6. Set up indicator system reflecting the defined framework
7. Conduct evaluation, iterative research, and stakeholder interaction through time

The process of establishing indicators and an indicator and monitoring system involves engaging with stakeholders (producers and users) who can contribute to the design of the indicators, engaging them in a process from development to implementation to evaluation. It defines the key questions (Box 6.2) the indicators are meant to address. Prototype indicators can be tested with users during this phase. Finally, a system should be set up to sustain the production and archiving of the indicators, and periodic evaluations should be carried out to ensure that the indicators continue to meet user needs and policy and management objectives.

Climate resiliency indicators

Effective indicators are resonant (i.e., strike a chord with the intended audience and are scientifically credible), salient (i.e., timely and relevant to decision-makers' needs), and targeted (i.e.,

tailored to the appropriate context) (de Sherbinin *et al.*, 2013). Indicators generated by government agencies can contribute to management and policy-making processes and have the potential to be sustained over time. Indicators also can be used for public engagement and outreach purposes to identify significant risks, impacts, and adaptation opportunities.

Figure 6.2 provides a flow diagram of the major climate extremes and the urban systems they impact. Although climate trends are important for medium- to long-term planning purposes, extremes are temporally limited events such as heat waves and coastal storms that generally have the greatest impact on urban systems. Major systems that are affected by extremes include energy supply, health, ecosystems, transportation infrastructure, water supply, and building stock.

Candidate indicators that could be included in the New York City Climate Resiliency Indicators and Monitoring System are shown in Tables 6.1, 6.2, 6.3, and 6.4. This list is not intended to be comprehensive because a final list would need to be vetted with stakeholders. Most are current trend indicators for New York City as a whole, but some are comparative and spatially discrete. Those with city-wide coverage allow



Figure 6.1. NPCC2 indicator development process.

Box 6.2. Key questions for development of urban climate indicators

Several questions need to be addressed regarding the role and purpose of urban climate impact, vulnerability, and adaptation indicators as well as their design.

Climate change impacts, vulnerability, and resiliency

- What important climate impacts are occurring or are predicted to occur in the future?
- What are fundamental vulnerabilities and resiliencies to climate variability and change?
- What systems are most at risk of climate impacts?
- What are the targeted policy questions for which indicators should be designed?
- What information is needed to improve resiliency to rapid change or extreme events related to climate?
- What adaptation measures are in place, and how may they change over longer time frames?

Climate change indicators and monitoring

- Is climate in the metropolitan region changing now?
- How is the climate projected to change in the future?
- What are the critical climate variables, indices, and extreme events to monitor?
- What is the baseline reference for the data (i.e., start date and end date)?
- For a given indicator, should it be calculated annually, seasonally, monthly, or weekly?
- What is the appropriate averaging period (e.g., 1-day or 4-day precipitation)?
- What is the appropriate spatial averaging (e.g., neighborhood, city, metropolitan region)?
- How should thresholds be chosen: statistically (e.g., 95th percentile) or relative to a critical value based on infrastructure vulnerability?
- What evidence is needed to determine if/when certain thresholds are being reached?

policy-makers to evaluate differences in indicator values and trends across administrative units within the city.

The social vulnerability indicators reflect an understanding that exposure to climate hazards alone does not explain outcomes but that differential levels of sensitivity (susceptibility) and adaptive capacity also play a role. In other words, the climate

impacts in terms of people’s experience will not be the same across all neighborhoods for an event of the same magnitude. Their measurement can help, when combined with climate risk information, to identify neighborhoods in need of intervention. These are particularly important for indicator development for public health (see Chapter 5, NPCC, 2015).

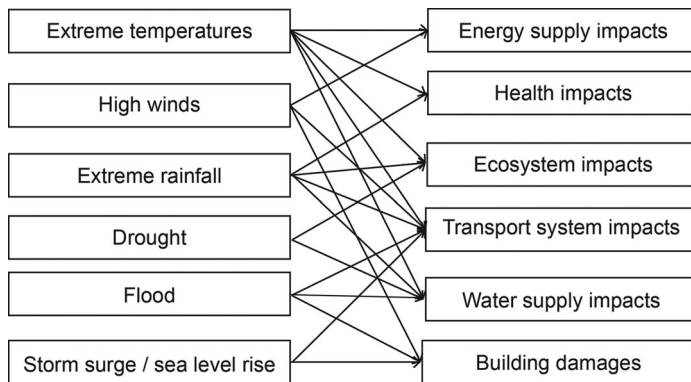


Figure 6.2. Climate extremes and potential impacts on urban systems.

Table 6.1. Potential climate indicators

-
- Number of heat advisories per year
 - Change in surface and air temperature during peak periods (July–August)
 - Number of extreme precipitation events (95th percentile values) per year
 - Number of coastal flooding advisories for major or moderate flooding
 - Trend in mean sea level
 - Trend in peak storm surge for 100-year and 500-year storms
 - Number of days per year with sustained winds or gusts exceeding certain thresholds
-

Regional and multi-institutional integration

The creation of a New York City Climate Resiliency Indicators and Monitoring System needs to encompass multiple institutions and to extend beyond city and even state borders, and thus should be metropolitan region in scope. Data need to be integrated across different spatial and temporal resolutions and across different formats. Planning must be undertaken to ensure that the incorporated data are of the appropriate quality, and funding must be provided to ensure that monitoring efforts remain consistent and continuous throughout the coming decades.

Regional integration. A clear need exists for a regional approach in the development of the New York City Climate Resiliency Indicators and Monitoring System. New York City’s drinking water supply sources, for example, lie outside city boundaries, and much of New York City’s labor force lives outside of the boundaries of the five boroughs. Disruptions to regional commuter transit can have serious economic consequences for the city. Furthermore, New York City is connected to a regional energy grid that provides more than 80% of its electricity and is

thus affected by regional storms and heat waves that may disrupt regional generation. A selected inventory of measurement systems for potential inclusion in an integrated New York City Climate Resiliency Indicators and Monitoring System is presented in Appendix IIF.

Multi-institutional integration. Some existing monitoring networks in New York City, including the Hudson River Environmental Conditions Observing System (HRECOS), the New York Harbor Observing and Prediction System (NYHOPS), and the New York City Meteorological Network (NYCMetNet) have already begun multi-institution data integration efforts. The New York City Environmental Public Health Tracking Portal provides an example of long-term public health data management; it is integrated across various agencies and made publicly available through a Web site: <http://a816-dohbosp.nyc.gov/IndicatorPublic/>.

The National Science Foundation’s Long-Term Ecological Research Network (LTER-NET; Redman *et al.*, 2004; see also <http://www.lternet.edu>) also may serve as a model for the integration of long-term interdisciplinary ecological data. The mission of LTER-NET is to provide scientists, policy-makers,

Table 6.2. Potential impact indicators

-
- Heat-related morbidity and excess mortality from extreme heat events per year
 - Other health-related heat impacts (e.g., heat-induced strokes)
 - Other climate hazard-related morbidity and mortality per year (e.g., drowning due to storms)
 - Number of days per year with observed air quality index > 100
 - Cooling (and heating) degree days per year
 - Duration of blackouts/brownouts per year associated with weather-related events
 - Number of weather-related transit and subway outages per year
 - Number of weather-related telecommunications outages and customer hours without telecommunications per year
 - Area of land inundated by coastal flooding per year
 - Costs of additional water treatment owing to extreme rainfall events per year
 - Total economic losses from climate-related events per year
-

Table 6.3. Potential social vulnerability indicators

-
- Disparity in heat-related morbidity and mortality across neighborhoods with respect to a variety of equity conditions (e.g., income, race/ethnicity, non-English speaking population, housing stock)
 - Disparity in other climate-related morbidity and mortality across neighborhoods with respect to a variety of equity conditions.
 - Disparity in households without air conditioning across neighborhoods with respect to a variety of equity conditions.
 - Percentage population with a disability (one or more of six types: hearing, vision, cognitive, ambulatory, self-care, independent living)
 - Social vulnerability indices, tailored as needed to specific climate hazards, for example:
 - Heat Vulnerability Index in census block groups experiencing relatively higher heat stress
 - Social Vulnerability Index scores related to access to green space
 - Social Isolation Index in census block groups in flood evacuation zones¹
-

¹The Heat Vulnerability Index (HVI) and Social Vulnerability Index (SVI) are composite measures based on multiple indicators that summarize population vulnerability by geography to extreme heat based on published epidemiological studies and, in the case of the HVI, prediction of increased mortality during extreme heat events (the SVI is described in Reid *et al.* 2009; the HVI in Madrigano pers. com., 2014). Social isolation has been a risk factor for heat-related mortality and can increase vulnerability to a variety of climate hazards. A commonly used index for assessing social connections and isolation among seniors is described in Lubben (1998).

and the general public with the scientific information needed to manage the nation’s ecosystems. Its disciplinary scope includes population and community ecology, ecosystem science, social and economic sciences, urban studies, oceanography, and science education. There are clear parallels

between this program and the multisectoral Climate Resiliency Indicators and Monitoring System needed in New York City.

Although these data integration programs vary considerably in their objectives, scope, and scale, they share four common features:

Table 6.4. Potential resiliency indicators

-
- Change in vegetation cover
 - Number of trees planted per year
 - Square footage of white/green roofs
 - Surface temperature change in areas that have adopted white/green roofs relative to non-white/green roof locations
 - Estimated percent of households with residential air conditioning
 - Number of citizen groups engaged in climate resiliency programs per year
 - Square footage of residential, commercial, industrial space not flood-proofed or elevated in areas within the 100-year floodplain
 - Number of residential units in 100-year floodplain implementing Core Flood Resiliency measures¹
 - Percentage of flood-affected areas with improved storm drainage
 - Acres of restored coastal wetlands
 - Miles of coastal defenses erected (dune replenishment/hard defenses)
 - Population growth/decline in the 100-year floodplain
 - Percentage of NYC transportation assets adapted for climate change resiliency
 - Financial expenditure on resiliency activities per year; as a percent of total expenditure
-

¹Core Flood Resiliency Measures, proposed in the *Special Initiative for Rebuilding and Resiliency* (City of New York, 2013), include elevation or other flood protection of critical building equipment and utilities: fire protection, electricity, heating, ventilation, air conditioning, plumbing, telecommunications, elevators, and emergency generators and associated fuel tanks and pumps.

- Early, documented planning to ensure data consistency and quality
- Dedicated resources and infrastructure to provide post-processing, harmonization, and long-term data management from different sources
- A coordinating institution or office responsible for data management
- A dedicated group of scientists to conduct on going evaluations

6.2 New York City environmental indicators

The section presents the current status of indicators now monitored by New York City, identifies gaps, and suggests potential ways that climate change can be incorporated.

An extensive web of environmental monitoring systems currently collects data that can support climate resiliency indicators monitoring for the New York metropolitan region. Many of these systems originally were developed to meet the requirements of environmental legislation and to address public health concerns, but they can also provide important information for climate change resiliency planning.

The ongoing monitoring of physical climate change variables is conducted through two approaches: site-based instrumentation and remote sensing. Site-based instruments monitor and provide long-term conditions at a particular location, complementing remotely sensed data. Site-based monitoring procedures must be harmonized in order to allow for rigorous comparison throughout the region.

Remote sensing can provide standardized, quantitative data on conditions throughout the entire metropolitan region at regular time intervals. For many physical climate change parameters, federal agencies such as the National Oceanic and Atmospheric Administration (NOAA) or the U.S. Geological Survey (USGS) provide standardized remote sensing data throughout the region. Making distributed observations with remote sensing techniques provides broad, continuous coverage. However, these must be integrated with ground-based data to enhance their utility.

The process of producing climate indicators is dependent on choosing appropriate sampling

strategies and effective combinations of these complementary monitoring systems. A selected inventory of the government agencies, nongovernmental organizations, and academic institutions conducting monitoring is presented in Appendix IIF (NPCC, 2015). This includes systems that measure relevant parameters in the atmosphere, on land, and throughout regional water bodies and coastal zones.

Weather and climate

Ongoing weather and climate monitoring is conducted by multiple federal agencies, academic institutions, and private companies. Long-term observation sites include the National Oceanic and Atmospheric Administration's Historic Climatology Network (HCN), with 712 sites in the 31-county region (Fig. 6.3). At these sites, instruments collect continuous data on basic meteorological variables such as surface temperature, precipitation, wind speed, and solar radiation, among many others. Data from these sites are subject to a common suite of quality-assurance reviews and integrated into a database of daily data. In addition to the HCN, NOAA also maintains one United States Climate Reference Network (USCRN) site (Milbrook, NY) in the 31-county region. USCRN sites are managed with the express purpose of detecting climate change signals, and they are located in pristine settings to exclude the impacts of development on local climate (Diamond *et al.*, 2013).

In addition to the NOAA surface observation sites, the Optical Remote Sensing Laboratory at the City University of New York maintains several upper-air measurement sites, which provide data on wind-speed profiles, aerosol concentrations, air quality, and atmospheric water content (Fig. 6.4). These have been highlighted in a recent publication by the National Academies of Science on Urban Meteorology (National Academy of Sciences, 2012). The observations from these ground-based remote-sensing instruments allow for the urban boundary layer (the layer in the atmosphere above a city where spatially integrated heat and moisture are exchanged with the overlying air) to be monitored and studied. Real-time displays from these observations are presented on the NYCMetNet web portal (<http://nycmetnet.cuny.cuny.edu/>) along with a large set of regional surface observations

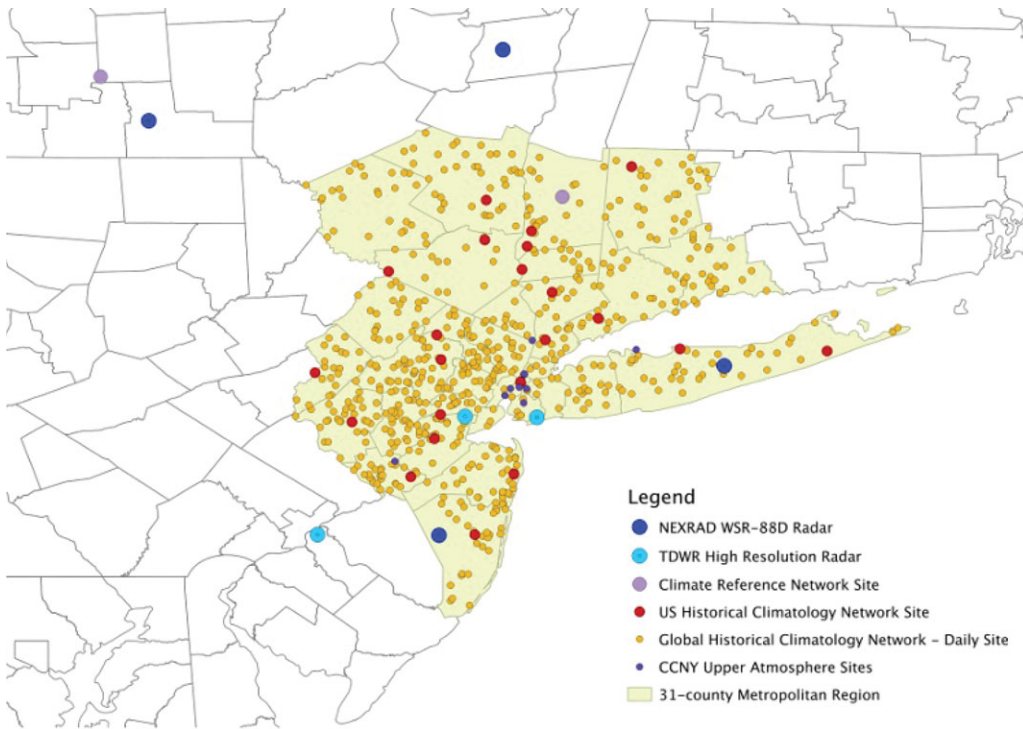


Figure 6.3. Sites important in supporting climate change monitoring in the New York metropolitan region. These include NOAA’s Historic Climatology Network (HCN) and Climate Change Reference Network (USRCN), the City College of New York Upper Atmosphere Monitoring Sites, and Weather Radar Sites operated by the National Weather Service and the Federal Aviation Administration.

from public and private agencies in the metropolitan region.

Next steps. Further integration is necessary to harmonize and adapt the weather and climate data from the various sources to support climate change–related monitoring. Weather and climate data collected at observing stations can be used to develop tailored climate projections requested by stakeholders. Examples of this are relative humidity projections and their potential application for electric utility providers. A Climate Resiliency Indicator and Monitoring Working Group with representatives from all the groups currently collecting weather and climate data should be formed to further the integration of these sources for climate change–related information.

Coastal zones and sea level rise

Sea level rise will produce some of the most significant climate change impacts on New York City. NOAA maintains tide gauge stations at the Battery and Kings Point/Willets Point. These are

indispensable for monitoring long-term changes in local mean sea level, water heights, and surge levels.

New York Harbor Observing and Prediction System (NYHOPS) maintains a network of buoy-mounted sensors, underwater probes, boat-mounted instruments, and unmanned underwater vehicles. These devices monitor water levels, currents, and water quality in the New York Harbor, the New Jersey Coast, and western Long Island Sound, all of which are critical for assessing the rate of sea level rise and the magnitude of storm surges. NYHOPS adheres to NOAA’s standards and guidelines for operational oceanographic products and services. The NYHOPS data as well as synthesized analyses are made accessible at <http://hudson.dl.stevens-tech.edu/maritimeforecast>.

Next steps. In order to support climate change–related monitoring of site-based and remote sensing data, it is important to integrate and modify the coastal zone data from the various sources. Efforts to coordinate the many sources of coastal zone data

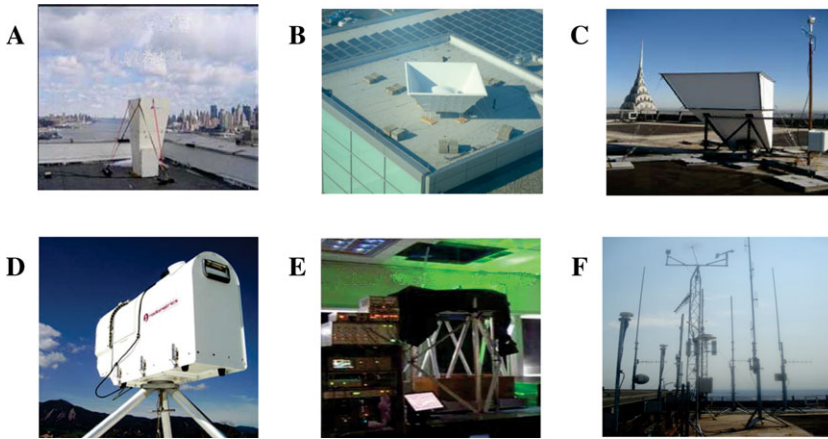


Figure 6.4. Instruments of the NYCMetNet: (A) and (C) Sodar wind vertical profiler (to ~1500 ft); (B) Radar wind vertical profiler (to 2 miles); (D) Temperature, humidity and liquid water vertical profiler (to ~1.3 miles); (E) CCNY Aerosol Raman lidar vertical profiler (to ~6 miles); (F) Skyscraper-mounted weather stations (Source: Mark Arend, CCNY Optical Remote Sensing Lab and NOAA CREST).

will require a Climate Resiliency Indicator and Monitoring Working Group with representatives from all the groups currently collecting the information.

Water resources

Currently, overall precipitation and heavy downpours are increasing in the New York metropolitan region (see Chapter 1 and Appendix I in NPCC, 2015). These climate change trends are expected to continue. Today, water levels in the upstate reservoirs that supply New York City's drinking water are closely monitored by the New York City Department of Environmental Protection (NYCDEP, 2011). In addition, the U.S. Geological Survey (USGS) collects continuous data on streamflow, tidal flow, and groundwater at numerous sites distributed throughout the 31-county region. This enables the assessment of how precipitation changes impact the region's other water resources as well as the frequency and magnitude of flooding events (Fig. 6.5).

Next steps. Hydrological data from the various sources need to be synchronized to support climate change-related monitoring. Representatives from the groups that currently gather hydrological data should join together to form a Climate Resiliency Indicators and Monitoring Working Group that will be able to link the many sources of climate change-related information.

Water quality

Climate change is expected to have significant impacts on water quality (Murdoch *et al.*, 2000). Numerous government agencies and NGOs conduct regular water-quality monitoring in the New York metropolitan region (see Appendix IIF, NPCC, 2015). However, the datasets they collect are not standardized across institutions, which makes comparison difficult and creates a challenge to their use in developing climate change indicators.

The recently established Hudson River Environmental Conditions Observing System (HRECOS), a network of water-quality monitoring stations in the Hudson River Estuary, may serve as a model for integrating water-quality monitoring data to support climate change indicators. HRECOS sites are operated by a consortium of government agencies, research institutes, and NGOs. Data from the network of stations along the length of the tidal Hudson River are collected using clear guidelines defined in the project's Quality Assurance Plan, and data are thus readily intercomparable. Further data collected through the project are integrated, archived, and made accessible through the project website <http://hrecos.org>.

Next steps. Water quality data from HRECOS, NYC DEP, USGS, and NYC DEC need to be combined to support climate change-related monitoring. A Climate Resiliency Indicator and Monitoring

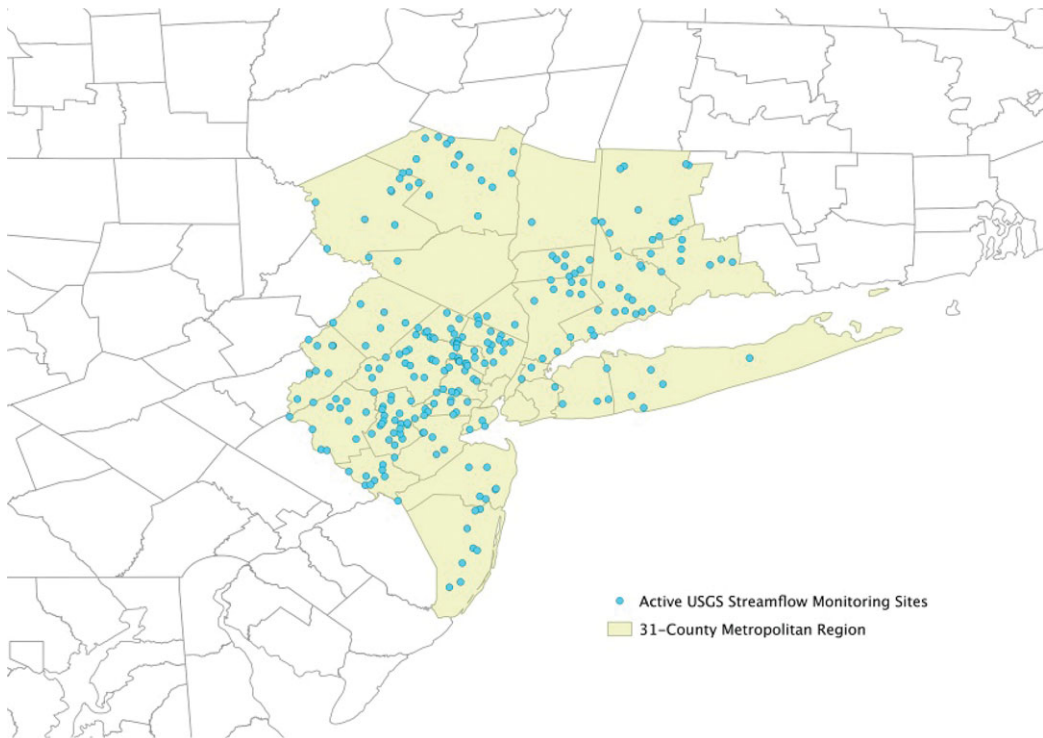


Figure 6.5. Active USGS streamflow sites in the New York metropolitan region.

Working Group with members from all the groups currently collecting water quality data should be formed to advance integration of these sources for climate change-related information.

Biodiversity and ecosystems

Climate change will have important but poorly understood impacts on the wildlife and ecosystems of the New York metropolitan region. Studies conducted in other parts of the Northeast have shown that the timing of spring migration of songbirds has changed over the last 40 years (Van Buskirk, 2012). Climate change has also been implicated in the northward expansion of kudzu (*Pueraria lobata*), an aggressive invasive plant that threatens New York City's native flora (Bradley *et al.*, 2010). However, there are currently limited observational data available to assess how climate change has impacted natural ecosystems in the New York metropolitan region. Field surveys are conducted in different parts of the region by the U.S. Fish and Wildlife Service, the National Parks Service, the New York City Department of Parks and Recreation, as well as many local organizations and academic researchers. To

date, few efforts have been made to synthesize the results and analyze them to better understand how climate change may be influencing regional ecosystems. Efforts to do so should be a priority in the development of the New York City Climate Resiliency Indicators and Monitoring System. The biodiversity indicators developed to support the global Convention on Biological Diversity (Butchart *et al.*, 2010) may provide a good model for a New York City framework. Examples of these indicators include metrics for wild bird population trends, trends in the areal extent of wetlands and marine grasses, and trends in numbers of invasive species.

Remote sensing data, such as aerial photography, provide an important source of fine-scale information on the ecosystems of the New York metropolitan region and how they are being affected by climate change (Morgan *et al.*, 2010). Aerial photos for New York City are managed by the Department of Information Technology and Telecommunications (NYC DoITT). Aerial imagery for the remainder of the 31-county area can be obtained from the New York Statewide Digital Orthophotography Program (NYSDOP), the New

Jersey Department of Environmental Protection, and the Connecticut Department of Environment. However, in order to utilize this imagery for the development of ecosystems indicators, algorithms will need to be developed to standardize these different datasets for the New York metropolitan region.

Regional land cover plays an important role in the interpretation of climate change—monitoring data and the development of indicator metrics. Land cover data sets that cover the entire 31-county region at 30-m resolution can be obtained from the National Land Cover Database (Homer *et al.*, 2012), developed in partnership by several federal agencies. Updates to this database are released approximately every 9 years.

However, although this data set provides important information on the vegetative or impervious land cover (i.e., deciduous forest, wetlands, urban, etc.), it would be greatly enhanced by analyzing supporting data on land use activities (i.e., commercial, residential, etc.). This type of information is provided for counties in New Jersey by the New Jersey Department of Environmental Protection (NJDEP, 2010), but similar data sets are not available for other parts of the New York metropolitan region.

Next steps. Ecosystem measurements at the regional scale should be synthesized as part of the development of the New York City Climate Resiliency Indicators and Monitoring System.

6.3 Climate resiliency indicators and monitoring test bed—Reducing the urban heat island

In this section, climate resiliency indicators and monitoring are explored in relation to a specific urban climate challenge and a program to address it. The urban heat island effect (UHI) is the phenomenon of cities being warmer (up to approximately 8°F) than surrounding suburban and rural areas due to the abundance of dry impermeable surfaces such as roads and buildings (see Box 6.3). The UHI effect increases ambient temperatures, heat stress, exposure during heat waves, and energy use for cooling.

Methods to reduce the UHI include cooling buildings through increasing the albedo of their roofs and increasing evapotranspiration. These methods are part of a set of green infrastructure

technologies, which include green vegetated roofs and bioswales (landscape features that improves drainage). Green roofs and bioswales can offer both UHI reduction and stormwater management.

This section addresses the following topics related to the challenges posed by the UHI effect in New York City and the NYC Cool Roofs Program designed to alleviate it:

- Science challenges
- NYC Cool Roofs Program
- Indicators and monitoring
- Next steps

Science challenges

A key challenge for UHI research and monitoring is quantifying the urban energy balance, especially the relationships between surface temperature and air temperature. This includes understanding by how much air temperatures can be reduced by lowering surface temperatures through increasing albedo and evapotranspiration.

Rooftops collectively comprise a substantial fraction of land area in urban settings. The percentage varies from city to city but may range from 10% to 20% (Rosenzweig *et al.*, 2009). For New York City, rooftops cover about 19% of its total land area. These rooftop surfaces and their micrometeorological fluxes interact with the atmosphere and thereby are part of the city's UHI phenomenon. They are thus key targets for UHI interventions.

The fundamental scientific principle that governs rooftop temperatures is that of the surface energy flow budget. This is the budget of energy into and energy out of a rooftop and any other surface exposed to the atmosphere. In sunlight, the energy flow fluxes are often more important than air temperature in determining surface temperatures; in other words, the energy flows involved in sunlight and thermal radiation often greatly outweigh the other surface energy flows such as windspeed and evaporative cooling. Evaporative and windspeed cooling, however, can strongly modulate the energy balance under some weather conditions and times of day (Gaffin *et al.*, 2010).

During peak sunlight times, black roofs can reach surface temperatures of 170°F (77°C) (Gaffin *et al.*, 2012b). Such peak temperatures are generally much more strongly dependent on incident sunlight conditions rather than high summertime air

Box 6.3. Urban heat island definitions

Air temperature (°F)

Temperature of the ambient air.

Albedo (%)

Ratio of solar radiation reflected by a surface to the radiation incident on it.

Cooling degree days

The number of degrees by which the daily mean temperature exceeds 65°F. Cooling degree days are calculated on a daily basis and are primarily used to track energy use.

Evapotranspiration (in. day⁻¹)

Sum of the physical processes of evaporation and plant transpiration that combine to return water to the atmosphere.

Surface temperature (°F)

The temperature at the surface of a body.

Urban energy balance

Energy balance between the fluxes of heat, moisture, and momentum in urban areas.

Urban heat island

Thermal characteristics of cities that cause them to be warmer than surrounding suburban areas.

temperatures. This presents an opportunity for albedo modification, i.e., changing from black to white roofs, to alleviate the high surface temperatures of New York City roofs. Surface temperatures are sometimes even higher during spring than summer when less hazy urban air prevails.

Extreme hot and cold temperature cycles have practical implications for rooftop service life and building energy gains or losses. The temperature cycles are a major factor in roof-membrane wear and tear as they lead to material expansion and contraction cycles.

During a typical summer day, flat, black asphalt rooftops can reach temperatures up to 170°F, which is 90°F hotter than the surrounding air temperature. Cool roof coatings have been shown to reduce external roof temperatures, thus helping to mitigate the UHI effect. They also reduce internal building temperatures by up to 30%, making the building cooler and more comfortable during the hot summer months. Further, cool roofs lower carbon emissions by reducing demand for power. Every 2500 square feet of roof that is coated can reduce the

city's carbon footprint by 1 ton of CO₂. Furthermore, cool roofs improve air quality by lowering air pollution and extend the lifespan of rooftops and HVAC equipment. A cool roof coating better regulates a roof's temperature as compared to typical rooftop surfaces. Decreasing the roof temperature and cooling loads can extend the life of the rooftop and cooling equipment.

NYC Cool Roofs Program

New York City has instituted the Cool Roofs Program to apply white paint to roofs in areas experiencing urban heat island effects. The goal of the program is to promote alleviation of the UHI and reduction in health risks associated with heat stress and heat exposure. By helping to cool buildings on hot days, NYC Cool Roofs contributes to reducing energy use and peak demand for electricity during extended heat waves (see www.nyc.gov/coolroofs).

In 2009, the City launched a Cool Roofs Pilot Program in Long Island City, Queens, a designated “hot spot” to test the effectiveness of cool roof coating in reducing energy consumption and cooling costs



Figure 6.6. Pilot paint program to brighten NYC dark roofs and monitoring sensors. The whitened test surface freshly coated is shown alongside an untreated square of the original asphaltic membrane. The surrounding gray area is the state of the paint two years after an initial coating. (Gaffin *et al.*, 2012b).

and to support the City’s goal to reduce greenhouse gas emissions by 80% by 2050 (City of New York, 2014). A group of 244 volunteers were trained to coat 100,000 square feet of rooftop with elastomeric acrylic paint. To measure the effects of the white roofs, the city partnered with Columbia University (Fig. 6.6). The study showed that daytime peak black temperatures were, on average, 75°F warmer than the test white surface on rooftops; thus white roofs significantly reduced the need for air conditioning and energy consumption, which can result in real cost savings for building owners and tenants.

Based on the pilot program’s initial success, a full program was launched citywide in 2010, in collaboration with NYC Service, the New York City Department of Buildings (DOB), and the New York City Mayor’s Office of Long-Term Planning and Sustainability (OLTPS) with the goal of coating 1 million square feet of rooftop per year. The technology can

be applied either by the building owner or by a labor service program created by the City. The Program focused on coating a range of nonprofit, low-income housing, and government buildings, among others.

To date, 5.8 million square feet of rooftops have been coated on 620 buildings, and 5600 volunteers have been engaged. In addition to the volunteer component, New York City also launched a “Cool-it-Yourself” campaign to encourage building owners to coat their own rooftops. This was promoted through bus shelters, several city websites, and word-of-mouth. New Yorkers who participate in the Cool-it-Yourself campaign log their data and address into the NYC Cool Roofs website.

Indicators and monitoring

New York City currently tracks the following metrics for the Cool Roofs Program:

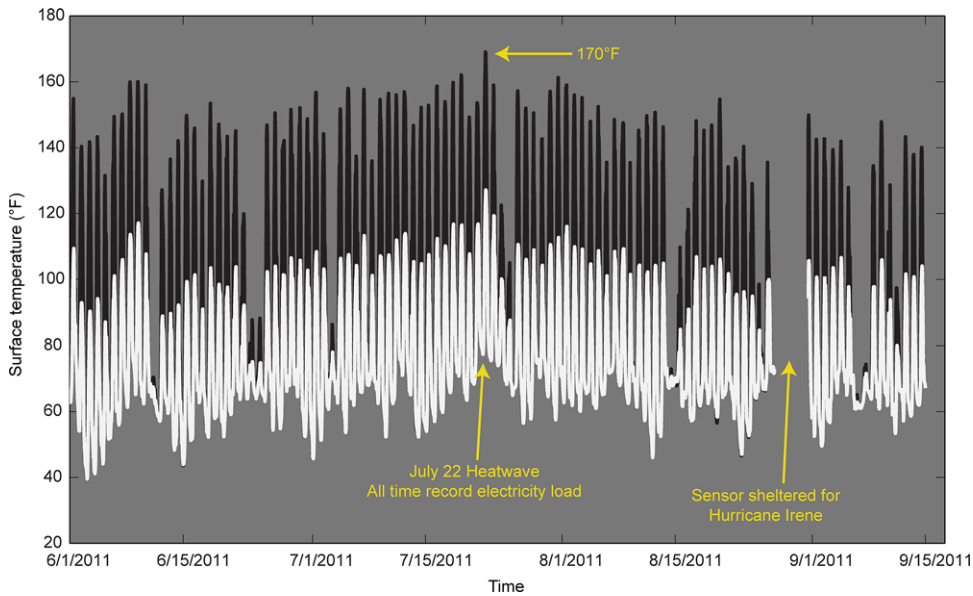


Figure 6.7. Surface temperatures for a freshly painted white roof compared to those of a control black roof at the Museum of Modern Art, Queens, NY. Source: Gaffin *et al.*, 2012.

1. Electricity usage in wattage and money spent in select buildings that have received an NYC Cool Roof coating
2. Number of square feet of rooftop coated
3. The amount of carbon reduced, calculated from the square footage of roofs coated
4. Number of volunteers engaged
5. Number of buildings coated
6. Number of green workforce^b participants
7. Number of green workforce participants who secure jobs and/or further their education.

A pilot monitoring system for the Cool Roofs program has been installed by the New York City Mayor's Office and Department of Buildings (DOB) (Gaffin *et al.*, 2012a). Data have been collected on surface temperatures, albedo, and thermal emissivity for a test-coated and an uncoated asphaltic control surface. The experimental set-up including sensors is shown in Figure 6.6.

^bGreen workforce members are men and women from underserved communities in New York City who have applied for and successfully completed a 17-week training program. Eligibility requirements include 18 years of age (or greater), a GED or high school diploma, and a strong interest in pursuing a career in clean energy.

The figure shows the sensor deployment including infrared radiometers used to measure surface temperature, as well as a contact temperature probe used to verify the emissivity that is assumed when programming the infrared sensors. Also shown is an albedometer on a boom-arm consisting of two back-to-back pyranometers.

Analyses of temperature data from white and black roofs show that a significant reduction in peak temperatures is achieved with the paint (Fig. 6.7). Of note in Figure 6.7 is the peak black surface temperature (170 °F) during a heat wave that also set a record at that time (but since has been broken) for citywide electricity load for air conditioning. It is likely that this surface temperature is representative of similar dark asphalt surfaces through the metropolitan region including pavements. This is a surface temperature load that urban climate resiliency measures can target to mitigate the urban heat island effect.

Nighttime temperatures on the white and black roofs are comparable. This is expected because rooftops of both types have low internal energy storage and comparable emissivities. Thus, at sunset, both roof surfaces cool off rapidly and similarly.

Using data gathered on the NYC Cool Roofs Program (www.nyc.gov/html/coolroofs), a team of scientists at the Princeton Plasma Physics Laboratory

conducted an energy-benchmarking study to analyze the building data collected by the program prior to and after the white roof coating. The study focused on months with the most cooling degree days: June, July, and August. With kilowatt hours provided from the utility companies, the researchers compared energy use from the months prior to the coating to energy use from the months following the coating. Using an average fractional analysis, they were able to determine the change in electric consumption from before the coating to after the coating.

Results of the energy-benchmarking analyses show that three of the five buildings analyzed had a 10–20% reduction in kilowatt hours used. The researchers concluded that if certain building characteristics (including high roof-area/wall-area ratio, low-rise and mid-rise structures, and overall air tightness, such that the contribution of roofs to total building energy gain is not negligible) are met, coating a rooftop with a light albedo paint or surface can help achieve significant reductions to building energy use.

Next steps

New York City will continue to monitor and analyze the benefits and science of cool roof coatings and is currently engaged on the following activities:

1. Indicators and monitoring
 - Deploy high-precision, high-resolution thermal infrared imaging cameras to further the studies of urban climate and of heat island causation and reduction technologies.
2. Site-specific analyses
 - Assess the performance of the sites coated so far, specifically the reflectivity and emissivity of buildings coated 1, 2, 3, and 4 years ago in designated neighborhoods.
 - Characterize positive impacts of increasing cool roofs as they affect carbon emissions reduction, health, and urban cooling.
 - Study the causes of albedo loss on treated roofs.
3. Regional scale research
 - Urban climate monitoring should increasingly pursue improved characterization of urban temperatures. Among the complicating factors are that air temperatures in a

given locale are mixing with surrounding air masses, and this tends to dominate the resulting air temperature locally.

- Additionally, a small area of cool surface temperatures, for example, is unlikely to have even a measurable effect on the overlying air parcels. To study this requires a large-enough footprint of specific types of surface temperatures (e.g., green areas, pavements, sidewalks, higher-albedo test surfaces) to assess any relationship.
- Research should also be completed to determine how areas large enough to affect urban climate scale.
- Monitoring should routinely include surface as well as air temperature. Currently, most monitoring of temperatures at official weather stations involves only air temperature.

The next phase of research will be to acquire temperature data on cool rooftops of different ages. A parallel effort to diagnose the causes for the losses in albedo and temperature control over time will be made. A third area of study will include an effort to better understand the temperature benefits of the Cool Roofs Program to air parcels overlying the treated roof surfaces.

Many green infrastructure options (e.g., urban forestry, green streets and roofs, and perhaps eventually green walls) are also increasingly being installed, and their effectiveness at providing desirable environmental services such as temperature and stormwater control needs to be further quantified.

It is also important to develop improved public awareness and education campaigns about heat wave risks and sensible strategies New Yorkers can use to protect themselves as well as to lower energy demand during such extreme events (see Chapter 5). Public awareness of the importance of green infrastructure will also aid in the maintenance of the projects, which is currently a challenge.

6.4 Conclusions and recommendations

New York City level efforts may benefit from linkages to broader national indicator efforts such as the U.S. National Climate Assessment's (NCA) Indicator System (<http://www.globalchange.gov/what-we-do/assessment/indicators-system>). Because this system is still under development and covers a

wide range of systems, New York City and the broader region have the opportunity to lead in the development and use of urban indicators. This is particularly important because many proposed indicators under the NCA are designed to prove that climate change is having an impact on environmental and human systems rather than to support decision-making in light of climate change. Although proving cause and effect may be important for spurring national mitigation policies, it will be of less utility for identifying local adaptation options.

Conclusions

Based on a review of the existing indicators and monitoring activities in general, and the Cool Roofs Program in particular, the NPCC2 concludes the following:

- Existing indicators and monitoring systems in New York City can be adapted to provide targeted information for climate resiliency decisions.
- A comprehensive, integrated, and adequately funded interagency/multijurisdictional system for indicator and monitoring assessment is needed to enhance the scope and the robustness of New York City's climate resiliency efforts.

Recommendations

The NPCC2 recommends New York City take the following steps to develop its Climate Resiliency Indicators and Monitoring System:

- Build on existing efforts by the NPCC, City Agencies, and Federal partners by engaging a wide range of stakeholders—including infrastructure specialists, city planners, and community representatives—in order to develop a program to integrate climate indicators, monitor data, and explore possibilities to secure funding to support these efforts.
- Identify the gaps between the existing systems and the demands of urban climate change and the best opportunities for effectively bridging these gaps. Target those existing monitoring systems that can be easily enhanced while identifying those systems where more extensive adjustments will have to take place.

- Engage stakeholders and scientists in regard to environmental monitoring and adaptation planning for climate change:
 - Organize and implement a comprehensive regional New York City Climate Resiliency Indicators and Monitoring System with proper protocols for resiliency and adaptation adjustments.
 - Form weather and climate, coastal zones and sea level rise, water resources and water quality, health (see Chapter 5), and biodiversity and ecosystems working groups to set up the Climate Resiliency Indicators and Monitoring System.
 - Ensure that the indicator and monitoring results are the main drivers used to assess implementation outcomes.
- Develop and foster a community-driven approach whereby local organizations and individuals are empowered and encouraged to participate in New York City's climate resiliency process, practice, and decisions.

References

- Blake, R., A. Grimm, T. Ichinose, *et al.* 2011. Urban climate: Processes, trends, and projections. In *Climate Change and Cities: First Assessment Report of the Urban Climate Change Research Network*. C. Rosenzweig, W.D. Solecki, and S.A. Hammer, S. Mehrotra, Eds., Cambridge University Press, 43–81.
- Bradley, B.A., D.S. Wilcove, and M. Oppenheimer. 2010. Climate change increases risk of plant invasion in the Eastern United States. *Biol. Invasions* **12**: 1855–1872.
- Butchart, S.H.M., *et al.* 2010. Global biodiversity: indicators of recent declines. *Science* **328**(5982): 1164–1168.
- Buxton, H.T., and D.A. Smolensky. 1999. *Simulation of the Effects of Development of the Ground-water Flow System of Long Island, New York*. Washington, DC: U.S. Department of the Interior, U.S. Geological Survey.
- C40 Cities. 2011. *Climate Action in Megacities: C40 Cities Baseline and Opportunities*. Version 1.0, June 2011. C40 Cities and Arup.
- CDP (Carbon Disclosure Project) and C40 Cities. 2012. *Measurement for Management: CDP Cities 2012 Global Report*. London: Carbon Disclosure Project.
- City of New York. 2014. *One City, Built to Last: Transforming New York City's Buildings for A Low-Carbon Future*. [Available online at <http://www.nyc.gov/html/builttolast/assets/downloads/pdf/OneCity.pdf>.]
- Davis, A.P., *et al.* 2009. Bioretention technology: Overview of current practice and future needs. *J. Environ. Eng.* **135.3**: 109–117.

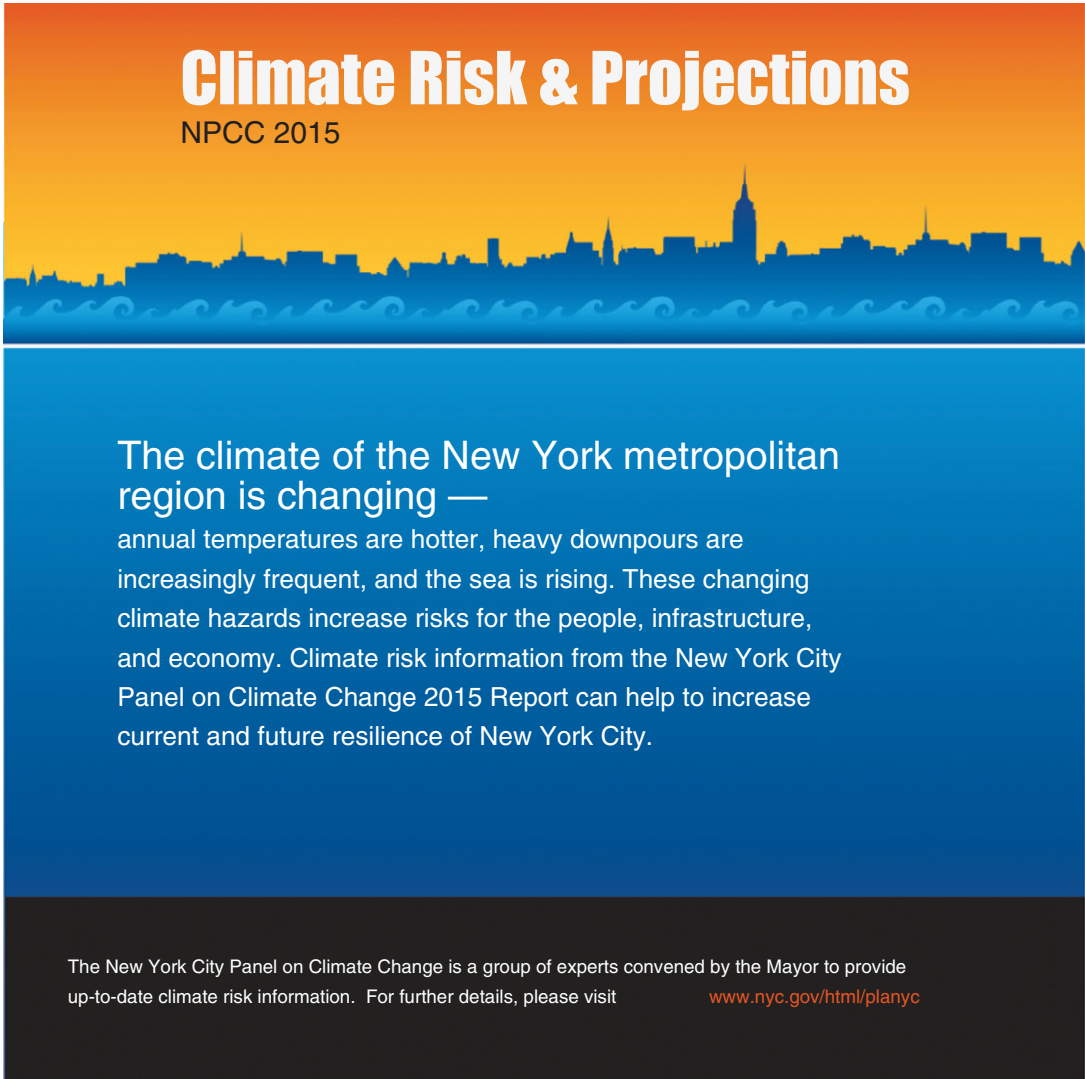
- de Sherbinin, A., A. Reuben, M. Levy, and L. Johnson. 2013. *Indicators in Practice: How Environmental Indicators are Being Used in Policy and Management Contexts*. New Haven and New York: Yale and Columbia Universities. Available at <http://ciesin.columbia.edu/binaries/web/global/news/2013/indicatorsinpractice.pdf>.
- Diamond, H.J., *et al.* 2013. US Climate Reference Network after one decade of operations. *Bull. Am. Meteorol. Soc.* **94.4**.
- EIU (Economist Intelligence Unit). 2012. *Green City Index*. Munich: Siemens AG. Accessed at http://www.siemens.com/entry/cc/features/greencityindex_international/all/en/pdf/gci_report_summary.pdf on March 31, 2014.
- Gaffin, S., R. Rosenzweig, and A.Y.Y. Kong. 2012. Adapting to climate change through urban green infrastructure. *Nature Climate Change*, **2**: 704.
- Gaffin, S.R., M. Imhoff, C. Rosenzweig, *et al.* 2012. Bright is the new black—multi-year performance of high-albedo roofs in an urban climate. *Environ. Res. Lett.* **7**. doi 10.1088/1748-9326/7/1/014029.
- Gaffin, S.R., C. Rosenzweig, R. Khanbilvardi, *et al.* 2011. *Stormwater Retention for a Modular Green Roof Using Energy Balance Data*. New York: Columbia University, Center for Climate Systems Research.
- Gaffin, S.R., C. Rosenzweig, J. Eichenbaum-Pikser, *et al.* 2010. *A Temperature and Seasonal Energy Analysis of Green, White, and Black Roofs*. New York: Columbia University, Center for Climate Systems Research. Available online at: <http://www.coned.com/newsroom/news/pr20100503.asp>
- Gaffin, S.R., C. Rosenzweig, R. Khanbilvardi, *et al.* 2008. Variations in New York City's urban heat island strength over time and space. *Theor. Appl. Climatol.* doi: 10.1007/s00704-007-0368-3.
- Georgas, N., and A.F. Blumberg. 2010. Establishing confidence in marine forecast systems: the design and skill assessment of the New York Harbor Observation and Prediction System, version 3 (NYHOPS v3). *Am. Soc. Civ. Eng.* doi: 10.1061/41121(388)39.
- Homer, C.H., J.A. Fry, and C.A. Barnes. 2012. *The National Land Cover Database, U.S. Geological Survey Fact Sheet 2012–3020*. Washington, DC: USGS.
- Hsu, A., J. Emerson, M. Levy, *et al.* 2014. *2014 Environmental Performance Index*. New Haven, CT: Yale Center for Environmental Law and Policy.
- IISD (International Institute for Sustainable Development). 2008. *Bellagio Sustainability Assessment and Measurement Principles (STAMP)*. Available at <http://www.iisd.org/measure/principles/progress/bellagiostamp/>.
- Karl, T.R., J.M. Melillo, and T.C. Peterson, Eds. 2009. *Global Climate Change Impacts in the United States*. Cambridge: Cambridge University Press.
- Li, D., E. Bou-Zeid, and M. Oppenheimer. 2014. The effectiveness of cool and green roofs as urban heat island mitigation strategies. *Environ. Res. Lett.* **9**: 055002.
- Moench, D., *et al.* 2011. *Catalyzing Urban Climate Resilience: Applying Resilience Concepts to Planning Practice in the ACCCRN Program*. Boulder, CO: Institute for Social and Environmental Transition.
- Monti, J. Jr., M. Como, and R. Busciolano. 2013. Water-table and Potentiometric-surface Altitudes in the Upper Glacial, Magothy, and Lloyd Aquifers beneath Long Island, New York, April–May 2010: U.S. Geological Survey, Scientific Investigations Map 3270, 4 sheets, scale 1:125,000. Available from <http://dx.doi.org/10.3133/sim3270>.
- Morgan, J.L., S.E. Gergel, and N.C. Coops. 2010. Aerial photography: a rapidly evolving tool for ecological management. *BioScience* **60.1**: 47–59.
- Moss, M., L. Qing, Y. Carson, and S. Kaufman. 2012. *Commuting to Manhattan. A Study of Residence Location Trends for Manhattan Workers from 2002 to 2009*. New York: Rudin Center for Transportation Policy and Management, New York University Wagner School of Public Service.
- Murdoch, P.S., J.S. Baron, and T.L. Miller. 2000. Potential effects of climate change on surface-water quality in North America. *J. Am. Water Resources Assoc.* **36.2**: 347–366.
- National Academy of Sciences, National Research Council. 2012. *Urban Meteorology: Forecasting, Monitoring, and Meeting Users' Needs*. Washington, DC: The National Academies Press.
- NJDEP. 2010. *NJDEP 2007 Land Use/Land Cover Update*. Trenton: New Jersey Department of Environmental Protection. Available at: <http://www.nj.gov/dep/gis/lulc07shp.html>.
- NYCDEP (New York City Department of Environmental Protection). 2011. *New York City Drinking Water 2011 Water Supply and Quality Report*. Available at: <http://www.nyc.gov/html/dep/pdf/wsstate11.pdf>. Accessed January 22, 2014.
- NYCDEP (New York City Department of Environmental Protection). 2012. *Drought Management Contingency Plan*. Available at: <http://www.nyc.gov/html/dep/pdf/droughtp.pdf>. Accessed January 22, 2014.
- NPCC. 2010. *Climate Change Adaptation in New York City: Building a Risk Management Response*. C. Rosenzweig and W. Solecki, Eds., *Ann. N.Y. Acad. Sci.* **1196**: 1–354.
- NPCC. 2015. *Building the Knowledge Base for Climate Resiliency: New York City Panel on Climate Change 2015 Report*. C. Rosenzweig and W. Solecki, Eds., *Ann. N.Y. Acad. Sci.* **1336**: 1–149.
- Pinter, L. 2013. *Measuring Progress Towards Sustainable Development Goals*. Winnipeg, Canada: International Institute for Sustainable Development.
- Redman, C.L., J.M. Grove, and L.H. Kuby. 2004. Integrating social science into the long-term ecological research (LTER) network: social dimensions of ecological change and ecological dimensions of social change. *Ecosystems* **7.2**: 161–171.
- Romero Lankao, P., and H. Qin. 2011. Conceptualizing urban vulnerability to global climate and environmental change. *Curr. Opin. Environ. Sustainability* **3**: 1–8.
- Rosenzweig, C., *et al.* 2005. Characterizing the urban heat island in current and future climates in New Jersey. *Global Environ. Change Part B: Environ. Hazards* **6.1**: 51–62.
- Rosenzweig, C., W.D. Solecki, L. Parshall, *et al.* 2009. Mitigating New York City's heat island: integrating stakeholder perspectives and scientific evaluation. *Bull. Am. Meteorol. Soc.* **90**: 1297–1312.
- Rotzoll, K., and C.H. Fletcher. 2013. Assessment of groundwater inundation as a consequence of sea-level rise. *Nature Climate Change* **3.5**: 477–481.
- Schauser, I., S. Otto, S. Schneiderbauer, *et al.* 2010. *Urban Regions: Vulnerabilities, Vulnerability Assessments by Indicators*

- and Adaptation Options for Climate Change Impacts*. The European Topic Centre on Air and Climate Change. Copenhagen: ETC - ACC Technical Paper 2010/12, December 2010.
- SCI (Sustainable Cities Initiative) and CIDA (Canadian International Development Agency). 2012. *Indicators for Sustainability: How Cities Are Monitoring and Evaluating Their Success*. Ottawa, Canada: CIDA.
- Shen, L.-Y., J.J. Ochoa, M.N. Shah, and X. Zhang. 2011. The application of urban sustainability indicators—A comparison between various practices. *Habitat Int.* **34**: 17–29.
- Solecki, W., L. Patrick, M. Brady, K. Grady, and A. Moroko. 2010. Climate Protection Levels: Incorporating Climate Change into Design and Performance Standards. In “New York City Panel on Climate Change. Climate Change Adaptation in New York City: Building a Risk Management Response.” C. Rosenzweig, and W. Solecki, Eds., *Ann. N.Y. Acad. Sci.* **1196**: 293–352.
- Soren, J. 1976. Basement flooding and foundation damage from water table rise in the East New York section of Brooklyn. In *USGS Water-Resources Investigation, Long Island*. Washington, DC: USGS, 76–95.
- Stewart, R.J., *et al.* 2013. Horizontal cooling towers: riverine ecosystem services and the fate of thermoelectric heat in the contemporary Northeast US. *Environ. Res. Lett.* **8.2**: 025010.
- Swart, R., J. Fons, W. Geertsema, *et al.* 2012. *Urban Vulnerability Indicators: A Joint Report of ETC-CCA and ETC-SIA*. Copenhagen: ETC-CCA and ETC-SIA Technical Report 01/2012, December 18, 2012.
- Tyler, S., E. Nugraha, H.K. Nguyen, *et al.* 2014. *Developing Indicators of Urban Climate Resilience. ISET Climate Resilience Working Paper 3, January 2014*. Available at: http://i-s-e-t.org/images/pdfs/ISET_DevelopingIndicatorsofUCR_140204.pdf.
- Van Buskirk, J., R.S. Mulvihill, and R.C. Leberman. 2009. Variable shifts in spring and autumn migration phenology in North American songbirds associated with climate change. *Global Change Biol.*, **15**(3): 760–771.
- Van Buskirk, J. 2012. Changes in the Annual Cycle of North American Raptors Associated with Recent Shifts in Migration Timing. *The Auk* **129**: 691–698.
- Yaro, R., and T. Hiss. 1996. *A Region at Risk: The Third Regional Plan for the New York-New Jersey-Connecticut Metropolitan Area*. Washington, DC: Island Press.

ANNALS OF THE NEW YORK ACADEMY OF SCIENCES

Issue: *Building the Knowledge Base for Climate Resiliency*

Appendix I: Climate Risk and Projections NPCC 2015 Infographics



Climate Risk & Projections
NPCC 2015

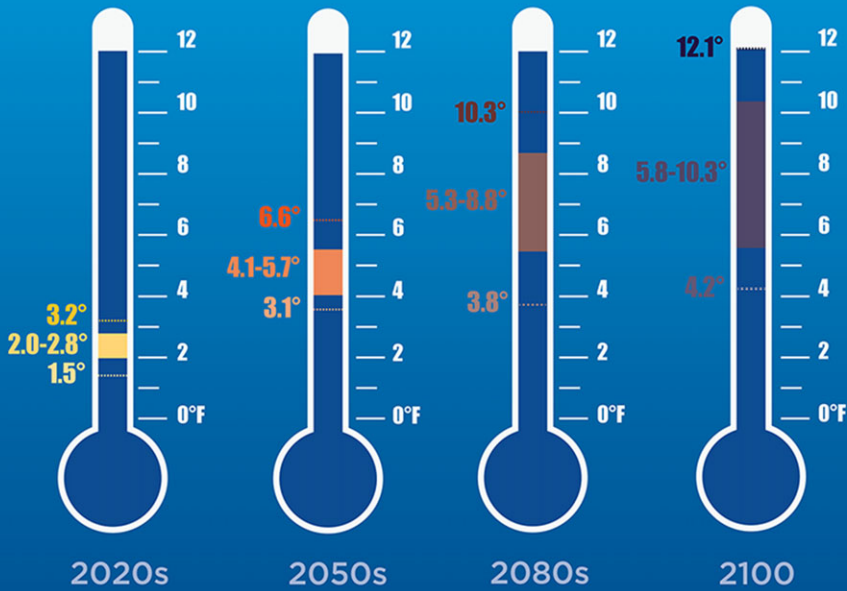
The climate of the New York metropolitan region is changing — annual temperatures are hotter, heavy downpours are increasingly frequent, and the sea is rising. These changing climate hazards increase risks for the people, infrastructure, and economy. Climate risk information from the New York City Panel on Climate Change 2015 Report can help to increase current and future resilience of New York City.

The New York City Panel on Climate Change is a group of experts convened by the Mayor to provide up-to-date climate risk information. For further details, please visit www.nyc.gov/html/planyc

Infographic 1.

Temperatures are extremely likely to increase in New York City through the end of the century

TEMPERATURE - MEAN ANNUAL CHANGES
Baseline (1971-2000) 54°F



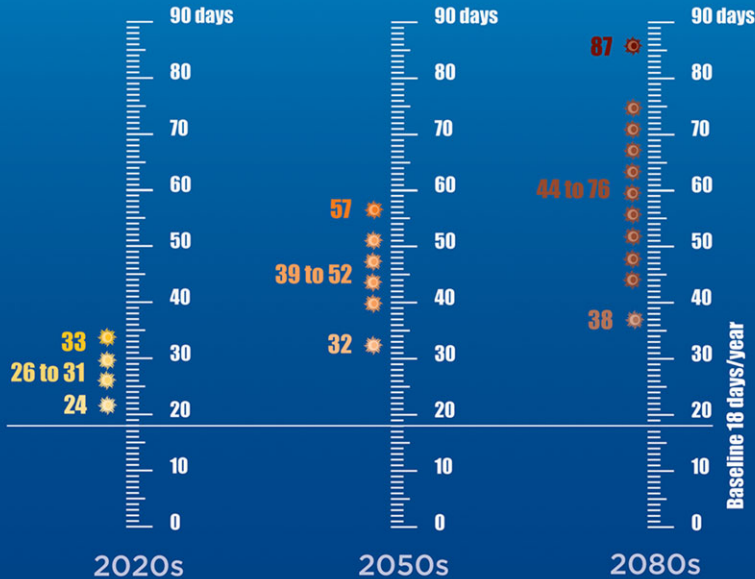
	2020s	2050s	2080s	2100
High
Middle
Low

The low estimate (10th percentile), middle range (25th percentile to 75th percentile), and high estimate (90th percentile).

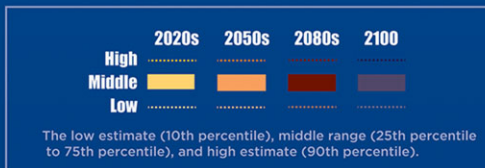
Infographic 2.

The number of hot days is projected to increase and the number of cold days is projected to decrease

Number of days/year with maximum temperature at or above 90°F (1971-2000 average is 18 days/year)



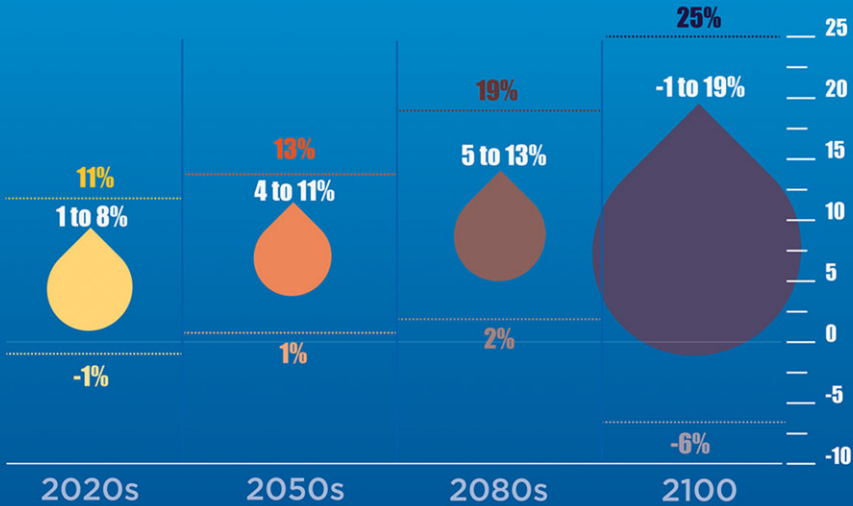
Based on 35 global climate models (GCMs) and 2 Representative Concentration Pathways (RCPs). Baseline data are from the National Oceanic and Atmospheric Administration (NOAA) National Climatic Data Center (NCDC).



Infographic 3.

Total annual precipitation in New York City will likely increase

PRECIPITATION - MEAN ANNUAL CHANGES (PERCENT)
Baseline (1971-2000) 50.1 inches



Based on 35 global climate models (GCMs) and 2 Representative Concentration Pathways (RCPs). Baseline data are from the National Oceanic and Atmospheric Administration (NOAA) National Climatic Data Center (NCDC).

	2020s	2050s	2080s	2100
High
Middle
Low

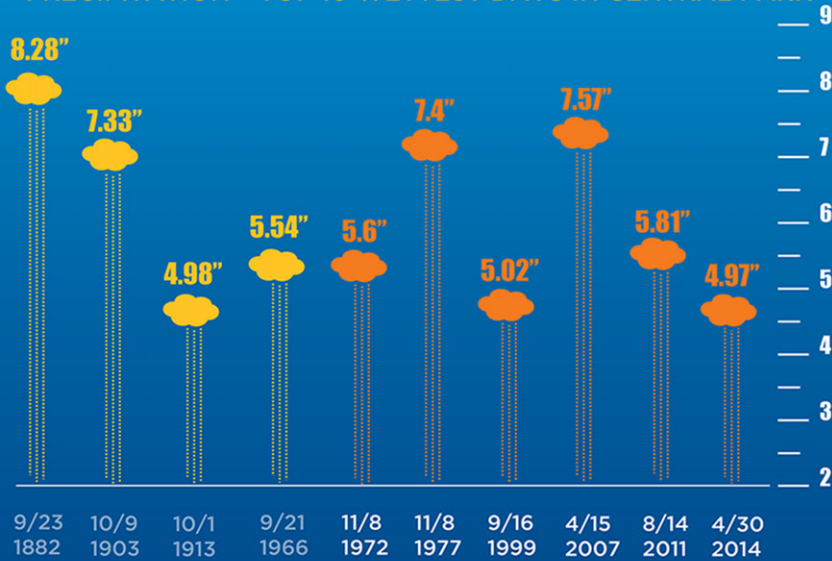
The low estimate (10th percentile), middle range (25th percentile to 75th percentile), and high estimate (90th percentile).

Infographic 4.

6 of the 10 wettest days on record in NYC have occurred since 1972

Heavy precipitation events in the Northeast have been increasing and this trend is projected to continue.

PRECIPITATION - TOP 10 WETTEST DAYS IN CENTRAL PARK

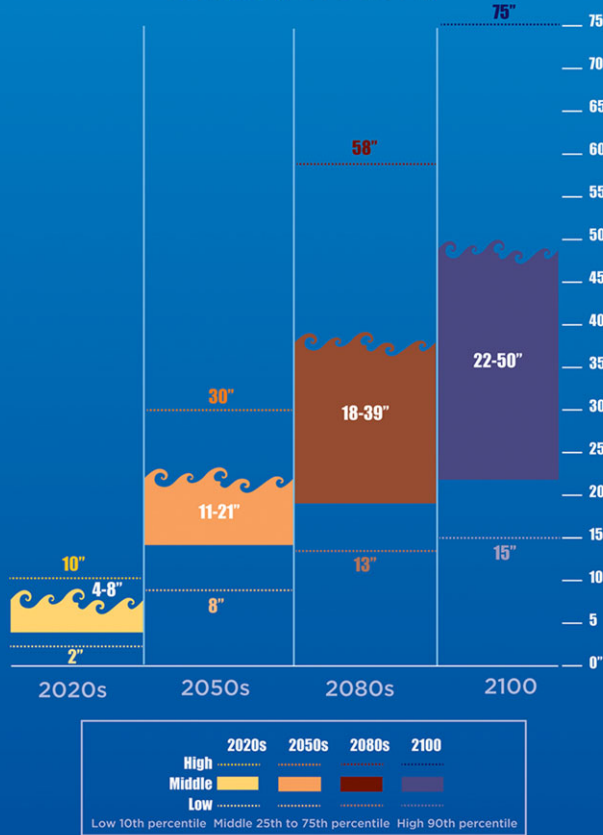


Data are from the National Weather Service and are for Central Park, New York. Record dates back to 1869.

Infographic 5.

Sea level rise in New York City is very likely to accelerate as the century progresses

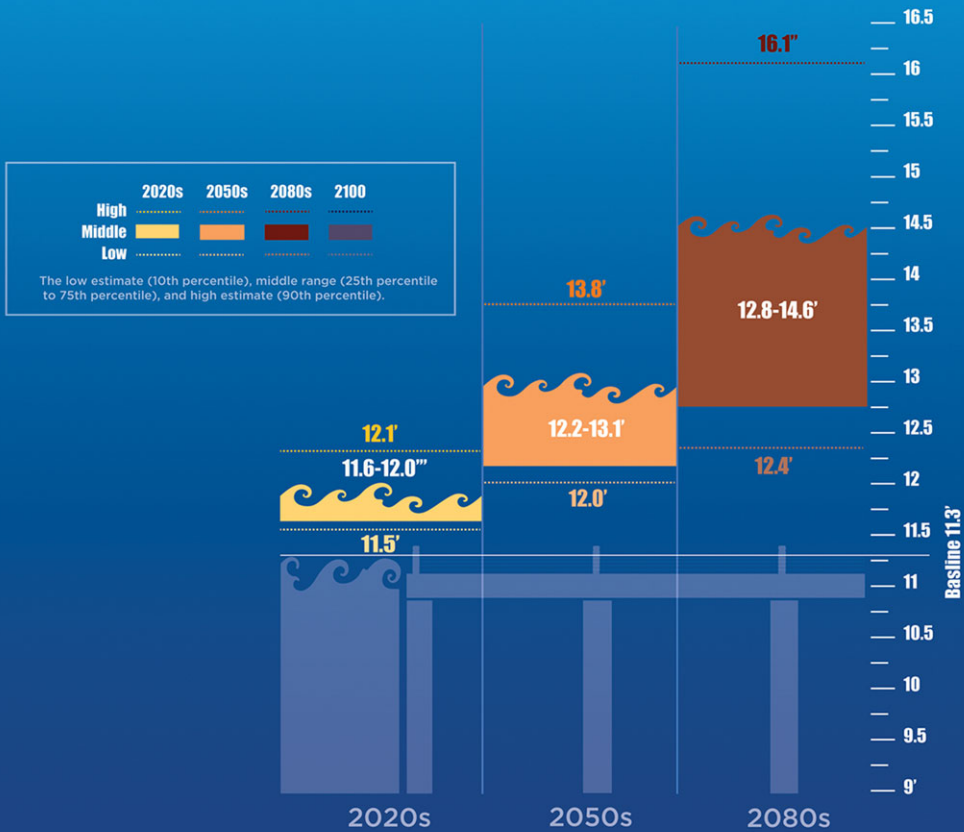
SEA LEVEL - MEAN ANNUAL CHANGES
Baseline (2000-2004)



Infographic 6.

Sea level rise is projected to cause an increase in coastal flooding

1-in-100 year Flood Heights (BASE HEIGHT: 11.3 FEET)



Infographic 7.

ANNALS OF THE NEW YORK ACADEMY OF SCIENCES

Issue: *Building the Knowledge Base for Climate Resiliency***Appendix II: NPCC 2015 Technical Details****A. Climate observations and projections: Methods and analyses^a****Contents**

- A.1 Observed extreme events
- A.2 Global climate models (GCMs)
- A.3 Climate projections

A.1 Observed extreme events

Temperature. Hot days, heat waves, and cold days in Central Park (1900–2013) based on maximum temperatures at or above 90°F, 100°F, at or above 90°F for three consecutive days, and minimum temperatures at or below 32°F (see Fig. A.1).

Precipitation. Heavy precipitation events in Central Park (1900–2013) based on daily precipitation at or above 1, 2, and 4 inches (see Fig. A.2).

Tropical storms and hurricanes. See Table A.1.

A.2 Global climate models

See Table A.2 for a list of the global climate models used in the NPCC 2015 report.

A.3 Climate projections

Methods for 2100 projections. Projections for 2100 require a different approach from the 30-year timeslices (10-year for sea level rise) that are centered on the 2020s, 2050s, and 2080s, which are what the New York City Panel on Climate Change (NPCC) traditionally uses. The primary difference is that because the vast majority of climate model simulations end in 2100, it is not possible to make a projection for the 30-year timeslice (10-year for sea level rise) centered on the year 2100.

Given this model availability constraint, the NPCC considered the alternate approaches listed below to generate projections for 2100. Both ap-

proaches share one thing in common: they involve adding a linear trend to the final timeslice (2080s for temperature and precipitation, 2090s for sea level rise), and extrapolating that trend to 2100. The final period linear trend (FPLT) is for 2085 to 2099 for temperature and precipitation, and 2095 to 2099 for sea level rise. The NPCC also considered quadratic trends as well, but determined that over the short time periods used for the trends, a linear approach produced comparable results. The two used approaches are:

1. Add each representative concentration pathway (RCP) ensemble mean FPLT to the final timeslice projections for the corresponding RCP, and calculate the four distribution points (i.e., 10th, 25th, 75th, and 90th percentiles).
2. Add the FPLT from each individual model and RCP to the final timeslice for the corresponding model and RCP, and then calculate the four distribution points (i.e., 10th, 25th, 75th, and 90th percentiles).

Approaches 1 and 2 were averaged to generate projections for 2100 (Table A.3).

It is also important to note that uncertainties are inherently much greater for the end of the century than the mid-century. For example, the RCP runs do not sample all the possible carbon and other biogeochemical cycle feedbacks associated with climate change. Even the few Earth System Models in the Coupled Model Intercomparison Project (CMIP5) used by the NPCC2 may underestimate the potential for increased methane and carbon releases from the Arctic under extreme warming scenarios. More generally, the potential for surprises increases further into the future one considers, such as technological innovations that could remove carbon from the atmosphere.

Maps of ensemble mean annual temperature and precipitation change. Figures A.3 and A.4 demonstrate that the mean temperature and

^aThis Appendix provides technical details for New York City Panel of Climate Change 2015 Report, Chapter 1: Climate Observations and Projections.

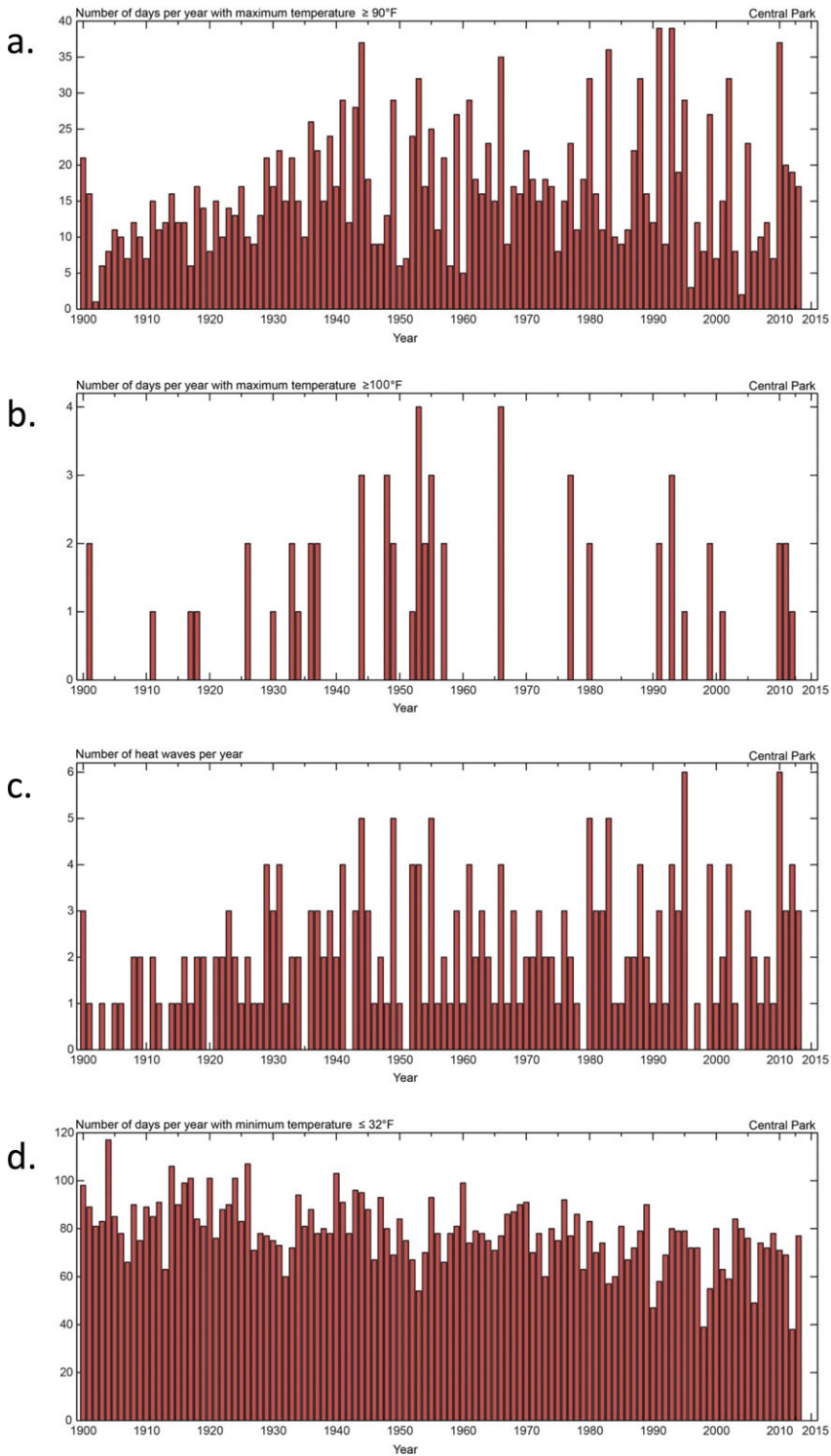


Figure A.1. Observed extreme temperature events (1900–2013): (a) maximum temperatures at or above 90°F ; (b) maximum temperatures at or above 100°F ; (c) heat waves (at or above 90°F for three consecutive days); and (d) minimum temperatures at or below 32°F .

Table A.1. Dates and major impacts from tropical storms and hurricanes that struck in New York metropolitan area

Date	Name	Category ^a	Central pressure ^{b,c}	Wind speed ^{b,c}	Notes
September 23, 1815	Great September Gale of 1815	3		(155)	
September 3, 1821	Norfolk and Long Island Hurricane	3	975 (970)	110 (130)	Only direct strike on New York City. Surge of 13 ft in 1 hour. Flooded parts of lower Manhattan as far north as Canal Street.
September 15, 1858	New England Storm	1	979 (976)	85 (100)	
September 8, 1869	Eastern New England Storm	2	963 (950)	100 (115)	
August 23, 1893	Midnight Storm	1	986 (952)	85 (115)	Flooded southern Brooklyn and Queens.
September 21, 1938	Long Island Express/New England Storm	3	945 (935)	110 (160)	Killed ~700 people. Storm surge of 10–12 feet on Long Island.
September 15, 1944	Great Atlantic Hurricane of 1944	1	965 (943)	80 (140)	Landfall over central Long Island.
August 31, 1954	Carol	2	975 (970)	100 (100)	Wind gusts between 115 and 125 mph over eastern Long Island.
September 12, 1960	Donna	2–3	965 (932)	110 (160)	Storm surge of 11 ft. Second highest recorded water level at the Battery (7.22 ft NAVD88). Lower Manhattan to West & Cortland Streets flooded nearly waist deep.
September 21, 1961	Esther	3	978 (927)	115 (145)	Minor flooding and power outages disrupted transportation on Long Island.
June 22, 1972	Agnes	TS – 1	980 (977)	70 (85)	Caused significant flooding.
August 10, 1976	Belle	1	980 (957)	85 (120)	Landfall on Long Island with wind gusts over 95 mph.
September 27, 1985	Gloria	2	951 (920)	105 (145)	Wind gusts over 110 mph. Struck at low tide with 5.45 ft water level (NAVD88).
August 19, 1991	Bob	2	962 (950)	105 (115)	Eye passed just east of Long Island.
September 16, 1999	Floyd	TS – 1	974 (921)	70 (155)	Major inland flooding with 24-hour rainfall totals between 10 and 15 inches in upstate New Jersey and New York.

Continued

Table A.1. Continued

Date	Name	Category ^a	Central pressure ^{b,c}	Wind speed ^{b,c}	Notes
August 28, 2011	Irene	TS	965 (942)	65 (120)	Center passed over Coney Island; 3–6 ft surge. Major inland flooding upstate NY and New England.
October 29, 2012	Sandy	PTS ^d -1	946 (941)	80 (115)	Major coastal flooding and power outages in New York City, New Jersey, and Long Island coasts. Record maximum water level of 11.28 ft above NAVD88 at the Battery.

NOTE: The above-mentioned storms have been selected based on their tracks and impacts on the New York metropolitan area. No single metric (i.e., location of landfall within a given distance of the city) was used to determine what storms to include.

^aCategory (based on the Saffir–Simpson Scale) is the estimated strength of the storm as it impacted the New York City area.

^bMinimum central pressure (in millibars (mb)) and maximum wind speed (in miles per hour (mph)).

^cThe central pressure and wind speed at the time the storm impacted the area; the numbers in parenthesis are the storm’s most intense observation(s).

^dPTS, posttropical storm. The term posttropical is used in National Weather Service advisory products to refer to any closed low-pressure system that no longer qualifies as a tropical cyclone (TC). However, such systems can continue carrying heavy rains and damaging winds. Post-TCs can be either frontal (extratropical) or nonfrontal lows.

SOURCE: Unisys Hurricane Archive (<http://weather.unisys.com/hurricane/>).

precipitation projections for the New York metropolitan region are part of a larger regional pattern. Shown are the national and regional changes in temperature and precipitation for the 2050s relative to 1971–2000. These changes are averaged across the 35 GCMs under RCP4.5 (top) and RCP 8.5 (bottom); while the two RCPs differ in the amount of changes projected, the spatial pattern across the United States is similar for both RCPs. Because these maps represent an average across 35 models, they obscure the substantial variations from one model to another that are evident in Table A.2.

Temperature. New York City’s proximity to the coast is projected to lead to approximately 0.5°F less warming than in the interior regions of the Northeast. The map also reveals that the Northeast is expected to experience slightly more warming than the mid-Atlantic.

Precipitation. Precipitation projections also show very little spatial variation across the Northeastern United States. However, the map does reveal a tendency for slightly greater precipitation increases to the north of New York City near the Canadian border, and slightly smaller increases in the mid-Atlantic region.

Seasonal and monthly projections. Throughout the 21st century, projected warming is comparable in each of the four seasons for the New York metropolitan region (Tables A.4 and A.5). As the century progresses, precipitation increases become highest during the winter season (Tables A.6 and A.7); for both the 2050s and the 2080s, winter is the only season where the 10th percentile projections show projected increases. This indicates that during the other three seasons, precipitation decreases cannot be ruled out.

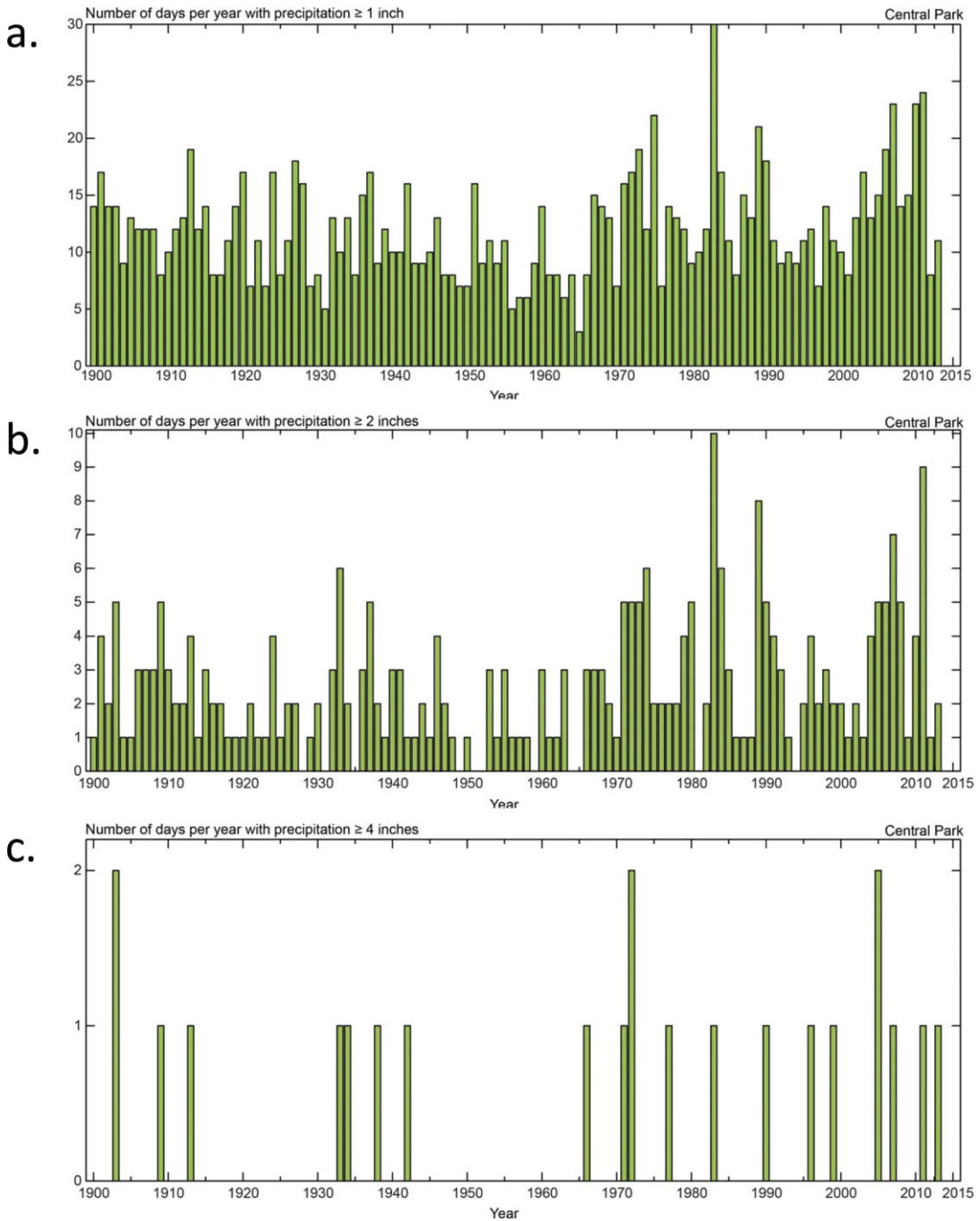


Figure A.2. Observed extreme precipitation events (1900–2013): (a) daily precipitation at or above 1 inch; (b) daily precipitation at or above 2 inches; and (c) daily precipitation at or above 4 inches.

Temperature Change-2050s

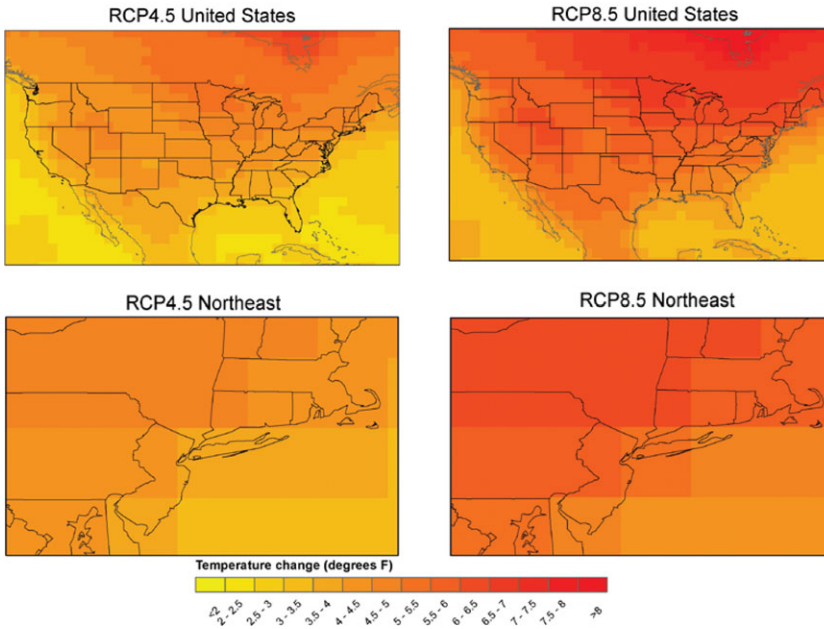


Figure A.3. Annual temperature changes in the 2050s.

Precipitation Change-2050s

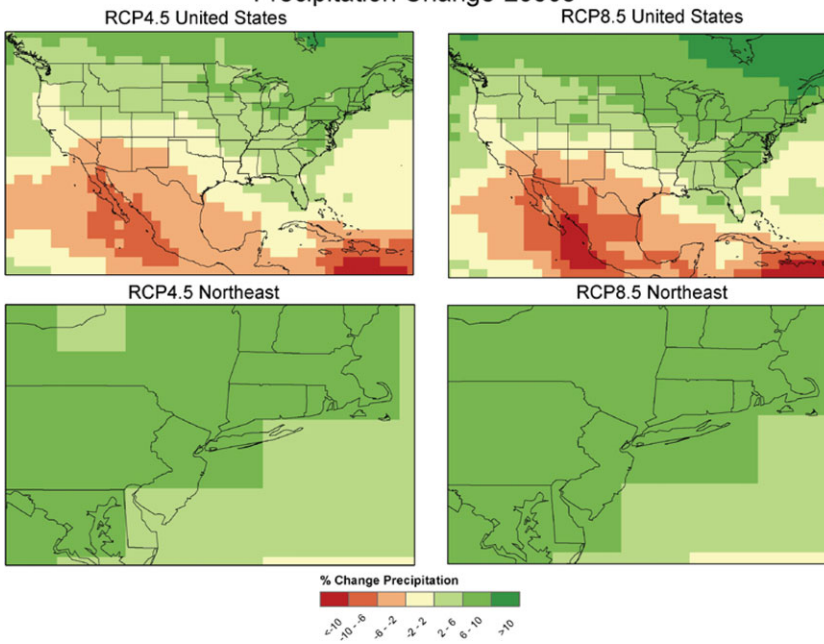


Figure A.4. Annual precipitation changes in the 2050s.

Table A.2. IPCC AR5 global climate models (GCMs) used by the NPCC2

Modeling center	Institute ID	Model name	Atmospheric resolution (lat° × lon°)
Commonwealth Scientific and Industrial Research Organization (CSIRO) and Bureau of Meteorology (BOM), Australia	CSIRO – BOM	ACCESS1.0	1.25 × 1.875
		ACCESS1.3	1.25 × 1.875
Beijing Climate Center, China Meteorological Administration	BCC	BCC-CSM1.1	2.8 × 2.8
		BCC-CSM1.1 (m)	1.1 × 1.1
College of Global Change and Earth System Science, Beijing Normal University	GCESS	BNU-ESM	2.8 × 2.8
Canadian Centre for Climate Modelling and Analysis	CCCMA	CanESM2	2.8 × 2.8
National Center for Atmospheric Research	NCAR	CCSM4	0.9 × 1.25
Community Earth System Model Contributors	NSF-DOE-NCAR	CESM1(BGC)	0.9 × 1.25
		CESM1(CAM5)	0.9 × 1.25
Centro Euro-Mediterraneo per i Cambiamenti Climatici	CMCC	CMCC-CM	0.75 × 0.75
		CMCC-CMS	1.9 × 1.9
Centre National de Recherches Météorologiques/Centre Européen de Recherche et Formation Avancée en Calcul Scientifique	CNRM-CEFRACS	CNRM-CM5	1.4 × 1.4
Commonwealth Scientific and Industrial Research Organization in collaboration with Queensland Climate Change Centre of Excellence	CSIRO-QCCE	CSIRO-Mk3.6.0	1.9 × 1.9
LASG, Institute of Atmospheric Physic, Chinese Academy of Sciences and CESS, Tsinghua University	LASG-CESS	FGOALS-g2	2.8 × 2.8
The First Institute of Oceanography, SOA, China	FIO	FIO-ESM	2.8 × 2.8
NOAA Geophysical Fluid Dynamics Laboratory	NOAA GFDL	GFDL-CM3	2.0 × 2.5
		GFDL-ESM2G	2.0 × 2.5
		GFDL-ESM2M	2.0 × 2.5
NASA Goddard Institute for Space Studies	NASA GISS	GISS-E2-H	2.0 × 2.5
		GISS-E2-R	2.0 × 2.5
National Institute of Meteorological Research/Korea Meteorological Administration	NIMR/KMA	HadGEM2-AO	1.25 × 1.875

Continued

Table A.2. Continued

Modeling center	Institute ID	Model name	Atmospheric resolution (lat° × lon°)
Met Office Hadley Centre (additional HadGEM2-ES realizations contributed by Instituto Nacional de Pesquisas Espaciais)	MOHC (additional realizations by INPE)	HadGEM2-CC HadGEM2-ES	1.25 × 1.875 1.25 × 1.875
Institute for Numerical Mathematics	INM	INM-CM4	1.5 × 2.0
Institut Pierre-Simon Laplace	IPSL	IPSL-CM5A-LR IPSL-CM5A-MR IPSL-CM5B-LR	1.9 × 3.75 1.3 × 2.5 1.9 × 3.75
Japan Agency for Marine-Earth Science and Technology, Atmosphere and Ocean Research Institute (The University of Tokyo), and National Institute for Environmental Studies)	MIROC	MIROC-ESM MIROC-ESM- CHEM	2.8 × 2.8 2.8 × 2.8
Atmosphere and Ocean Research Institute (The University of Tokyo), National Institute for Environmental Studies, and Japan Agency for Marine-Earth Science and Technology	MIROC	MIROC5	1.4 × 1.4
Max Planck Institute for Meteorology	MPI-M	MPI-ESM-MR MPI-ESM-LR	1.9 × 1.9 1.9 × 1.9
Meteorological Research Institute	MRI	MRI-CGCM3	1.1 × 1.1
Norwegian Climate Centre	NCC	NorESM1-M NorESM1-ME	1.9 × 2.5 1.9 × 2.5

NOTE: This table provides information about the 35 GCMs used by the NPCC2. The 35 models were developed by 22 modeling centers (left column). Some centers support multiple GCMs, and/or versions (for example, some institutions conducted multiple simulations at varying spatial resolutions) of their GCM.

Table A.3. NPCC2 2100 projections for temperature, precipitation, and sea level rise

	Low estimate (10th percentile)	Middle range (25th to 75th percentile)	High estimate (90th percentile)
(a) Temperature projections for 2100^a			
Approach 1	+4.5°F	+6.0 to 10.4°F	+11.9°F
Approach 2	+3.9°F	+5.5 to 10.3°F	+12.3°F
2100 Projections (average of Approaches 1 and 2)	+4.2°F	+5.8 to 10.4°F	+12.1°F
(b) Precipitation projections for 2100^b			
Approach 1	-1%	+2 to +14%	+18%
Approach 2	-11%	-5 to +24%	+32%
2100 Projections (average of Approaches 1 and 2)	-6%	-1 to +19%	+25%
(c) Sea-level rise projections for 2100^{c,d}			
Approach 1	7 inches	9 to 18 inches	24 inches
Approach 2	6 inches	9 to 19 inches	26 inches
Model-based component average	6 inches	9 to 18 inches	25 inches
2100 Total SLR projections (average of Approaches 1 and 2)	15 inches	22 to 50 inches	75 inches

^aBased on 35 global climate models (GCMs) and two representative concentration pathways (RCPs). Projections are relative to the 1971–2000 base period.

^bBased on 35 GCMs and two RCPs. Projections are relative to the 1971–2000 base period.

^cBased on 24 GCMs and two RCPs. Projections are relative to the 2000–2004 base period.

^dRows 1, 2, and 3 are for model-based sea level rise components only; the final row shows row three plus all other sea level change components.

Table A.4. NPCC2 projected seasonal temperature changes (°F)

	Low estimate (10th percentile)	Middle range (25th to 75th percentile)	High estimate (90th percentile)
(a) 2020s			
Winter	1.4°F	2.0°F to 3.2°F	3.7°F
Spring	1.2°F	1.6°F to 2.7°F	3.1°F
Summer	1.8°F	2.1°F to 3.1°F	3.3°F
Fall	1.9°F	2.3°F to 3.2°F	3.6°F
(b) 2050s			
Winter	3.1°F	4.2°F to 6.0°F	6.8°F
Spring	2.7°F	3.6°F to 5.2°F	6.4°F
Summer	3.1°F	4.3°F to 5.8°F	6.6°F
Fall	3.6°F	4.3°F to 5.7°F	6.8°F
(c) 2080s			
Winter	3.9°F	5.6°F to 8.8°F	10.5°F
Spring	3.7°F	4.7°F to 7.9°F	8.9°F
Summer	4.1°F	4.9°F to 9.5°F	10.5°F
Fall	3.9°F	5.5°F to 9.2°F	10.8°F

NOTES: Winter, December to February; Spring, March to May; Summer, June to August; Fall, September to November. Based on 35 GCMs and two representative concentration pathways. Projections are relative to the 1971–2000 base period.

Model-based range of outcomes (distribution) for temperature changes (°F) in New York City, relative to the 1971–2000 base period for the 2020s, 2050s, and 2080s. Projections are based on 35 GCMs and 2 representative concentrations pathways.

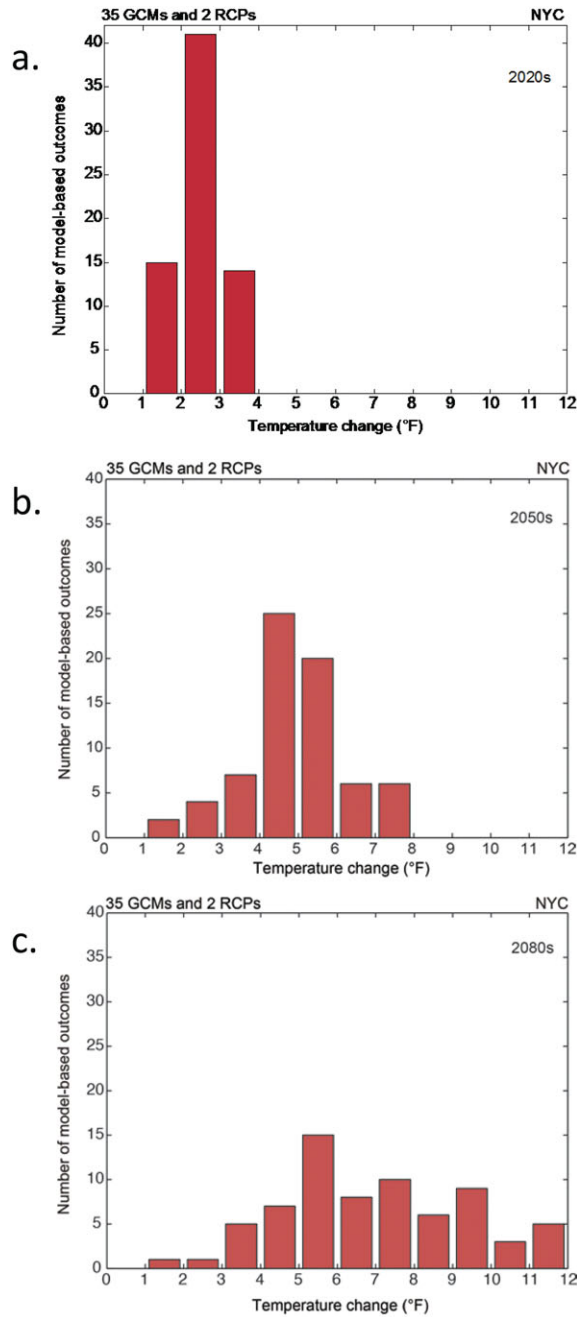


Figure A.5. Model-based range of outcomes (distribution) of projected temperature changes: (a) 2020s, (b) 2050s, and (c) 2080s.

Table A.5. Projected monthly temperature changes (°F)

	Low estimate (10th percentile)	Middle range (25th to 75th percentile)	High estimate (90th percentile)
(a) 2020s			
January	0.9°F	1.6°F to 3.6°F	4.4°F
February	0.8°F	1.6°F to 2.9°F	4.0°F
March	0.3°F	1.3°F to 2.7°F	3.6°F
April	1.1°F	1.5°F to 2.6°F	3.4°F
May	0.9°F	1.4°F to 2.9°F	3.5°F
June	1.0°F	1.7°F to 2.8°F	3.3°F
July	1.4°F	2.0°F to 3.0°F	3.3°F
August	1.5°F	2.2°F to 3.1°F	3.5°F
September	1.5°F	2.3°F to 3.2°F	3.7°F
October	1.2°F	2.0°F to 3.2°F	3.6°F
November	1.1°F	1.8°F to 3.2°F	3.8°F
December	0.6°F	1.8°F to 3.5°F	4.3°F
(b) 2050s			
January	2.9°F	3.9°F to 6.1°F	7.0°F
February	2.8°F	3.6°F to 5.7°F	6.7°F
March	2.6°F	3.6°F to 5.2°F	6.4°F
April	2.5°F	3.3°F to 5.1°F	6.5°F
May	2.4°F	3.2°F to 5.3°F	6.4°F
June	2.5°F	3.8°F to 5.9°F	6.3°F
July	2.9°F	4.1°F to 5.9°F	6.8°F
August	3.2°F	4.3°F to 6.1°F	7.0°F
September	3.3°F	4.4°F to 6.2°F	7.0°F
October	3.0°F	4.1°F to 5.9°F	6.8°F
November	3.2°F	3.9°F to 5.6°F	6.6°F
December	2.8°F	3.7°F to 6.1°F	7.0°F
(c) 2080s			
January	3.4°F	5.6°F to 8.9°F	10.7°F
February	3.5°F	5.4°F to 8.4°F	10.0°F
March	3.0°F	4.5°F to 7.4°F	8.8°F
April	3.6°F	4.7°F to 7.9°F	9.4°F
May	3.4°F	4.6°F to 8.0°F	9.2°F
June	3.3°F	4.7°F to 8.6°F	9.9°F
July	3.6°F	5.0°F to 9.3°F	10.4°F
August	4.1°F	5.1°F to 9.6°F	11.3°F
September	4.2°F	5.3°F to 9.6°F	11.0°F
October	3.7°F	4.9°F to 9.0°F	11.0°F
November	3.1°F	4.9°F to 8.4°F	9.9°F
December	3.6°F	5.3°F to 8.3°F	10.6°F

NOTE: Based on 35 GCMs and two representative concentration pathways. Projections are relative to the 1971–2000 base period.

Table A.6. Projected seasonal precipitation changes (%)

	Low estimate (10th percentile)	Middle range (25th to 75th percentile)	High estimate (90th percentile)
(a) 2020s			
Winter	-3%	+1% to +12%	+20%
Spring	-3%	+1% to +9%	+15%
Summer	-5%	-1% to +11%	+15%
Fall	-5%	-2% to +7%	+10%
(b) 2050s			
Winter	+2%	+7% to +18%	+24%
Spring	-1%	+3% to +12%	+18%
Summer	-9%	-5% to +11%	+18%
Fall	-2%	+1% to +10%	+14%
(c) 2080s			
Winter	+4%	+10% to +25%	+33%
Spring	-1%	+4% to +15%	+21%
Summer	-10%	-5% to +18%	+23%
Fall	-7%	-1% to +11%	+18%

NOTES: Winter, December to February; Spring, March to May; Summer, June to August; Fall, September to November. Based on 35 GCMs and two representative concentration pathways. Projections are relative to the 1971–2000 base period.

Model-based range of outcomes (distribution) for precipitation changes (%) in New York City, relative to the 1971–2000 base period for the 2020s, 2050s,

and 2080s. Based on 35 GCMs and 2 representative concentrations pathways.

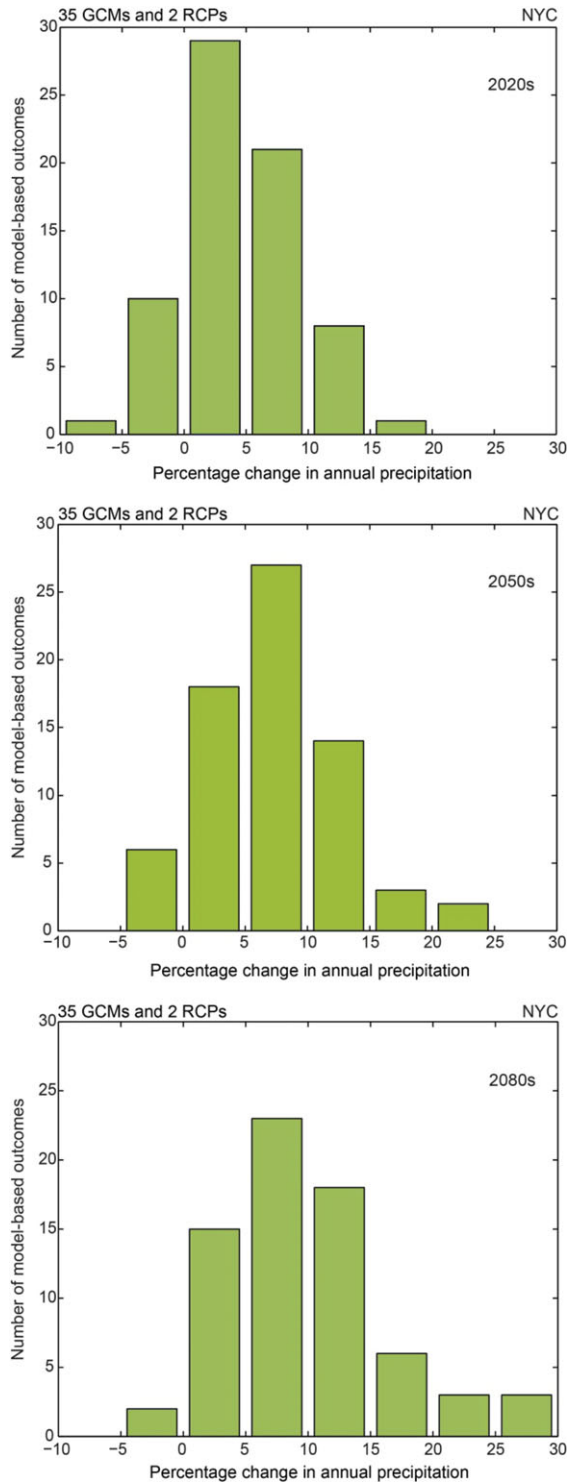


Figure A.6. Model-based range of outcomes (distribution) of projected precipitation changes: (a) 2020s, (b) 2050s, and (c) 2080s.

Table A.7. Projected monthly precipitation changes (%)

	Low estimate (10th percentile)	Middle range (25th to 75th percentile)	High estimate (90th percentile)
(a) 2020s			
January	-8%	-1% to +14%	26%
February	-9%	-2% to +16%	31%
March	-7%	-1% to +12%	19%
April	-12%	-4% to +11%	18%
May	-13%	-6% to +10%	20%
June	-14%	-4% to +9%	18%
July	-12%	-4% to +12%	20%
August	-7%	+1% to +13%	20%
September	-18%	-11% to +7%	14%
October	-19%	-7% to +12%	19%
November	-9%	-4% to +12%	21%
December	-6%	-1% to +12%	20%
(b) 2050s			
January	-4%	+1% to +25%	+35%
February	-4%	+2% to +26%	+36%
March	-3%	+1% to +18%	+25%
April	-5%	-1% to +14%	+26%
May	-10%	-5% to +11%	+17%
June	-14%	-5% to +13%	+18%
July	-14%	-9% to +10%	+23%
August	-13%	-4% to +14%	+26%
September	-20%	-8% to +11%	+16%
October	-17%	-6% to +14%	+22%
November	-5%	-1% to +18%	+23%
December	-8%	+4% to +19%	+23%
(c) 2080s			
January	-4%	+7% to +28%	+40%
February	-4%	+5% to +28%	+44%
March	-1%	+5% to +22%	+27%
April	-10%	+2% to +19%	+25%
May	-10%	-1% to +14%	+22%
June	-14%	-2% to +15%	+20%
July	-16%	-9% to +19%	+32%
August	-19%	-9% to +20%	+35%
September	-16%	-8% to +10%	+22%
October	-20%	-9% to +9%	+23%
November	-10%	-2% to +21%	+29%
December	-5%	+5% to +26%	+31%

NOTES: Based on 35 GCMs and two representative concentration pathways. Projections are relative to the 1971–2000 base period.

B. Sea level rise observations and projections: methods and analyses^b

Contents

- B.1 NPCC2 sea level rise methods and projections
- B.2 Ocean changes
- B.3 Ice mass change
- B.4 Vertical land movements—glacial isostatic adjustment (GIA)
- B.5 Anthropogenic land water storage

This section describes the New York City Panel on Climate Change (NPCC2) methodology for projecting future sea level rise in New York City.

B.1 NPCC2 sea level rise methods and projections

The regionalized sea level projection methodology used in NPCC (2010) and Horton *et al.* (2010) is updated here in NPCC2. Individual sea level rise components are described in Chapter 2, NPCC 2015. NPCC2 sea level projections do not comprise the full range of possible sea level rise contributions, but rather present the estimated 10th, 25th, 75th, and 90th percentile sea level contributions by component; the sum of components at each percentile is used to generate a total sea level rise projection for each percentile. As noted in Chapter 2 (NPCC, 2015), this approach neglects correlations between sea level rise components, which could influence the robustness of the projections.^c

The cumulative sea level change S_{TOT} (at a given likelihood) in New York City is equal to:

$$S_{TOT} = S_{OCEAN} + S_I + S_{GIA} + S_{LWS}, \quad (1)$$

where S_{TOT} is the change in mean sea level for each component since the base period. S_{OCEAN} refers to ocean changes, S_I to ice mass change, S_{GIA} to vertical

land movements, and S_{LWS} to anthropogenic land water storage.

Uncertainty and confidence in the quantitative ranges of individual terms are assessed using a variety of techniques, including model-based approaches, expert judgment, and literature review. Subsequent sections describe the basis for projections of each component in greater detail.

B.2 Ocean changes

For NPCC2, future thermosteric and dynamic ocean changes are determined using outputs (the variables ZOSTOGA and ZOS in the CMIP5 archive) from 24 CMIP5 GCMs under both RCP4.5 and RCP8.5 (see later), yielding a total of 48 outcomes. As in Yin *et al.* (2012), dynamic sea level is now defined as the grid point anomaly from the global mean field.

$$S_{OCEAN} = ZOSTOGA_t - ZOSTOGA_{tbase} + ZOS_t - ZOS_{tbase}, \quad (2)$$

ZOSTOGA = global mean sea level rise due to thermal expansion, relative to a 2000 to 2004 baseline;

ZOS = local sea level rise due to changes in dynamic ocean height (caused by changes in local ocean density and circulation), relative to the 2000 to 2004 local mean.^d

Projections of ZOS, particularly the 75th and 90th percentile, reflect a local sea level rise greater than the global mean. This local anomaly has been linked to a slowdown of the Gulf Stream/Atlantic Meridional Ocean Circulation (AMOC) in some GCMs^e (Yin *et al.*, 2009, 2010; Hu *et al.*, 2009; 2011).

^bThis Appendix provides technical details for New York City Panel of Climate Change 2015 Report, Chapter 2: Sea Level Rise and Coastal Storms.

^cFor example, the NPCC2 approach does not consider whether our estimated 90th percentile land-based ice loss, through its effects on the Gulf Stream, might be inconsistent with a 90th percentile increase in relative ocean height (as estimated using global climate models that do not include the possibility of large land-based ice loss) along the Northeast coast.

^dGiven time constraints and metadata limitations, it was difficult to ascertain whether all modeling centers used the same definitions for zos and zostoga, respectively. For example, at least one model in the CMIP3 archive allowed globally averaged zos to vary in time, while the majority of models did not. Inconsistent definitions of zos and zostoga could lead to inconsistencies in the resulting ocean change term. In general such inconsistencies are expected to have a small effect on the sea level rise projections.

^eSea levels are lower to the west of the Gulf Stream than to the east. If the Gulf Stream weakens, a compensating increase in sea level along the Northeast coast is expected; this is an example of a dynamical, or motion related, change in sea level.

Table B.1. New York metropolitan region sea level rise and land subsidence

Station	NOAA		PSMSL		Peltier	Englehart	Englehart & Horton
	SLR (in/year) ^a	Years	SLR (in/year) ^b	Years	GIA (in/year) ^c	(2009) Paleo-SLR (in/year) ^d	(2012) Paleo-SLR (in/year) ^d
New London	0.10	73	0.10	68	0.04	0.04	~0.04
Bridgeport	0.11	47	0.10	43	0.04	0.04	~0.04
Montauk	0.12	64	0.12	53	0.05	0.03	~0.04
Port Jefferson	0.10	35	0.09	31	0.05	0.03	~0.04
Willets Point	0.10	80	0.10	65	0.05	0.03	~0.04
The Battery/New York City	0.11	155	0.11	138	0.05	0.05	~0.05
Sandy Hook	0.16	79	0.16	79	0.05	0.06	~0.06
Atlantic City	0.16	100	0.16	100	0.05	0.05	~0.06

^a<http://tidesandcurrents.noaa.gov/sltrends/index.shtml/> (see: updated mean sea level trends; current through 2011).

^b<http://www.psmsl.org/products/trends/trends.txt/> (posted January 16, 2013).

^cGIA corrections for tide gauges predicted by W.R. Peltier's ICE 5G v 1.3, VM2, with 90 km lithosphere resolution. <http://www.psmsl.org/train'and'info/geo.signal/gia/peltier/drs1250.PSMSL.ICE5Gv1.3'VM2'L90'2012b/> (posted August 13, 2012).

^dEngelhart *et al.* (2009).

^eEngelhart and Horton (2012).

A higher-than-average rate of local sea level rise has also been observed in recent decades. Tide gauges along the Atlantic coast show a distinct regional sea level acceleration “hotspot” from Cape Cod to Cape Hatteras since the early 1990s (Sallenger *et al.*, 2012; Boon, 2012; Ezer and Corlett, 2012), although the record is still too short to attribute to climate change because of high interannual to multidecadal ocean variability.

B.3 Ice mass change

In NPCC2, sea level rise contributions from four separate ice masses—the Greenland (GR), West Antarctic (WAIS), and East Antarctic (EAIS) ice sheets, and small glaciers and ice caps (GICs)—are projected independently. At each percentile (10th, 25th, 75th, and 90th), the sea level rise due to changes in ice mass balance at New York City (S_I) is given by the sum of mass changes in each component (where M_x is expressed in sea level equivalent (360 gigatonne mass loss = 1 mm sea level rise) and f_x is the local “fingerprint” of ice mass loss):

$$S_I = - (f_{GIC} M_{GIC} + f_{GR} M_{GR} + f_{WAIS} M_{WAIS} + f_{EAIS} M_{EAIS}). \quad (3)$$

The subsections below discuss the projections of the individual terms in Eq. (3) in more detail.

Mass balance of the Greenland and Antarctic ice sheets. Processes that modify continental ice sheet mass balance (and thus their effect of sea level) can be segregated into those that act on an ice sheet's surface mass balance (or SMB, including snow accumulation, melting, and sublimation) and those that affect ice flow (dynamic changes). Recent observations indicate that dynamic changes underlie virtually all of recently observed mass changes in Antarctica, and approximately half in Greenland (Rignot *et al.*, 2011).

Because robust, process model-based projections of ice sheet contributions to sea level rise are still under development and a complete quantitative assessment is currently unavailable, NPCC2 utilizes the projections of Bamber and Aspinall (2013) for the Greenland and Antarctic ice sheets. Although this study relies exclusively on expert elicitation, it provides a consistent, probabilistic approach for each ice sheet that includes a combined estimate of uncertainty in SMB and ice dynamics.

Mass balance of glaciers and small ice caps^f. Projections of the future sea level rise contribution of

^fUncertainty exists in the assignment of percentiles of GICs.

Box B.1. What is glacial isostatic adjustment (GIA)?

GIA derives from changes in the size of large ice masses, which distort the Earth's lithosphere and change the elevation of the land surface relative to the ocean. Regions formerly beneath ice sheets around 20,000 years ago (e.g., central Canada and Scandinavia) are still uplifting, while peripheral regions (e.g., New York down to Chesapeake Bay) are subsiding in response to the slow, viscous component of glacial isostatic rebound.

GIA models (such as ICE-5G v1.3 VM2 L90; Peltier, 2012, 2004; see also Mitrovica and Milne, 2003) calculate gravitational interactions among ice sheets, land, and ocean over time and separate effects of glacial loading/unloading on sea level from the climatic signal. Specific GIA corrections^a for NYC area tide gauges are listed in Table B.1.

^aNOTE: These GIA corrections apply to the last deglaciation, not to future ice melting.

GICs have been made using: (1) extrapolations of observed rates of mass change (Bahr *et al.*, 2009); (2) regional, process-based, mass balance models forced by GCMs (Radic *et al.*, 2013; Marzeion *et al.*, 2012), and (3) a statistical approach, whereby mass or volume changes are parameterized as a function of climate (e.g., global mean temperature; Perrette *et al.*, 2013, and references therein). We use the process-based approach of Radic *et al.* (2013) and Marzeion *et al.* (2014), since it does not rely on stationarity as the climate system, and the GICs, evolves over this century.

Fingerprints. Land-based ice compresses the lithosphere, exerts a gravitational pull on the surrounding ocean, and alters the Earth's rotation. Localized ice mass changes thus give a spatially varying pattern of sea level change that is known as a "fingerprint" (Tamisiea and Mitrovica, 2011; Mitrovica *et al.*, 2009, 2001; see Eq. (3)).

For NPCC2, the value of the fingerprint for each ice component in New York City is included as a multiplier of mass change. Here, we assign a single value estimated from the literature (e.g., Mitrovica *et al.*, 2009; Perrette *et al.*, 2013; Gomez *et al.*, 2010; Miller *et al.*, 2013).

B.4 Vertical land movements—glacial isostatic adjustment (GIA)

Vertical land motion in New York City today is primarily "slow" GIA-related subsidence (see Box B.1). Other causes of local vertical land movements (neotectonic activity, sediment loading and compaction, and subsidence due to excess subsurface fluid withdrawal) are expected to remain negligible at the Battery in New York City.

NPCC2 calculates the future subsidence due to GIA as a linear trend where S_{GIA} is the number of years since the start date (t_{base} , 2002, average of 2000–2004) times the annual subsidence rate, R , in mm/year:

$$S_{\text{GIA}} = (t - t_{\text{base}}) \times R. \quad (4)$$

Table B.1 lists annual subsidence rates, R , for individual tide stations in the New York metropolitan area. Current GIA-related subsidence rates are now much improved over earlier values and compare favorably with millennial sea level rise trends in this region (Engelhart and Horton, 2012; Engelhart *et al.*, 2009). Therefore, $R = 1.26$ mm/year for New York City is used to calculate S_{GIA} . This is roughly 40% of the sea level rise in the observed period.

For historical sea level rise trends, see <http://tidesandcurrents.noaa.gov/sltrends/index.shtml/>. Updated mean sea level rise trends (current through 2011) for each of the New York metro area tide gauge stations are listed in Table B.1.

B.5 Anthropogenic land water storage

Continental water storage fluctuates due to variability in precipitation, and increasingly since the 1950s due to human interventions in the hydrological cycle. By storing water on land, reservoirs have reduced sea level rise by 0.55 mm/year since the 1950s (Chao *et al.*, 2008) and 0.44 mm/year since the 1970s (Church *et al.*, 2011). Conversely, groundwater mining (water withdrawal in excess of natural recharge) raises sea level.

We also adopted the IPCC (2013) approach in calculating the contribution of changes in land water storage to sea level rise (Church *et al.*, 2013). Specifically, the NPCC 10th, 25th, 75th, and 90th percentile distribution points were calculated by

assuming that IPCC projections of sea level rise are based on a normal distribution. The land water storage rates were treated as linear over time; therefore, the 2020s, 2050s, and 2080s projections could be calculated directly from the IPCC timeslices.

References

- Bahr, D.B., M. Dyurgerov & M.F. Meier. 2009. Sea level rise from glaciers and ice caps: a lower bound. *Geophys. Res. Lett.* **36**: L03501, doi:10.1029/2008GL036309.
- Bamber, J.L. & W.P. Aspinall. 2013. An expert judgment assessment of future sea level rise from the ice sheets. *Nature Clim. Change* **3**: 424–427.
- Boon, J.D. 2012. Evidence of sea level acceleration at U.S. and Canadian tide station, Atlantic Coast, North America. *J. Coast. Res.* **28**: 1437–1445.
- Chao, B.F., Y.H. Wu & Y.S. Li. 2008. Impact of artificial reservoir water impoundment on global sea level. *Science* **320**: 212–214.
- Church, J.A., P.U. Clark, A. Cazenave, *et al.* 2013. Sea level change.” In *Climate Change 2013: The Physical Science Basis. Contribution of Working Group I to the Fifth Assessment Report of the Intergovernmental Panel on Climate Change*. T.F. Stocker, D. Qin, G.-K. Plattner, M. Tignor, S.K. Allen, J. Boschung, A. Nauels, Y. Xia, V. Bex, P.M. Midgley, Eds.: 1137–216. Cambridge, UK: Cambridge University Press.
- Church, J.A., *et al.* 2011. Revisiting the earth’s sea-level and energy budgets from 1961 to 2008. *Geophys. Res. Lett.* **38**: L188601.
- Engelhart, S.E., *et al.* 2009. Spatial variability of late Holocene and 20th century sea-level rise along the Atlantic coast of the United States. *Geology* **37**: 1115–1118.
- Engelhart, S.E. & B.P. Horton. 2012. Holocene sea level database for the Atlantic coast of the United States. *Quater. Sci. Rev.* **54**: 12–25.
- Ezer, T. & W.C. Corlett. 2012. Is sea level rise acceleration in the Chesapeake Bay? A demonstration of a novel new approach for analyzing sea level data. *Geophys. Res. Lett.* **39**: L19606, doi: 10.1029/2012GL053435.
- Gomez, N., J.X. Mitrovica, P. Huybers, & P.U. Clark. 2010. Sea level as a stabilizing factor for marine-ice-sheet grounding lines. *Nature Geosci.* **3**: 850–853.
- Horton, R., Rosenzweig, C., Gornitz, V., Bader, D., & O’Grady, M. 2010. Climate Risk Information. In “Climate Change Adaptation in New York City: Building a Risk Management Response. New York City Panel on Climate Change 2010 Report”, Rosenzweig, C. and Soleski, W, Eds. *Ann. N.Y. Acad. Sci.* **1196**: 147–228.
- Hu, A., G.A. Meehl, W. Han & J. Yin. 2009. Transient response of the MOC and climate to potential melting of the Greenland ice sheet in the 21st century. *Geophys. Res. Lett.* **36**: L10707.
- Hu, A., G.A. Meehl, W. Han & J. Yin. 2011. Effect of the potential melting of the Greenland Ice Sheet in the Meridional Overturning Circulation and global climate in the future. *Deep-Sea Res. II* **58**: 1914–1926.
- IPCC. 2013. *Climate Change 2013: The Physical Science Basis. Contribution of Working Group I to the Fourth Assessment Report of the Intergovernmental Panel on Climate Change*. Stocker, T.F., D. Qin, G.-K. Plattner, M. Tignor, S.K. Allen, J. Boschung, A. Nauels, Y. Xia, V. Bex and P.M. Midgley, Eds: Cambridge University Press Cambridge, United Kingdom and New York, NY, USA, 1535 pp
- Marzeion, B. A.H. Jarosch, & M. Hofer. 2012. Past and future sea-level change from the surface mass balance of glaciers. *Cryosphere* **6**: 1295–1322.
- Marzeion, B., J. G. Cogley, K. Richter, and D. Parkes. 2014. Attribution of global glacier mass loss to anthropogenic and natural causes. *Science* **345**: 919–921.
- Miller, K.G., R.E. Kopp, B.P. Horton, *et al.* 2013. A geological perspective on sea-level rise and its impacts along the U.S. mid-Atlantic coast. *Earth’s Future* **1**: 3–18.
- Mitrovica, J.X. & G.A. Milne. 2003. On post-glacial sea level: I. General theory. *Geophys. J. Int.* **154**: 253–267.
- Mitrovica, J.X., M.E. Tamisiea, J.L. Davis, & G.A. Milne. 2001. Recent mass balance of polar ice sheets inferred from patterns of global sea-level change. *Nature* **409**: 1026–1029.
- Mitrovica, J.X., N. Gomez & P.U. Clark. 2009. The sea-level fingerprint of West Antarctic collapse. *Science* **323**: 753.
- NPCC. 2010. Climate Change adaptation in New York City: building a risk management response. New York City Panel on Climate Change 2010 Report. C. Rosenzweig and W. Solecki, Eds. *Ann. N.Y. Acad. Sci.* **1196**: 1–354.
- NPCC. 2015. Building the Knowledge Base for Climate Resiliency: New York City Panel on Climate Change 2015 Report. C. Rosenzweig and W. Solecki, Eds. *Ann. N.Y. Acad. Sci.* **1336**: 1–149.
- Peltier, W.R. 2012. GIA data sets. http://www.psmsl.org/train_and_info/geo_signals/gia/peltier/drs250.PSMSL.ICE5GV1.3_VM2_L90_2012b.txt. Accessed March 1, 2013.
- Peltier, W.R. 2004. Global glacial isostasy and the surface of the ice-age earth: the ICE-5G (VM2) Model and GRACE. *Annu. Rev. Earth Planet. Sci.* **32**: 111–149.
- Perrette, M., F. Landerer, R. Riva, K. Frieler, & M. Meinschausen. 2013. A scaling approach to project regional sea level rise and its uncertainties. *Earth Syst. Dyn.* **4**: 11–29.
- Radic, V., A. Bliss, A.C. Beedlow, *et al.* 2013. Regional and global projections of twenty-first century glacier mass changes in response to climate scenarios from global climate models. *Clim. Dyn.*: **42**: 37–58.
- Rignot, E., I. Velicogna, M.R. van den Broeke, *et al.* 2011. Acceleration of the contribution of the Greenland and Antarctic ice sheets to sea level rise. *Geophys. Res. Lett.* **38**: L05503, doi:10.1029/2011GL046583.
- Sallenger, A.H., Jr., K.S. Doran & P.A. Howd. 2012. Hotspot of accelerated sea-level rise on the Atlantic coast of North America. *Nature Clim. Change* **2**: 884–888.
- Tamisiea, M.E. & J.X. Mitrovica. 2011. The moving boundaries of sea level change: Understanding the origins of geographic variability. *Oceanography* **24**: 24–39.
- Yin, J., M.E. Schlesinger & R.J. Stouffer. 2009. Projections of rapid sea-level rise on the northeast coast of the United States. *Nature Geosci.* **2**: 262–266.
- Yin, J., S.M. Griffies & R.J. Stouffer. 2010. Spatial variability of sea level rise in twenty-first century projections. *J. Clim.* **23**: 4585–4606.
- Yin, J. 2012. Century to multi-century sea level rise projections from CMIP5 models. *Geophys. Res. Lett.* **39**: L17709.

C. Static coastal flood mapping^g

Contents

- C.1 United States Army Corps of Engineers hurricane storm surge inundation areas
- C.2 NPCC2 baseline flood elevation datasets
- C.3 line flood elevation datasets: Lateral variations
- C.4 Baseline flood elevation datasets: Rounded integer values
- C.5 Vertical datum
- C.6 Vertical accuracy of elevation data
- C.7 Future work: Mapping uncertainty in the elevation dataset
- C.8 Future work: Combined uncertainties

This section includes technical material supplementary to Chapter 3, Static Coastal Flood Mapping (NPCC, 2015). It was created to add detail about the mapping methodology and limitations, datasets, and accuracy issues that were touched upon in the main chapter.

C.1 United States Army Corps of Engineers hurricane storm surge inundation areas

The United States Army Corps of Engineers (USACE) develops storm surge inundation maps from the National Hurricane Center's SLOSH (Sea, Lake, and Overland Surges from Hurricanes) model.

The NYC Office of Emergency Management (OEM) uses these inundation maps to understand worst-case scenario storm surge in New York City to develop the city's evacuation zone maps. Storm surge inundation zones are delineated for hurricane categories 1–4, with six possible bearings, ranging from Northeast (NE) to West North West (WNW). The bearing is the direction in which the hurricane is headed. OEM uses two SLOSH products, MEOWs (Maximum Envelope of Water) and MOMs (Maximum of MEOWs), in its planning and preparedness efforts. The MEOW is based on a set of storms with fixed intensity and bearing, but with varying sizes, forward speeds, and landfall locations. Surge inundation zones based on the MEOWs were used to create New York City's hurricane evacuation zones,

which are the primary tool for communicating the surge hazard to the public. Surge inundation zones created from the MOMs are used to plan for the worst-case inundation for a category of hurricane without regard to the probability of occurrence. The SLOSH data used for OEM's planning assume that the hurricane makes landfall at high tide.

C.2 NPCC2 baseline flood elevation datasets

Base flood elevations (BFEs) and still-water elevation (SWEL) data from FEMA's Preliminary Flood Insurance Study (FIS) and FIRMs serve as the baseline to which projections of sea level rise were added to create maps of the future 100- and 500-year flood scenarios. The 500-year SWEL raster was calculated by FEMA and their mapping partners using the Advanced Circulation Model for Oceanic, Coastal and Estuarine Waters (ADCIRC) coupled to the unstructured numerical wave model Simulating Waves Nearshore (unSWAN), referred to as SWAN + ADCIRC hydrodynamic models (FEMA, 2013). This modeled output of SWELs considers the projected elevation of floodwaters in the absence of wave heights and wave runup, but with consideration of wave setup.^h

The 100-year coastal BFEs are founded on 100-year SWEL data, and then wave height (derived through the Wave Height Analysis for Flood Insurance Studies (WHAFIS) model) and wave runup (derived through various runup models, where applicable) were incorporated.ⁱ The use of the SWEL depth grid (raster) values instead of BFE values for the 500-year flood extent is a departure from the 2013 flood map methodology, in which BFE values were used for both the 100- and 500-year flood maps. Because BFEs incorporating wave heights and wave runup were not calculated for the 2013 Preliminary FIRM 500-year flood extent, 500-year SWEL data were used as a proxy. The older FEMA Advisory BFE values for the 500-year flood (released in

^gThis Appendix provides technical details for New York City Panel of Climate Change 2015 Report, Chapter 3: Static Coastal Flood Mapping.

^hWave setup is the increase in the water level caused by the onshore mass transport of water that occurs due to waves breaking during a storm. Wave runup is the rush of water that extends inland when waves come ashore.

ⁱFEMA's Flood Insurance Study (FIS) for the city of New York (revised December 5, 2013) details the baseline engineering methods used in determining the 100- and 500-year floodplains. The 2013 FIS revision can be accessed through the FEMA Map Service Center website: <https://msc.fema.gov/>.

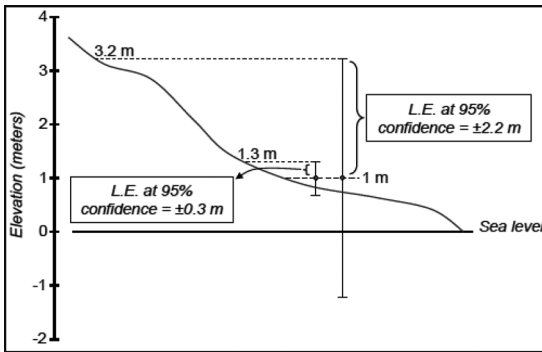


Figure C.1. An example of linear error (L.E.) mapping using two elevation (topographic) models with differing vertical accuracies: one with a 95% confidence interval of 7.2 feet (2.2 m), and the other with a 95% confidence interval of 0.98 feet (30 cm; Source: Gesch, 2009).

February 2013, followed by the Preliminary FIRM dataset released that December) were considered for use, but the 0.2% SWEL data were ultimately selected as the best available data. The 0.2% SWEL data are based on a completely revised coastal modeling analysis for all New York City neighborhoods and approximate BFE values in inland areas where wave action is negligible (A. Martin, 2014, personal communication). Exceptions are areas where wave runup is the dominant coastal process: in these few areas, BFE values exceed 500-year SWEL values by many feet and produce a 100-year flood zone that extends beyond the 500-year projection. For mapping purposes, this issue was resolved by merging the 100- and 500-year datasets such that the runup areas are also included in the 500-year flood extent.

C.3 Baseline flood elevation datasets: Lateral variations

FEMA's BFE and SWEL elevations vary both parallel and perpendicular to the shoreline and thus are not at a constant elevation. The transitions in flood elevation values along the coasts should be reflected in the landward movement of floodwaters, such that the inland shape and extent of the flood zone reflects the changing BFE values nearer to shore. The NPCC approach incorporates these lateral variations in flood elevation values by assuming that landward values of floodwater elevation are likely to be more similar to neighboring flood elevation values and less similar to more distant values. To execute this concept in a geographic information system, Thiessen polygons are created in the coastal area. These polygons define and assign

a value to the area closest to a given point relative to all other points in the dataset. They are used to delineate the new boundaries between BFE zones as floodwaters are projected landward. However, by this process, areas of low topography that are not connected to open water will nonetheless appear as islands of flooding among nonflooded terrain. These "orphans" are later removed using spatial selection queries of the raster pixels.

C.4 Baseline flood elevation datasets: Rounded integer values

On FEMA's 2013 Preliminary FIRM for New York City, BFEs are given as values rounded to the nearest whole number (feet). BFEs represent the height (referenced to the NAVD 1988 vertical datum) to which floodwaters will rise during the 100-year flood. On FIRMs they are represented as single-value zones (e.g., "8" or "10" feet); however, they actually represent a range of values. For example, the BFE labeled as 10 feet actually encompasses all values from 9.6 feet to 10.5 feet—a range just larger than the NPCC2 90th percentile sea level rise projection of 10 inches for the 2020s. By contrast, FEMA's SWEL raster elevation dataset (used for the 500-year flood maps) contains values presented as decimals (e.g., 9.6, 9.7); however, in the process of preparing the SWEL data for mapping, the decimals were converted to whole integers by rounding the values. Rounded integer values are less accurate than decimal values and introduce a margin of uncertainty into the future flood map products.

C.5 Vertical datum

It is important that the topographic and floodwater elevations used in the NPCC2 mapping effort are referenced to a common vertical standard in order to create consistency among elevation data. Tidal data, which reference average water levels, and geodetic data, which reference ground-based benchmarks, have both been used to standardize to flood map elevations within a data system. The NPCC2 work references elevation data to the North American Vertical Datum of 1988 (NAVD88).

The east and west coasts of the United States experience semidiurnal tides consisting of two high and two low tides per day. The "higher high water" elevation represents the height of the higher of the two daily high tides and the "lower low water" elevation represents height of the lower of the two daily low tides. The Mean Higher High Water (MHHW)

tidal datum is defined as the average of daily higher high water heights during the current National Tidal Datum Epoch (NTDE; current is 1983–2001). Common practice is to use the MHHW tidal datum as baseline when mapping sea level rise inundation because MHHW represents the highest level of daily inundation (Cooper *et al.* 2013). Despite this convention, the extents of the future flood maps developed by NPCC2 are calculated with reference to NAVD88, a geodetic datum situated 2.5 inches (0.21 feet) above mean sea level and 30 inches (2.5 feet) below MHHW at the Battery NY (at lower Manhattan). The NAVD88 was selected as the NPCC2 baseline because (1) the NYC Digital Elevation Model (DEM) and FEMA FIRMs datasets used in developing the future flood maps are already referenced to NAVD88; and (2) MHHW is not the optimal foundational datum for the purposes of approximating future flood events since sea level rise is a slow and long-term event.

As a gradual decadal process that affects the full tidal cycle at a given location, sea level rise slowly elevates both the mean high and low water levels relative to previous values. For this reason it is practical to map sea level rise inundation onto the highest level of daily inundation, that is, MHHW, to ensure coverage of the fullest extent of daily water level ranges. However, unlike sea level rise inundation, flood events can be very brief, with peak waters often lasting less than a full tidal cycle and do not always occur during high tides. If the flood event is minor or occurs coincident with Mean Lower Low Water (MLLW), water levels may never reach or exceed the height of MHHW. For this reason, using the NAVD88 for mapping reference is appropriate for flood events because NAVD88 approximates mean sea level and does not superimpose the effects of daily tidal cycles on flood elevation.

C.6 Vertical accuracy of elevation data

The topographic dataset used by the NPCC2 was a DEM created from Light Detection and Ranging (LiDAR) data collected in spring 2010 over New York City. Vertical accuracy of this dataset was reported as 9.5 cm root mean square error (RMSE). RMSE is a common method of accuracy reporting^j calculated

as the square root of the average of the set of squared differences between dataset coordinate values and coordinate values from an independent source of higher accuracy (NDEP, 2004). These higher accuracy sources can often include geodetic ground surveys, Global Positioning System ground surveys, photogrammetric surveys, and spatial databases of substantially higher accuracy (ICSM, 2009):

$$\text{RMSE}_Z = \sqrt{\frac{\sum (Z_{\text{data } i} - Z_{\text{check } i})^2}{n}}, \quad (5)$$

where $Z_{\text{data } i}$ is the vertical coordinate of the i th checkpoint in the dataset, $Z_{\text{check } i}$ is the vertical coordinate of the i th checkpoint in the independent source of higher accuracy, i is an integer from 1 to n , and n is the number of points being checked.

In addition to RMSE, the National Standard for Spatial Data Accuracy (NSSDA) uses the linear uncertainty value at the 95% confidence interval to report vertical accuracy (Federal Geographic Data Committee, 1998). This metric is expressed as:

$$\begin{aligned} \text{Linear Error at 95\% confidence (LE95)} \\ = 1.96 \times \text{RMSE}_Z. \end{aligned} \quad (6)$$

Using Eq. (2) above, the DEM RMSE value of 9.5 cm equates to a linear error at 95% confidence value of 5.3 inches (18.6 cm). Thus the 90th percentile sea level rise projections of 10 inches (25.4 cm) for the 2020s, 30 inches (76.2 cm) for the 2050s, 58 inches (145.3 cm) for the 2080s, and 75 inches (190.5 cm) for 2100 all exceed the 95% error bounds of the elevation data.

C.7 Future work: Mapping uncertainty in the elevation dataset

It is important to convey the vertical uncertainty of the underlying elevation dataset in any flood or inundation mapping exercise. The term uncertainty is used to express a quantitative indication of the quality of elevation data using a specified level of confidence. In topographic elevation data uncertainty is often depicted by one of two techniques. The first is the NSSDA linear error technique mentioned above (Eq. (2), which is based on “. . . a linear uncertainty value such that the true or theoretical location of the point falls within \pm of that linear uncertainty value 95-percent of the time” (Federal Geographic Data Committee, 1998). This calculation of linear error of the topographic data can be depicted on sea level

^j Accuracy refers to the closeness of a measured value to a standard or known value.

rise inundation maps as a second boundary above or outside the inundation boundary (Fig. C.1; Gesch, 2009, Cooper *et al.*, 2013). In this way the magnitude of uncertainty of the topographic dataset is captured visually as the distance between the sea level rise and linear error boundaries. Greater width between the two indicates greater uncertainty.

In contrast to uncertainty, error refers to the difference between the measured and true values of elevation data. It is reported as the RMSE or Accuracy_z (see Eq (1), which for the purposes of the NPCC2 work, are assumed to be equivalent to the standard deviation and 95% confidence interval, respectively. Mapping uncertainty in the elevation dataset can also be done using a basic equation to compute a standard score, which is the number of standard deviations a value falls from the mean.

$$\text{Standard Score}_{(X,Y)} = (\text{Inundation}_{(\text{watersurface})} - \text{Elevation}_{(X,Y)}) / \text{RMSE}_{(\text{ElevationData})} \quad (7)$$

Standard scores are critical in conveying the accuracy of the elevation data, as mapping an inundation extent can be done with data of any quality irrespective of its accuracy. However, standard-score maps delineate zones of high and low confidence in the elevation data. Standard scores also reflect areas of high and low uncertainty that are independent of data accuracy, but instead are connected to slope; low slopes will have higher uncertainty and areas of high slopes will have lower uncertainty since a large vertical error will result in less of a horizontal error. A given location can also have different uncertainties relative to the level of inundation: a low level of inundation may correspond to an area of low slope, while high inundation at the same location may fall along an area of high slope (NOAA 2010). Future flood map work could use either linear boundary or standard score methods to display the uncertainty in the underlying elevation dataset.

C.8 Future work: Combined uncertainties

In addition to vertical error in the LiDAR dataset, the modeled sea level rise projections for the 2020s, 2050s, 2080s, and 2100, and the FEMA base flood and SWEL datasets upon which the future

flood zones are founded, have ranges of error that can also be expressed as confidence intervals. The error in these three sources can be combined into an “uncertainty envelope” and mapped above and below the projected future flood boundary. Several studies have used this probabilistic technique, combining the vertical error of LiDAR elevation data and vertical error of the tidal grids (which are calculated using NOAA’s VDatum tool) to give the probability of inundation for a given location at 90% and 95% confidence intervals (Mitsova *et al.*, 2012; NOAA, 2010).

An important disclaimer to the NPCC2 future flood maps is that they are used for illustrative purposes only and should not be used for site-specific planning or insurance requirements. This statement is intended to prevent users from assuming the maps are a perfect representation of projected future flood extents. Future work should attempt to account for the uncertainty in map data sources and products and to illustrate this uncertainty directly on the map as confidence intervals.

References

- Cooper, H.M., Q. Chen, C.H. Fletcher & M.M. Barbee. 2013. Assessing vulnerability due to sea-level rise in Maui, Hawai‘i using LiDAR remote sensing and GIS. *Clim. Change* **116**: 547–563.
- FEMA. 2013. *Flood Insurance Study: City of New York, New York, Bronx County, Richmond County, New York County, Queens County, Kings County*, pp. 131. FEMA.
- Federal Geographic Data Committee. 1998.
- Gesch, D.B. 2009. Analysis of lidar elevation data for improved identification and delineation of lands vulnerable to sea-level rise. *J. Coast. Res.* **53**: 49–58.
- ICSM. 2009. Australian Map and Spatial Data Horizontal Accuracy Standard. Intergovernmental Committee on Surveying and Mapping, pp. 16.
- Mitsova, D., A.-M. Esnard, Y. Li. 2012. Using enhanced dasymetric mapping techniques to improve the spatial accuracy of sea level rise vulnerability assessments. *J. Coastal Conservation* **16**: 355–372.
- NDEP. 2004. *Guidelines for Digital Elevation Data, Version 1.0*. National Digital Elevation Program. pp. 93.
- NOAA. 2010. *Mapping Inundation Uncertainty*. Charleston, NC: NOAA Coastal Services Center.
- NPCC. 2015. Building the Knowledge Base for Climate Resiliency: New York City Panel on Climate Change 2015 Report. C. Rosenzweig and W. Solecki, Eds. *Ann. N.Y. Acad. Sci.* **1336**: 1–149.

D. Dynamic coastal flood modeling^k

Contents

- D.1 The FEMA Region II flood mapping study (2014)
- D.2 Overland wave heights
- D.3 Storm set
- D.4 Statistics
- D.5 Dynamic coastal flood mapping

D.1 The FEMA Region II flood mapping study (2014)

FEMA recently performed its first complete coastal flood zone reassessment for Region II since 1983 (FEMA, 2014a), and draft maps (2013 Preliminary FIRMs), and the reports are currently out for public comment (<http://www.region2coastal.com/>). The study used a computer modeling approach for its assessment (e.g., Niedoroda *et al.*, 2010; Toro *et al.*, 2010). Historical storm and sea level data from 1938 to 2009 were used to help define a regional “climatology” of storms that cause coastal flooding, comprising 159 synthetic tropical cyclones (TCs) and 30 historical extratropical cyclones (ETCs). Hydrodynamic modeling was performed with the coupled modeling system ADCIRC (ADvanced CIRCulation model)/SWAN (Booij *et al.*, 1996; Luetlich *et al.*, 1992). With ADCIRC/SWAN, wave/hydrodynamic interactions such as wave set-up are included in SWELs.

The FEMA methods were designed not only to make maximum use of the available detailed historical storm data (1938–2009), but also be useful for looking at a wider range of possible events. They are also designed to include small variations on these historical events that are possible with shifts to the tide phase at storm landfall, or variations in TC variables such as wind speed or storm track (FEMA, 2014c; Toro *et al.*, 2010).

The 30 “worst” ETCs over the period 1950–2009 were defined based on ranking storm surge heights from area tide gauges. Retrospective best estimates (“reanalyses”) of wind and atmospheric pressure were constructed using observations and models to represent the meteorology of these historical storms.

Representing TCs is more difficult as they are rare in the New York metropolitan region, so the historical storms were utilized with a method called Joint Probability Method Optimal Sampling Quadrature (JPM-OS-Q; Toro *et al.*, 2010) that defines a set of 159 synthetic TCs that covers a wider range of events similar to the historical storms (see Fig. 4.1 in NPCC, 2015). Winds and pressure for TCs were developed using idealized parametric models and a detailed boundary layer model (FEMA, 2014b). The maximum water elevation during a storm in this region is strongly affected by the tide phase relative to the time of peak storm surge. This effect was included in the analysis by assigning a random tide phase to the ADCIRC/SWAN simulation of each of the TCs and ETCs.

Each of the 159 TCs was run one time with a random tide phase, but each of the 30 historical ETCs was run two times with different tide phases, totaling 60 ETCs. Each ETC was run once with a random tide phase, and once with that random storm timing offset by 7 days (nearly half a neap-spring tidal period)—this spreads out the “random” phasing so that storms are run on a wider range of tide phases. As a result, the production simulations covered 159 TCs and 60 ETCs—a total of 219 storms (FEMA, 2014c). Extensive details on the storms, grid development guidelines, the model grid, model validation, and quality control are included in the FEMA report (FEMA, 2014a).

D.2 Overland wave heights

The NPCC2 did not simulate overland wave heights using the WHAFIS model, which was part of FEMA’s study—the primary vertical flood level results are SWELs, not BFEs. Note that some studies that map the extent of flood zones with sea level rise utilize BFE data (e.g., NPCC, 2013; also 100-year flood zones in chapter 3 of NPCC, 2015), and in areas with large waves (e.g., Staten Island’s southeastern shore), this can lead to flood zone boundaries that are substantially further inland than flood zones mapped using SWEL data. However, at most locations in the New York metropolitan region, the spatial difference in the flood zone boundary is negligible.

D.3 Storm set

Storm surge simulations with the ADCIRC/SWAN computer model are computationally intensive, and

^kThis Appendix provides technical details for New York City Panel of Climate Change 2015 Report, Chapter 4: Dynamic Coastal Flood Modeling.

the short 6-month project timetable precluded running all the storms for each future sea level scenario. As a result, methods were also developed for only simulating a subset of the storms, and yet still utilizing the complete hazard assessment technique that accounts for all the storms. Information on these methods and the added uncertainty they cause in the assessment is given in Orton *et al.* (2014). In short, many of the storms in the FEMA assessment did not cause over-land flooding in New York City, and so the modeling was focused primarily on the storms that caused flooding, indicative of 100- to 500-year events.

D.4 Statistics

Temporal maximum water elevation data computed at each location over the entire domain for each storm were utilized for statistical analysis. For each of the 188,390 grid points in the study area, probability distributions of water elevation were built separately for TCs and ETCs. A detailed description of the statistical methods utilized for converting these distributions to flood-exceedance curves (return period vs. water elevation) is found in Orton *et al.* (2014). As a consistency check, NPCC2 results for the baseline flood assessment were verified against FEMA results. The NPCC2 modeling outputs closely reproduced FEMA flood-exceedance curves, generally within two inches (see Fig. 4.3).

D.5 Dynamic coastal flood mapping

Results of the dynamic coastal flood modeling are shown in flood maps for the baseline and future timeslices. They represent the 100- and 500-year SWEL values taken from the flood-exceedance curves for each grid location. The resulting water elevation data were imported into ArcMAP and interpolated (inverse-distance weighting, IDW) to form a raster surface over the entire region (New York City and the New Jersey Harbor regions). The ADCIRC land-surface elevation (essentially a coarse, 70-m resolution DEM) was also interpolated using IDW to the same cell size as the water elevation rasters. The land surface raster was subtracted from each water elevation raster to compute a map (raster) of

flood depth, and the zero contour is the boundary of the flood zone.

For comparison to the static flood zone maps, the ADCIRC land-surface elevations were used, and superposition and the bathtub approach were applied to the baseline SWELs using ArcMAP. The flooded areas with hydraulic connectivity to the open water were identified, keeping only these connected areas and removing all isolated areas. Again, the zero contour is the boundary of the flood zone. This work was done using similar methods to the maps presented in chapter 3, using lower resolution.

References

- Booij, N., L. Holthuijsen & R. Ris. 1996. The "SWAN" wave model for shallow water. *Coastal Eng. Proc.* **1**: 668–676.
- FEMA. 2014a. *Region II Coastal Storm Surge Study: Overview Report*. 15 p. Washington, DC. Federal Emergency Management Agency.
- FEMA. 2014b. *Region II Storm Surge Project: Development of Wind and Pressure Forcing in Tropical And Extra-Tropical Storms Report*. 62 p. Washington DC. Federal Emergency Management Agency.
- FEMA. 2014c. *Region II Storm Surge Project: Joint Probability Analysis of Hurricane and Extratropical Flood Hazards Report*. 95 p. Washington, DC. Federal Emergency Management Agency.
- Luetlich, R., J. Westerink & N.W. Scheffner. 1992. ADCIRC: an advanced three-dimensional circulation model for shelves, coasts, and estuaries. Report 1. theory and methodology of ADCIRC-2DDI and ADCIRC-3DL. C. E. R. C. US Army Corps of Engineers, Ed. Vicksburg, MS. US Army Engineer Waterways Experimentation Station.
- Niedoroda, A., D. Resio, G. Toro, *et al.* 2010. Analysis of the coastal Mississippi storm surge hazard. *Ocean Eng.* **37**: 82–90.
- NPCC. 2013. *Climate Risk Information 2013: Climate Change Scenarios and Maps Report*. 38 p. New York, NY. New York City Panel on Climate Change.
- NPCC. 2015. Building the Knowledge Base for Climate Resiliency: New York City Panel on Climate Change 2015 Report. C. Rosenzweig and W. Solecki, Eds. *Ann. N.Y. Acad. Sci.* **1336**: 1–149.
- Orton, P., S. Vinogradov, N. Georgas & A. Blumberg. 2014. Hydrodynamic mapping of future coastal flood hazards for New York City, edited, 37 p. Final report prepared for New York City Office of Emergency Management.
- Toro, G., A. Niedoroda, C. Reed & D. Divoky. 2010. Quadrature-based approach for the efficient evaluation of surge hazard. *Ocean Eng.* **37**: 114–124.

E. Public health impacts and resiliency¹

Contents

- E.1 Workshop results for coastal storm resiliency
- E.2 Workshop results for extreme heat resiliency

Recommendations are presented regarding improving health resiliency to coastal storms and extreme heat events that were distilled from discussions that occurred during the December 13, 2013, NPCC2 Health Workshop held at Columbia University's Mailman School of Public Health.

E.1 Workshop results for coastal storm resiliency

A range of measures are available to improve resiliency before and during extreme coastal storm events. This means refining early-warning and emergency-response mechanisms, as well as strengthening infrastructure, among other things.

Here, we summarize suggestions discussed at the December 13, 2013, NPCC Health Workshop held at Columbia University's Mailman School of Public Health. Table E.1 describes the short-term strategies for building resiliency to coastal storms, while Table E.2 outlines the long-term strategies.

E.2 Workshop results for extreme heat resiliency

A range of measures are available to reduce heat-health risks before and during extreme heat events, including enhancing access to air conditioning for vulnerable individuals, urban greening initiatives, and others. Here, we summarize suggestions discussed at the December 13, 2013, NPCC2 Health Workshop held at Columbia University's Mailman School of Public Health. Table E.3 describes the short-term strategies for dealing with health risks to extreme heat, while Table E.4 outlines the long-term strategies.

Table E.1. Shorter term strategies to build resiliency to coastal storm events

-
- Improve early warning systems.
 - Develop visual, map-based, and accessible probabilistic aids for predicting and contextualizing risk.
 - Create a system for knowing where vulnerable people are located within the New York metropolitan region.
 - Enhance capacity-building and resource planning for community-based organizations to be optimally helpful.
 - Encourage residents to develop storm-preparation plans for themselves and for their apartment building or neighborhoods.
 - Improve public messaging about: (1) meteorological information and public health, (2) checking in on neighbors, and (3) using community leaders as avenue for messages and checking on people.
 - Centralize communication systems, including the utilization of neighborhood groups, in order to distribute reliable information about risks, preparedness, and support.
 - Extend communication systems before and after storm season, and include a variety of avenues.
 - Implement a continuous training program to reach residents of all cultures.
 - Stockpile infrastructure supplies before storm events to allow for speedier repair of damages.
 - Assure that the science on sea level rise and storm surge is applied to New York City flood risk maps.
 - Develop real-time floor forecasts at fine scales that take into account special vulnerabilities (e.g., transportation, communications, health, and neighborhood).
 - Send rapid-response teams to assess impacts and infrastructure problems, including through community groups and social networks.
 - Implement a public education program to increase an "awareness of nature."
 - Establish more accurate baselines of locational risks, especially waste sites and locational opportunities (e.g., shelters, care centers).
 - Run emergency drills and practices to prepare response teams for extreme coastal storm events.
 - Identify concentrations of at-risk populations, and target messaging to isolated groups using key messengers.
 - Augment preparedness further in advance of extreme storms.
 - Work with local industrial businesses and community-based organizations to assess the vulnerability to hazardous exposures (i.e., toxic chemicals) in industrial waterfront neighborhoods and assess the local capacity for implementation.
-

SOURCE: NPCC2 Health Group Workshop, December 13, 2013.

¹This Appendix provides technical details for New York City Panel of Climate Change 2015 Report, Chapter 5: Public Health Impacts and Resiliency.

Table E.2. Long-term strategies to build resiliency to coastal storm events

-
- Incorporate emergency bypasses to connected transportation systems.
 - Add more waterway transportation during pre- and postemergency time periods.
 - Change building codes to facilitate preparedness (e.g. location of generator fuel).
 - Retool and raise wastewater treatment plants to accommodate for projected sea level rise, storm surge, and rainfall.
 - Build resilient power sources for critical infrastructure during storm impacts (e.g., shelters, health facilities).
 - Keep power grid on by burying lines underground and using emergency electricity repair vehicles that have the ability to move through deep water.
 - Infrastructure improvements, such as those that prevent water from entering subways.
 - Instill power back-up plans for buildings.
 - Keep health care, internet, and cell service functioning during extreme events.
 - Research the utility of microgrids.
 - Better match at-risk populations and emergency healthcare provision.
 - Increase urban floodwater retention between 1.5 and 12 inches.
 - Update building standards (e.g., elevate gear).
 - Retrofit multifamily housing and industrial areas to maintain minimum habitability and functionality for at least a few days in the wake of extreme storm: boilers, water, power, etc.; prioritize public housing in these scenarios.
 - Promote a layered approach to flood adaptation: not just walls, but also zoning changes, microgrids, and building-level adaptations.
 - Research and design flood protections that do not worsen public health risk when design heights or protective capabilities are exceeded (e.g., drowning, water quality).
 - Introduce city-scale improvements: hospitals, transportation sewage, green infrastructure, and communications systems.
 - Implement neighborhood-scale improvements: shelters, communication systems, and emergency generators.
 - Recommend and provide assistance for household improvements: fact-sheets on hardening home, financial support for these measures, and having gas and water storage elevated and stockpiled before storms.
 - Research and design best practices to prevent the exposure of hazardous substances and toxic chemicals that are stored, transferred, or handled in waterfront industrial areas in the event of severe weather.
-

SOURCE: NPCC2 Health Group Workshop, December 13, 2013.

Table E.3. Short-term strategies to build resiliency to extreme heat events

-
- Improve early warning systems (e.g., earlier messaging and text message alerts that warn people to stay inside during heat-wave events).
 - Make cooling centers more accessible, especially in high-risk areas.
 - Provide air conditioning subsidies for low-income individuals and households.
 - Instill community watch programs, such as the *Look-in on a neighbor* program.
 - Target heat-risk awareness to the caregivers of vulnerable populations like student athletes, firemen, kids, meals on wheels, and teachers (e.g., pharmacists can attach letters about heat-risk to prescriptions).
 - Expand syndromic surveillance networks to more locations in the metropolitan region.
 - Allow pets inside of cooling shelters.
 - Research how coupled events (e.g., simultaneous extreme heat and power outage) impact behavioral adaptations.
 - Implement regulations on thermostat-use and other energy-related conditions to prevent blackout (i.e., for commercial and public buildings).
 - Consider scaled responses to prolonged heat waves and complex disasters.
 - Offer ongoing and prewarm season vulnerability education (e.g., how to identify if you're especially vulnerable to heat, what to do about it).
 - Provide early warning system for electrical brownouts/blackouts (e.g., possibly incorporating SMS-based, GPS-located warning for load reduction).
 - Make better use of mobile devices, social media, and mainstream media to disseminate heat warning, a secondary health risks.
 - Implement urban-greening initiatives such as green buildings, "greener" rooms, and planting trees.
-

SOURCE: NPCC2 Health Group Workshop, December 13, 2013.

Table E.4. Long-term strategies to build resiliency to extreme heat events

- Install infrastructure improvements to the power grid.
 - Provide air conditioning units to those who need them (i.e., the most at-risk and vulnerable populations).
 - Increase access to green spaces, especially in high-risk areas.
 - Increase roof albedo (e.g., require or subsidize cool roofs).
 - Develop alternative energy sources for cooling.
 - Make sure all buildings have windows that can open to allow for proper ventilation and air flow.
 - Design buildings for both heat and cold events.
 - Encourage behavior shift by having the City “bring” common organizations of high-risk groups to cooling centers in nonemergency times.
 - Install more robust electrical infrastructure, especially in vulnerable neighborhoods and public housing
 - Combine urban heat-island mitigation (white roofs, greening, etc.), efficiency improvements, and the expansion of load-shaving programs in order to reduce electrical load.
 - Research building designs that reduce need for air conditioning to maintain safe indoor temperatures.
 - Develop strategies to “throttle” or limit consumers’ use of power during peak demand (e.g., via behavior shifts, technical measures, and pricing).
 - Apply a combined heat vulnerability index to target urban heat island interventions, and organize before/after health outcome measures once implemented.
 - Increase energy efficiency to cope with excess power demand during extreme heat events.
 - Switch to greener energy sources (i.e., renewables).
 - Raise public awareness through education so that they know how to anticipate, access, and deal with the risks of heat-wave events.
 - Relocate hospitals and care centers to the most populous and most vulnerable areas.
-

SOURCE: NPCC2 Health Group Workshop, December 13, 2013.

F. Indicators and monitoring^m

Contents

- F.1 Inventory of data sources relevant to climate change in New York City
- F.2 Extending climate resilience indicators and monitoring to the New York metropolitan region
- F.3 Technical and research support for the NYC Cool Roofs Program

F.1 Inventory of data sources relevant to climate change in New York City

The New York metropolitan region has extant monitoring systems that, although they were not put in place specifically for climate resiliency, can now be utilized for this purpose. Table F.1 provides an inventory of some of these existing data sources.

Additional sources of data (and the climate-related variable they track) in the New York metropolitan region include National Weather Service Automated Surface Observing System (ASOS) locations (meteorological variables), the NOAA-CREST NYCMetNet/Urban Atmospheric Observatory (atmospheric observations, NYS DEC (air quality; see Fig. F.1)), the NYCDEP Harbor Survey (water quality), and the Stevens Institute of Technology New York Harbor Observing and Prediction System (NYHOPS; ocean/coastal).

F.2 Extending climate resilience indicators and monitoring to the New York metropolitan region

While New York City has emerged as a global leader in climate change mitigation and resiliency planning, significant gaps remain between the existing indicators and monitoring systems and what will be needed to support climate change efforts. It will be important to (i) expand the spatial domain included in climate change monitoring for New York City, (ii) maintain and, in some cases, increase the observations that support climate indicators, and (iii) better integrate information from numerous agencies and institutions currently conducting climate change-

related monitoring. While funding constraints will be a key challenge for the implementation of the first two recommendations, improved coordination between different monitoring programs may allow for the most efficient use of resources and allow for the needed expansion of existing monitoring.

Climate change will have a significant impact on many sectors critical to New York City, including water resources, energy supply and use, transportation, agriculture, ecosystems, and human health (NPCC, 2010). These systems extend beyond city borders, and as a result, in order to assess the multisectoral impacts of climate change on New York City, it will be important to take a regional approach. The New York metropolitan region includes 31 counties in New York, New Jersey, and Connecticut (Rosenzweig and Solecki, 2001).

Integrating across multiple institutions. Although indicators can be produced in an *ad hoc* manner, with agencies developing and using indicators as needed for various risk management and adaptation needs, the development of a more comprehensive indicators and monitoring system would promote cross-agency collaboration and give high-level decision-makers and the public a broader view of key impacts, vulnerabilities, and adaptation responses. Although the potential policy impact of such a system is significant, investments will be needed to set up a sustainable system for collecting raw data from agencies, climate monitoring systems, remote sensing, census and survey data, and other sources, and for transforming them into indicators. Here we review important considerations and design elements for an integrated system to develop and maintain a robust set of climate change indicators.

A first step will be to identify a coordinating unit for the system. This could be located in the Mayor's Office of Sustainability, Mayor's Office of Recovery and Resiliency, or within an agency such as the Department of Environmental Protection or the Office of Emergency Management. However, it would need to be at a high enough level to be able to coordinate across agencies and address risks across sectors. Second, a technical unit for data processing, indicator calculation, and analysis would need to be set up. This could be within the government, but it might be preferable to have this hosted by an independent institution with

^mThis Appendix provides technical details for New York City Panel of Climate Change 2015 Report, Chapter 6: Indicators and Monitoring.

Table F.1. Data sources in the New York metropolitan region

Data source	Stations in the metropolitan region	Variables monitored	Notes
US HCN v. 2.5 (NOAA NCDC)	22 stations	Monthly average temperature, monthly minimum temperature, monthly maximum temperature, precipitation	Well-documented, consistent data. Adjusted for changes to observational methods, siting and other potential sources of bias as described in Menne <i>et al.</i> (2009). Data represents the synergistic impacts of climate and urban land management.
GHCN-Daily (NOAA NCDC)	690 stations	Precipitation, snowfall, snow depth, maximum temperature, minimum temperature	Provides the measured variables, length of record, and period of record by station. There are numerous other variables in addition to the five core ones at daily time step.
US Climate Reference Network (NOAA NCDC)	One station (Milbrook, NY, in Dutchess County)	Three independent measurements of temperature and precipitation at each station. Also observes solar radiation, surface skin temperature, surface winds, soil moisture, and soil temperature at five depths, atmospheric relative humidity.	Reference data: climate change without urban influence. Provides 50-year sustainable, high-quality climate observation network.
NEXRAD WSR-88D Radar	Two stations (KDIX in Mount Holly, NJ, and KOKX in Coram, NY)	Spatial and temporal variability and intensity of precipitation.	Short record.

technical expertise in data analysis and management as well as indicator development. Hosts could include a university or a coalition of universities in the city that could jointly set up a technical unit that has the requisite expertise in the types of data to be managed and processed, including climate, environmental, health, and socioeconomic data. The technical unit would need strong skills in stakeholder engagement, data management, data processing (especially geospatial data processing), and statistics.

The coordinating and technical units together would be responsible for managing stakeholder engagement processes to modify the framework and identify suitable indicators. Often indicators identified in stakeholder processes are vague and open to interpretation. Thus, the technical unit would be responsible for developing a methodology for each indicator. This would include technical specifications such as measurement units, source data, geographic coverage, output resolution, frequency of update, type (current status

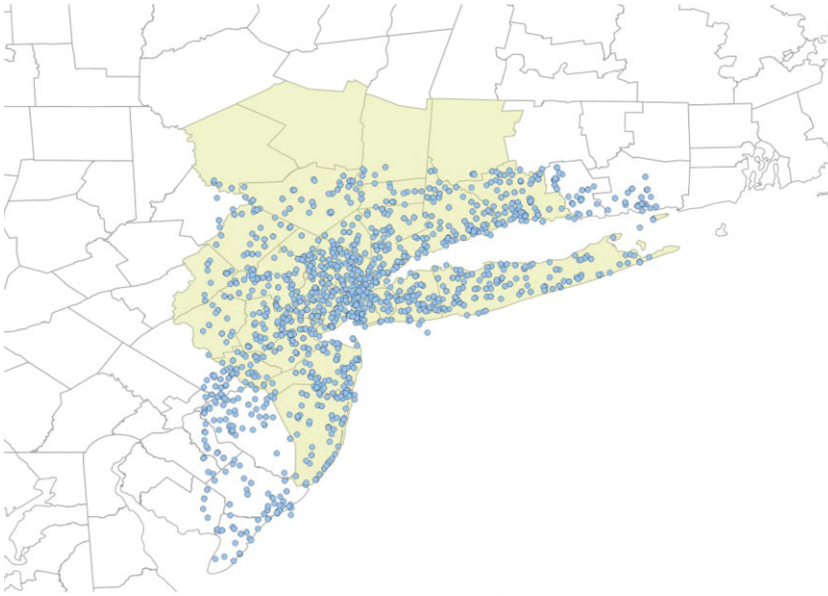


Figure F.1. The 5253 surface meteorological sites that provide data included in the CCNY NYCMetNet Database, which are noted by the blue dots on this map. These sites are operated by multiple public and private institutions.

NASA Landsat 7 Surface Temperature Map Aug 14, 2002 -10:30AM 60 meter resolution

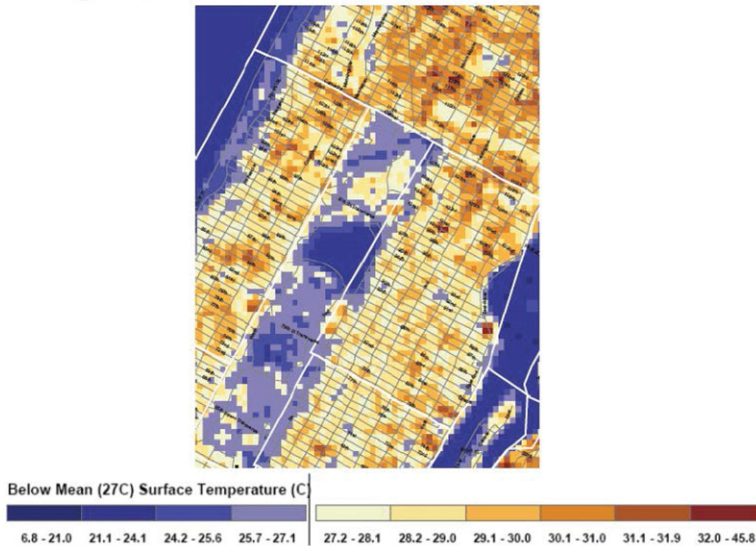


Figure F.2. NASA LANDSAT surface temperature map of Midtown Manhattan with Central Park in the center.

or trend), and statistical transformations needed. This may involve a degree of experimentation with alternative approaches and the production of sample indicators. Once one or more designs/methodologies for each indicator have been

developed, it is important to hold a further round of consultations with stakeholders to seek feedback and ensure that the indicators meet user needs. Once agreement is reached regarding a final set of indicators, indicator production methods

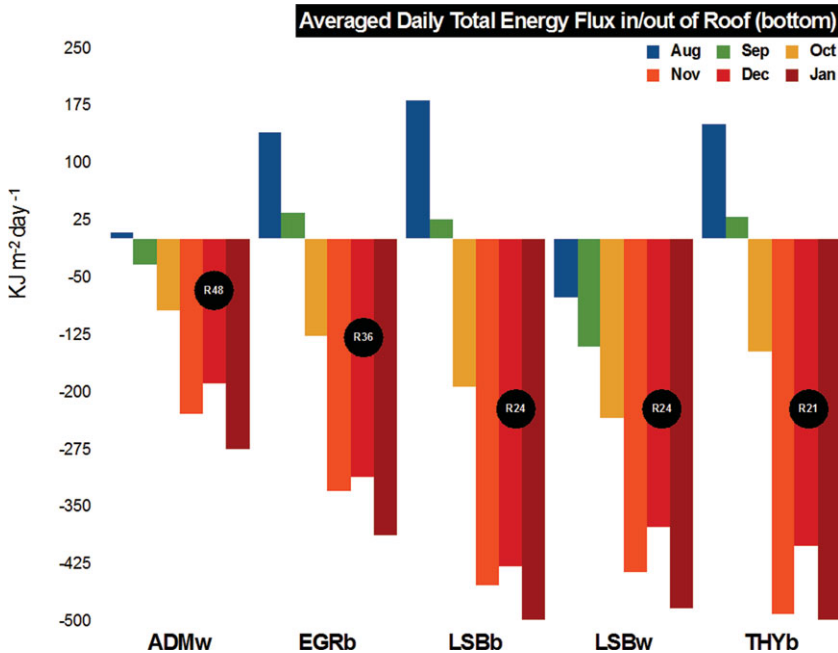


Figure F.3. Measurement of heat gain and loss from five roofs with different colors (albedos) and insulation thicknesses (R -values) over buildings in the Princeton Plasma Physic Laboratory.

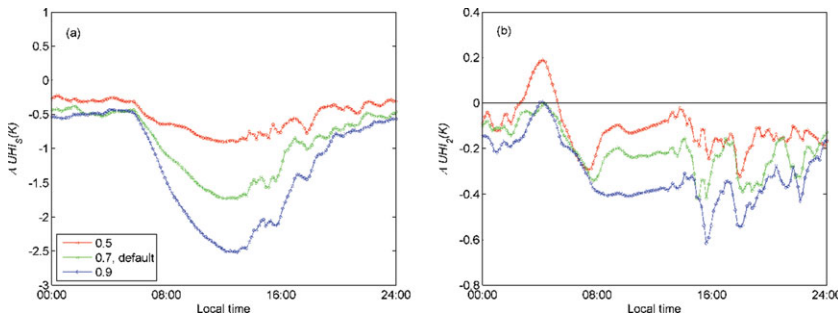


Figure F.4. Impacts of cool roof implementation at the city scale (simulation for Baltimore, MD, from Li *et al.* 2013) as a function of albedo values (the fraction of cool roofs is 50% and the conventional roofs have an albedo value of 0.3). The image on the left shows changes in the surface urban heat island (UHI) and the image on the right shows changes in the near-surface UHI. $\Delta UHI = T_{\text{urban}} - T_{\text{rural}}$ the subscripts are s for surface and 2 for 2 m above surface. The different lines are for albedos of 0.5 (red), 0.7 (green), and 0.9 (blue) as indicated in the legend.

can be standardized and automated to the extent possible.

The technical unit would collate data for the relevant indicators from existing data custodians, with primary sources including city agencies, federal meteorological and climate data managers, climate modeling groups, the U.S. Census, and NASA Centers. Where important indicators are identified but no existing monitoring system exists, the city will need to consider the costs and benefits of adding

monitoring systems. The existence of relatively low-cost systems for collecting data (e.g., cheap digital thermometers that can report data wirelessly, which could be placed in a dense network throughout the city), or new crowd-sourcing methods (e.g., for collection of data on the flowering dates of certain plant species or bird migration arrival dates), could mean that costs are in fact quite reasonable.

The coordinating and technical units would be jointly responsible for setting up a Web portal for

indicator reporting, including interactive tools for indicator exploration (map services, data query tools, and data visualization tools). An annual “state of the climate” report could be produced for the city and the wider metropolitan area that summarizes spatial patterns, trends, and results of adaptation efforts, and explains any salient climate phenomena that occurred in that year based on climate indicators. The portal could also include reference information in the form of a bibliographic database searchable by topic, date, geographic scope, and type of climate event.

It must be emphasized that for such a system to be successful, it must not be viewed as an academic exercise, but instead needs to be closely tied to city policy and planning processes.

F.3 Technical and research support for the New York City Cool Roofs Program

Rooftops provide a testbed for studying a number of fundamental urban surface energy balance and climate principles. Indeed, roof scientists and engineers share many concepts and interests with climate scientists, such as weather, climate, extreme events, sunlight and the solar spectrum (including UV radiation, which also can damage membranes), albedo and solar reflectance, temperature cycles, and building energy needs for both heating and cooling. Traditional waterproof roofing systems take many different material forms depending on a number of factors, including local climate conditions, consumer preferences, and historical precedents.

In this section of the appendix, the focus will be on high-albedo roofing for temperature control.

Urban surfaces and rooftop science. Among the many projections of future climate change impacts, ranging from ecological to oceanic to storms and extreme events, increases in heat and heat-wave extreme events in urban areas are a great risk. Further, the urban heat island (UHI) is not a disputed concept. Indeed cities are increasingly becoming “crystal balls” into future global warming in so many ways—higher temperatures due to anthropogenic factors, dominant as global sources of CO₂ emissions, vulnerable populations and expensive assets, proactive policies to reduce emissions and develop adaptation, low per capita carbon intensities, and high local ambient atmospheric CO₂ levels.

A major question UHI research faces is how to quantify the relationship between radiometric surface temperature and overlying air temperature, and by how much can ambient air temperatures be lowered by reducing surface temperatures through methods such as increasing albedo and evapotranspiration through the use of new and old green infrastructure technologies.

Rooftops collectively comprise a substantial fraction of land area in urban settings. The percentage varies from city to city, but ranges from 10% to 20% (Rosenzweig *et al.*, 2009). The ubiquitous waterproof rooftop membrane is therefore a fundamental urban surface interacting with the atmosphere and affecting the environment in ways that are increasingly being appreciated and studied.

Among the most salient features of the rooftop environment is that they are hot. During peak sunlight times, membranes can easily reach surface temperatures of 170°F (77°C) (Gaffin *et al.*, 2012). And, such peak temperatures do not require high summertime air temperatures, but are generally much more strongly dependent on incident sunlight conditions; it is sometimes the case that the surface temperatures are even higher during spring rather than summer, when less hazy urban air prevails.

Contrastingly, night-time rooftop surfaces temperatures can drop remarkably low, especially under calm, clear conditions. Nocturnal temperatures as low as −11°F (−24°C) have been observed (Gaffin *et al.*, 2012). The explanation for how temperatures can drop this low has to do with the fact that the rooftop is experiencing net negative long-wave radiation imbalance, in that downward long-wave radiation is emanating from high tropospheric altitudes with correspondingly low blackbody radiation temperatures. The rooftop is emitting long-wave radiation at much higher terrestrial surface temperatures and hence a negative energy imbalance ensues. Under such conditions surface, the surface temperature on the rooftop will keep dropping until it matches the extremely cold high-altitude tropospheric effective longwave radiation temperature. An important contributing factor here is that rooftop mass is also quite low to minimize structural roof dead load, and so there is little internal mass energy that might otherwise slow down the nocturnal cooling.

Whether such extreme nocturnal cooling is occurring on other prototypical urban surfaces such

as pavement, streets, and walls is less well known although it is unlikely to be as strong. One reason is that in these cases the surface materials are quite dense, and considerable internal energy can be stored during the day that is slowly released at night and probably leads to slower nocturnal cooling as compared to roofs. In addition, if not more important, urban streets and walls have a low sky-view factor compared to roofs, meaning they are often receiving longwave radiation from nearby buildings with correspondingly higher terrestrial and blackbody radiative temperatures than the atmosphere.

The general principle involved is that the surface energy balance radiation fluxes, especially in sunlight, are often more important than air temperature in determining surface temperatures. Latent heat and conductive heat flows however can strongly modulate the radiative energy balance (Gaffin *et al.*, 2010).

Such extreme hot and cold membrane temperatures cycles have practical implications for rooftop service life and building energy gains or losses from the roof. The temperature cycles are a major factor in roof membrane wear and tear as they lead to material expansion and contraction cycles. Also, although peak daytime roof surface temperatures can be very hot, this is counterbalanced significantly by the cold nocturnal cycles, resulting in less energy gain during the summer than might otherwise be expected.

Surface temperature versus air temperature. Urban climate scientists take pains to distinguish the difference between material surface temperatures and air temperatures. To the general public, air temperature is more commonly understood as it is the one reported in daily weather reports and the one individuals bear in mind to prepare for daily activities or travel to different climates. However, surface temperature and its extremes are also clearly familiar in many daily experiences, such as walking barefoot on a sunny beach or touching sliding ponds exposed to long periods of sunlight. To scientists, surface temperature has a number of different names, such as “skin,” “radiometric,” or “black body radiating” temperature.

With respect to urban climate, these two categories of temperature have different roles to play and are both important, though in different ways.

Regarding human thermal comfort and building energy use, air temperature is arguably the more relevant indicator as this is the temperature people feel where they live, work, or play outdoors. The primary goal of UHI mitigation is to ultimately lower such air temperatures during extreme heat events.

However climate science does not have technology to lower air temperatures directly on a large scale, such as the size of a city. On small scales there are a number of familiar thermodynamic methods to reduce air temperatures, but ability for cities to deliberately cool large-scale air masses does not exist. In contrast to air temperature, it is very easy to materially control surface temperatures by altering albedo or creating surfaces that can evaporate or transpire water to vapor, that is, using plant–soil systems. By viewing a surface temperature thermal map of a city (Fig. F.1), it is evident that all the surfaces detected by the satellite sensor are anthropogenic and the extreme range of surface temperatures from hot to cold result from their specific land use and surface material choices.

Cool Roof research conducted in 2012 and 2013: Princeton, NJ, and City of Baltimore, MD. The measurement of heat gain and loss from five roofs with different albedos and insulation thickness over buildings in the Princeton Plasma Physics Laboratory reveals that Cool Roofs offer significant advantages in the summer time, while producing very minimal adverse impacts in the winter (Fig. F.2). Comparing, for example, the LSBb and LSBw roofs in Figure F.2, which have the same insulation (R -value of 24) but different albedos (LSBw is a white roof with an albedo of 0.65 m; LSBb is black with an albedo of 0.07), one can notice that their winter months heat losses are comparable. However, during the summer, the figure shows that the heat gains over the black roofs are significantly more substantial. In fact, on average over a day, the white roofs do not gain heat in the summer due to their night-time radiative cooling. In addition, one can see that heat gains in the summer are high for the three black roofs (EGRb, LSBb, and THYb) and much lower for the two white roofs (ADWm and LSBw). The difference between winter time and summer time impact of albedo can be attributed to the diurnal cycle of solar radiation. Roof albedo is only an important factor in roofs performance during hours of high insolation where a high albedo can reflect a

large fraction of that radiation. During the summer months, peak heat gains associated with peak cooling loads occur during the longer summer daytime when insolation is high and the impact of albedo is significant, creating large differences between cool and dark roofs. During the winter, insolation occurs over shorter periods and peak heat losses associated with peak heating loads occur during the nighttime, when albedo has no relevance.

Cool roofs have an impact beyond the scale of a single building. If implemented widely throughout a city, they can reduce surface and air temperatures significantly at the city scale. Simulations using the weather and research forecasting (WRF) model over Baltimore show that these reductions depend almost linearly on the fraction of roofs in the city converted to high-albedo surfaces (Li *et al.*, 2014). Figure F.3 shows a reduction of up to 0.9°F (0.4°C) in air temperature with 50% of the roofs converted to an albedo of 0.7. With 100% penetration of roofs across Baltimore, this cooling effect almost doubles.

The NYC Cool Roofs program: regulatory framework. To help decrease the effects of UHI, the NYC Building Code requires that 75% of the roof area or setback surface on buildings permitted on or after July 1, 2009, be coated white or rated as highly reflective by ENERGY STAR®. In addition, alterations involving the recovery or replacement of an existing roof covering shall comply with Section 1504.8 of the New York City Building Code, unless the area to be recovered or replaced is less than 50% of the roof area and less than 500 square feet.

Local Law 21, 2011, amended this to align with LEED requirements. Effective January 1, 2012, existing buildings making alterations that involve the recovery or replacement of an existing roof must use more reflective and emissive materials.

All building and Cool Roof maintenance is the responsibility of the building owner or manager. This information is conveyed at the initial inspection where the overall condition of the roof is evaluated, as well as type of roof, drainage, ponding, and warranty. No roof will be coated through NYC Cool Roofs if a warranty will be jeopardized. An inspection sheet must be signed off by a building operator prior to any work taking place. In addition, for Cool Roofs to be optimally successful, the roofs must be properly maintained and cleaned throughout the year.

Research questions. In addition to the question of temperature relationships, there are many fundamental research questions associated with high-albedo urban surfaces including cool roofs. Some of these questions that could expand the scope of mitigating the UHI in the New York metropolitan region are as follows:

- How much shortwave radiation is reflected and how does albedo and temperature control decline over time?
- What is the effective transmissivity of this light upwards in the atmosphere and what fraction ultimately reaches the top of the atmosphere (TOA)?
- For reflected light escaping the TOA, this creates a negative radiative forcing, and the carbon equivalence for this forcing can, in principle, be calculated. What is that equivalence?
- What land area worldwide is amenable to this benign form of geo-engineering?
- What does this mean regionally and locally for climate control in the face of global warming?
- What is the public acceptance of higher albedo surfaces and roofs (i.e., neutral, low)? How significant is the scattering of light into neighboring buildings?
- Is there a winter heat penalty in colder climates?
- What are the best protocols for measuring albedo, emissivity, and temperatures in real urban settings where shading, for example, can be quite significant?
- Are there positive synergies between cool roofs and other rooftop infrastructure, such as PV and HVAC systems?
- How can the practical challenges to brightening street-level surfaces—such as pedestrian and vehicular usage—be addressed to allow additional urban surfaces like street pavement and sidewalks to be lightened?

References

- Gaffin, S.R., M. Imhoff, C. Rosenzweig, *et al.* 2012. Bright is the new black—multi-year performance of high-albedo roofs in an urban climate. *Environ. Res. Lett.* 7: 014029.
- Gaffin, S.R., C. Rosenzweig, J. Eichenbaum-Pikser, *et al.* 2010. *A Temperature and Seasonal Energy Analysis of Green, White, and Black Roofs*. 19 pp. Center for Climate Systems Research, Columbia University.

- Li, T., R.M. Horton, and P.L. Kinney. 2013. Projections of seasonal patterns in temperature-related deaths for Manhattan, New York. *Nature Clim. Change* **3**: 717–721.
- Li, D., E. Bou-Zeid & M. Oppenheimer. 2014. The effectiveness of cool and green roofs as urban heat island mitigation strategies. *Environ. Res. Lett.* **9**: 055002.
- Menne, M.J., C.N. Williams & R.S. Vose. 2009. The U.S. historical climatology network monthly temperature data, version 2. *Bull. Am. Meteorol. Soc.* **90**: 993–1007.
- NPCC. 2010. Climate change adaptation in New York City: building a risk management response. New York City panel on climate change 2010 report. C. Rosenzweig and W. Solecki, Eds. *Ann. N.Y. Acad. Sci.* **1196**: 1–354.
- Rosenzweig, C., W.D. Solecki, J. Cox, *et al.* 2009. Mitigating New York City's heat island: integrating stakeholder perspectives and scientific evaluation. *Bull. Am. Meteorol. Soc.* **90**: 1297–1312.
- Rosenzweig, C. & W. Solecki. 2001. *Climate Change and a Global City: The Potential Consequences of Climate Variability and Change: Metro East Coast*. 224 pp. For the U.S. Global Change Research Program, National Assessment of the Potential Consequences of Climate Variability and Change for the United States, Columbia Earth Institute.